Nutritional programming of white adipose tissue and mitochondrial function Fat quality matters

Nutritional programming of white adipose tissue and mitochondrial function

Fat quality matters

Andrea Kodde

Propositions

1. Programming of mitochondrial function by the perinatal diet has a long-lasting impact on adult metabolic health.
(this thesis)

2. A postnatal diet with lipid droplets mimicking the human milk fat globule structure improves adult metabolic health.
(this thesis)

3. The effect of a lower environmental temperature on energy expenditure is a positive side effect of the energy crisis.

4. This is the last generation PhD candidates that writes their PhD thesis without the use of artificial intelligence.

5. *Luctor et Emergo* is the motto of the Dutch province Zealand and of PhD projects.

6. A beneficial side effect of giving studies space names is that you learn more about space.

Propositions belonging to the thesis, entitled

Nutritional programming of white adipose tissue and mitochondrial function: Fat quality matters

F.D. (Andrea) Kodde

Wageningen, 3 April 2024

NUTRITIONAL PROGRAMMING OF WHITE ADIPOSE TISSUE AND MITOCHONDRIAL FUNCTION:

Fat quality matters

F. D. (Andrea) Kodde

Thesis committee

Promotors

Prof. Dr J. Keijer
Professor of Human and Animal Physiology
Wageningen University & Research

Prof. Dr E. M. van der Beek
Professor of Nutritional Programming
University of Groningen

Other members

Prof. Dr R. Witkamp, Wageningen University & Research
Dr M.C. Michalski, Carmen-Inrae, Lyon, France
Dr M. Palou March, University of the Baleares, Palma, Spain
Prof. Dr A. Kalsbeek, Academic Medical Center, University of Amsterdam

This research was conducted under the auspices of the Graduate School VLAG

Nutritional programming of white adipose tissue and mitochondrial function: Fat quality matters

Francina Dorothea (Andrea) Kodde

Thesis

submitted in fulfilment of the requirements for the degree of doctor
at Wageningen University
by the authority of the Rector Magnificus,
Prof. Dr C. Kroeze
in the presence of the
Thesis Committee appointed by the Academic Board
to be defended in public
on Wednesday 3 April 2024
at 1:30 p.m. in the Omnia Auditorium.

F.D. (Andrea) Kodde
Nutritional programming of white adipose tissue and mitochondrial function: Fat quality matters
252 pages

PhD thesis, Wageningen University, Wageningen, the Netherlands (2024)
With references, with summary in English and Dutch

ISBN: 978-94-6395-015-2
DOI: 10.18174/644648

CONTENTS

Chapter 1

General introduction

Early life programming of later life metabolic health

The prevalence of obesity in children, adolescents and adults is at a worrying high level and, despite stabilizing trends in most high-income countries, obesity still is increasing worldwide (1). Although there is still some controversy, obesity is recognized as a disease by the World Health Organization and has a direct impact on mobility and cardiac, pulmonary and immune function as well as endocrine regulation (2, 3). Importantly, obesity is also strongly associated with an increased risk for metabolic diseases, such as type 2 diabetes (T2D), non-alcoholic fatty liver disease (NAFLD) and cardiovascular disease, especially when the onset of obesity occurs in early life (4). Causes of metabolic disease are often multi-factorial and include genetic factors, a sedentary lifestyle, and a high intake of foods rich in (saturated) fatty acids and carbohydrates. In addition to these causes, environmental factors in pre- and postnatal life have shown to be linked to the adult metabolic phenotype. Epidemiological evidence has shown strong correlations between birth weight and incidence of cardiovascular death and T2D in later life (5, 6). Being born small for gestational age, specifically in combination with subsequent catch-up growth, is associated with a higher fat mass, T2D, hypertension and cardiovascular disease in later life (7-11). Also, being born large for gestational age is associated with metabolic dysregulations like adult obesity, T2D and cardiovascular disease (9, 12).

Interestingly, the maternal diet has also shown to be a potential contributing factor for obesity and metabolic disease in the adult offspring. Exposure to severe, but short-lasting maternal undernutrition during the Dutch famine, in the winter 1944-45, not only had short term consequences for birth weight, but also increased the risk for coronary heart disease, glucose intolerance and obesity in adult offspring (13-15). Similar effects were found in animal studies, showing increased adiposity and disturbed insulin signalling upon maternal undernutrition during pregnancy in rodents and sheep (16-19). Additionally, maternal overnutrition also showed to increased risk of obesity, T2D, cardiovascular disease and NAFLD in the offspring (20-23). Similar insights had led to the hypothesis previously formulated by David Barker, who was the first to postulate that origins of adult disease can be traced back to the foetal and infant environment (24). As such, those environmental factors in early life can cause sustained and definitive changes to organ structure and function, including the underlying molecular wiring. The induction of later-life changes to metabolic organs by early life influences is called metabolic programming (25, 26), which consequently may increase or reduce the risk of later disease.

In addition to being a potential origin for later life metabolic disease, early life may also be a window of opportunity for beneficial (nutritional) metabolic programming i.e.,

reaching an individual's growth potential or attenuate adverse metabolic consequences of maternal over- or undernutrition. Obesity has a large impact on quality of life and life expectancy, and as treatment is difficult, prevention is pivotal (4). Beneficial programming by early life nutrition may therefore be a crucial opportunity in the battle to reduce later life obesity and its associated disease risks. Indeed, evidence exists for the potential to beneficial impact later life metabolic health by nutrition in early life. For example, postnatal caloric restriction attenuated some of the metabolic consequences of maternal under- and overnutrition in mice (27, 28). Furthermore, (the duration of) breastfeeding is associated with reduced overweight risk in childhood and adolescence and T2D risk in later life (29, 30). Several factors have been suggested to underlie the association between breastfeeding, bodyweight status and metabolic health in later life. Those factors include the social-economic environment and food intake regulation, but it may also be related to the specific properties of human milk (31, 32).

Specific nutrients, more specifically, fatty acids and carbohydrates, fed in postnatal life have been shown to affect later life metabolism. N-3 long-chain polyunsaturated fatty acids and medium-chain fatty acids fed to mice postnatally reduced adult adiposity and insulin resistance in an obesogenic environment (33, 34). Further, feeding a mixture of arachidonic acid and docosahexaenoic acid (ratio of 1.46:1) to mice after weaning also reduced adiposity in adulthood, but did not affect insulin sensitivity (35). The latter may be explained by the relative late introduction of the diet (postnatal day 28). Reduction of the amount of n-6 polyunsaturated fatty acids in the postnatal diet of mice also reduced adult adiposity (36). Also, changes in dietary carbohydrate composition i.e., replacing part of the glucose for galactose and low vs. high digestible-starch, reduced adult adiposity, insulin resistance and increased metabolic flexibility, in female mice only (37, 38). Together this data shows that there is indeed a window in postnatal life to beneficially program metabolic health.

Possible processes underlying postnatal programming of adult metabolic health need further investigation. One factor proposed to be involved in perinatal programming of adult metabolic health is programming of white adipose tissue (WAT) function and mitochondrial function and will be discussed in the next sections (39-41). Subsequently, the role of impaired WAT health on liver function and the programming of liver function by the perinatal diet are discussed. Finally, I will introduce a specific nutritional concept, a postnatal diet containing large, (milk)phospholipid coated lipid droplets, which was hypothesized to have a programming effect on WAT function and mitochondrial function.

White adipose tissue development and programming

Programming of WAT function and lipid storage capacity is suggested to underlie programming of body fatness and metabolic health in later life. Reasons include the important role of WAT in the development of T2D as well as the early life setpoint for total adipocyte number, relevant for total fat mass capacity, as explained in the following section (39, 40).

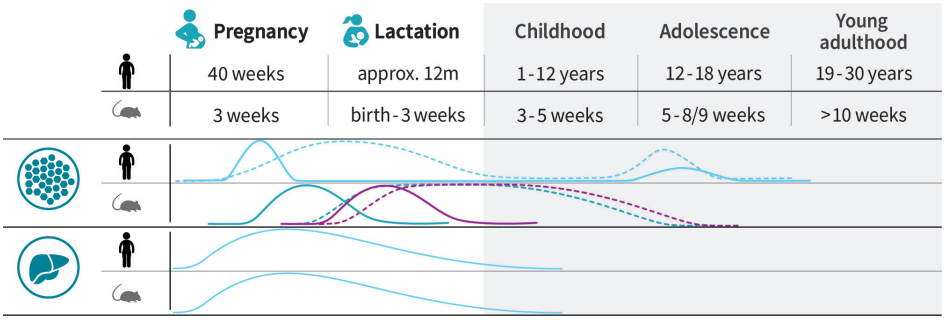

Figure 1: Schematic representation of the developmental stages in humans and mice with below the perinatal development of white adipose tissue (50, 53, 54) and liver (89, 90). Development of hyperplasia (---) and hypertrophy (- - -) as reported for human WAT (blue lines) and mouse subcutaneous (green lines) and visceral (purple lines) WAT and development of human and mice liver (blue lines). Time periods with the highest developmental activity are shown as peaks in the graphs.

WAT is important in the regulation of whole-body energy metabolism. Excess postprandial glucose and lipids are taken up by the WAT and stored as triglycerides, and in times of energy need, like fasting or exercise, released again in the form of fatty acids. When WAT function is impaired, it fails to store the excessive lipids and glucose, resulting in fat deposition in other organs (ectopic fat deposition), an important step in the development of T2D and NAFLD. The location of WAT depots, either under the skin (subcutaneous WAT) or in the abdominal cavity (visceral WAT), is thought to determine the role of WAT depots in metabolic health (42, 43). Visceral WAT mass is inversely correlated with insulin sensitivity and an independent risk factor for metabolic diseases (44, 45), while the subcutaneous WAT has a higher mitochondrial density and oxidative capacity (46). The reduced insulin sensitivity of WAT, calculated as product of fasting free fatty acids and insulin levels, and the reduced insulin sensitivity of subcutaneous adipocytes in obese and T2D patients has indicated a crucial role for WAT in regulation of systemic insulin sensitivity (47-49).

WAT develops in the second trimester of pregnancy in humans and is fully functional at birth (50). During this period WAT develops from loose connective tissue from the start of the second trimester to WAT depots with fully developed adipocytes, preadipocytes and a stromal vascular fraction around birth. Evidence of prenatal development of WAT in humans is scarce and mainly obtained from older studies (50, 51). However, a recent study on the development of fat mass relative to body weight gain from birth to 2 years of age has shown that the relative fat mass of infants increased up to 6 months of life, after which it decreased to some extent (52). In mice, WAT is first detected at day 16 of pregnancy, but lipid storage is, in contrast with humans where it starts during third trimester of pregnancy, not found before postnatal day 2 (**Figure 1**) (51, 53). Studies in rodents also show distinct developmental patterns between subcutaneous WAT and visceral WAT, adipocyte commitment and differentiation being set before day 18 of pregnancy in the subcutaneous, but mostly postnatally in visceral WAT depots (54). WAT development starts with the formation of adipocytes from progenitor cells (adipogenesis), resulting in an increase in adipocyte number (hyperplasia), followed by storage of lipids as large lipid droplets in the cytoplasm resulting in increased adipocyte size (hypertrophy). The growth and development of WAT depots continues after birth, by hyperplasia and hypertrophy and functional changes (55). For example, WAT depots of rodents are subjected to transient browning postnatally followed by a gradual transition towards a whiter phenotype around weaning (56, 57). A similar transition towards a whiter phenotype is seen in large animals starting soon after birth (58, 59). In humans, adipocyte number is relatively stable after childhood and puberty, and a setpoint is suggested for adipocyte number in early life (39). In specific circumstances, like following long-term high fat exposure, hyperplasia was observed in adulthood as well (54).

Adult WAT health can be programmed by nutritional conditions prenatally, like maternal under- and overnutrition. Maternal undernutrition during pregnancy reduced insulin sensitivity of WAT in adult rats, while maternal overnutrition increased later life WAT hypertrophy and expression of lipolytic and adipogenic genes in a depot- and sex-specific manner (17, 60-63). Adult WAT function can also be programmed by early postnatal nutrition. For example, overfeeding during the lactation period induced by litter-size reduction resulted in WAT inflammation and increased adipogenic and lipid storage capacity later in life (64, 65). Adult WAT health may also be programmed by specific nutrients, like medium-chain fatty acids, n-3 long-chain polyunsaturated fatty acids and reduced linoleic acid intake in postnatal life, as postnatal exposure to those nutrients reduced adult WAT hypertrophy, but processes underlying are unknown (33, 34, 36). Thus, WAT health can be programmed by the early diet, but processes underlying are not fully understood, especially regarding the possible contribution of postnatal nutritional programming.

Programming of mitochondrial function

An essential determinant of WAT health is mitochondrial function. Mitochondria are the energy generators of all cells and produce adenosine triphosphate (ATP) through oxidative phosphorylation (OXPHOS, **Figure 2**). In OXPHOS, fuels are oxidized via the electron transport chain resulting in electron transfer coupled to the generation of a proton gradient over the mitochondrial inner membrane, which is essential for the production of ATP. Uncoupling of the electron transport chain from ATP production especially by uncoupling protein 1 (UCP1), predominantly found in brown adipose tissue, results in the production of heat (thermogenesis) which is particularly relevant in early life for the regulation of body temperature. Well-functioning mitochondria are required for all functional processes in the body, including for lipid storage and release in the WAT. Furthermore, well-functioning mitochondria in WAT respond to changes in nutrient supply and, in this way, impact whole-body energy metabolism (66).

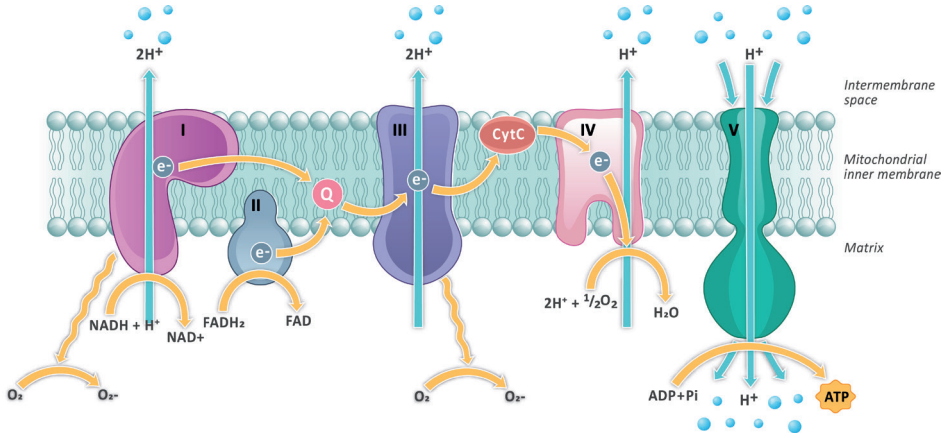

Figure 2: The oxidative phosphorylation (OXPHOS). NADH, which is produced in the tricarboxylic acid cycle, is oxidized to NAD^+ by complex I of OXPHOS (NADH dehydrogenase). An electron pair of NADH is, by enzyme activity of complex I, transferred to ubiquinone which is then reduced to ubiquinol (coenzyme Q). The released energy from this reaction is used to pump H^+ across the mitochondrial inner membrane (MIM) into the intermembrane space (IMS). In complex II of OXPHOS (succinate dehydrogenase), $FADH_2$ is oxidized to FAD and electrons from $FADH_2$ are also transferred to ubiquinone which is then reduced to ubiquinol. The ubiquinol produced in complex I and II is transported to complex III of OXPHOS (cytochrome C reductase), where electrons from ubiquinol are used for the reduction of cytochrome C. The energy produced by this reaction is used to pump H^+ across the MIM into the IMS. Complex IV of OXPHOS (cytochrome C oxidase) oxidizes cytochrome C and electrons from cytochrome C are transferred to the terminal electron acceptor oxygen, resulting in the production of H_2O. Simultaneous H^+ ions are pumped across the MIM into the IMS with the released energy. In Complex V of OXPHOS (ATP synthase) uses the proton motive force created by the H^+ gradient across the MIM to synthesize ATP from ADP. ADP: Adenosine diphosphate; ATP: Adenosine triphosphate; FAD: flavin adenine dinucleotide; $FADH_2$: reduced FAD; H: hydroxide; H_2O: water; NAD: Nicotinamide adenine dinucleotide; NADH: reduced NAD; OXPHOS: oxidative phosphorylation.

An impaired fatty acid storage capacity and a decreased mitochondrial oxidative capacity are important features in obesity and T2D. WAT mitochondrial density and oxidative capacity were reduced in obese mice as evidenced by reduced OXPHOS protein expression and oxygen consumption in functional measurements (67, 68). Moreover, body mass index in obese and non-obese individuals was inversely correlated to mitochondrial density and oxidative capacity, and WAT mitochondrial density as well as oxidative capacity were reduced even in the absence of glucose intolerance (68, 69). In addition, WAT mitochondrial function was also disturbed in rodents with glucose intolerance and T2D (68, 70).

Moreover, hepatic and skeletal muscle mitochondrial function was impaired in T2D (71, 72). Together these data indicate a pivotal role for mitochondrial function in the regulation of whole-body energy metabolism and insulin sensitivity.

Mitochondrial density and function can be programmed by early life events. Low birth weight in a rat model for intra-uterine growth restriction was accompanied by mitochondrial dysfunction in pancreatic β-cells, skeletal muscle and liver and followed by the development of T2D (73-75). Mitochondrial dysfunction i.e., reduced oxidative capacity and mitochondrial density in skeletal muscle and liver, was also seen in offspring upon maternal underfeeding of sheep and rats (41, 76, 77). Interestingly, maternal overnutrition also resulted in reduced oxidative capacity, mitochondrial density and altered mitochondrial dynamics in rat skeletal muscle (78, 79). Together this provides an evidence base that mitochondrial function can be affected by the prenatal environment in several organs. The effect of the maternal diet on WAT mitochondrial function in the offspring has not been intensively investigated and thus is less clear. However, in mice the effect of maternal protein restriction during pregnancy on offspring WAT was assessed (80). Insulin sensitivity of the adult male offspring was improved and adiposity reduced, and those improvements in metabolic outcome were accompanied by an increased expression of markers for mitochondrial biogenesis and mitochondrial density in WAT, suggesting an improved WAT oxidative capacity (80). Mitochondrial function was also assessed in mesenchymal stem cells, progenitor cells of adipocytes, collected from children born to mothers with gestational diabetes (81). The mesenchymal stem cells showed a reduced adipogenic differentiation potential and display a reduced mitochondrial oxidative capacity. Together, this may indicate that indeed prenatal conditions can alter offspring mitochondrial function in WAT. However, the effect of the postnatal diet on mitochondrial function in WAT later in life remains to be elucidated.

The liver and metabolic health

When WAT function is impaired and WAT insulin sensitivity is reduced, WAT releases free fatty acids both in the fasted and postprandial state and postprandial WAT glucose uptake is reduced. The subsequent increased free fatty acid and glucose levels in the blood induces hepatic lipid storage and increased blood insulin levels. In a healthy liver, insulin reduces postprandial glucose release and *de novo* lipogenesis from carbohydrates. However, in case of high hepatic lipid storage, hepatic insulin resistance is induced, the postprandial suppression of glucose release is blunted and *de novo* lipogenesis remains elevated, together inducing NAFLD and T2D (82). Mitochondrial functionality is essential for the regulation of the hepatic lipid metabolism, but excessive lipid accumulation can impair hepatic mitochondrial function, as shown in a mice model for obesity (83). Indeed, hepatic mitochondrial function was altered in T2D and NAFLD, suggested to be affected by excessive lipid storage in the liver (84, 85). In particular, hepatic accumulation of intermediates of triglyceride synthesis, like diacylglycerols, and changes in specific phospholipid species, like ceramides, are associated with adverse metabolic consequences (86, 87). Those lipid species interfere with the insulin signaling pathway and, in this way, mediate lipid-induced insulin resistance (88).

The development of the liver starts early in pregnancy (Figure 1). In humans, a rudiment of the liver appears from week 3 of pregnancy and development continues throughout pregnancy (89). At birth, there is a major change in the venous circulation of the liver resulting from the ligation of the umbilical vein, which supplied oxygenated blood to the liver during pregnancy. The change in blood flow i.e., from the umbilical vein to the portal vein, temporary reduces growth of the left side of the liver and changes the liver vascular territories i.e., liver segments supplied via different branches of the portal vein (89). Postnatally, the hepatocytes maturate and the metabolic functions of different hepatic regions are defined, the so-called metabolic zonation develops (90). In mice, development of the liver starts at day 9 of pregnancy (Figure 1). Single cell transcriptomics analyses in mice showed that functional changes in hepatocytes continue until postnatal day 56, which may indicate that the liver may be susceptible to metabolic programming in postnatal life (91).

Prenatal under- as well as overnutrition can increase hepatic lipid storage leading to NAFLD and insulin resistance (22, 92). Hepatic insulin resistance and mitochondrial dysfunction in the liver are suggested to contribute to long-term consequences of prenatal adverse conditions (93). Indeed, reduced mitochondrial oxygen consumption at weaning preceded adult hyperglycemia in intra-uterine growth restricted rats and reduced OXPHOS enzyme activity in livers of offspring exposed to maternal overfeeding

preceded adult whole body insulin resistance and NAFLD (22, 75). Also, expression of insulin receptors and other regulators of the insulin signaling pathway were reduced in livers of offspring exposed to maternal under- or overnutrition (92, 94). The postnatal diet can also change hepatic function, as shown by increased hepatic lipid storage and changes in hepatic lipid and oxidative stress metabolism in mice overfed during lactation (95). Moreover, changes in nutrient composition in the postnatal diet i.e., replacing glucose partly with galactose, reduced hepatic lipid accumulation and expression of inflammatory pathways in the liver (96). Together, the role of the liver in the programming of adult metabolic health is evident. However, the specific role and possible contribution of hepatic mitochondria in postnatal programming is less clear.

Postnatal programming impact of dietary lipid droplet structure

Although the susceptible processes and associated underlying mechanisms are not fully elucidated, adult metabolic health can clearly be programmed by the perinatal diet (16, 18-21). Moreover, as mentioned above, there are several examples of programming of adult metabolic health by the postnatal diet (33, 34, 36, 96). However, research on the programming of WAT health and mitochondrial function in WAT and liver by nutrition in the early postnatal period is still scarce.

Observational studies showed that breastfeeding and duration of breastfeeding were associated with reduced overweight, obesity and T2D risk in children and adolescents (29, 30). Causes for the development of (childhood) overweight and metabolic diseases are multifactorial (97). The beneficial effects of breastfeeding may partly be explained by differences in demographics or lifestyle factors compared to formula fed infants (98) or specific composition of human milk. As such, the distinct differences in features of the lipid droplets between human milk and infant milk formula (IMF) may also play a role (**Figure 3A and B**). The human milk lipid droplet has a mode diameter of ~4 µm and is enveloped by a native membrane (99). The milk fat globule membrane (MFGM) has similarities to the cell membrane and contains phospholipids, cholesterol, glycolipids and membrane proteins. But instead of a bilayer of phospholipids as is present in the cell membrane, the MFGM has a trilayer of phospholipids. The inner phospholipid layer originating from the endoplasmic reticulum where the lipid droplet is formed, and a bilayer envelops this lipid droplet during the extrusion process (100). Lipid droplets in IMF have an average mode diameter of 0.4 µm, a core of vegetable oil and/or milk fat, and no MFGM surrounding the lipid core (99). Thus, in addition to other differences, the human milk lipid droplet is 10 times larger compared to the lipid droplet in IMF, and

has a lipid trilayer which is absent in the IMF droplet. Differences in the supramolecular structure of the dietary lipid droplets impact the postprandial kinetics in adult humans as shown by the faster lipid digestion and delayed gastric emptying upon feeding of small *vs.* large lipid droplets (101, 102).

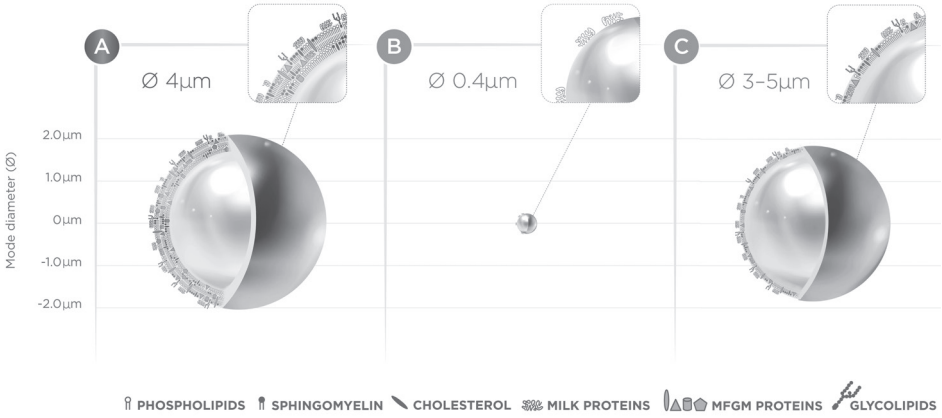

Figure 3: Schematic representation of the lipid droplets in **A**) human milk with the tri-layer MFGM, **B**) standard infant milk formula with proteins at the droplets interface and **C**) the Concept with MFGM fragments at the droplet interface. Mean mode diameter and a visual representation of the surface structure are indicated in the figure. Reprinted with permission (108).

We hypothesized that differences in the supramolecular structure of the dietary lipid droplet in early postnatal life may program adult metabolic health. To mimic some of the structural properties of human milk, an IMF with large (3-5 µm), (milk)phospholipid coated lipid droplets was developed (Nuturis®, **Figure 3C**) (103).

To create this Concept IMF (containing the Nuturis concept, alias complex lipid matrix, further referred to as "Concept"), bovine-derived MFGM fragments were added during the adapted production process, with as a result in large fat droplets coated by the added phospholipids (103). Feeding the Concept to young healthy males resulted in differences in postprandial kinetics compared to feeding a control IMF (104). In line with our programming hypothesis, studies in mice showed that feeding a diet containing Concept in early postnatal life (postnatal day 16 until day 42) followed by an adult Western style diet challenge, reduced adult adiposity and plasma insulin and glucose levels (105-107). The mice fed the Concept had smaller adipocytes in adulthood and showed reduced WAT mRNA expression of markers for adipocyte differentiation, lipogenesis and adipose tissue expansion i.e., *Ppary*, RxRα, *Leptin* and *Mest/Peg1*, indicating that the Concept changed lipid handling in the WAT (107). Together, this indicates that indeed mimicking the structure

of the human milk lipid droplets has the potential to program adult metabolic health. More research is needed to understand the underlying processes. We hypothesized that programming of WAT health and mitochondrial function may explain the reduced adiposity and improved metabolic health in adult mice fed the Concept postnatally, which was further investigated in this thesis.

Aim and outline of the thesis

Obesity and associated metabolic health problems are a major world-wide health issue and preventive strategies are needed. Providing adequate nutrition to optimally support growth and development in early life is considered to potentially be a substantial contributor to preventive strategies. Although early life programming of adult metabolic health i.e., nutritional programming, is acknowledged for years, most research to date focused on the effect of prenatal conditions and thus on the adverse consequences of maternal diet and health on offspring's metabolic health. An evidence base exists for the potential postnatal programming by early life nutrition for later life metabolic health, however the processes underlying are often not well understood, which hampers effective translation and implementation. Therefore, I here **aim to investigate the processes underlying the postnatal dietary programming of adult metabolic health in a mouse model for nutritional programming**. More specifically, the effect of a postnatal diet containing large, (milk)phospholipid coated lipid droplets on WAT health and mitochondrial function in the liver was investigated, as well as potential predictors thereof.

The sub-aims of this thesis are 1) to investigate if the previous observed effects of the Concept on adiposity can be explained by (programmed) changes in mitochondrial function (markers) in WAT and liver; **2)** to investigate the developmental trajectory of different WAT depots to gain insight in the potential window of opportunity for programming of WAT health; and **3)** to explore underlying processes for the observed programming of adult metabolic health.

Chapter 2 addresses sub-aim 1 and investigated the impact of a postnatal diet containing large, (milk)phospholipid coated lipid droplets on mitochondrial density and oxidative capacity markers in WAT in adulthood, in a mouse model for nutritional programming (**Figure 4A**). We hypothesized that programming of mitochondrial function in WAT may underlie previously observed reductions in adult adiposity in mice fed Concept in early postnatal life.

Chapter 3 addresses sub-aim 2 and investigated the developmental trajectory of different WAT depots in a mouse model for nutritional programming (**Figure 4B**). With

this, we aimed to substantiate and extend current knowledge on the depot specific development of WAT in early life and thus obtain a better understanding of the potential window for programming of WAT health.

Chapter 4 addresses sub-aim 1 and 3 and investigated the effect of a postnatal diet containing large, (milk)phospholipid coated lipid droplets on mitochondrial function markers in early life and underlying processes in a mouse model for nutritional programming (**Figure 4C**). We hypothesized that the Concept changed WAT mitochondrial density and oxidative capacity markers in early life and that those changes were programmed via epigenetic mechanisms.

Chapter 5 addresses sub-aim 1 and investigated the effect of the Concept diet on hepatic lipid metabolism and mitochondrial oxidative capacity in a mouse model for nutritional programming (**Figure 4D and E**). We hypothesized that the postnatal diet could improve later life mitochondrial function in the liver and in this way improve metabolic health.

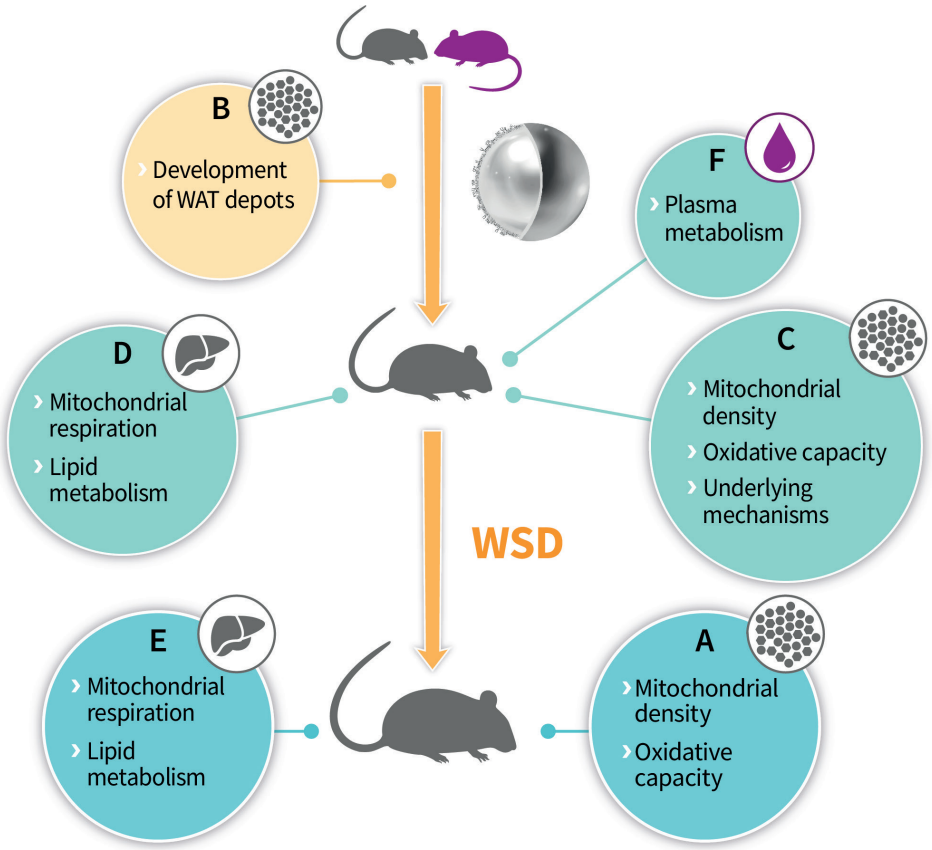

Figure 4: Graphic overview of the investigated aspects.

Chapter 6 addresses sub-aim 3 and investigated the effect of the Concept on serum metabolomics in early life and its correlation to later life metabolic health outcomes in intra-uterine growth restricted rat offspring (**Figure 4F**). We hypothesized that early life serum metabolomics may predict adult metabolic health.

Chapter 7 discusses the answers to the research questions and the overall conclusions. Further, I discuss the relevance of the research and proposals for follow up.

References:

1. Collaboration NCDRF. Worldwide trends in body-mass index, underweight, overweight, and obesity from 1975 to 2016: a pooled analysis of 2416 population-based measurement studies in 128.9 million children, adolescents, and adults. Lancet. 2017;390(10113):2627-42.
2. Conway B, Rene A. Obesity as a disease: no lightweight matter. Obes Rev. 2004;5(3):145-51.
3. Steele M, Finucane FM. Philosophically, is obesity really a disease? Obes Rev. 2023;24(8):e13590.
4. Reilly JJ, Kelly J. Long-term impact of overweight and obesity in childhood and adolescence on morbidity and premature mortality in adulthood: systematic review. Int J Obes (Lond). 2011;35(7):891-8.
5. Barker DJ, Winter PD, Osmond C, Margetts B, Simmonds SJ. Weight in infancy and death from ischaemic heart disease. Lancet. 1989;2(8663):577-80.
6. Mi D, Fang H, Zhao Y, Zhong L. Birth weight and type 2 diabetes: A meta-analysis. Exp Ther Med. 2017;14(6):5313-20.
7. Meas T, Deghmoun S, Armoogum P, Alberti C, Levy-Marchal C. Consequences of being born small for gestational age on body composition: an 8-year follow-up study. J Clin Endocrinol Metab. 2008;93(10):3804-9.
8. Martin-Calvo N, Goni L, Tur JA, Martinez JA. Low birth weight and small for gestational age are associated with complications of childhood and adolescence obesity: Systematic review and meta-analysis. Obes Rev. 2022;23 Suppl 1:e13380.
9. Harder T, Rodekamp E, Schellong K, Dudenhausen JW, Plagemann A. Birth weight and subsequent risk of type 2 diabetes: a meta-analysis. Am J Epidemiol. 2007;165(8):849-57.
10. Huxley RR, Shiell AW, Law CM. The role of size at birth and postnatal catch-up growth in determining systolic blood pressure: a systematic review of the literature. J Hypertens. 2000;18(7):815-31.
11. Milovanovic I, Njuieyon F, Deghmoun S, Chevenne D, Levy-Marchal C, Beltrand J. SGA children with moderate catch-up growth are showing the impaired insulin secretion at the age of 4. PLoS One. 2014;9(6):e100337.
12. Derraik JGB, Maessen SE, Gibbins JD, Cutfield WS, Lundgren M, Ahlsson F. Large-for-gestational-age phenotypes and obesity risk in adulthood: a study of 195,936 women. Scientific reports. 2020;10(1):2157.
13. Roseboom TJ, van der Meulen JH, Osmond C, Barker DJ, Ravelli AC, Schroeder-Tanka JM, et al. Coronary heart disease after prenatal exposure to the Dutch famine, 1944-45. Heart. 2000;84(6):595-8.
14. Ravelli AC, van der Meulen JH, Michels RP, Osmond C, Barker DJ, Hales CN, et al. Glucose tolerance in adults after prenatal exposure to famine. Lancet. 1998;351(9097):173-7.
15. Ravelli AC, van Der Meulen JH, Osmond C, Barker DJ, Bleker OP. Obesity at the age of 50 y in men and women exposed to famine prenatally. Am J Clin Nutr. 1999;70(5):811-6.
16. Jones AP, Simson EL, Friedman MI. Gestational undernutrition and the development of obesity in rats. J Nutr. 1984;114(8):1484-92.
17. Thompson N, Huber K, Bedurftig M, Hansen K, Miles-Chan J, Breier BH. Metabolic programming of adipose tissue structure and function in male rat offspring by prenatal undernutrition. Nutr Metab (Lond). 2014;11(1):50.
18. Ford SP, Hess BW, Schwope MM, Nijland MJ, Gilbert JS, Vonnahme KA, et al. Maternal undernutrition during early to mid-gestation in the ewe results in altered growth, adiposity, and glucose tolerance in male offspring. J Anim Sci. 2007;85(5):1285-94.
19. Gardner DS, Tingey K, Van Bon BW, Ozanne SE, Wilson V, Dandrea J, et al. Programming of glucose-insulin metabolism in adult sheep after maternal undernutrition. Am J Physiol Regul Integr Comp Physiol. 2005;289(4):R947-54.

20. Desclee de Maredsous C, Oozeer R, Barbillon P, Mary-Huard T, Delteil C, Blachier F, et al. High-Protein Exposure during Gestation or Lactation or after Weaning Has a Period-Specific Signature on Rat Pup Weight, Adiposity, Food Intake, and Glucose Homeostasis up to 6 Weeks of Age. J Nutr. 2016;146(1):21-9.
21. Blackmore HL, Niu Y, Fernandez-Twinn DS, Tarry-Adkins JL, Giussani DA, Ozanne SE. Maternal diet-induced obesity programs cardiovascular dysfunction in adult male mouse offspring independent of current body weight. Endocrinology. 2014;155(10):3970-80.
22. Bruce KD, Cagampang FR, Argenton M, Zhang J, Ethirajan PL, Burdge GC, et al. Maternal high-fat feeding primes steatohepatitis in adult mice offspring, involving mitochondrial dysfunction and altered lipogenesis gene expression. Hepatology. 2009;50(6):1796-808.
23. Oben JA, Mouralidarane A, Samuelsson AM, Matthews PJ, Morgan ML, McKee C, et al. Maternal obesity during pregnancy and lactation programs the development of offspring non-alcoholic fatty liver disease in mice. J Hepatol. 2010;52(6):913-20.
24. Barker DJ. The fetal and infant origins of adult disease. BMJ. 1990;301(6761):1111.
25. Hales CN, Barker DJ. Type 2 (non-insulin-dependent) diabetes mellitus: the thrifty phenotype hypothesis. Diabetologia. 1992;35(7):595-601.
26. Lucas A. Role of nutritional programming in determining adult morbidity. Arch Dis Child. 1994;71(4):288-90.
27. Jimenez-Chillaron JC, Hernandez-Valencia M, Lightner A, Faucette RR, Reamer C, Przybyla R, et al. Reductions in caloric intake and early postnatal growth prevent glucose intolerance and obesity associated with low birthweight. Diabetologia. 2006;49(8):1974-84.
28. Turdi S, Ge W, Hu N, Bradley KM, Wang X, Ren J. Interaction between maternal and postnatal high fat diet leads to a greater risk of myocardial dysfunction in offspring via enhanced lipotoxicity, IRS-1 serine phosphorylation and mitochondrial defects. Journal of molecular and cellular cardiology. 2013;55:117-29.
29. Harder T, Bergmann R, Kallischnigg G, Plagemann A. Duration of breastfeeding and risk of overweight: a meta-analysis. Am J Epidemiol. 2005;162(5):397-403.
30. Owen CG, Martin RM, Whincup PH, Smith GD, Cook DG. Does breastfeeding influence risk of type 2 diabetes in later life? A quantitative analysis of published evidence. Am J Clin Nutr. 2006;84(5):1043-54.
31. Dewey KG. Is breastfeeding protective against child obesity? J Hum Lact. 2003;19(1):9-18.
32. Gillman MW, Rifas-Shiman SL, Camargo CA, Jr., Berkey CS, Frazier AL, Rockett HR, et al. Risk of overweight among adolescents who were breastfed as infants. JAMA. 2001;285(19):2461-7.
33. Oosting A, Kegler D, Boehm G, Jansen HT, van de Heijning BJ, van der Beek EM. N-3 long-chain polyunsaturated fatty acids prevent excessive fat deposition in adulthood in a mouse model of postnatal nutritional programming. Pediatr Res. 2010;68(6):494-9.
34. van de Heijning BJM, Oosting A, Kegler D, van der Beek EM. An Increased Dietary Supply of Medium-Chain Fatty Acids during Early Weaning in Rodents Prevents Excessive Fat Accumulation in Adulthood. Nutrients. 2017;9(6).
35. Wielinga PY, Harthoorn LF, Verschuren L, Schoemaker MH, Jouni ZE, van Tol EA, et al. Arachidonic acid/docosahexaenoic acid-supplemented diet in early life reduces body weight gain, plasma lipids, and adiposity in later life in ApoE*3Leiden mice. Molecular nutrition & food research. 2012;56(7):1081-9.
36. Oosting A, Kegler D, van de Heijning BJ, Verkade HJ, van der Beek EM. Reduced linoleic acid intake in early postnatal life improves metabolic outcomes in adult rodents following a Western-style diet challenge. Nutr Res. 2015;35(9):800-11.
37. Fernandez-Calleja JMS, Bouwman LMS, Swarts HJM, Oosting A, Keijer J, van Schothorst EM. Direct and Long-Term Metabolic Consequences of Lowly vs. Highly-Digestible Starch in the Early Post-Weaning Diet of Mice. Nutrients. 2018;10(11).

38. Bouwman LMS, Fernandez-Calleja JMS, van der Stelt I, Oosting A, Keijer J, van Schothorst EM. Replacing Part of Glucose with Galactose in the Postweaning Diet Protects Female But Not Male Mice from High-Fat Diet-Induced Adiposity in Later Life. J Nutr. 2019;149(7):1140-8.
39. Spalding KL, Arner E, Westermark PO, Bernard S, Buchholz BA, Bergmann O, et al. Dynamics of fat cell turnover in humans. Nature. 2008;453(7196):783-7.
40. Mostyn A, Symonds ME. Early programming of adipose tissue function: a large-animal perspective. Proc Nutr Soc. 2009;68(4):393-400.
41. Jorgensen W, Gam C, Andersen JL, Schjerling P, Scheibye-Knudsen M, Mortensen OH, et al. Changed mitochondrial function by pre- and/or postpartum diet alterations in sheep. Am J Physiol Endocrinol Metab. 2009;297(6):E1349-57.
42. Yang YK, Chen M, Clements RH, Abrams GA, Aprahamian CJ, Harmon CM. Human mesenteric adipose tissue plays unique role versus subcutaneous and omental fat in obesity related diabetes. Cellular physiology and biochemistry : international journal of experimental cellular physiology, biochemistry, and pharmacology. 2008;22(5-6):531-8.
43. Bjorndal B, Burri L, Staalesen V, Skorve J, Berge RK. Different adipose depots: their role in the development of metabolic syndrome and mitochondrial response to hypolipidemic agents. J Obes. 2011;2011:490650.
44. Pouliot MC, Despres JP, Nadeau A, Moorjani S, Prud'Homme D, Lupien PJ, et al. Visceral obesity in men. Associations with glucose tolerance, plasma insulin, and lipoprotein levels. Diabetes. 1992;41(7):826-34.
45. Ross R, Aru J, Freeman J, Hudson R, Janssen I. Abdominal adiposity and insulin resistance in obese men. Am J Physiol Endocrinol Metab. 2002;282(3):E657-63.
46. Schottl T, Kappler L, Braun K, Fromme T, Klingenspor M. Limited mitochondrial capacity of visceral versus subcutaneous white adipocytes in male C57BL/6N mice. Endocrinology. 2015;156(3):923-33.
47. Gastaldelli A, Gaggini M, DeFronzo RA. Role of Adipose Tissue Insulin Resistance in the Natural History of Type 2 Diabetes: Results From the San Antonio Metabolism Study. Diabetes. 2017;66(4):815-22.
48. Eriksson-Hogling D, Andersson DP, Backdahl J, Hoffstedt J, Rossner S, Thorell A, et al. Adipose tissue morphology predicts improved insulin sensitivity following moderate or pronounced weight loss. Int J Obes (Lond). 2015;39(6):893-8.
49. Hammarstedt A, Graham TE, Kahn BB. Adipose tissue dysregulation and reduced insulin sensitivity in non-obese individuals with enlarged abdominal adipose cells. Diabetol Metab Syndr. 2012;4(1):42.
50. Poissonnet CM, LaVelle M, Burdi AR. Growth and development of adipose tissue. J Pediatr. 1988;113(1 Pt 1):1-9.
51. Poissonnet CM, Burdi AR, Garn SM. The chronology of adipose tissue appearance and distribution in the human fetus. Early Hum Dev. 1984;10(1-2):1-11.
52. de Fluiter KS, van Beijsterveldt I, Goedegebuure WJ, Breij LM, Spaans AMJ, Acton D, et al. Longitudinal body composition assessment in healthy term-born infants until 2 years of age using ADP and DXA with vacuum cushion. Eur J Clin Nutr. 2020;74(4):642-50.
53. Birsoy K, Berry R, Wang T, Ceyhan O, Tavazoie S, Friedman JM, et al. Analysis of gene networks in white adipose tissue development reveals a role for ETS2 in adipogenesis. Development. 2011;138(21):4709-19.
54. Wang QA, Tao C, Gupta RK, Scherer PE. Tracking adipogenesis during white adipose tissue development, expansion and regeneration. Nat Med. 2013;19(10):1338-44.
55. DiGirolamo M, Fine JB, Tagra K, Rossmanith R. Qualitative regional differences in adipose tissue growth and cellularity in male Wistar rats fed ad libitum. Am J Physiol. 1998;274(5 Pt 2):R1460-7.

56. Xue B, Rim JS, Hogan JC, Coulter AA, Koza RA, Kozak LP. Genetic variability affects the development of brown adipocytes in white fat but not in interscapular brown fat. J Lipid Res. 2007;48(1):41-51.
57. Lasar D, Julius A, Fromme T, Klingenspor M. Browning attenuates murine white adipose tissue expansion during postnatal development. Biochim Biophys Acta. 2013;1831(5):960-8.
58. Symonds ME. Adipose tissue development during early life: novel insights into energy balance from small and large mammals. Proceedings of the Nutritional Society. 2012;0:1-8.
59. Basse AL, Dixen K, Yadav R, Tygesen MP, Qvortrup K, Kristiansen K, et al. Global gene expression profiling of brown to white adipose tissue transformation in sheep reveals novel transcriptional components linked to adipose remodeling. BMC Genomics. 2015;16(1):215.
60. Palou M, Konieczna J, Torrens JM, Sanchez J, Priego T, Fernandes ML, et al. Impaired insulin and leptin sensitivity in the offspring of moderate caloric-restricted dams during gestation is early programmed. The Journal of nutritional biochemistry. 2012;23(12):1627-39.
61. Samuelsson AM, Matthews PA, Argenton M, Christie MR, McConnell JM, Jansen EH, et al. Diet-induced obesity in female mice leads to offspring hyperphagia, adiposity, hypertension, and insulin resistance: a novel murine model of developmental programming. Hypertension. 2008;51(2):383-92.
62. Lecoutre S, Deracinois B, Laborie C, Eberle D, Guinez C, Panchenko PE, et al. Depot- and sex-specific effects of maternal obesity in offspring's adipose tissue. J Endocrinol. 2016;230(1):39-53.
63. Alfaradhi MZ, Kusinski LC, Fernandez-Twinn DS, Pantaleao LC, Carr SK, Ferland-McCollough D, et al. Maternal Obesity in Pregnancy Developmentally Programs Adipose Tissue Inflammation in Young, Lean Male Mice Offspring. Endocrinology. 2016;157(11):4246-56.
64. Kayser BD, Goran MI, Bouret SG. Perinatal overnutrition exacerbates adipose tissue inflammation caused by high-fat feeding in C57BL/6J mice. PLoS One. 2015;10(3):e0121954.
65. Dias I, Salviano I, Mencalha A, de Carvalho SN, Thole AA, Carvalho L, et al. Neonatal overfeeding impairs differentiation potential of mice subcutaneous adipose mesenchymal stem cells. Stem Cell Rev Rep. 2018;14(4):535-45.
66. Heilbronn L, Smith SR, Ravussin E. Failure of fat cell proliferation, mitochondrial function and fat oxidation results in ectopic fat storage, insulin resistance and type II diabetes mellitus. Int J Obes Relat Metab Disord. 2004;28 Suppl 4:S12-21.
67. Wilson-Fritch L, Nicoloro S, Chouinard M, Lazar MA, Chui PC, Leszyk J, et al. Mitochondrial remodeling in adipose tissue associated with obesity and treatment with rosiglitazone. J Clin Invest. 2004;114(9):1281-9.
68. Schottl T, Kappler L, Fromme T, Klingenspor M. Limited OXPHOS capacity in white adipocytes is a hallmark of obesity in laboratory mice irrespective of the glucose tolerance status. Mol Metab. 2015;4(9):631-42.
69. Fischer B, Schottl T, Schempp C, Fromme T, Hauner H, Klingenspor M, et al. Inverse relationship between body mass index and mitochondrial oxidative phosphorylation capacity in human subcutaneous adipocytes. Am J Physiol Endocrinol Metab. 2015;309(4):E380-7.
70. Choo HJ, Kim JH, Kwon OB, Lee CS, Mun JY, Han SS, et al. Mitochondria are impaired in the adipocytes of type 2 diabetic mice. Diabetologia. 2006;49(4):784-91.
71. Schrauwen P, Schrauwen-Hinderling V, Hoeks J, Hesselink MK. Mitochondrial dysfunction and lipotoxicity. Biochim Biophys Acta. 2010;1801(3):266-71.
72. Szendroedi J, Chmelik M, Schmid AI, Nowotny P, Brehm A, Krssak M, et al. Abnormal hepatic energy homeostasis in type 2 diabetes. Hepatology. 2009;50(4):1079-86.
73. Simmons RA, Suponitsky-Kroyter I, Selak MA. Progressive accumulation of mitochondrial DNA mutations and decline in mitochondrial function lead to beta-cell failure. J Biol Chem. 2005;280(31):28785-91.

74. Selak MA, Storey BT, Peterside I, Simmons RA. Impaired oxidative phosphorylation in skeletal muscle of intrauterine growth-retarded rats. Am J Physiol Endocrinol Metab. 2003;285(1):E130-7.
75. Peterside IE, Selak MA, Simmons RA. Impaired oxidative phosphorylation in hepatic mitochondria in growth-retarded rats. Am J Physiol Endocrinol Metab. 2003;285(6):E1258-66.
76. Park HK, Jin CJ, Cho YM, Park DJ, Shin CS, Park KS, et al. Changes of mitochondrial DNA content in the male offspring of protein-malnourished rats. Ann N Y Acad Sci. 2004;1011:205-16.
77. Park KS, Kim SK, Kim MS, Cho EY, Lee JH, Lee KU, et al. Fetal and early postnatal protein malnutrition cause long-term changes in rat liver and muscle mitochondria. J Nutr. 2003;133(10):3085-90.
78. Pileggi CA, Hedges CP, Segovia SA, Markworth JF, Durainayagam BR, Gray C, et al. Maternal High Fat Diet Alters Skeletal Muscle Mitochondrial Catalytic Activity in Adult Male Rat Offspring. Front Physiol. 2016;7:546.
79. Borengasser SJ, Faske J, Kang P, Blackburn ML, Badger TM, Shankar K. In utero exposure to prepregnancy maternal obesity and postweaning high-fat diet impair regulators of mitochondrial dynamics in rat placenta and offspring. Physiol Genomics. 2014;46(23):841-50.
80. Jousse C, Muranishi Y, Parry L, Montaurier C, Even P, Launay JM, et al. Perinatal protein malnutrition affects mitochondrial function in adult and results in a resistance to high fat diet-induced obesity. PLoS One. 2014;9(8):e104896.
81. Kim J, Piao Y, Pak YK, Chung D, Han YM, Hong JS, et al. Umbilical cord mesenchymal stromal cells affected by gestational diabetes mellitus display premature aging and mitochondrial dysfunction. Stem Cells Dev. 2015;24(5):575-86.
82. Azzu V, Vacca M, Virtue S, Allison M, Vidal-Puig A. Adipose tissue-liver cross talk in the control of whole-body metabolism: implications in non-alcoholic fatty liver disease. Gastroenterology. 2020.
83. Arruda AP, Pers BM, Parlakgul G, Guney E, Inouye K, Hotamisligil GS. Chronic enrichment of hepatic endoplasmic reticulum-mitochondria contact leads to mitochondrial dysfunction in obesity. Nat Med. 2014;20(12):1427-35.
84. Koliaki C, Szendroedi J, Kaul K, Jelenik T, Nowotny P, Jankowiak F, et al. Adaptation of hepatic mitochondrial function in humans with non-alcoholic fatty liver is lost in steatohepatitis. Cell Metab. 2015;21(5):739-46.
85. Schmid AI, Szendroedi J, Chmelik M, Krssak M, Moser E, Roden M. Liver ATP synthesis is lower and relates to insulin sensitivity in patients with type 2 diabetes. Diabetes Care. 2011;34(2):448-53.
86. Puri P, Baillie RA, Wiest MM, Mirshahi F, Choudhury J, Cheung O, et al. A lipidomic analysis of nonalcoholic fatty liver disease. Hepatology. 2007;46(4):1081-90.
87. Gorden DL, Ivanova PT, Myers DS, McIntyre JO, VanSaun MN, Wright JK, et al. Increased diacylglycerols characterize hepatic lipid changes in progression of human nonalcoholic fatty liver disease; comparison to a murine model. PLoS One. 2011;6(8):e22775.
88. Roden M, Shulman GI. The integrative biology of type 2 diabetes. Nature. 2019;576(7785):51-60.
89. Champetier J, Yver R, Tomasella T. Functional anatomy of the liver of the human fetus: applications to ultrasonography. Surg Radiol Anat. 1989;11(1):53-62.
90. Lemaigre FP. Mechanisms of liver development: concepts for understanding liver disorders and design of novel therapies. Gastroenterology. 2009;137(1):62-79.
91. Liang Y, Kaneko K, Xin B, Lee J, Sun X, Zhang K, et al. Temporal analyses of postnatal liver development and maturation by single-cell transcriptomics. Developmental cell. 2022;57(3):398-414 e5.

92. Ashino NG, Saito KN, Souza FD, Nakutz FS, Roman EA, Velloso LA, et al. Maternal high-fat feeding through pregnancy and lactation predisposes mouse offspring to molecular insulin resistance and fatty liver. The Journal of nutritional biochemistry. 2012;23(4):341-8.
93. Baker PR, 2nd, Friedman JE. Mitochondrial role in the neonatal predisposition to developing nonalcoholic fatty liver disease. J Clin Invest. 2018;128(9):3692-703.
94. Carlin G, Chaumontet C, Blachier F, Barbillon P, Darcel N, Blais A, et al. Maternal High-Protein Diet during Pregnancy Modifies Rat Offspring Body Weight and Insulin Signalling but Not Macronutrient Preference in Adulthood. Nutrients. 2019;11(1).
95. Conceicao EP, Moura EG, Carvalho JC, Oliveira E, Lisboa PC. Early redox imbalance is associated with liver dysfunction at weaning in overfed rats. J Physiol. 2015;593(21):4799-811.
96. Bouwman LMS, Swarts HJM, Fernandez-Calleja JMS, van der Stelt I, Schols H, Oosting A, et al. Partial replacement of glucose by galactose in the post-weaning diet improves parameters of hepatic health. The Journal of nutritional biochemistry. 2019;73:108223.
97. Verduci E, Bronsky J, Embleton N, Gerasimidis K, Indrio F, Koglmeier J, et al. Role of Dietary Factors, Food Habits, and Lifestyle in Childhood Obesity Development: A Position Paper From the European Society for Paediatric Gastroenterology, Hepatology and Nutrition Committee on Nutrition. Journal of pediatric gastroenterology and nutrition. 2021;72(5):769-83.
98. Dieterich CM, Felice JP, O'Sullivan E, Rasmussen KM. Breastfeeding and health outcomes for the mother-infant dyad. Pediatr Clin North Am. 2013;60(1):31-48.
99. Michalski MC, Briard V, Michel F, Tasson F, Poulain P. Size distribution of fat globules in human colostrum, breast milk, and infant formula. J Dairy Sci. 2005;88(6):1927-40.
100. Lopez C, Menard O. Human milk fat globules: polar lipid composition and in situ structural investigations revealing the heterogeneous distribution of proteins and the lateral segregation of sphingomyelin in the biological membrane. Colloids and surfaces B, Biointerfaces. 2011;83(1):29-41.
101. Armand M, Pasquier B, Andre M, Borel P, Senft M, Peyrot J, et al. Digestion and absorption of 2 fat emulsions with different droplet sizes in the human digestive tract. Am J Clin Nutr. 1999;70(6):1096-106.
102. Maljaars PW, van der Wal RJ, Wiersma T, Peters HP, Haddeman E, Masclee AA. The effect of lipid droplet size on satiety and peptide secretion is intestinal site-specific. Clin Nutr. 2012;31(4):535-42.
103. Gallier S, Vocking K, Post JA, Van De Heijning B, Acton D, Van Der Beek EM, et al. A novel infant milk formula concept: Mimicking the human milk fat globule structure. Colloids and surfaces B, Biointerfaces. 2015;136:329-39.
104. Baumgartner S, van de Heijning BJM, Acton D, Mensink RP. Infant milk fat droplet size and coating affect postprandial responses in healthy adult men: a proof-of-concept study. Eur J Clin Nutr. 2017;71(9):1108-13.
105. Oosting A, Kegler D, Wopereis HJ, Teller IC, van de Heijning BJ, Verkade HJ, et al. Size and phospholipid coating of lipid droplets in the diet of young mice modify body fat accumulation in adulthood. Pediatr Res. 2012;72(4):362-9.
106. Oosting A, van Vlies N, Kegler D, Schipper L, Abrahamse-Berkeveld M, Ringler S, et al. Effect of dietary lipid structure in early postnatal life on mouse adipose tissue development and function in adulthood. Br J Nutr. 2014;111(2):215-26.
107. Baars A, Oosting A, Engels E, Kegler D, Kodde A, Schipper L, et al. Milk fat globule membrane coating of large lipid droplets in the diet of young mice prevents body fat accumulation in adulthood. Br J Nutr. 2016;115(11):1930-7.
108. Oosting A, Harvey L, Ringler S, van Dijk G, Schipper L. Beyond ingredients: Supramolecular structure of lipid droplets in infant formula affects metabolic and brain function in mouse models. PLoS One. 2023;18(8):e0282816.

[1] Early Life Nutrition Division , Nutricia Research, P.O. Box 801413508 TC Utrecht, The Netherlands;
[2] Department of Pediatrics, University Medical Centre Groningen, Groningen, The Netherlands;
[3] Department of Human Biology, Maastricht University, Maastricht, The Netherlands.

Chapter 2

Supramolecular structure of dietary fat in early life modulates expression of markers for mitochondrial content and capacity in adipose tissue of adult mice

Andrea Kodde[1], Eline M. van der Beek[1,2], Esther Phielix[3], Eefje Engels[1], Lidewij Schipper[1] and Annemarie Oosting[1]

Nutrition & Metabolism, 2017: 14(37)
DOI: 10.1186/s12986-017-0191-5

Abstract

Background: Previous studies have shown that early life nutrition can modulate the development of white adipose tissue and thereby affect the risk on obesity and metabolic disease later in life. For instance, postnatal feeding with a concept infant milk formula with large, phospholipid coated lipid droplets (Concept, Nuturis®), resulted in reduced adiposity in adult mice. The present study investigated whether differences in cell energy metabolism, using markers of mitochondrial content and capacity, may contribute to the observed effects.

Methods: C57BL/6j male mice were exposed to a rodent diet containing the Concept (Concept) or standard (CTRL) infant milk formula from postnatal day 16 until postnatal day 42, followed by a western style diet challenge until postnatal day 98. Markers for mitochondrial content and capacity were analyzed in retroperitoneal white adipose tissue and gene expression of metabolic markers was measured in both retroperitoneal white adipose tissue and muscle tibialis (M. tibialis) at postnatal day 98.

Results: In retroperitoneal white adipose tissue, the Concept group showed higher citrate synthase activity and mitochondrial DNA expression compared to the CTRL group ($p<0.05$). In addition, protein expression of mitochondrial cytochrome c oxidase subunit I of the oxidative phosphorylation pathway/cascade was increased in the Concept group compared to CTRL ($p<0.05$). In the *M. tibialis*, gene expression of uncoupling protein 3 was higher in the Concept compared to the CTRL group. Other gene and protein expression markers for mitochondrial oxidative capacity were not different between groups.

Conclusion: Postnatal feeding with large, phospholipid coated lipid droplets generating a different supramolecular structure of dietary lipids enhances adult gene and protein expression of specific mitochondrial oxidative capacity markers, indicative of increased substrate oxidation in white adipose tissue and skeletal muscle. Although functional mitochondrial capacity was not measured, these results may suggest that adaptations in mitochondrial function via early feeding with a more physiological structure of dietary lipids, could underlie the observed beneficial effects on later life adiposity.

Keywords: Postnatal programming, White adipose tissue, Mitochondrial content, Oxidative capacity, Lipid droplet structure

Background

Obesity is a global health threat and increasingly emerges at a young age (1). Early onset obesity is associated with metabolic disease, including diabetes and cardiovascular disease (1). Increased energy intake and decreased physical activity are well-established lifestyle risk factors in obesity (2). When energy intake exceeds energy expenditure, the surplus energy is stored in white adipose tissue (WAT) resulting in increased adipocyte size (hypertrophy) and eventually increased adipocyte numbers (hyperplasia) (3- 5). When WAT fails to store the excessive energy, fat accumulates ectopically in the liver and skeletal muscle, an important step in the development of type 2 diabetes (T2D) (6). A mismatch between storage of fat in the form of triglycerides and oxidation of fatty acids (FA) in the mitochondria is an important feature in both obesity and T2D (7). Moreover, compromised mitochondrial function in skeletal muscle (8–10), as well as in liver and WAT (11, 12) evaluated using functional measurements, is a well know feature seen in obesity and T2D. In line with these observations, gene expression of a subset of genes coding for mitochondrial proteins (i.e. pyruvate dehydrogenase, cytochrome C, carnitinepalmitoyl-transferase I (*Cpt1*) and the uncoupling proteins (*Ucp*s)) were lower in WAT of transgenic diabetic mice models and in high fat diet (HFD)-induced insulin-resistant mice (11, 13). Taken together, these data strongly indicate a pivotal role of mitochondrial energy metabolism in WAT in obesity and T2D.

The development of WAT starts in the third trimester of gestation and continues throughout childhood and adolescence (3). Nutrition (excess or scarcity) during pregnancy and infancy has a substantial effect on adipose tissue development. For instance, maternal exposure to a HFD during pregnancy and lactation resulted in increased adiposity in rodent offspring (14, 15). This indicates that the nutrition in early life programs adiposity in adulthood.

Observational studies have demonstrated a moderate but consistent association between breastfeeding (duration) and reduced prevalence of later life overweight and obesity (16, 17). Studies from our lab suggest that the supramolecular structure of lipids in milk may contribute to these beneficial effects (18–20). We have shown that early postnatal exposure to a diet containing a concept IMF with large lipid droplets coated by phospholipids (Concept, Nuturis®) reduced body fat accumulation in adolescence and early adulthood in a mouse model for nutritional programming (18, 19). The reduced adult fat mass was associated with reduced adipocyte size and altered adipocyte function as well as improved metabolic health (19). This provides clear evidence that early life dietary lipid supramolecular structure may effectively program metabolic health later in life.

Nutrition during fetal and early postnatal life has been shown to affect mitochondrial content and oxidative capacity throughout life (21–24). For instance, hepatic enzyme activity of the mitochondrial oxidative phosphorylation was decreased in offspring of dams fed a HFD during pregnancy and lactation (21). Thus, differences in mitochondrial development and function may underlie programming of adiposity and metabolic health later in life.

In the current study, we investigate if postnatal exposure to large, phospholipid coated lipid droplets affects markers for mitochondrial content and oxidative capacity in WAT. We hypothesize that the supramolecular lipid structure affects the expression of genes involved in the energy utilization in both WAT and skeletal muscle and the expression of markers for mitochondrial content and oxidative capacity in WAT.

Methods

Animals and study design

All experimental procedures were approved by an external, independent Animal Experimental Committee (DEC consult, Soest, The Netherlands) and complied with the principles of good laboratory animal care following the EU-directive for the protection of animals used for scientific purposes. C57BL/6jOlaHsd mice (Harlan, Horst, The Netherlands) were kept at the animal facility of Wageningen University and Research Centre under a 12 h light − 12 h dark cycle (lights on at 06:00 h). Room temperature and humidity were kept at a constant level (21 ± 2 °C and 50 ± 5% respectively) and standard cage enrichment was added to allow mice to build a nest. Food and water were available ad libitum during the entire experimental period, except for an 8 h fastening period before dissection. Breeders were time-mated and female mice were provided with the American Institute of Nutrition-93G synthetic diet (AIN93G) (25) during pregnancy and lactation. At postnatal day 2 (PN2), litters were randomly cross-fostered to reduce between-litter variability and avoid litter effects, and culled to four male and two female pups per dam. On PN16, litters were randomly assigned to either the *i.* control (CTRL), *ii.* Concept or *iii.* Non-challenged reference group (REF), resulting in n = 12 male pups per experimental group (3 litters per group). The Concept group was fed the Concept-IMF based diet and CTRL and REF group were fed a control-IMF based diet from PN16 until PN42 (**Figure 1**). Male littermates were housed in pairs after weaning at PN21 and continued their respective IMF-based diets. From PN42 until PN98, Concept and CTRL group were challenged with a western style diet containing 20 *w/w* % fat (WSD, Figure 1). The REF group was fed AIN93M (25) from PN42 until PN98 and was included as a nonchallenged reference to compare to the effects of the WSD challenge (CTRL

group). Body weight was measured twice a week as of the period of weaning and body composition was monitored by DEXA using a PIXImus imager (GE Lunar, Madison, WI, USA) under general anesthesia (isoflurane/N2O/O2). At PN98, mice were fasted for 8 h, subjected to terminal anesthesia (isoflurane/N2O/O2) and dissected. *M.tibialis* and retroperitoneal (RP) WAT depots (as proxy for visceral WAT) were weighed, snap frozen and stored at −80 °C. Epididymal (EPI) WAT depots were weighed and immediately used for fat cell analysis, as RP WAT depots were too small to use for all analyses.

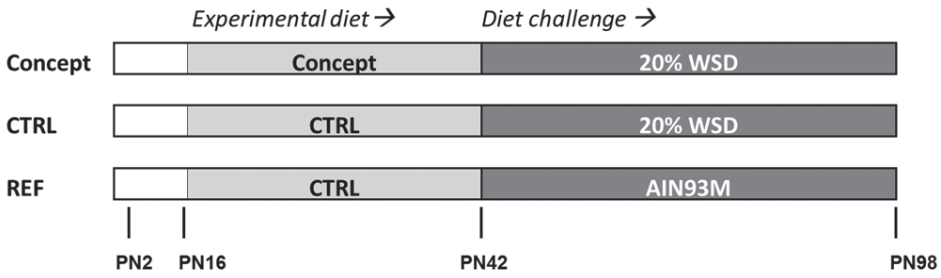

Figure 1: Study design; WSD: western style diet; PN: postnatal day.

IMF production

The CTRL IMF was produced according to a Standard stage 1 IMF recipe and processing procedure (Nutricia Research, Utrecht, the Netherlands). For the Concept IMF powder 0.5 g/l phospholipids of bovine milk origin (SM2, Corman Food industry, Goé, Belgium) was added and processing procedure was adjusted as described previously (19, 26). The mode diameter of the lipid droplets in the Concept IMF was 2.924 µm versus 0.267 µm in the CTRL IMF.

Experimental diets

Control and Concept IMF-based diets were semi-synthetic and contained 28.2 *w/w* % control or Concept IMF powder, respectively. The diets were complemented with protein and carbohydrates to establish macronutrient composition appropriate for normal growth and development in rodents and match a macronutrient composition according to AIN93G standards (**Table 1**). The macronutrient composition of CTRL and Concept diet was similar except for phospholipid (0.2 versus 1.44 g/kg, respectively) content. The moderate WSD consisted of 20% (*w/w*) fat of which 17% (*w/w*) lard, 3% (*w/w*) soy oil and 0.1% (*w/w*) cholesterol (Table 1).

Table 1: Composition of the early programming diets and the WSD diet.

Diet		Programming diet		WSD
		CTRL	Concept	
Carbohydrates	(g/kg)	646	646	520
Sugars [a]	(g/kg)	236	236	70
Polysaccharides [b]	(g/kg)	410	410	450
Protein	(g/kg)	179	179	180
Fat	(g/kg)	70	70	200
Saturated Fatty Acids (SFA)	(g/kg)	30	30	81,2
Mono Unsaturated Fatty Acids (MUFA)	(g/kg)	28	28	84,9
Poly Unsaturated Fatty Acids (PUFA)	(g/kg)	12	12	32,7
LA/ALA ratio		5.5	5.5	14,9
Phospholipids [c]	(g/kg)	0.2	1.44	-
Cholesterol	(g/kg)	-	-	1.0
Fiber	(g/kg)	47.5	47.5	50
Vitamin & mineral mix	(g/kg)	45	45	45

[a] Total sugars, including lactose, glucose and sucrose; [b] including starch and maltodexintrin; [c] Phospolipids derived from bovine milk.

Fat cell analysis

Fresh EPI WAT depots were used to determine cell size distribution according to the optical method of DiGirolamo and Fine (27) and Hirsch and Gallian (28) as described in detail previously (19).

Gene expression

RNA from RP WAT and *m.tibialis* were isolated using Trizol®/chloroform (Invitrogen, Breda, The Netherlands) and purified with a RNeasy Mini Kit (Qiagen Benelux b.v., Zwijndrecht, The Netherlands) including a DNase treatment with a RNase-free DNase Set (Qiagen Benelux b.v., Zwijndrecht, The Netherlands) as previously described (29). Quantity and quality of the RNA samples was analysed with the Nanodrop 2000 (Thermo Scienctific, Breda, The Netherlands) and the Bioanalyzer (Agilent, Santa Clara, USA). Samples with a RIN below 8.0 and a 260/280 ratio below 1.9 were excluded from analyses. cDNA was synthesized with the iScript™ cDNA synthese kit (Bio-Rad, Veenendaal, The Netherlands) according to manufacturer instructions. 9,4 and 25 ng cDNA was used as input for each Q-PCR reaction of the RP WAT and *m.tibialis* samples, respectively. 5× Hot FirePol Evagreen ® qPCR mix Plus (Bio-Connect, Huissen, The Netherlands) was used according to manufacturer instructions and qPCR was

performed with a 7900HT Fast Real Time PCR System (Applied Biosystems, Bleiswijk, The Netherlands). Acetyl-CoA carboxylase 1 (*Acc1*), adipose triglyceride lipase (*Atgl*), fatty acid transfer protein/cluster of differentiation 36 (*Cd36*), Cell death-inducing DNA fragmentation factor, alpha subunit-like effector A (*Cidea*), *Cpt1*α, fatty acid binding protein 4 (*Fabp4*), fatty acid synthase (*Fasn*), fatty acid transfer protein 1 (*Fatp1*), glucose transporter 4 (*Glut4*), glycerol-3-phosphate acyltransferase (*Gpat*), hexokinase II (*HkII*), hormone sensitive lipase (*Hsl*), lipoprotein lipase (*Lpl*), pyruvate dehydrogenase kinase 4 (*Pdk4*), peroxisome proliferator activated receptor α (*Ppar*α), stearoyl-Coenzyme A desaturase 1 (*Scd1*), sterol regulatory element binding protein 1c (*Srebp1c*), *Ucp1* and *Ucp3* mRNA expression were measured in RP WAT. *Cpt1*α, *Glut4*, *Pdk4* and *Ucp3* gene expression were measured in *m.tibialis*. See **Table 2** for the complete list of primers. RP WAT qPCR data was normalized using the method of relative normalization as described by Hellemans et al. (30) and performed with qbase+ (Biogazelle, Genth, Belgium). In short, gene expression of genes of interest was analyzed relative to mean expression of multiple reference genes and scaled to the expression of the CTRL group. Four reference genes were used for the RP WAT: ribosomal protein L19 (*Rpl19*) and S29 (*Rps29*), 18S ribosomal RNA (*18SrRNA*) and Calnexin (*Canx*). *Rpl19*, *Rps29* and *18SrRNA* were used as reference genes for the *M. tibialis*.

Enzyme activity

Citrate synthase (CS) and Hydroxyacyl-CoA dehydrogenase (HAD) activity were measured as described elsewhere (31). In short, RP WAT samples were homogenized and dissolved in sucrose-Tris-EDTA buffer (250 mM Sucrose, 10 mM Tris, 2 mM EDTA, pH 7.4). CS activity was analyzed by adding sample to reaction reagent (100 mM Tris, 100 µM DTNB, 50 µM acetyl-CoA, pH 8.0) and start reagent (50 mM Oxaloacetic acid), in the proportion 1:50:1, followed by a kinetic reading (421 nm, 37 °C). HAD activity was analyzed by adding sample to reaction reagent (100 mM tetra-sodiumpyrophosphate, 250 µM NADH, pH 7.3) and start reagent (5 mM Acetoacetyl-CoA), in the proportion 1:10:1, followed by a kinetic reading (340 nm, 37 °C).

OXPHOS protein expression

Protein expression of 5 subunits of the oxidative phosphorylation (OXPHOS) was measured as previously described (32). Briefly, RP WAT samples were homogenized and dissolved in Radio-Immunoprecipitation Assay buffer (RIPA, Fisher Scientific, Landsmeer, The Netherlands) with protease inhibitor cocktail (Roche diagnostics, Almere, the Netherlands). Per sample 15 µg was used for gel electrophoreses with a 4–15% gradient and transferred to a PVDF membrane with a Trans-Blot® Turbo™ Blotting System using the Trans-Blot®

Turbo™ Midi PVDF Transfer pack (Bio-Rad, Veenendaal, The Netherlands). OXPHOS protein expression was determined using the Mito-Profile® Total OXPHOS rodent western blot antibody cocktail (Abcam, Cambridge, UK) with ECL anti mouse IgG (Fisher Scientific, Landsmeer, The Netherlands) as a secondary antibody. Protein expression was detected with the ChemiDoc™ XRS, analyzed by Quantity One (Biorad, Veenendaal, The Netherlands) and adjusted for total protein levels per lane, using Coomassie brilliant blue staining.

Mitochondrial DNA content

Nuclear and mitochondrial DNA (mtDNA) was isolated from RP WAT with the QIAamp DNA micro kit (Qiagen Benelux b.v., Zwijndrecht, The Netherlands), according to manufacturers protocol. DNA quantity was determined with a Nanodrop 2000 (Thermo Scienctific, Breda, The Netherlands). Relative mitochondrial DNA expression was determined as previously described (33). Briefly, 135 ng input DNA was used for each qPCR reaction, with NADH dehydrogenase 1 (*Nd1*) as a marker for mitochondrial DNA and *Lpl* to normalize for nuclear DNA. Primers sequences are shown in Table 2. Data were analyzed using qbase+ (Biogazelle, Genth, Belgium).

Table 2: primer sequences.

Gene name	NCBI Reference number	Forward primer	Reverse primer
Genes of interest:			
Acc1	NM_133360.2	tggtgcagaggtaccgaagtg	cgtagtggccgttctgaaact
Atgl	NM_025802.3	atccgcttgttggagtggct	ctcttggccctcatcaccag
Cd36	NM_001159558.1	attgcgacatgattaatggcac	gatagacctgcaaatgtcagaggaa
Cidea	NM_007702.2	aggccgtgttaaggaatctg	cccagtactcggagcatgta
Cpt1α	NM_013495.2	gcccatgttgtacagcttcc	tcatcagtggcctcacagac
Fabp4	NM_024406.2	tcataaccctagatggcggg	ttccaccaccagcttgtcac
Fas	NM_007988.3	gctgggctctatggattaccc	ggtccattgtgtgtgcctgc
Fatp1	NM_011977.3	attgtggtgcacagcaggtacta	tggtagagtggcaggcagtca
Glut4	NM_009204.2	cggatgctatgggtccttacg	aacgtccggcctctggttt
Gpat	NM_008149.3	tgtccacaacttcagcggtc	cagcgtacacggcaacgtt
HkII	NM_013820.3	aagacgataaggacggaattcaga	gagcgcgtggacacaatct
Hsl	NM_010719.5	cctgcttggttcaactggaga	tcactccataggctgctgcc
Lpl	NM_008509.2	cacttgtcatctcattcctggatt	ccgttaccgtccatccatg
Pdk4	NM_013743.2	aagagctggtatatccagagcctg	ttgaccagcgtgtctacaaactc
Pparα	NM_011144.6	agtgccctgaacatcgagtgt	ttcgccgaaagaagcccttа
Scd1	NM_009127.4	cacctgcctcttcgggatttt	gcagccgtgccttgtaagttc
Srebp1c	NM_011480.3	ccggctattccgtgaacatc	caagggcatctgagaactccc
Ucp1		assay ID qMmuCID0005832	
Ucp3	NM_009464.3	aacgctcccctaggcaggta	gcagaaaggagggcacaaatc

Table 2: Continued

Gene name	NCBI Reference number	Forward primer	Reverse primer
Reference genes:			
Canx	NM_007597.3	agagctcagcctggatcaattc	ttgtagtcctctccacacttatctgg
Rpl19	NM_009078.2	ttgcctctagtgtcctccgc	cttcctgatctgctgacggg
Rps29	NM_009093.2	agtcacccacggaagttcgg	gtccaacttaatgaagcctatgtcctt
18SrRNA	NR_003278.1	cgattccgtgggtggtggtg	catgccagagtctcgttcgttatc
DNA primers			
Nd1	NC_005089.1	accaatacgccctttaacaac	aatgggtgtggtattggtagg
Lpl	NM_008509	tcctgatgacgctgattttg	atgtcaacatgccctactgg

Statistical analysis

Statistical analyses were performed using SPSS® 19.0 (SPSS Benelux, Gorinchem, The Netherlands). The primary focus for the study was to assess the difference between the Concept and the CTRL group, which was tested using a TTest. The latter will give insight into the window of opportunity to be influenced by our nutritional intervention as well as to understand the direction of change. The effect of the WSD challenge was tested separately using a TTest. Concept and REF group were not directly compared based on the differences in dietary exposure both in early postnatal life (Concept vs. Control) and also later life (WSD vs. AIN). Gaussian distribution was tested with a Kolmogorov-Smirnov test. Differences in adipocyte size distribution were analyzed with a Mann-Whitney. Correlations between parameters were analyzed using a Pearson test. Data are presented as mean + SD, except for the qPCR data which are presented as mean relative expression (scaled to the average expression) with 95% confidence intervals. Differences were considered significant at $p<0.05$ and tendencies reported when $0.05<p<0.1$.

Results

Effect of the western-style diet challenge during adolescence and adulthood

Body composition

As a consequence of the WSD challenge, body weight, fat mass, EPI and RP WAT weight were increased in the CTRL compared to the non-challenged REF group. Lean body mass was slightly higher although no significant effect on *m. tibialis* weight was found (**Table 3**). These data are discussed elsewhere (20).

Adipocyte size and number in EPI WAT

The WSD challenge resulted in a 44% increase in average EPI adipocyte size in the CTRL group compared to the non-challenged REF group (p<0.001; Table 3). Furthermore, a shift was seen in adipocyte size distribution towards larger cells in the CTRL group (**Figure 2**). Percentages of cells in the size categories between 30 and 90 µm were lower for the CTRL group while higher in the size categories between 100 and 240 (p<0.05). EPI adipocyte numbers tended to be lower in the CTRL group (p=0.07; Table 3).

Table 3: Body composition, organ weight and EPI WAT adipocyte characteristics (mean adipocyte size and number).

Diet group	**REF (n = 12)**	**CTRL (n = 12)**	**Concept (n = 12)**
Body weight (g)	28.48 (SD 1.8)	31.7 (SD 2.5) $^{\#\#}$	29.23 (SD 2.4) *
Lean body mass (g)	23.5 (SD 1.4)	24.4 (SD 1.3) †	23.5 (SD 1.8)
Fat mass (g)	4.9 (SD 1.1)	7.5 (SD 1.8) $^{\#\#\#}$	5.8 (SD 1.6) *
RP WAT (g)	0.14 (SD 0.06)	0.31 (SD 0.10) $^{\#\#\#}$	0.20 (SD 0.10) *
EPI WAT (g)	0.48 (SD 0.15)	1.00 (SD 0.29) $^{\#\#\#}$	0.63 (SD 0.27) **
m. tibialis (g)	0.05 (SD 0.00)	0.05 (SD 0.01)	0.05 (SD 0.01)
Adipocyte characteristics:	**REF (n = 11)**	**CTRL (n = 10)**	**Concept (n = 9)**
Mean adipocyte size (µm)	74.4 (SD 10.3)	107.1 (SD 15.7) $^{\#\#\#}$	81.3 (SD 14.0) **
Adipocyte number (x 10^6)	7.44 ± (SD 2.44)	5.79 (SD 1.07) †	7.55 (SD 3.67)

Data expressed as mean plus SD. Early diet and WSD challenge effects were analyzed separately. Difference between Concept and REF groups were not tested, as groups were fed different postnatal and adult diets. $^{\#\#}$p<0.01; $^{\#\#\#}$p<0.001; †p=0.05-0.10, CTRL different from REF group; *p<0.05; **p<0.01, Concept different from CTRL group.

Markers for mitochondrial content and β-oxidation in the WAT

Mitochondrial content of the RP depot, as measured by CS activity and relative mtDNA content, was significantly lower in the CTRL group compared to the REF group (p<0.05; **Figure 3A and B**). FA oxidation of the RP WAT, reflected by HAD activity, was similar in both groups (**Figure 3C**).

OXPHOS protein expression in the WAT

No effect of the WSD challenge was shown on the protein expression of OXPHOS complexes I (NDUFB8; **Figure 4A**), II (SDHB; **Figure 4B**), III (UQCRC2; **Figure 4C**) and IV (MTCOI; **Figure 4D**) in the RP depot. Expression levels of the ATP synthase subunit of complex V (ATP5A) tended to be increased in the CTRL group as a consequence of the WSD challenge (p=0.08; **Figure 4E**). OXPHOS protein expression was lower for all complexes in the CTRL compared to the REF group when corrected for CS activity (**Figure 5A-E**).

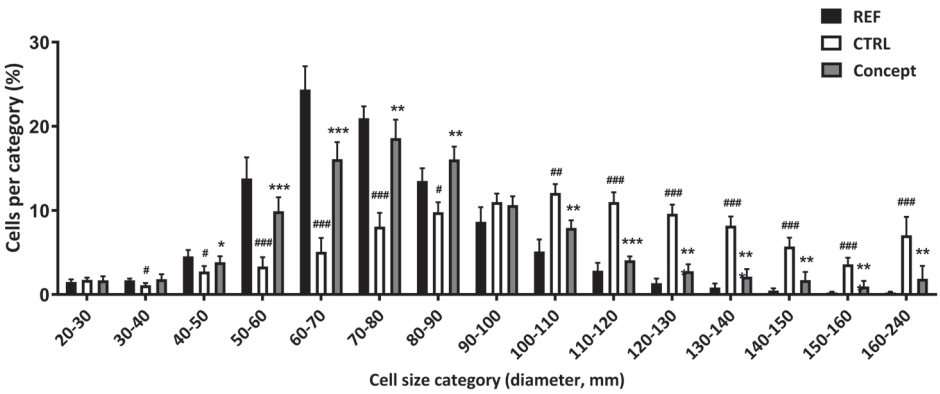

Figure 2: Effect of postnatal Concept diet on adult adipocyte size distribution of epididymal white adipose tissue (n = 10, n = 9 and n = 11 for CTRL, Concept and REF group respectively). Early diet and WSD challenge effects were analyzed separately. Difference between Concept and REF group not tested, as groups were fed different postnatal and adult diets. $^{\#}$p<0.05; $^{\#\#}$p<0.01; $^{\#\#\#}$p<0.001, CTRL different from REF group; *p<0.05; **p<0.01; ***p<0.001 Concept different from CTRL group.

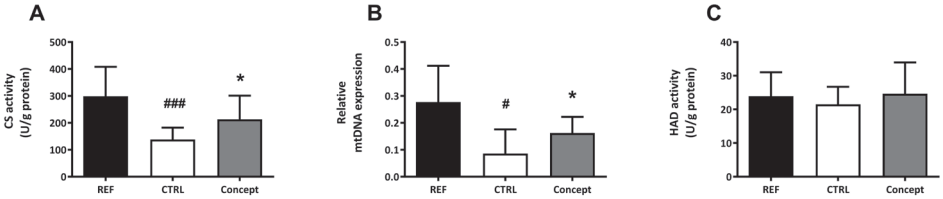

Figure 3: Effect of postnatal Concept diet on markers for mitochondrial content and β-oxidation in the retroperitoneal (RP) white adipose tissue; (**A**) citrate synthase (CS) activity (n = 10 per group), (**B**) mtDNA/nDNA ratio (n = 8 per group) and (**C**) hydroxyacyl-CoA dehydrogenase (HAD; n = 10 per group). DNA ratio displayed as mean plus 95% confidence interval. Early diet and WSD challenge effects were analyzed separately. Difference between Concept and REF group not tested, as groups were fed different postnatal and adult diets. $^{\#}$p<0.05; $^{\#\#\#}$p<0.001, CTRL different from REF group; *p<0.05, Concept different from CTRL group.

Gene expression profiles RP WAT

Expression levels of the lipogenic genes *Gpat* and *Srebp1c* in RP WAT were lower in the CTRL compared to the REF group as were the expression levels of the lipogenic enzymes *Acc1*, *Fas* and *Scd1* (p<0.05 for all parameters; **Table 4**). Gene expression of the lipolytic enzyme *Atgl* tended to be lower in the CTRL group (p=0.09). Expression of *Hsl* was similar in both groups. Expression levels of *Pdk4* and *HkII*, both part of the glucose oxidative pathway, were significantly lower in the CTRL compared to the REF group as were the levels of the glucose transporter *Glut4* (p<0.05 for all parameters; Table 4). The CTRL group showed elevated expression levels of the FA transporters

*Cpt1*α and *Cd36* and lower *Fatp1* and *Fabp4* levels compared to the non-challenged REF group ($p<0.05$ for all parameters). No difference was observed in expression levels of *Lpl* (Table 4). *Ppar*α expression levels were lower in the CTRL group compared to the REF group ($p<0.001$), as was the *Ucp3* gene expression ($p<0.01$; Table 4). Expression of WAT browning markers *Ucp1* and *Cidea* were decreased in the CTRL compared to the Ref group ($p<0.001$; Table 4).

Gene expression profiles in skeletal muscle

The CTRL group showed lower *Ucp3* expression levels in the m. tibialis compared to the REF group ($p<0.01$). Expression profiles of *Pdk4*, *Cpt1*α and *Glut4* were not affected by the adult WSD challenge (Table 4).

Programming effect of concept IMF diet

Body composition

In accordance to previous findings (18, 19), body weight, fat mass, EPI and RP WAT weight were reduced in the Concept compared to the CTRL group. Lean body mass and *m. tibialis* weight were similar in both groups (Table 3). These data are part of a more extensive study concerning the potential protective effects of structural aspect of lipids in human milk against later life obesity and therefore reported in a separate paper (20).

Adipocyte size and number in EPI WAT

Average EPI adipocyte size (Table 3) was 24% lower in the Concept group compared to the CTRL group ($p<0.01$). This was confirmed by a shift in adipocyte size distribution towards smaller cells in the Concept compared to the CTRL group (Figure 2). EPI adipocyte numbers were similar in both groups (Table 3). Most striking differences were found in size categories between 50 and 90 μm with more cells for the Concept compared to the CTRL group ($p<0.05$). In addition, the Concept group showed fewer cells in the size categories between 100 and 240 μm ($p<0.01$) compared to the CTRL group.

Markers for mitochondrial content and β*-oxidation in WAT*

In the RP depot mitochondrial content, as measured by CS activity and relative mtDNA expression, was significant higher in the Concept compared to the CTRL group ($p<0.05$; Figure 3A and B respectively). Groups had similar HAD activity, which reflects FA oxidation (Figure 3C).

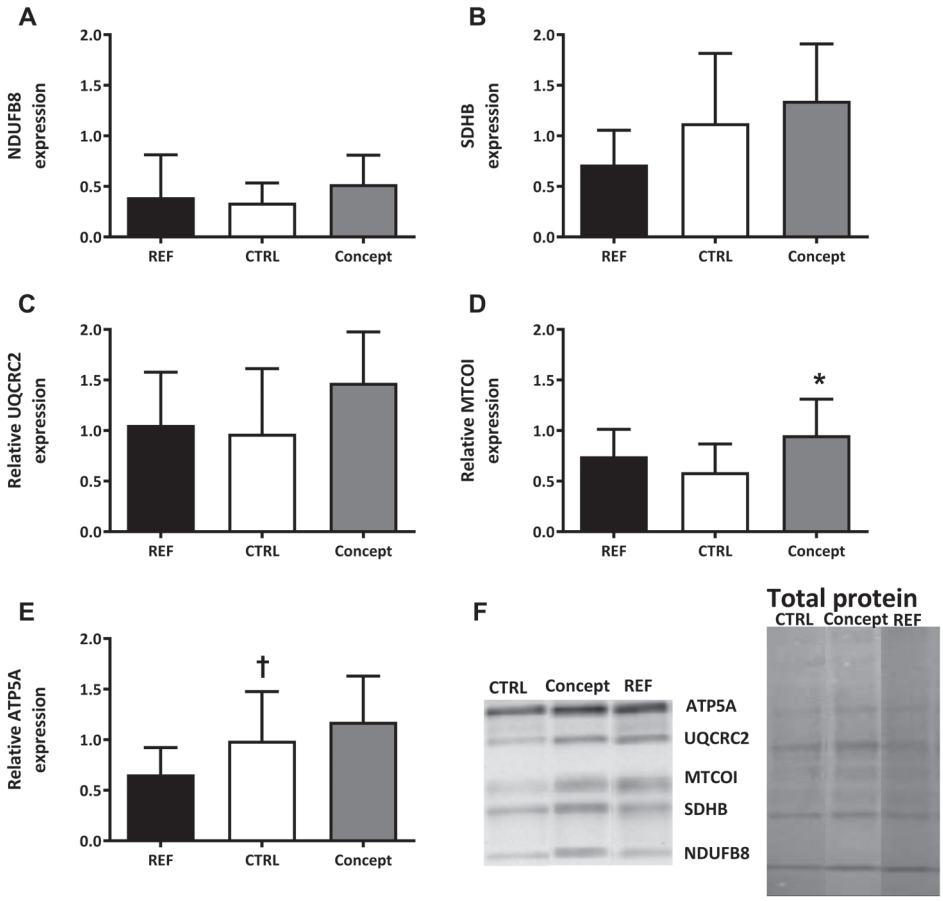

Figure 4: Effect of postnatal Concept diet on relative protein expression of 5 oxidative phosphorylation complex (OXPHOS) subunits (**A – E**) in the retroperitoneal (RP) white adipose tissue (n = 8 for CTRL, n = 7 for Concept and n = 10 for REF group) and (**F**) total protein and western blot bands of one sample per group, samples came from one blot, but not from adjacent lanes, a picture of the whole blot is added as Additional file 1. Early diet and WSD challenge effects were analyzed separately. Difference between Concept and REF group not tested, as groups were fed different postnatal and adult diets. *p<0.05, Concept different from CTRL group; †p=0.05–0.1 REF different from CTRL group.

OXPHOS protein expression in WAT

Mitochondrial cytochrome c oxidase I subunit (subunit of complex IV, MTCOI) expression levels were significantly higher in the Concept group compared to the CTRL group (p<0.05; Figure 4D). Protein expression of complex I (NDUFB8; Figure 4A) II (SDHB; Figure 4B), III (UQCRC2, Figure 4C) and V (ATP5A; Figure 4E) did not significantly differ between the two groups. OXPHOS protein expression was not significantly lower in the Concept compared to the CTRL group when corrected for CS activity (Figure 5A-E).

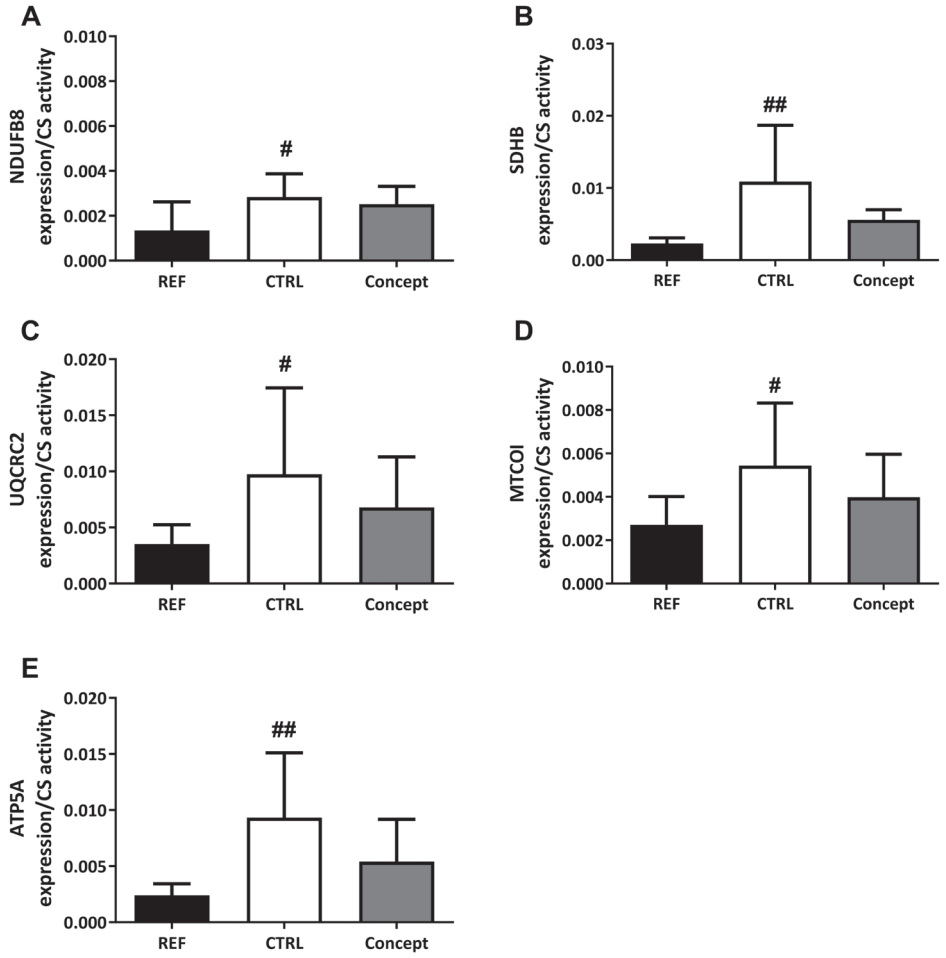

Figure 5: Effect of postnatal Concept diet on relative protein expression of 5 oxidative phosphorylation complex (OXPHOS) subunits (**A - E**) in the retroperitoneal (RP) white adipose tissue when corrected for citrate synthase (CS) activity (n = 7 for CTRL, n = 6 for Concept and n = 9 for REF group). Early diet and WSD challenge effects were analyzed separately. Difference between Concept and REF group not tested, as groups were fed different postnatal and adult diets. $^{\#}p<0.05$; $^{\#\#}p<0.01$ different from CTRL group.

Gene expression profiles in RP WAT

RP WAT expression levels of lipogenic genes *Gpat*, *Srebp1c*, *Acc1*, *Fas* and *Scd1* were similar in the Concept and the CTRL group as were the expression levels of lipolytic enzymes *Atgl* and *Hsl* (Table 4). Glucose oxidative pathways (*Pdk4* and *HkII*) were unaffected by the early diet (Table 4). The *Cd36* expression levels of the Concept group tended to be lower compared to the CTRL group (p=0.09), but expression levels of

other FA transporters (*Cpt1*α, *Fatp1*, *Fabp4* and *Lpl*) and glucose transporter *Glut4* were comparable between the Concept and the CTRL group (Table 4). *Ppar*α (fat oxidative pathway) expression levels were also similar in the Concept and CTRL group as was the RP WAT expression of the uncoupling protein *Ucp3* (Table 4). Expression of *Ucp1*, as marker for WAT browning, was similar between the Concept and CTRL group, but expression of another marker for WAT browning, *Cidea* tended to be higher in Concept compared to CTRL group (p=0.08; Table 4).

Table 4: Relative mRNA expression in arbitrary units (AU).

Gene name	**REF (n = 10)**	**CTRL (n = 12)**	**Concept (n = 12)**
RP WAT:			
Acc1	2.953 (1.912-4.562)	1.000 (0.747-1.338) ###	1.212 (0.815-1.803)
Atgl	1.264 (1.118-1.429)	1.000 (0.786-1.273) †	1.058 (0.831-1.347)
Cd36	0.863 (0.741-1.006)	1.000 (0.939-1.064) #	0.882 (0.764-1.018) ‡
Cidea	10.066 (6.317-16.038)	1.000 (0.603-1.659) ###	1.962 (1.035-3.717) ‡
*Cpt1*α	0.711 (0.595-0.849)	1.000 (0.816-1.225) #	0.978 (0.764-1.251)
Fabp4	1.199 (1.020-1.408)	1.000 (0.892-1.121) #	1.097 (1.002-1.200)
Fas	3.012 (1.816-4.995)	1.000 (0.730-1.371) #	1.080 (0.715-1.633)
Fatp1	1.352 (1.097-1.665)	1.000 (0.821-1.218) #	0.995 (0.804-1.230)
Glut4	1.939 (1.315-2.858)	1.000 (0.863-1.159) ###	1.221 (0.935-1.594)
Gpat	1.514 (1.298-1.766)	1.000 (0.846-1.181) ###	1.167 (0.925-1.472)
HkII	1.390 (1.093-1.767)	1.000 (0.786-1.272) #	1.068 (0.795-1.434)
Hsl	1.146 (1.048-1.252)	1.000 (0.837-1.194)	0.931 (0.809-1.071)
Lpl	0.902 (0.784-1.038)	1.000 (0.874-1.144)	0.866 (0.706-1.061)
Pdk4	1.878 (1.215-2.904)	1.000 (0.780-1.283) ##	1.377 (0.887-2.140)
*Ppar*α	1.911 (1.648-2.216)	1.000 (0.785-1.274) ###	1.124 (0.944-1.338)
Scd1	1.891 (1.544-2.317)	1.000 (0.812-1.232) ###	1.079 (0.854-1.363)
Srebp1c	1.426 (1.146-1.775)	1.000 (0.810-1.235) ##	1.087 (0.910-1.300)
Ucp1	27.480 (15.828-47.709)	1.000 (0.337-2.968) ###	2.621 (0.860-7.993)
Ucp3	1.432 (1.248-1.644)	1.000 (0.833-1.200) ##	1.168 (0.883-1.544)
Skeletal muscle:	**REF (n = 10)**	**CTRL (n = 12)**	**Concept (n = 11)**
Cpt1a	1.029 (0.881-1.202)	1.000 (0.752-1.331)	1.074 (0.906-1.273)
Glut4	1.009 (0.811-1.256)	1.000 (0.811-1.233)	1.089 (0.939-1.262)
Pdk4	1.600 (1.124-2.277)	1.000 (0.684-1.461)	1.296 (0.929-1.808)
Ucp3	1.577 (1.286-1.933)	1.000 (0.830-1.204) ##	1.299 (1.105-1.527) *

mRNA expression listed as the mean expression level, scaled to expression of the CTRL group, plus 95% confidence intervals, n = 10 - 12 per group. Early diet and WSD challenge effects were analyzed separately. Difference between the Concept and REF group were not tested, as groups were fed different postnatal and adult diets. #p<0.05; ##p<0.01; ###p<0.001; †p=0.05-0.10, CTRL different from REF group; *p<0.05; ‡p=0.05-0.10, Concept different from CTRL group.

Gene expression profiles in skeletal muscle

The Concept group showed higher *Ucp3* expression levels in the *m. tibialis* compared to the CTRL group (p<0.05; Table 4). Expression profiles of *Pdk4* (involved in the transport of pyruvate –the glycolytic end product– into the mitochondria), *Cpt1*α (involved in the transport of long-chain fatty acids over the mitochondrial membrane) and *Glut4* (glucose transporter) in the m. tibialis were not affected by the early postnatal diet (Table 4).

Correlations

Markers for mitochondrial content, CS activity and mtDNA, were inversely correlated to RP WAT weight (r=−0.741; p<0.001 and r=−0.655; p<0.001, respectively; **Figure 6**). No correlations between protein expression of the OXPHOS complexes and RP WAT weight were found.

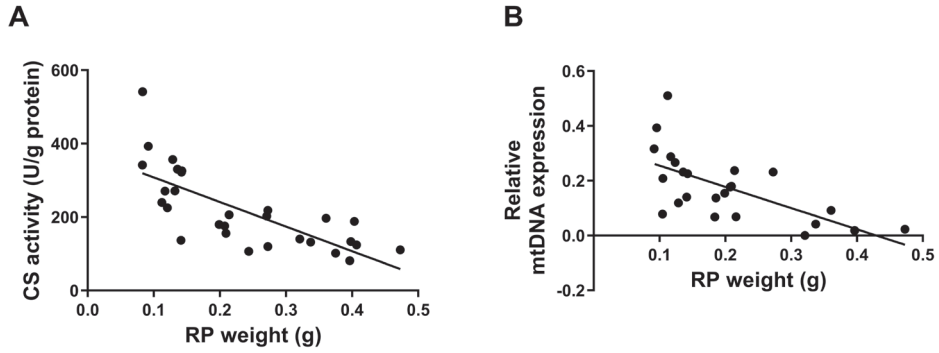

Figure 6: Correlation between retroperitoneal (RP) white adipose tissue weight and (**A**) citrate synthase (CS) activity (r=−0.741; p<0.001) and (**B**) mtDNA/nDNA ratio(r =−0.655; p<0.001).

Discussion

The present study showed that early life exposure to large, phospholipid-coated lipid droplets leads to altered expression of markers for mitochondrial oxidative capacity in RP WAT and *m. tibialis*. Although functional mitochondrial capacity was not measured, these markers suggest that adapted mitochondrial oxidative capacity may underlie the previously reported reduced body fat accumulation in adolescence and adulthood (18–20).

Programming of metabolic health is well established, but possible underlying mechanisms are still largely unknown although many have been suggested. Aberrant mitochondrial function has been suggested in a limited amount of studies as possible link between adverse fetal environment and the development of T2D (22, 34). Yet, little is known on how nutritional programming may improve lifelong metabolic health and protect against obesity.

In the present study, markers for mitochondrial oxidative capacity appeared to be increased due to the supramolecular structure of milk lipids in the early postnatal diet. The elevation in CS activity and relative mtDNA expression in the WAT imply higher mitochondrial content, suggesting a higher oxidative capacity. In addition, the elevated protein expression levels for the mitochondrial cytochrome c oxidase subunit I indicate that possibly more substrate is oxidized in RP WAT of Concept mice as well. As OXPHOS protein levels corrected for CS activity were similar between CTRL and Concept groups, total oxidative capacity per cell may be increased by the Concept diet rather than the intrinsic activity per mitochondrion. The expression levels of *Ucp3* in the Concept group were slightly increased in skeletal muscle. A higher *Ucp3* expression could elevate substrate oxidation via its uncoupling activity or via export of FA anions out of the mitochondria (35, 36). Taken together, these data suggest that mitochondrial oxidative capacity may be elevated in mice fed a Concept diet in early postnatal life, resulting in a better ability to cope with an increased FA load in adulthood, which could explain the lower adiposity seen upon the WSD challenge. The WSD challenge had, apart from the early diet, a clear effect on markers for oxidative capacity. Expression of markers for mitochondrial content (CS activity and relative mtDNA expression) in the WAT and mitochondrial uncoupling (*Ucp3*) in the skeletal muscle were decreased in the CTRL compared to the non-challenge REF group. No effect of the WSD diet on OXPHOS protein levels was found. OXPHOS protein levels corrected for CS activity were however elevated in the CTRL compared to the REF group, which points towards increased intrinsic activity per mitochondrion as compensatory mechanism. These results are in line with the literature showing decreased expression of oxidative capacity markers in

the WAT upon a high fat diet (37) and are opposite from the early diet effect. This may indicate that mice fed the Concept diet in early life were protected against the adverse effects of the WSD challenge by preserving WAT health and were different from the CTRL mice, able to increase mitochondrial oxidative capacity in response to the WSD challenge.

Gene expression of markers for lipogenesis, lipolysis or lipid uptake were unaffected by the supramolecular lipid structure of the early postnatal diet, suggesting that these metabolic processes may not contribute the observed effects on adult adiposity. In addition, gene expression of markers for β-oxidation, transfer of long-chain acyl-CoA into the mitochondria, other substrate transporters, the glucose oxidative pathway and browning of the WAT depot were not affected by the postnatal diet intervention.

It should be noted that functional measurements are pivotal to confirm whether the higher levels of mitochondrial content and capacity markers truly result in increased substrate oxidation upon a change in nutrient status. There is some evidence showing that mitochondrial function can be reduced or elevated upon caloric restriction and/or physical activity with similar numbers of mitochondria (38, 39), indicating that similar numbers of mitochondria still may result in differences in mitochondrial function. In contrast, other studies have shown that mitochondrial content and complex IV protein content and activity were correlated to ADP stimulated respiration (40–42), suggesting that differences in levels of these markers may reflect an actual difference in mitochondrial function. Thus, although functional measurements were not performed, the lower adiposity and adipocyte size of the Concept group found, does suggest that the Concept mice showed a less exaggerated respond to the WSD challenge. This supports oxidation of the surplus of energy instead of storage into WAT.

Altered mitochondrial oxidative capacity in WAT could affect substrate selection and competition in other oxidative organs like skeletal muscle and liver, thereby affecting whole body insulin sensitivity (43, 44). Further studies focusing on functional measurements of mitochondrial function in liver and skeletal muscle are required to confirm that postnatal dietary lipid structure indeed programs adult mitochondrial function.

CS activity and mtDNA content, representative for mitochondrial content, were inversely correlated with RP WAT weight. Whether or not the higher mitochondrial content in the Concept group caused the reduced RP WAT weight or the other way around remains to be determined. Interestingly cytochrome c oxidase subunit I expression was not related to RP WAT weight, suggesting that OXPHOS protein expression may be driven by the interaction between the early diet and the WSD challenge although further investigation is needed to establish this.

Previous studies showed that mitochondrial oxidative capacity was decreased in rodents and sheep by exposure to HFD and/or malnutrition during fetal life (45–47). The present results show a beneficial programming of mitochondrial oxidative capacity markers by a relatively mild diet intervention during the postnatal period. Based on these observations we could speculate that decreased oxidative capacity following an adverse fetal environment could potentially be reprogrammed by an adjusted diet in the postnatal period.

Conclusion

We showed that exposure to adapted supramolecular structure of dietary lipids (Nuturis®) in early postnatal life results in increased expression of markers for mitochondrial content and capacity which may enable adult mice to cope better with the surplus of fat provided by the WSD challenge diet. Although functional measurements are not performed, these adaptations in mitochondrial function markers could underlie the observed reduced body fat accumulation in an obesogenic adult environment in these animals.

Additional information

Acknowledgements We thank Diane Kegler for help in performing the animal experiment and Annemarie Baars for skeletal muscle gene expression analyses.

Funding Nutricia Research funded the study.

Availability of data and materials The datasets generated during the current study are available from the corresponding author on reasonable request.

Authors' contributions AK, AO, EP, EE, LS and EvdB design of the study; AK, EE, LS, performed experiments, AK analyzed data; AK, AO, EP, EvdB interpreted results; AK prepared figures; AK, AO, EP and EvdB drafted manuscript; AK, AO, EP, EE, LS, EvdB edited and revised manuscript; AK, AO, EP, EE, LS, EvdB approved the final version of manuscript.

Competing interests Andrea Kodde, Annemarie Oosting, Eefje Engels, Lidewij Schipper and Eline van der Beek are employees of Nutricia Research.

Ethics approval and consent to participate All experimental procedures were approved by an external, independent Animal Experimental Committee (DEC consult, Soest, The Netherlands) and complied with the principles of good laboratory animal care following the EU-directive for the protection of animals used for scientific purposes.

References:

1. Lobstein T, Baur L, Uauy R. Obesity in children and young people: a crisis in public health. Obes Rev. 2004;5 Suppl 1:4-104.
2. Rennie KL, Johnson L, Jebb SA. Behavioural determinants of obesity. Best Pract Res Clin Endocrinol Metab. 2005;19(3):343-58.
3. Spalding KL, Arner E, Westermark PO, Bernard S, Buchholz BA, Bergmann O, et al. Dynamics of fat cell turnover in humans. Nature. 2008;453(7196):783-7.
4. Surwit RS, Feinglos MN, Rodin J, Sutherland A, Petro AE, Opara EC, et al. Differential effects of fat and sucrose on the development of obesity and diabetes in C57BL/6J and A/J mice. Metabolism. 1995;44(5):645-51.
5. Berger JJ, Barnard RJ. Effect of diet on fat cell size and hormone-sensitive lipase activity. J Appl Physiol. 1999;87(1):227-32.
6. Kahn BB, Flier JS. Obesity and insulin resistance. J Clin Invest. 2000;106(4):473-81.
7. Rogge MM. The role of impaired mitochondrial lipid oxidation in obesity. Biol Res Nurs. 2009;10(4):356-73.
8. Phielix E, Mensink M. Type 2 diabetes mellitus and skeletal muscle metabolic function. Physiol Behav. 2008;94(2):252-8.
9. Kelley DE, He J, Menshikova EV, Ritov VB. Dysfunction of mitochondria in human skeletal muscle in type 2 diabetes. Diabetes. 2002;51(10):2944-50.
10. Mogensen M, Sahlin K, Fernstrom M, Glintborg D, Vind BF, Beck-Nielsen H, et al. Mitochondrial respiration is decreased in skeletal muscle of patients with type 2 diabetes. Diabetes. 2007;56(6):1592-9.
11. Wilson-Fritch L, Nicoloro S, Chouinard M, Lazar MA, Chui PC, Leszyk J, et al. Mitochondrial remodeling in adipose tissue associated with obesity and treatment with rosiglitazone. J Clin Invest. 2004;114(9):1281-9.
12. Holmstrom MH, Iglesias-Gutierrez E, Zierath JR, Garcia-Roves PM. Tissue-specific control of mitochondrial respiration in obesity-related insulin resistance and diabetes. Am J Physiol Endocrinol Metab. 2012;302(6):E731-9.
13. Rong JX, Qiu Y, Hansen MK, Zhu L, Zhang V, Xie M, et al. Adipose mitochondrial biogenesis is suppressed in db/db and high-fat diet-fed mice and improved by rosiglitazone. Diabetes. 2007;56(7):1751-60.
14. Bayol SA, Simbi BH, Bertrand JA, Stickland NC. Offspring from mothers fed a 'junk food' diet in pregnancy and lactation exhibit exacerbated adiposity that is more pronounced in females. J Physiol. 2008;586(13):3219-30.
15. Turdi S, Ge W, Hu N, Bradley KM, Wang X, Ren J. Interaction between maternal and postnatal high fat diet leads to a greater risk of myocardial dysfunction in offspring via enhanced lipotoxicity, IRS-1 serine phosphorylation and mitochondrial defects. Journal of molecular and cellular cardiology. 2013;55:117-29.
16. Harder T, Bergmann R, Kallischnigg G, Plagemann A. Duration of breastfeeding and risk of overweight: a meta-analysis. Am J Epidemiol. 2005;162(5):397-403.
17. Owen CG, Martin RM, Whincup PH, Smith GD, Cook DG. Effect of infant feeding on the risk of obesity across the life course: a quantitative review of published evidence. Pediatrics. 2005;115(5):1367-77.
18. Oosting A, Kegler D, Wopereis HJ, Teller IC, van de Heijning BJ, Verkade HJ, et al. Size and phospholipid coating of lipid droplets in the diet of young mice modify body fat accumulation in adulthood. Pediatr Res. 2012;72(4):362-9.
19. Oosting A, van Vlies N, Kegler D, Schipper L, Abrahamse-Berkeveld M, Ringler S, et al. Effect of dietary lipid structure in early postnatal life on mouse adipose tissue development and function in adulthood. Br J Nutr. 2014;111(2):215-26.

20. Baars A, Oosting A, Engels E, Kegler D, Kodde A, Schipper L, et al. Milk fat globule membrane coating of large lipid droplets in the diet of young mice prevents body fat accumulation in adulthood. Br J Nutr. 2016;115(11):1930-7.
21. Bruce KD, Cagampang FR, Argenton M, Zhang J, Ethirajan PL, Burdge GC, et al. Maternal high-fat feeding primes steatohepatitis in adult mice offspring, involving mitochondrial dysfunction and altered lipogenesis gene expression. Hepatology. 2009;50(6):1796-808.
22. Taylor PD, McConnell J, Khan IY, Holemans K, Lawrence KM, Asare-Anane H, et al. Impaired glucose homeostasis and mitochondrial abnormalities in offspring of rats fed a fat-rich diet in pregnancy. Am J Physiol Regul Integr Comp Physiol. 2005;288(1):R134-9.
23. Shelley P, Martin-Gronert MS, Rowlerson A, Poston L, Heales SJ, Hargreaves IP, et al. Altered skeletal muscle insulin signaling and mitochondrial complex II-III linked activity in adult offspring of obese mice. Am J Physiol Regul Integr Comp Physiol. 2009;297(3):R675-81.
24. Simmons RA, Suponitsky-Kroyter I, Selak MA. Progressive accumulation of mitochondrial DNA mutations and decline in mitochondrial function lead to beta-cell failure. J Biol Chem. 2005;280(31):28785-91.
25. Reeves PG, Nielsen FH, Fahey GC, Jr. AIN-93 purified diets for laboratory rodents: final report of the American Institute of Nutrition ad hoc writing committee on the reformulation of the AIN-76A rodent diet. J Nutr. 1993;123(11):1939-51.
26. Gallier S, Vocking K, Post JA, Van De Heijning B, Acton D, Van Der Beek EM, et al. A novel infant milk formula concept: Mimicking the human milk fat globule structure. Colloids and surfaces B, Biointerfaces. 2015;136:329-39.
27. DiGirolamo M, Fine JB. Cellularity measurements. Methods Mol Biol. 2001;155:65-75.
28. Hirsch J, Gallian E. Methods for the determination of adipose cell size in man and animals. J Lipid Res. 1968;9(1):110-9.
29. Vanhoutvin SA, Troost FJ, Hamer HM, Lindsey PJ, Koek GH, Jonkers DM, et al. Butyrate-induced transcriptional changes in human colonic mucosa. PLoS One. 2009;4(8):e6759.
30. Hellemans J, Mortier G, De Paepe A, Speleman F, Vandesompele J. qBase relative quantification framework and software for management and automated analysis of real-time quantitative PCR data. Genome Biol. 2007;8(2):R19.
31. Shepherd D, Garland PB. The kinetic properties of citrate synthase from rat liver mitochondria. Biochem J. 1969;114(3):597-610.
32. Meex RC, Phielix E, Schrauwen-Hinderling V, Moonen-Kornips E, Schaart G, Schrauwen P, et al. The use of statins potentiates the insulin-sensitizing effect of exercise training in obese males with and without Type 2 diabetes. Clin Sci. 2010;119(7):293-301.
33. Kaaman M, Sparks LM, van Harmelen V, Smith SR, Sjolin E, Dahlman I, et al. Strong association between mitochondrial DNA copy number and lipogenesis in human white adipose tissue. Diabetologia. 2007;50(12):2526-33.
34. Warner MJ, Ozanne SE. Mechanisms involved in the developmental programming of adulthood disease. Biochem J. 2010;427(3):333-47.
35. Schrauwen P, Hoeks J, Schaart G, Kornips E, Binas B, Van De Vusse GJ, et al. Uncoupling protein 3 as a mitochondrial fatty acid anion exporter. FASEB J. 2003;17(15):2272-4.
36. Brand MD, Pamplona R, Portero-Otin M, Requena JR, Roebuck SJ, Buckingham JA, et al. Oxidative damage and phospholipid fatty acyl composition in skeletal muscle mitochondria from mice underexpressing or overexpressing uncoupling protein 3. Biochem J. 2002;368(Pt 2):597-603.
37. Cummins TD, Holden CR, Sansbury BE, Gibb AA, Shah J, Zafar N, et al. Metabolic remodeling of white adipose tissue in obesity. Am J Physiol Endocrinol Metab. 2014;307(3):E262-77.
38. Rabol R, Svendsen PF, Skovbro M, Boushel R, Haugaard SB, Schjerling P, et al. Reduced skeletal muscle mitochondrial respiration and improved glucose metabolism in nondiabetic obese women during a very low calorie dietary intervention leading to rapid weight loss. Metabolism. 2009;58(8):1145-52.

39. Menshikova EV, Ritov VB, Toledo FG, Ferrell RE, Goodpaster BH, Kelley DE. Effects of weight loss and physical activity on skeletal muscle mitochondrial function in obesity. Am J Physiol Endocrinol Metab. 2005;288(4):E818-25.
40. Larsen S, Nielsen J, Hansen CN, Nielsen LB, Wibrand F, Stride N, et al. Biomarkers of mitochondrial content in skeletal muscle of healthy young human subjects. J Physiol. 2012;590(Pt 14):3349-60.
41. Kraunsoe R, Boushel R, Hansen CN, Schjerling P, Qvortrup K, Stockel M, et al. Mitochondrial respiration in subcutaneous and visceral adipose tissue from patients with morbid obesity. J Physiol. 2010;588(Pt 12):2023-32.
42. Deveaud C, Beauvoit B, Salin B, Schaeffer J, Rigoulet M. Regional differences in oxidative capacity of rat white adipose tissue are linked to the mitochondrial content of mature adipocytes. Mol Cell Biochem. 2004;267(1-2):157-66.
43. Vernochet C, Damilano F, Mourier A, Bezy O, Mori MA, Smyth G, et al. Adipose tissue mitochondrial dysfunction triggers a lipodystrophic syndrome with insulin resistance, hepatosteatosis, and cardiovascular complications. FASEB J. 2014;28(10):4408-19.
44. Choo HJ, Kim JH, Kwon OB, Lee CS, Mun JY, Han SS, et al. Mitochondria are impaired in the adipocytes of type 2 diabetic mice. Diabetologia. 2006;49(4):784-91.
45. Jorgensen W, Gam C, Andersen JL, Schjerling P, Scheibye-Knudsen M, Mortensen OH, et al. Changed mitochondrial function by pre- and/or postpartum diet alterations in sheep. Am J Physiol Endocrinol Metab. 2009;297(6):E1349-57.
46. Latouche C, Heywood SE, Henry SL, Ziemann M, Lazarus R, El-Osta A, et al. Maternal overnutrition programs changes in the expression of skeletal muscle genes that are associated with insulin resistance and defects of oxidative phosphorylation in adult male rat offspring. J Nutr. 2014;144(3):237-44.
47. Park KS, Kim SK, Kim MS, Cho EY, Lee JH, Lee KU, et al. Fetal and early postnatal protein malnutrition cause long-term changes in rat liver and muscle mitochondria. J Nutr. 2003;133(10):3085-90.

Supplementary Material Chapter 2

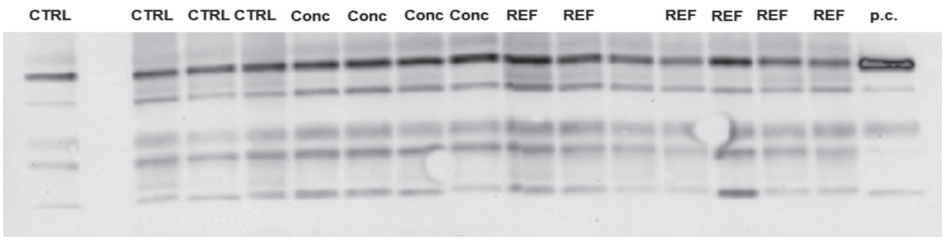

Supplementary Figure S1: OXPHOS western blot. CTRL: sample of CTRL group; Conc: sample of Concept group; REF: sample of REF group; p.c.: positive control sample. (PDF 85 kb)

[1] Danone Nutricia Research, Utrecht, The Netherlands; [2] Department of Pediatrics, University Medical Center Groningen - University of Groningen, Groningen, The Netherlands; [3] Human and Animal Physiology, Wageningen University, Wageningen, The Netherlands.

Chapter 3

Maturation of white adipose tissue function in C57BL/6j mice from weaning to young adulthood

Andrea Kodde[1], Eefje Engels[1], Annemarie Oosting[1], Kees van Limpt[1], Eline M. van der Beek[1,2], and Jaap Keijer[3]

Frontiers in Physiology, 2019; 10: 835
DOI: 10.3389/fphys.2019.00836

Abstract

White adipose tissue (WAT) distribution and WAT mitochondrial function contribute to total body metabolic health throughout life. Nutritional interventions starting in the postweaning period may impact later life WAT health and function. We therefore assessed changes in mitochondrial density and function markers in WAT depots of young mice. Inguinal (ING), epididymal (EPI) and retroperitoneal (RP) WAT of 21, 42 and 98 days old C57BL/6j mice was collected. Mitochondrial density [citrate synthase (CS), mtDNA] and function [subunits of oxidative phosphorylation complexes (OXPHOS)] markers were analyzed, together with gene expression of browning markers (*Ucp1*, *Cidea*). mRNA of ING WAT of 21 and 98 old mice was sequenced to further investigate functional changes of the mitochondria and alterations in cell populations. CS levels decreased significantly over time in all depots. ING showed most pronounced changes, including significantly decreased levels of OXPHOS complex I, II, and III subunits and gene expression of *Ucp1* (PN21-42 and PN42-98) and *Cidea* (PN42-98). White adipocyte markers were higher at PN98 in ING WAT. Analyses of RNA sequence data showed that the mitochondrial functional profile changed over time from "growth-supporting" mitochondria focused on ATP production (and dissipation), to more steady-state mitochondria with more diverse functions and higher biosynthesis. Mitochondrial density and energy metabolism markers declined in all three depots over time after weaning. This was most pronounced in ING WAT and associated with reduced browning markers, increased whitening and an altered metabolism. In particular the PN21-42 period may provide a time window to study mitochondrial adaptation and effects of nutritional exposures relevant for later life metabolic health.

Keywords: white adipose tissue, mitochondria, browning, maturation, uncoupling protein, oxidative phosphorylation, obesity

Introduction

Obesity prevalence is high in adults and considerably increased nowadays in children and adolescents (1). Childhood obesity increases the risk for early onset metabolic diseases, like type 2 diabetes mellitus (T2D) and cardiovascular disease (2). An important link between obesity and metabolic diseases is the metabolic function of the white adipose tissue (WAT), i.e., WAT health (3).

Mitochondrial density in adulthood appears to be strongly correlated to WAT health as shown by a reduced WAT mitochondrial density in obesity (4) and T2D (5). Nutrition may regulate WAT function as feeding a high fat diet reduced WAT mitochondrial density (6), a process that is already initiated after 5 days of western style diet (WSD) (7), while caloric restriction and diets enriched in poly-unsaturated fatty acids increased WAT mitochondrial density, oxidative capacity and biogenesis (8, 9). Dependent on their location in the body, WAT depots differ in their impact on metabolic health (10, 11). Visceral WAT is located in the abdominal cavity and visceral WAT mass is inversely correlated to total body insulin sensitivity and as such considered a risk factor for development of the metabolic syndrome (12, 13). In contrast, subcutaneous WAT is located directly under the skin and is shown to have a higher oxidative capacity compared to the visceral depots in mice (14).

Experimental evidence suggests that growth and distribution of WAT as well as mitochondrial density of WAT depots can be programmed by early life environmental factors. For example, maternal obesity, over-nutrition or undernutrition during pregnancy can all drive increased visceral adiposity and an adapted mitochondrial density in rodent offspring (15-18). In addition, mild caloric restriction or a high fat diet exposure in the lactation period also programmed adult adiposity and metabolic health of pups (19, 20). Those studies show that suboptimal nutrient conditions in early life can have long-term metabolic consequences. Programming of the oxidative and storage capacity of WAT, which develops from the third trimester of gestation until adolescence (21), may be an underlying mechanism.

The postnatal development of WAT includes differentiation from progenitor cells to fully developed adipocytes containing lipid droplets, a process starting before birth in subcutaneous depots and after birth in visceral depots (22, 23). After weaning WAT depots continue to grow and adipocytes increase in size (hypertrophy) and number (hyperplasia) in a depot specific manner (24). Furthermore, WAT depots develop postnatally from a white phenotype at PN10 to a brown phenotype at PN20 where the majority of the adipocytes are multilocular and express UCP1, after which these cells disappear again and are replaced by unilocular adipocytes which only express UCP1 upon cold-induction (25-27).

Many nutritional intervention studies, including postnatal programming studies, i.e., studies with a nutritional intervention in early life with the aim to improve adult metabolic health (28-31), take the postweaning period (around PN21) as starting point. Comprehensive and extended comparison of postweaning changes of markers for mitochondrial function and WAT browning in different WAT depots is crucial for the interpretation of those studies. Therefore, we here investigate early life changes in markers for mitochondrial density, function and browning in the developing WAT depots with the aim to substantiate and extend, in terms of number of markers and WAT depots analyzed, available research. To this end we collected inguinal (ING), epididymal (EPI) and retroperitoneal (RP) WAT, of 21, 42 and 98 days old mice, housed under standardized experimental conditions (ambient temperature) and comprehensively measured markers of mitochondrial density, function and browning as well as the effect of a WSD on these markers. In addition, we newly examined changes within mitochondrial functional profile by analyzing transcription of all established mitochondrial proteins and categorize them to function.

Material and methods

Study Design

Mice were kept at the animal facility of Intravacc (Bilthoven, Netherlands) under a 12 h light – 12 h dark cycle (lights on at 06:00 h). Room temperature and humidity were kept at constant level (21 ± 2°C and 50 ± 5%, respectively). This housing temperature was chosen to adhere to the most common temperature used for animal experiments. C57BL/6jOlaHsd breeders were purchased from Harlan (Envigo since 2015, Horst, Netherlands), acclimatized for 2 weeks, time mated and fed a American Institute of Nutrition-93G synthetic diet (AIN93G) (32) during breeding, pregnancy and lactation. Within 2 days after birth, litters were culled to four males and two females and randomly assigned to a dam. At postnatal day 21 (PN21) female mice were killed, while male mice were weaned, housed in littermate-pairs and continued on AIN93G until PN42. From PN42 until sacrifice at PN98 mice were fed AIN93M (32) or WSD (containing 39 en% fat; diet composition in **Table 1**). Food and water were available *ad libitum* during the entire experimental period. A very limited amount of food was supplied the night before dissection to ensure that the animals were in a fasted state (approximately 8 h). Body weight and food intake were measured twice a week. At different time points (PN21, PN42, and PN98) mice were sacrificed to assess the development of WAT depots and the effect of the WSD challenge, resulting in the following experimental groups (i) PN21 (n = 8), (ii) PN42 (n = 8), (iii) PN98-AIN (n = 11), and (iv) PN98-WSD (n = 11; **Figure**

1A). At dissection mice were anesthetized (isoflurane/N2O/O2), terminated by bleeding (eye extraction) and ING, EPI, and RP WAT were collected, weighted, snap frozen and stored at -80°C.

Table 1: Diet composition

Diet		**AIN93GG**	**AIN93M**	**WSD**
Carbohydrates	(g/kg)	629.5	720,7	499.5
Dextrose	(g/kg)	-	50	150
Sucrose	(g/kg)	100	100	-
Starch	(g/kg)	397.5	415.7	150
Maltodextrin	(g/kg)	132	155	199.5
Proteins	(g/kg)	203	141.8	203
Casein	(g/kg)	200	140	200
Cystine	(g/kg)	3.0	1.8	3.0
Fat	(g/kg)	70	40	200
Soy oil	(g/kg)	70	40	30
Lard	(g/kg)	-	-	169
Cholesterol	(g/kg)	-	-	1.0
Fiber (Cellulose)	(g/kg)	50	50	50
Vitamin & mineral mix	(g/kg)	47.5	47.5	47.5
Energy %				
Carbohydrates	(en%)	64	76	43
Proteins	(en%)	21	15	18
Fat	(en%)	16	9	39

Sample Homogenization

The EPI, ING, and RP WAT depots were homogenized with a Cellcrusher (Cellcrusher, Cork, Ireland) and aliquots of the resulting homogenized powder where made to enable separate analyses. EPI and RP WAT at PN21 were too small to make aliquots and were therefore only used for RNA extractions and enzyme activity measurements, respectively. In addition, RP WAT of PN42 was too small to analyze mitochondrial DNA levels.

Gene Expression

RNA of EPI, ING and RP WAT was isolated using Trizol (Thermo Fisher Scientific, Landsmeer, Netherlands) followed by purification with a RNeasy Mini Kit (Qiagen Benelux b.v., Zwijndrecht, Netherlands) including a DNase treatment with a RNase-

free DNase Set (Qiagen Benelux b.v.) as previously described (33). RNA quantity and chemical purity were assessed with the Nanodrop 2000 (Thermo Fisher Scienctific) and integrity with the Agilent 2100 Bioanalyzer (Agilent, Santa Clara, CA, United States). iScriptcDNA synthesis kit (Bio-Rad, Veenendaal, Netherlands) was used according to manufacturer instructions. 6.25 ng cDNA was used as input for each Q-PCR reaction. SYBR Select Master Mix (Life Technologies Europe, Bleiswijk, Netherlands) was used according to manufacturer instructions and qPCR was performed with a QuantStudio 6 Flex Real-Time PCR System (Life Technologies Europe). mRNA expression of cell death-inducing DNA fragmentation factor, alpha subunit-like effector A (*Cidea*), Leptin (*Lep*), mesoderm specific transcript (*Mest*, also known as *Peg1*), delta-like 1 homolog (*Dlk1*, better known as *Pref1*, which will be used here) and uncoupling protein 1 (*Ucp1*) were analyzed relative to mean expression of two reference genes, hypoxanthine guanine phosphoribosyl transferase (*Hprt*) and zinc finger, AN1-type domain 6 (*Zfand6*). For a complete list of primers used see Table 2. Normalization of qPCR data was performed using the qbaseC (Biogazelle, Genth, Belgium) based on the method of relative normalization as described (29, 34). Reference genes *Hprt1* and *Zfand6* were selected based on transcriptome data and stability checked by Q-PCR analyses. Primers for *Ucp1* were purchased from Biorad, all other primers from Biolegio (Biolegio, Nijmegen, Netherlands).

Enzyme Activity

Citrate synthase (CS) and hydroxyacyl-Coenzyme A dehydrogenase (HADH) activities were measured as described (29, 35).

Table 2: Primer sequences

Gene name	NCBI Reference number	Forward primer (5' - 3')	Reverse primer (5' - 3')
Genes of interest:			
Cidea	NM_007702.2	aggccgtgttaaggaatctg	cccagtactcggagcatgta
Lep	NM_008493_3	aggatgacaccaaaaccctcat	agtccaagccagtgaccctct
Mest	NM_008590.1	tcagtgacaagccgagacca	gttgattctgcggttctggag
Pref1	NM_010052.5	tgcgaggctgacaatgtctg	atgcactgccatggttcctt
Ucp1		assay ID qMmuCID0005832	
Reference Genes:			
Hprt	NM_013556.2	ggacctctcgaagtgttggat	ccaacaacaaacttgtctggaa
Zfand6	NM_022985.6	tgggacttactgggtttgaa	ttctcagcagcatcagcttt
DNA primers:			
mt-Nd1	NC_005089.1	accaatacgccctttaacaac	aatgggtgtggtattggtagg
Lpl	NM_008509	Tcctgatgacgctgattttg	atgtcaacatgccctactgg

OXPHOS and UCP1 Protein Levels

Protein levels of five subunits (NDUFB8, SDHB, UQCRC2, MTCOI, ATP5A1) representing the five oxidative phosphorylation (OXPHOS) complexes (I–V, respectively) were measured with western blot (29, 36). Briefly, 15 mg of total protein per sample was used for SDS-PAGE, transfer to a PVDF membrane was done using the TransBlot Turbo (Biorad). Blots were blocked with 5% Protifar (Nutricia, Zoetermeer, Netherlands), incubated with Mito-Profile Total OXPHOS rodent western blot antibody cocktail (Abcam, Cambridge, United Kingdom) as primary antibody and ECL anti mouse IgG (Thermo Fisher Scienctific) as a secondary antibody. OXPHOS protein levels, detected with Supersignal West Dura (Thermo Fisher Sceintific), were related to total protein levels as analyzed by Coomassie brilliant blue staining. Protein levels were detected with the Chemidoc XRS and analyzed by Quantity One (Biorad). The same procedure was used for detection of UCP1 protein levels, except that 5% BSA was used as blocking agent, rabbit anti mouse UCP1 (Abcam, Cambridge, United Kingdom) was used as primary antibody, goat anti rabbit IgG (Santa Cruz, Dallas, United States) as secondary antibody and Supersignal West Femto (Thermo Fisher Scientific) was used for signal detection. A representative Western blot stained for the OXPHOS and for UCP1 proteins and the corresponding Coomassie brilliant blue stained blots are shown in **Supplementary Figures 3, 4**, respectively.

Mitochondrial DNA Density

Mitochondrial copy number was assessed by the ratio (ΔCt) between nuclear DNA (abundance of lipoprotein lipase (*Lpl*) DNA) and mitochondrial DNA (abundance of mitochondrial gene NADH dehydrogenase 1 (*mt-Nd1*) DNA) (37). Briefly, total DNA was isolated with the QIAamp DNA micro kit (Qiagen Benelux), following instructions of the manufacturer. DNA quantity was determined with Quant-iT Picogreen dsDNA assay kit (Thermo Fisher Scientific). 10 ng input DNA was used for each qPCR reaction. Primers sequences are shown in **Table 2**.

mRNA Sequencing

RNA samples of ING depots from PN21 and PN98 (n = 4 per time point) were used for mRNA sequencing analysis (NXT-Dx, Gent, Belgium). After RNA quantification (Rediplate 96 Ribogreen RNA Quantitation kit, Life Technologies), RNA libraries were prepared (NEBNext Ultra Directional RNA library Prep Kit for Illumina, New England Biolabs INC., Ipswich, United Kingdom), intact poly(A)+ RNA was isolated (NEBNext poly(A) mRNA Magnetic isolation Module, New England Biolabs INC., Ipswich, United Kingdom) and cDNA libraries were sequenced (paired end, 100 base pairs) on an Illumina HiSeq

sequencer (Illumina Netherlands, Eindhoven, Netherlands). FASTQ sequences were generated using the llumina Casava pipeline 1.8.2. Quality of the data was assessed using the Illumina Chasitity filter and quality of the reads using the FASTQC quality control tool version 0.10.0. Subsequently, data were mapped on the mouse reference genome mm10 using STAR Aligner 2.3.0 and analyzed with Cufflinks v2.1.1 on Gencode annotation v15. mRNA sequence data have been deposited at the NCBI Gene expression omnibus (GSE116313).

Data Analyses mRNA Sequence Data

Data analysis included contrast analysis (R package Limma) between PN21 and PN98, omitting transcripts whit a FPKM (fragments per kilobase million) of zero in at least one of the samples and including transcripts with an average FPKM $>$ 2 at PN21 or PN98. Principal Component Analysis (PCA) was performed to visualize the samples and results are reported in **Supplementary Figure 1**. Transcripts with a p-value below 0.05 were used for Ingenuity Pathway Analysis (Qiagen Bioinformatics, Aarhus, Denmark) and targeted analysis as described below. The data set was examined for changes in brown and white (pre)adipocyte markers derived from Gesta et al. (38) to get insight in the change in cell population in ING WAT between PN21 and 98. To further explore changes in mitochondrial function, a list of genes encoding proteins with strong support of mitochondrial localization was derived from Mitocarta (Mouse MitoCarta 2.0, Broad institute), checked for their regulation in the data set, annotated with Nextprot (SIB Swiss institute for bioinformatics) and sorted per function category. When more than one transcript per gene was present in the data set, the transcript with the lowest p-value was used. Some of the genes are listed as non-mitochondrial (11 of 327) in the results table, because these are annotated in Nextprot having a ribosomal, extracellular matrix or cell membrane localization rather than a mitochondrial localization. Next to this, a list of genes known to be involved in mitophagy was examined in the same data set, to get a better understanding of underlying mechanisms for WAT whitening.

Statistical Analysis

SPSS 19.0 (SPSS Benelux, Gorinchem, Netherlands) was used for statistical analyses. Gaussian distribution was tested with Levene's test for equality of error variances in all parameters. Differences over time (per depot) were analyzed using Univariate ANOVA. Depot differences over time were analyzed using a two-way ANOVA (Brown-Forsyte) with time and depot as factors. A t-test was used to analyze the effect of the WSD. Data that did not show a Gaussian distribution was analyzed by Kruskall-Wallis for time

differences and Mann-Whitney for the adult diet effect. qPCR data is presented as mean relative expression (scaled to average expression) + SEM and all other data is displayed as mean + SEM. Differences were considered significant at $p<0.05$ and tendency was reported when $0.05<p<0.1$. Correlations were analyzed with Pearson's test.

Results

Body Weight, WAT Weight and Markers of Adiposity

Body weight increased significantly between weaning (PN21) and young adulthood (PN98) ($p<0.001$) (**Figure 1B**), as did the weight of ING, EPI and RP WAT ($p<0.01$; **Figures 1C–E**). In accordance with increased WAT weight, gene expression levels of adiposity (*Lep*) and adipocyte expansion (*Mest*) markers increased over time in EPI WAT ($p<0.05$ for *Lep* and $p<0.001$ for *Mest*) and RP WAT ($p=0.06$ for *Lep* and $p<0.05$ for *Mest*), but not ING WAT (**Figures 1F–K**). *Mest* and *Lep* expression levels were increased in ING WAT upon WSD exposure ($p<0.001$ for both parameters; Figures 1F,I). *Lep* expression levels were also moderately increased in EPI and RP WAT upon WSD ($p<0.05$ for EPI and $p=0.08$ for RP WAT; Figures 1G,H), whereas *Mest* expression levels were unaffected upon WSD in EPI and RP WAT (Figures 1J,K). *Pref1* expression levels, a pre-adipocyte number marker, decreased in all depots over time ($p<0.001$) and most pronounced from PN21 to 42 (**Figures 1L–N**). In contrast, *Pref1* expression levels were in EPI and RP WAT not affected by the WSD, but levels were slightly elevated in ING WAT ($p<0.01$).

Markers of Mitochondrial Density

Mitochondrial density measured by citrate synthase (CS) levels, assayed as activity, decreased over time in all WAT depots ($p<0.01$; **Figures 2A–C**). Between PN21 and PN42 CS levels decreased substantially (56%) in ING WAT ($p<0.05$). CS levels were not affected by the WSD in any depot (Figures 2A–C). Activity-based levels of hydroxyacyl-Coenzyme A dehydrogenase (HADH), a mitochondrial enzyme involved in b-oxidation, decreased over time in ING and EPI WAT ($p<0.001$; **Figures 2G,H**), but not in RP WAT (**Figure 2I**). However, HADH activity tended to decrease in RP WAT upon WSD exposure ($p=0.07$; Figures 2G–I). When mitochondrial density was measured as mtDNA copy number no significant decrease over time or upon WSD was found (**Figures 2D–F**).

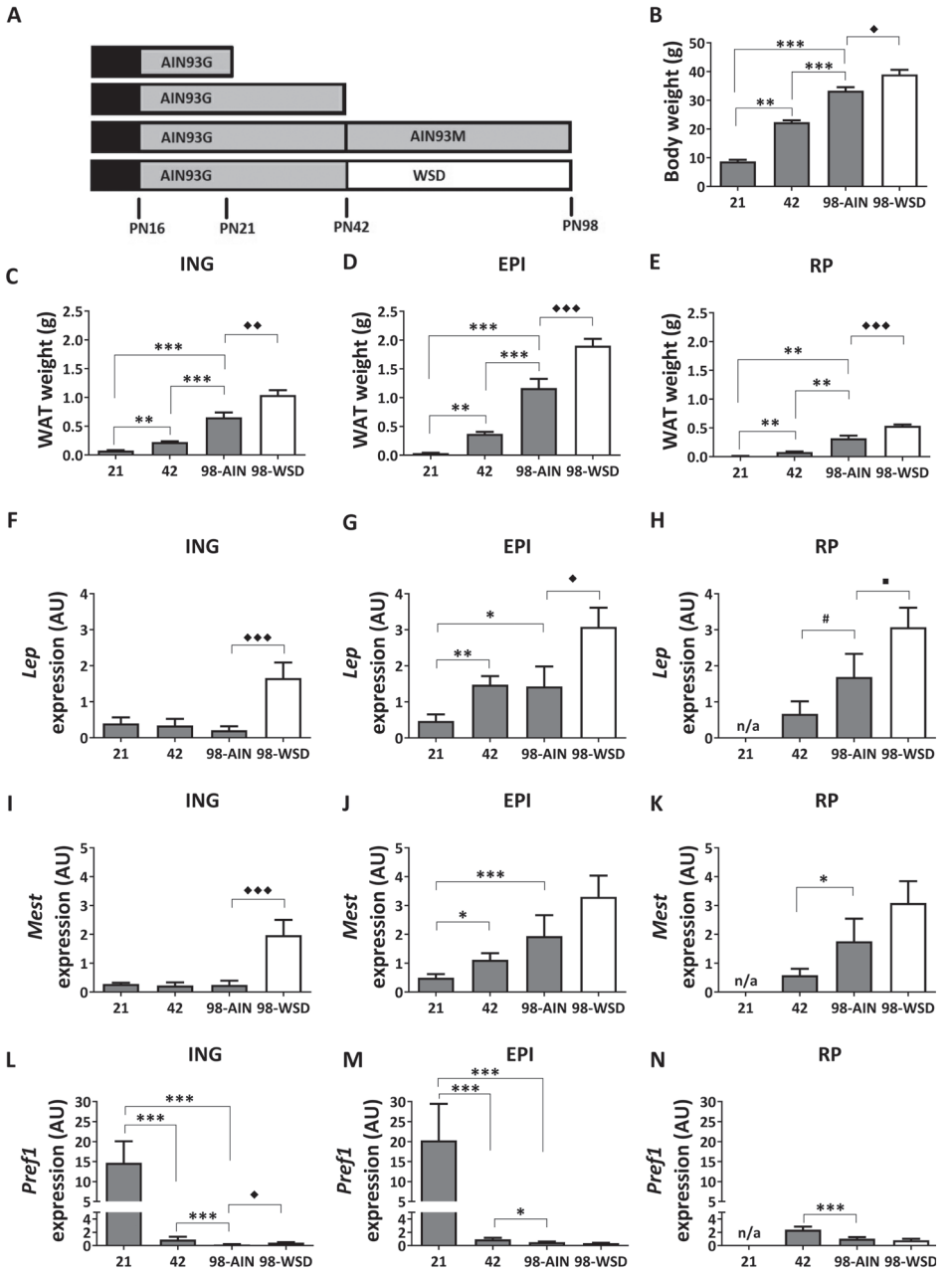

Figure 1: Study design, development of body weight, WAT weight and gene expression of adiposity markers between PN21 and PN98. (**A**) Study design with at PN16 start of weaning to full weaning at PN21; (**B**) body weight; weight of (**C**) ING WAT, (**D**) EPI WAT, (**E**) RP WAT; *Lep* expression in (**F**) ING WAT, (**G**) EPI WAT, (**H**) RP WAT; *Mest* expression in (**I**) ING WAT, (**J**) EPI WAT, (**K**) RP WAT; *Pref1* expression in (**L**) ING WAT, (**M**) EPI WAT and (**N**) RP WAT. PN: postnatal day; AIN: AIN-93G diet from PN16-42 and AIN-93M from PN42-98 (gray); WSD: western style diet (white); n/a: data not available. Data expressed as mean + SEM. WAT weight: n = 8 for PN 21 and PN42, n = 11 for PN98;

Figure 1: Continued
gene expression: n = 8 for PN 21 and PN42, n = 11 for PN98, no data available for RP WAT at PN21. Time and WSD effects were analyzed separately; time effect: *p<0.05; **p<0.01; ***p<0.001; #0.05<p<0.1; WSD effect: ◆p<0.05; ◆◆p<0.01; ◆◆◆p<0.001; ■0.05<p<0.1.

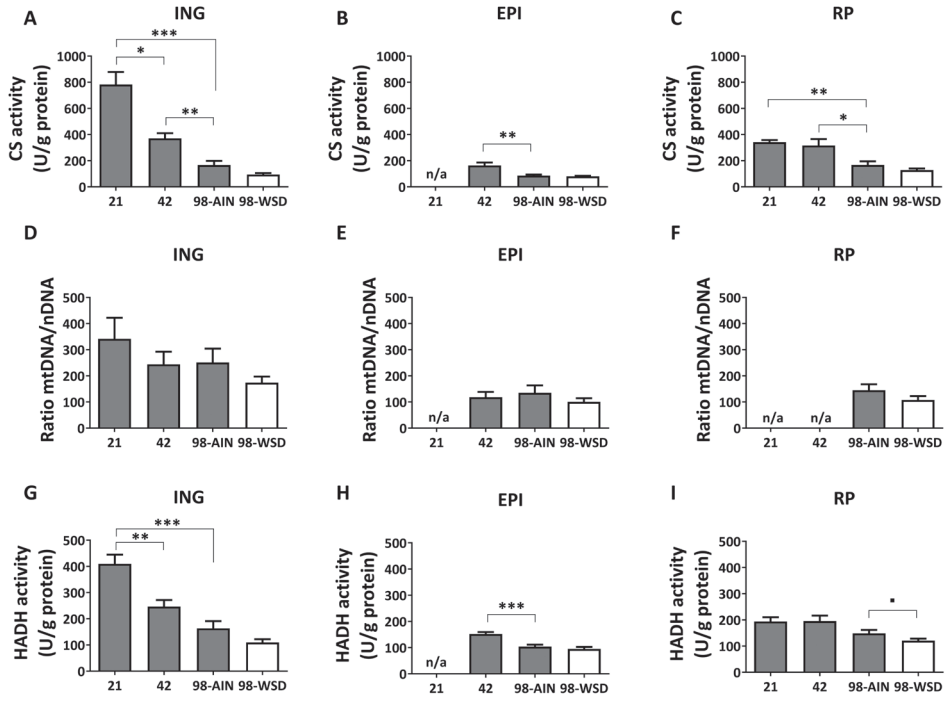

Figure 2: Changes in mitochondrial content markers, citrate synthase (CS), mtDNA and hydroxyacyl-Coenzyme A dehydrogenase (HADH), between PN21 and PN98. CS activity in (**A**) ING WAT, (**B**) EPI WAT, (**C**) RP WAT; mtDNA copy number in (**D**) ING WAT, (**E**) EPI WAT, (**F**) RP WAT; HADH activity in (**G**) ING WAT, (**H**) EPI WAT, and (**I**) RP WAT. PN: postnatal day; AIN: AIM93-M diet; WSD: western style diet. Data expressed as mean + SEM, n = 8 for PN 21 and PN42 and n = 11 for PN98, no data available (n/a) for EPI WAT at PN21 and for RP WAT at PN21 and PN42 for mtDNA copy number. Time and WSD effects were analyzed separately; time effect: *p<0.05; **p<0.01; ***p<0.001; WSD effect: ■0.05<p<0.1.

Markers of Mitochondrial Oxidative Capacity

Mitochondrial oxidative capacity, measured by protein levels of five subunits representing the five oxidative phosphorylation (OXPHOS) complexes, decreased in ING WAT over time for NDUFB8 (p<0.01; **Figure 3A**), SDHB and UQCRC2 (p<0.01; **Figures 3D,G**) and upon WSD for UQCRC2 (Figure 3G) and MTCOI (**Figure 3J**). ATP5A protein expression decreased over time in EPI WAT (p<0.05; **Figure 3N**) but was not affected in the ING WAT (**Figure 3M**). Other complexes of EPI WAT and all complexes in RP WAT remained stable over time and were not affected by the WSD (Figure 3).

Markers of WAT Browning

Gene expression levels of the uncoupling protein *Ucp1*, as marker for browning of WAT, was relatively high in ING WAT at PN21 and decreased substantial over time ($p<0.001$; **Figure 4A**). *Ucp1* expression levels were low in visceral depots, but also decreased over time in EPI WAT ($p<0.01$; **Figures 4B,C**). *Cidea* gene expression levels were substantially higher in ING WAT compared to visceral depots (**Figures 4D,E**), but in contrast to *Ucp1* remained stable in ING WAT between PN21 and 42, after which *Cidea* levels declined from PN42 to 98 ($p<0.01$). UCP1 protein levels tended to decline from PN21 to 42 and 98 ($p=0.09$; **Figure 4G**) and were low and not changing over time in the visceral depots (**Figures 4H,I**). Upon WSD exposure, *Ucp1* and *Cidea* gene expression levels decreased in ING WAT ($p<0.05$), but remained unaffected in the visceral EPI and RP WAT depots. UCP1 protein levels tended to decline upon the WSD exposure in ING WAT ($p=0.1$), was not affected by the WSD in the EPI WAT but increased upon the WSD in RP WAT ($p<0.01$). *Ucp1* and *Cidea* expression levels did not change over time in RP WAT (**Figures 4C,F**). It should be noted that UCP1 protein levels were very heterogeneous at PN98, showing some animals with much higher levels than on average.

Depot Differences

ING WAT had overall lower expression of adiposity markers (*Lep*, *Mest*; $p<0.001$) and higher levels of mitochondrial (CS and HADH activity and OXPHOS subunits I – IV; $p<0.001$) and browning markers (*Ucp1* and *Cidea* gene expression and UCP1 protein levels; $p<0.001$) compared to both EPI and RP WAT. Especially at PN21 and 42 CS and HADH levels were higher in ING compared to EPI and RP WAT ($p<0.01$) and at PN42 levels of OXPHOS complexes I–IV were also higher in ING compared to RP and EPI WAT ($p<0.01$). Subsequent decline in CS, HADH and OXPHOS complexes I–IV levels was steeper in ING WAT compared to the visceral depots and resulted in similar CS, HADH and OXPHOS subunit II levels in ING WAT and RP WAT and HADH and subunit II levels being similar in ING WAT and EPI WAT at PN98. *Ucp1* and *Cidea* gene expression levels were also significant higher in ING compared to EPI and RP WAT at PN21 and 42 ($p<0.01$) and had a steeper decline over time resulting in comparable *Ucp1* gene expression levels in ING and RP WAT at PN98. OXPHOS complex I-IV from the electron transport system, which drives ATP synthesis by OXPHOS complex V, the final step that is bypassed by UCP1 mediated uncoupling. Remarkably, unlike complex I–IV, levels of complex V (represented by ATP5A) were similar between depots.

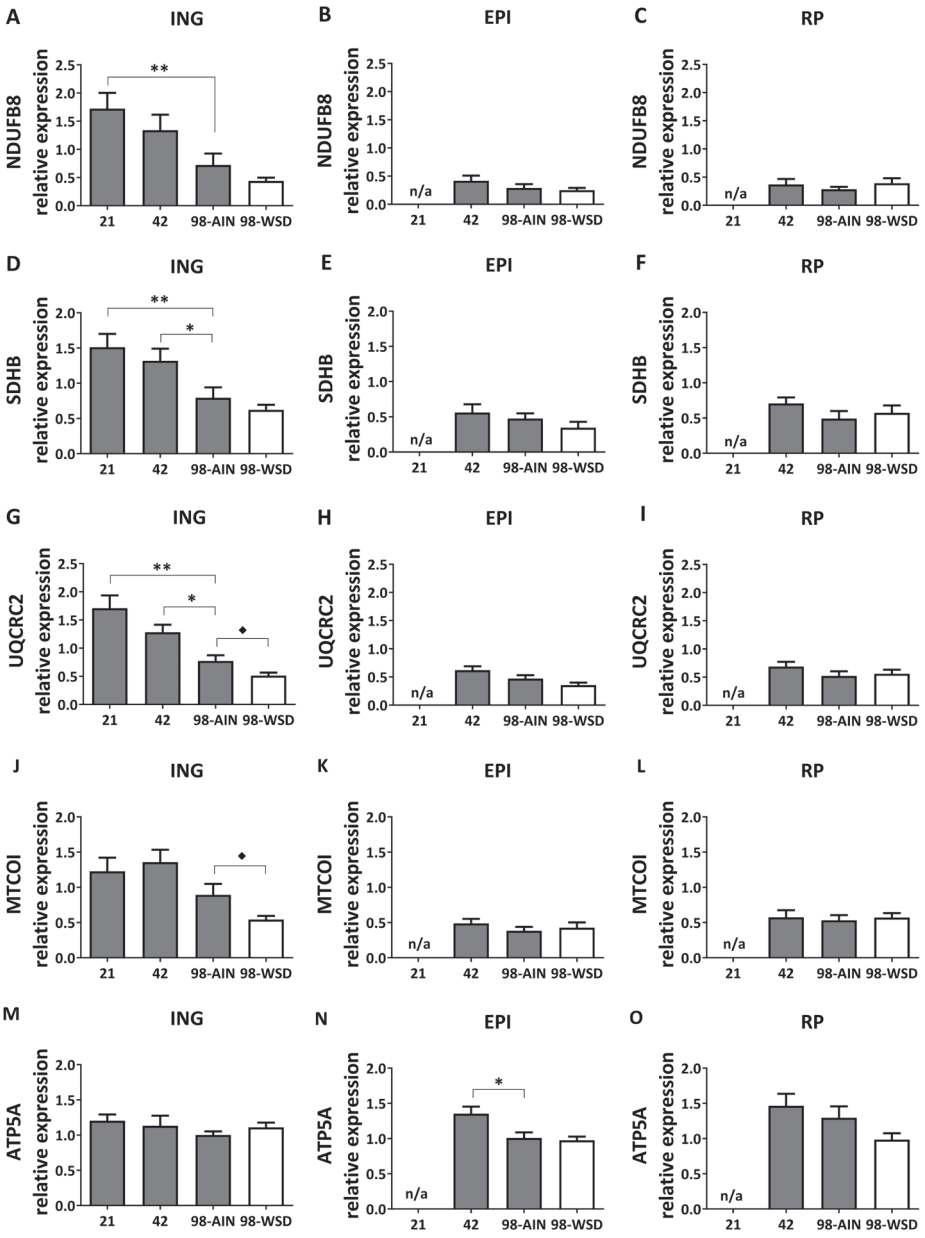

Figure 3: Changes in protein levels of subunits of oxidative phosphorylation complexes I-V between PN21 and PN98. NDUFB8 (Complex I) levels in (**A**) ING WAT, (**B**) EPI WAT, (**C**) RP WAT; SDHB (complex II) levels in (**D**) ING WAT, (**E**) EPI WAT, (**F**) RP WAT; UQCRC2 (complex III) levels in (**G**) ING WAT, (**H**) EPI WAT, (**I**) RP WAT; MTCOI (complex IV) levels in (**J**) ING WAT, (**K**) EPI WAT, (**L**) RP WAT; ATP5A (complex V) levels in (**M**) ING WAT, (**N**) EPI WAT and (**O**) RP WAT. PN: postnatal day; AIN: AIM93-M diet; WSD: western style diet. Data expressed as mean expression levels corrected for total protein expression (Coomassie staining) + SEM, n = 8 for PN 21 and PN42 and n = 11 for PN98, no data available (n/a) for EPI and RP WAT at PN21. Time and WSD effects were analyzed separately; time effect: *p<0.05; **p<0.01; WSD effect: ◆p<0.05.

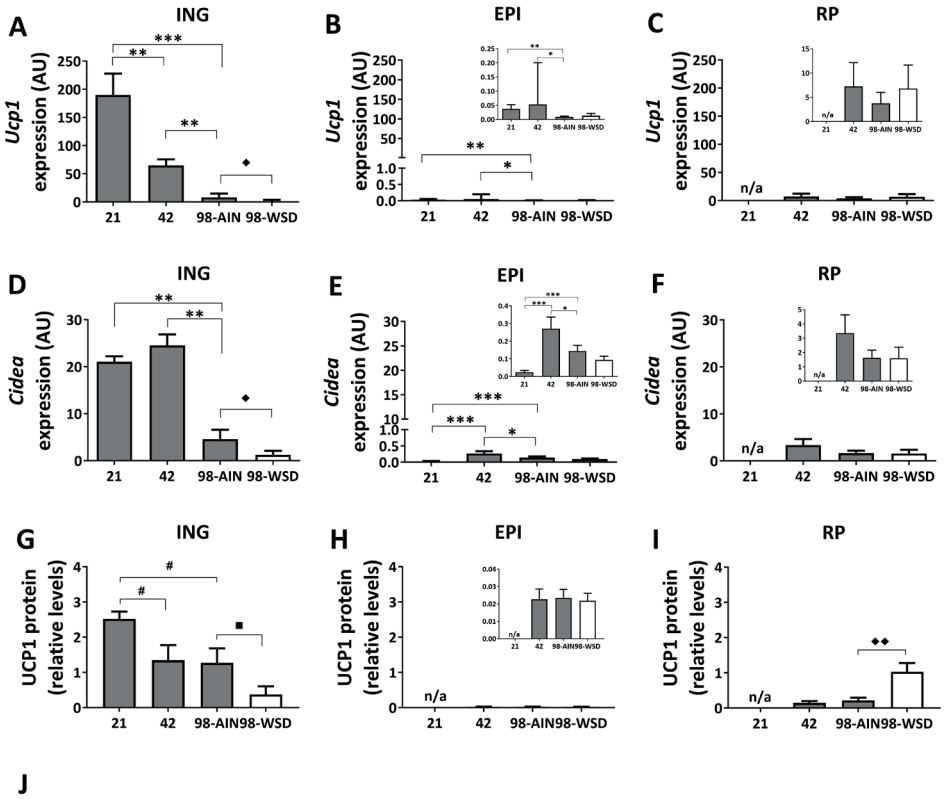

J

White adipocyte		Brown adipocyte		White preadipocyte		Brown preadipocyte	
Aldh1a1	3.5	*Cox7a1*	-5.6	*Cfb*	2.0	*Fn1*	-2.3
App	1.7	*Cpn2*	-9.0			*Maged2*	-4.7
Fads3	3.4	*Ppargc1a*	-2.2			*Mme*	2.3
Fbn1	-3.3	*S100b*	-1.9			*Myl1*	3.6
Lep	4.7	*Ucp1*	-7.3			*Mylpf*	4.7
Serpina3k	5.1					*Ndn*	-2.6
						Snrpa	-1.4
						Tnnt3	12.6

Figure 4: Changes in gene expression of browning markers between PN21 and PN98. *Ucp1* gene expression in (**A**) ING WAT, (**B**) EPI WAT, (**C**) RP WAT; *Cidea* expression in (**D**) ING WAT, (**E**) EPI WAT, (**F**) RP WAT; UCP1 protein levels in (**G**) ING WAT, (**H**) EPI WAT, (**I**) RP WAT; and (**J**) Regulation of genes selective for brown or white (pre)adipocytes over time, analyzed with mRNA sequencing, gene list derived from Gesta et al. (38) and expression levels of transcripts with p<0.05 included in table. Inserts in figures B, C, E, F, and H show the same data with adapted y-axis for better visualization of the low expression data. PN: postnatal day; AIN: AIM93-G diet; WSD: western style diet. Gene expression data expressed as mean + SEM and protein levels as mean levels corrected for total protein (Coomassie staining) + SEM, n = 8 for PN 21 and PN42, n = 11 for PN98, no data available (n/a) for RP WAT at PN21. Time and WSD effects were analyzed separately; time effect: *p<0.05; **p<0.01; ***p<0.001; #0.05<p<0.1; WSD effect: ◆p<0.05; ◆◆p<0.01; ■0.05<p<0.1. Sequence data reported as fold changes between postnatal day 21 over 98. Up regulated values red and down regulated values green.

Pathway Analysis of mRNA Sequence Data

To better understand the changes in mitochondrial density and function markers in ING WAT over time, mRNA of ING WAT at PN21 and 98 was sequenced (n = 4 per time point). For pathway analysis 5040 transcripts with a p-value <0.05 were used, resulting in a list of pathways which were significant regulated over time (**Table 3**). Most differentially regulated pathways include those involved in regulation of cell proliferation and growth and pathways involved in hormonal regulation and immune response. Protein synthesis was down regulated over time and pathways involved in the FA metabolism were up regulated over time. Overlap between the regulated pathways was plotted as a network map, showing much overlap between pathways, including those involved in the regulation of cell proliferation and growth as well as pathways involved in hormonal regulation and immune response.

Table 3: List of significant regulated pathways at PN98 as analyzed by Ingenuity pathway analysis (IPA). Expression of transcripts determined with mRNA sequencing and data analyzed with ingenuity Pathway Analysis (Qiagen Bioinformatics, Aarhus, Denmark). Difference between postnatal day 21 over 98.

Canonical Pathways	-log(p-value)	Ratio	z-score
Top 10 down regulated pathways			
EIF2 signaling	12.10	0.34	-3.833
Estrogen-mediated S-phase entry	5.96	0.58	-3.051
STAT3 pathway	5.58	0.37	-0.577
Cyclins and cell cycle regulation	4.96	0.35	-2.524
Regulation of eIF4 and p70S6K signaling	4.13	0.27	-1.155
mTOR signaling	4.02	0.25	-0.408
Acute phase response signaling	4.00	0.26	-1.333
Phospholipase C signaling	3.78	0.24	-2.359
NF-κB activation by viruses	3.68	0.30	-2.353
14-3-3-mediated signaling	3.61	0.27	-0.378
Top 10 up regulated pathways			
Cell cycle: G1/S checkpoint regulation	5.72	0.39	1.706
Aryl hydrocarbon receptor signaling	5.45	0.30	2.000
Protein kinase A signaling	4.71	0.23	1.732
Cell Cycle: G2/M DNA damage checkpoint regulation	4.44	0.39	1.414
Androgen signaling	4.34	0.30	0.535
Sumoylation pathway	4.02	0.30	1.043
PPARα/RXRα activation	3.75	0.25	2.874
LXR/RXR activation	3.20	0.26	0.557

Table 3: Continued

Canonical Pathways	-log(p-value)	Ratio	z-score
PPAR signaling	2.74	0.27	2.858
Apoptosis swignaling	2.67	0.27	0.816
Top 10 pathways without available activity pattern*			
Cell cycle control of chromosomal replication	8.08	0.55	NaN
RAR activation	6.75	0.30	NaN
Estrogen receptor signaling	6.15	0.32	NaN
Adipogenesis pathway	6.00	0.31	NaN
Glucocorticoid receptor signaling	5.47	0.25	NaN
Mitochondrial dysfunction	3.87	0.26	NaN
Lipid antigen presentation by CD1	3.85	0.46	NaN
T cell receptor signaling	3.72	0.28	NaN
TR/RXR activation	3.46	0.29	NaN
Assembly of RNA polymerase II complex	3.24	0.34	NaN

* No information on activity pattern was available in IPA and no Z-score calculated as a consequence

Two pathways were less connected to the central network: “mitochondrial dysfunction” and “lipid antigen presentation by CD1” (**Supplementary Figure 2**). The “mitochondrial dysfunction” pathway contained genes representing subunits of the oxidative phosphorylation and other genes involved in the function of mitochondria, and its IPA name follows the general idea that downregulation of the genes contained in this pathway is associated with dysfunctional mitochondria, like in T2D, Alzheimer’s or Parkinson’s disease. Although ingenuity pathway analysis did not indicate a direction for the change in the mitochondrial dysfunction pathway, 35 of the 44 regulated genes in this pathway were down regulated over time, what may indicate that mitochondrial function is reduced at PN98 compared to PN21 in ING WAT (**Supplementary Table 1**).

Targeted Analysis of mRNA Sequence Data

A list of brown and white preadipocyte and adipocyte markers was extracted from literature (38) and checked for their expression in the mRNA sequence data (the 5040 transcripts with $p<0.05$) to get insight in possible changes in cell populations in ING WAT between PN21 and 98. Expression levels of brown adipocytes markers declined and levels of white adipocytes markers increased from PN21 to 98 (**Figure 4G** and **Supplementary Table 2** for the complete list of markers). For preadipocytes the picture is less clear, some brown preadipocytes markers were up and others were down regulated over time.

Of note, the list of markers was extracted from the review of Gesta et al. (38) and based on results of different experiments, the brown preadipocytes markers which were up regulated over time originate from another experiment than the down regulated markers (39, 40). The list of white preadipocytes markers is short and only one of these genes was abundant in our data set and up regulated over time.

A list of genes of which mitochondrial localization is strongly supported (Mitocarta, 1158 genes) were checked for expression in the data set to further explore functional changes of the mitochondria over time. 327 genes of this list were identified in the data set, of which 231 gene were down regulated, 88 up regulated and 8 genes had discrepancy in regulation between different transcripts. Genes involved in energy metabolism and protein syntheses were down regulated over time, including oxidative phosphorylation, citric acid (TCA) cycle, b-oxidation, import, transport and translation. The up regulated genes showed more diversity in function, including glycolytic metabolism, lipid synthesis, biosynthesis and mitophagy. The list with genes categorized to function is shown in **Supplementary Tables 3, 4**. A summary of these findings is presented in **Figure 5**.

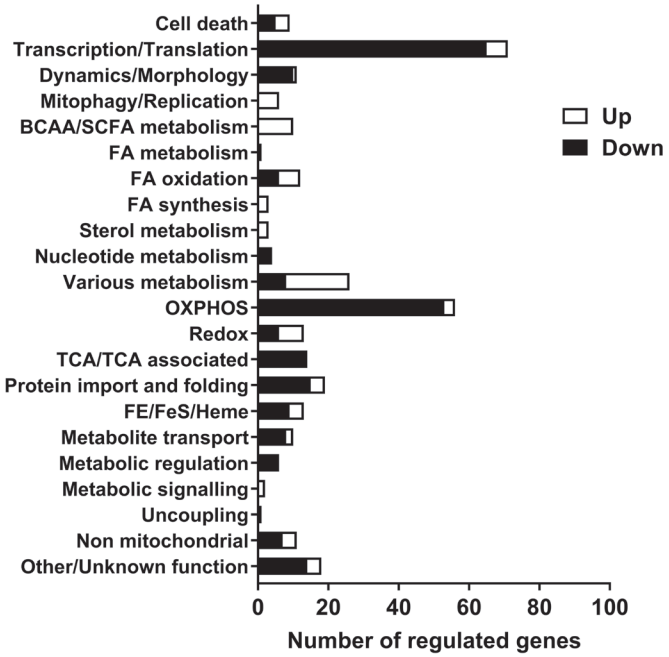

Figure 5: Functional categorization of regulated genes (PN21 over 98) with a strong support for mitochondrial localization. Expression of transcripts analyzed with mRNA sequence, of the transcripts with $p<0.05$ genes encoding proteins with strong support of mitochondrial localization (Mouse MitoCarta 2.0, Broad institute) were selected and functional categorized with Nextprot (SIB Swiss institute for bioinformatics). The full list of genes with functional categorization is shown in Supplementary Tables 3, 4.

Established mitophagy/autophagy markers (41) were extracted from the mRNA sequence data and their regulation was studied for insight in potential underlying mechanisms of WAT whitening and results are reported in **Table 4**. Microtubule-associated protein one light chain three alpha (*Map1lc3a*, better known as *Lc3*), sequestosome 1 (*Sqstm1*, better known as *p62*), unk-51 like kinase 2 (*Ulk2*), PTEN induced putative kinase 1 (*Pink1*) and BCL2/adenovirus E1B interacting protein 3 (*Bnip3*) were upregulated at PN98 compared to PN21. To further support this data, LC3 protein levels were analyzed with western blot. LC3.2 protein levels increased between PN21 and 98 in ING and RP WAT and were unchanged in EPI WAT (**Supplementary Materials and Supplementary Figure 5**). Regrettably, LC3.1 protein levels were not detectable in these samples under these conditions and ratios between LC3.2 and LC3.1 could therefore not be calculated.

Table 4: Regulation of mitophagy/autophagy markers in ING WAT from PN21 to 98 as measured with RNA sequencing. Expression reported as fold changes between postnatal day 21 over 98.

Gene name	ENSBL ID	FC	p-value	Adjusted p-value
Map1lc3a (Lc3)	ENSMUSG00000027602	**1.90**	**0.020**	0.169
Sqstm1 (p62)	ENSMUSG00000015837	**1.80**	**0.004**	0.099
Ulk1	ENSMUSG00000029512	1.22	0.253	0.466
Ulk2	ENSMUSG00000004798	**1.39**	**0.028**	0.190
Atg7	ENSMUSG00000030314	1.24	0.100	0.300
Pink1	ENSMUSG00000028756	**2.66**	< **0.001**	**0.024**
Prkn (Parkin)	ENSMUSG00000023826	Not detected		
Bnip3l	ENSMUSG00000022051	Mean count at PN21 < 2		
Bnip3	ENSMUSG00000078566	**2.70**	< **0.001**	**0.026**
Fundc1	ENSMUSG00000025040	Mean count at PN21 < 2		

Correlations

There were many correlations between mitochondrial density and function markers and WAT weight (**Table 5**). Specifically, the inverse correlation between CS and HADH levels and weight of the corresponding depot was consistently strong in all depots. ING WAT weight was also inversely correlated to levels of the electron transport system complexes (OXPHOS complexes I–IV). In contrast, no correlation was found between ING WAT weight and the level of OXPHOS complex V (ATP5A; Table 5). RP WAT demonstrated opposite findings: the electron transport system complexes did not correlate with WAT weight, but complex V (ATP5A) showed a mild, inverse correlation with WAT weight. *Lep* gene expression was correlated to WAT weight for each of the depots, but this correlation was stronger in the visceral depots compared to ING WAT. *Ucp1* expression, a key marker for browning of WAT, in ING WAT was correlated to mitochondrial density

(CS and mtDNA, Table 5) and function markers (OXPHOS complexes I–IV), but not in RP WAT. In EPI WAT *Ucp1* expression was only to some extent correlated to CS and HADH levels. *Ucp1* expression in ING WAT was not correlated to complex V levels.

Table 5: Correlations between WAT weight v. *Ucp1* gene expression and mitochondrial function markers, *Lep* gene expression:

	ING WAT		EPI WAT		RP WAT	
	r	**p**	**r**	**p**	**r**	**p**
Correlations with WAT weight						
CS activity	-0.738	< 0.001	-0.579	< 0.001	-0.788	< 0.001
HADH activity	-0.759	< 0.001	-0.615	< 0.001	-0.725	< 0.001
mtDNA	-0.444	< 0.05	-0.335	0.076	-0.607	< 0.01
NDUFB8	-0.681	< 0.001	-0.484	< 0.01	-0.02	n.s.
SDHB	-0.695	< 0.001	-0.451	< 0.05	-0.01	n.s.
UQCRC2	-0.734	< 0.001	-0.687	< 0.001	-0.04	n.s.
MTCOI	-0.585	< 0.001	-0.150	n.s.	-0.098	n.s.
ATP5A	-0.091	n.s.	-0.571	< 0.001	-0.478	< 0.05
Correlations with *Ucp1*						
CS activity	0.664	< 0.001	0.393	< 0.05	0.049	n.s.
HADH activity	0.696	< 0.001	0.490	< 0.01	-0.048	n.s.
mtDNA	0.473	< 0.01	0.049	n.s.	-0.136	n.s.
NDUFB8	0.583	< 0.001	0.155	n.s.	0.197	n.s.
SDHB	0.582	< 0.001	0.113	n.s.	-0.306	n.s.
UQCRC2	0.599	< 0.001	0.287	n.s.	-0.182	n.s.
MTCOI	0.511	< 0.001	0.031	n.s.	-0.154	n.s.
ATP5A	0.126	n.s.	0.221	n.s.	-0.221	n.s.
Lep	-0.402	< 0.05	-0.118	n.s.	-0.023	n.s.

Discussion

In this study, we show clear changes in markers for mitochondrial density, mitochondrial function and browning in ING, EPI, and RP WAT depots of C57BL/6j mice after weaning up to young adulthood. We show that an increase in WAT depot mass and elevated levels of adiposity markers is associated with a decline in mitochondrial density over time in all depots. This decline was depot specific, being most pronounced in ING WAT with the steepest drop from PN21 to 42 and was accelerated by the WSD challenge. RNA sequence data from the ING depot showed that the decline in mitochondrial density was accompanied by a transfer from active, ATP producing mitochondria with a clear uncoupling potential toward mitochondria with a more diverse metabolic function and a higher biosynthesis. The RNA sequence data also showed that ING WAT developed from a “browner” toward a “whiter” phenotype with increased coupled mitochondria.

These data also show that this is accompanied by an increased mRNA expression of mitophagy markers.

The present study aimed to comprehensively compare postweaning changes of markers for mitochondrial function and WAT browning in three different WAT depots. There is evidence from one other study showing decreasing mitochondrial enzyme activity in human subcutaneous WAT from the postnatal period to adulthood (42), which is in accordance with the findings in our study. Previous experiments in rats showed lower mitochondrial respiration, enzyme activity and mitochondrial abundance in ING compared to EPI WAT, both when measured in whole tissue or isolated adipocytes (43, 44). But a study in adult mice showed a higher mitochondrial performance in isolated mitochondria of ING compared to EPI WAT while mitochondrial density was not different between the depots (14). In the present study respiration was not measured, but the results were more in agreement with the later study, showing higher mitochondrial enzyme, OXPHOS protein and RNA marker levels in ING compared to EPI WAT of young mice. Moreover, the results of this study showed that the differences in mitochondrial density and function markers between ING and visceral WAT are age specific, being prominent at weaning and much smaller in early adulthood.

The declining mitochondrial density and function markers from weaning to young adulthood in ING WAT was accompanied by a diminished gene expression of the WAT browning markers *Ucp1* and *Cidea*. UCP1 proteins levels tended to decrease accordingly, although statistical significance was not reached for the older AIN93 animals. Subcutaneous depots are more prone to WAT browning than visceral depots and have a higher abundancy of adipocytes with a brown-like phenotype, that can be activated upon cold exposure (45). The higher levels of WAT browning markers at weaning may therefore be part of a protective response of the vulnerable pups to the colder environment in the postnatal period, comparable to the uncoupling response in the brown adipose tissue (46). Indeed, the decreased expression of brown adipocyte markers in the RNA sequence data at PN98 suggests that abundance of brown or brown-like adipocytes, with the capacity to produce heat, is declining over time. This is in line with evidence of other mice studies showing browning of the WAT depots from PN10 to 20 and subsequent whitening from PN20 to 30 (25-27) a process that has shown to be strongly genetically controlled (47). The increased abundancy of white adipocytes, with their lipid storage and insulation capacity, at the same time point further supports this explanation. This also provides an explanation for the differences between subcutaneous and visceral WAT, of which the latter showed a much lower expression of the browning makers *Ucp1* and *Cidea*. Again, this it is fully in line with the

developmental needs of a young pup, being small and vulnerable to cold stress, to a large, more mature individual with a sufficient layer of thermal insulation provided by WAT. This notion is supported by the substantial decline in preadipocyte marker expression from PN21 to PN42 and the increased expression of white adipocyte markers at PN98. The latter indicates that preadipocytes differentiated to adipocytes between those time points, a process that is probably already ongoing at PN21. Indeed, the decline in preadipocyte marker expression is previously reported and there coincided with an increased expression of adipocyte marker expression (25). Environmental factors, like dietary interventions or early life stress (48), may change the pace of whitening and subsequently have long-lasting effects on the oxidative and storage capacity of WAT depots. It would be of interest to investigate the effects of temperature on postweaning changes, in particular by repeating the experiment under thermoneutrality, but also at intermediate and lower low-ambient temperatures, and what the consequence of changes in the pace of whitening of the WAT depots is for later life metabolic health and WAT function. Moreover, investigating the pace of whitening and subsequent later life health consequences in UCP1 knockout or other relevant genetic mouse models or investigating the consequences of different aspects of the weaning process (maternal separation, dietary switch and early/late weaning) can give insight in the underlying mechanisms.

Recent publications revealed that the whitening of WAT is controlled by autophagy induced mitochondrial clearance (mitophagy), indicated by the activation of mitophagy during the beige to white transition in cultured adipocytes following b3-AR agonist withdrawal and the impaired whitening when autophagy is deleted in knock-out mouse models (49, 50). Therefore, we checked the regulation of genes known to be involved in mitophagy (41) in ING WAT between PN21 and 98, the depot where changes in mitochondrial abundance and expression of browning markers was biggest. Indeed, genes involved in mitophagy were upregulated over time, as was the protein level of the autophagy marker LC3.2, confirming the role of mitophagy in whitening of WAT depots. Our data on mitochondrial metabolic pathways show that mitochondria develop from organelles with a high expression of pathways directed at energy production (and dissipation), as in brown adipocytes (51), toward coupled mitochondria which display a wider variety of biochemical pathways. Part of the changes may be related to maturation of ING WAT, since expression of proteins involved in fatty acid metabolism and of mitochondrial chaperones has been shown to increase during adipogenesis (52). In ING WAT of the more mature PN98 mice we observe a much smaller number of genes related to especially protein import, translation and OXPHOS as well as nucleotide

metabolism, suggestion a decrease in mitochondrial “growth”/biogenesis, while genes related to lipid synthesis, branched chain amino acid/short chain fatty acid metabolism, steroid metabolism and redox signaling appear, as well as a substantial number of genes related to diverse biosynthetic pathways (Figure 5). This indicates that the mitochondria have reached a condition where they interact more with the rest of the cell, no longer unilaterally focused on growth and energy metabolism (and dissipation) only. This especially suggests that ING WAT mitochondria have reached a steady state, which is supported by the appearance of autophagy and apoptosis genes, essential for mitochondrial (and cellular) turnover and quality control (53). Our data further indicate that ING WAT between PN21 (and possibly earlier) and PN42 provides a physiological relevant model to study and better understand functional changes in mitochondria related to adipose tissue development and mitochondrial adaptive capacity and to understand mitochondrial changes related to WAT whitening.

The changes in the functionality of the mitochondria in the WAT depots and the remodeling of these depots in early life may have an impact for intervention studies starting in early life, as the effect of the intervention may be very dependent on the starting point of the intervention. In line with the developmental origins of health and disease theory (54, 55), developmental processes may respond in a manner to optimally match an individual to anticipate later life conditions (56). Previous studies in our lab showed that the postnatal period is amendable to nutritional programming since a relative mild dietary intervention at weaning indeed increased levels of later life mitochondrial oxidative capacity (29). Although the perspective is there, additional studies are needed to fully understand to which extent nutritional interventions in the timeframe of weaning provides a window of opportunity for protection against later life metabolic disease.

Conclusion

The present study showed a decline in mitochondrial density and oxidative capacity markers in WAT depots of young C57BL/6j mice over time while adipose tissue mass increased in size. The decline is more explicit in ING WAT compared to the visceral depots and is accompanied by an evolution from a browner, energy dissipating, to a whiter, biosynthetic, adipose tissue phenotype. These developmental changes may provide an opportunity to program a healthy WAT mitochondrial phenotype by nutritional interventions during the weaning period.

Additional information

Ethic statement All animal procedures were in accordance with the principles of good laboratory animal care following the EU directive for the protection of animals used for scientific purposes and approved by an external, independent Animal Experimental Committee (DEC consult, Soest, Netherlands).

Author contributions AK, EE, and KvL conducted the experiments. AK and JK analyzed the data and drafted the manuscript. AK, AO, and JK interpreted the results. AK prepared the figures. All authors contributed to the design of the study, edited and revised the manuscript, and approved the final version of the manuscript.

Funding This work was funded by the Danone Nutricia Research.

Acknowledgements We thank Jan Polman for help in carrying out the data analyses of the mRNA sequence results and Joris Hoeks and Gert Schaart (Maastricht University) for sharing their UCP1 western blot protocol.

References

1. Ng M, Fleming T, Robinson M, Thomson B, Graetz N, Margono C, et al. Global, regional, and national prevalence of overweight and obesity in children and adults during 1980-2013: a systematic analysis for the Global Burden of Disease Study 2013. Lancet. 2014;384(9945):766-81.
2. Reilly JJ, Kelly J. Long-term impact of overweight and obesity in childhood and adolescence on morbidity and premature mortality in adulthood: systematic review. Int J Obes (Lond). 2011;35(7):891-8.
3. Hammarstedt A, Graham TE, Kahn BB. Adipose tissue dysregulation and reduced insulin sensitivity in non-obese individuals with enlarged abdominal adipose cells. Diabetol Metab Syndr. 2012;4(1):42.
4. Wilson-Fritch L, Nicoloro S, Chouinard M, Lazar MA, Chui PC, Leszyk J, et al. Mitochondrial remodeling in adipose tissue associated with obesity and treatment with rosiglitazone. J Clin Invest. 2004;114(9):1281-9.
5. Choo HJ, Kim JH, Kwon OB, Lee CS, Mun JY, Han SS, et al. Mitochondria are impaired in the adipocytes of type 2 diabetic mice. Diabetologia. 2006;49(4):784-91.
6. Sutherland LN, Capozzi LC, Turchinsky NJ, Bell RC, Wright DC. Time course of high-fat diet-induced reductions in adipose tissue mitochondrial proteins: potential mechanisms and the relationship to glucose intolerance. Am J Physiol Endocrinol Metab. 2008;295(5):E1076-83.
7. Derous D, Kelder T, van Schothorst EM, van Erk M, Voigt A, Klaus S, et al. Network-based integration of molecular and physiological data elucidates regulatory mechanisms underlying adaptation to high-fat diet. Genes Nutr. 2015;10(4):470.
8. Flachs P, Horakova O, Brauner P, Rossmeisl M, Pecina P, Franssen-van Hal N, et al. Polyunsaturated fatty acids of marine origin upregulate mitochondrial biogenesis and induce beta-oxidation in white fat. Diabetologia. 2005;48(11):2365-75.
9. Nisoli E, Tonello C, Cardile A, Cozzi V, Bracale R, Tedesco L, et al. Calorie restriction promotes mitochondrial biogenesis by inducing the expression of eNOS. Science. 2005;310(5746):314-7.
10. Yang YK, Chen M, Clements RH, Abrams GA, Aprahamian CJ, Harmon CM. Human mesenteric adipose tissue plays unique role versus subcutaneous and omental fat in obesity related diabetes. Cellular physiology and biochemistry : international journal of experimental cellular physiology, biochemistry, and pharmacology. 2008;22(5-6):531-8.
11. Bjorndal B, Burri L, Staalesen V, Skorve J, Berge RK. Different adipose depots: their role in the development of metabolic syndrome and mitochondrial response to hypolipidemic agents. J Obes. 2011;2011:490650.
12. Pouliot MC, Despres JP, Nadeau A, Moorjani S, Prud'Homme D, Lupien PJ, et al. Visceral obesity in men. Associations with glucose tolerance, plasma insulin, and lipoprotein levels. Diabetes. 1992;41(7):826-34.
13. Ross R, Aru J, Freeman J, Hudson R, Janssen I. Abdominal adiposity and insulin resistance in obese men. Am J Physiol Endocrinol Metab. 2002;282(3):E657-63.
14. Schottl T, Kappler L, Braun K, Fromme T, Klingenspor M. Limited mitochondrial capacity of visceral versus subcutaneous white adipocytes in male C57BL/6N mice. Endocrinology. 2015;156(3):923-33.
15. Bruce KD, Cagampang FR, Argenton M, Zhang J, Ethirajan PL, Burdge GC, et al. Maternal high-fat feeding primes steatohepatitis in adult mice offspring, involving mitochondrial dysfunction and altered lipogenesis gene expression. Hepatology. 2009;50(6):1796-808.
16. Jousse C, Muranishi Y, Parry L, Montaurier C, Even P, Launay JM, et al. Perinatal protein malnutrition affects mitochondrial function in adult and results in a resistance to high fat diet-induced obesity. PLoS One. 2014;9(8):e104896.

17. Claycombe KJ, Vomhof-DeKrey EE, Garcia R, Johnson WT, Uthus E, Roemmich JN. Decreased beige adipocyte number and mitochondrial respiration coincide with increased histone methyl transferase (G9a) and reduced FGF21 gene expression in Sprague-Dawley rats fed prenatal low protein and postnatal high-fat diets. The Journal of nutritional biochemistry. 2016;31:113-21.
18. Lecoutre S, Deracinois B, Laborie C, Eberle D, Guinez C, Panchenko PE, et al. Depot- and sex-specific effects of maternal obesity in offspring's adipose tissue. J Endocrinol. 2016;230(1):39-53.
19. Mitra A, Alvers KM, Crump EM, Rowland NE. Effect of high-fat diet during gestation, lactation, or postweaning on physiological and behavioral indexes in borderline hypertensive rats. Am J Physiol Regul Integr Comp Physiol. 2009;296(1):R20-8.
20. Palou M, Priego T, Sanchez J, Torrens JM, Palou A, Pico C. Moderate caloric restriction in lactating rats protects offspring against obesity and insulin resistance in later life. Endocrinology. 2010;151(3):1030-41.
21. Spalding KL, Arner E, Westermark PO, Bernard S, Buchholz BA, Bergmann O, et al. Dynamics of fat cell turnover in humans. Nature. 2008;453(7196):783-7.
22. Han J, Lee JE, Jin J, Lim JS, Oh N, Kim K, et al. The spatiotemporal development of adipose tissue. Development. 2011;138(22):5027-37.
23. Wang QA, Tao C, Gupta RK, Scherer PE. Tracking adipogenesis during white adipose tissue development, expansion and regeneration. Nat Med. 2013;19(10):1338-44.
24. DiGirolamo M, Fine JB, Tagra K, Rossmanith R. Qualitative regional differences in adipose tissue growth and cellularity in male Wistar rats fed ad libitum. Am J Physiol. 1998;274(5 Pt 2):R1460-7.
25. Xue B, Rim JS, Hogan JC, Coulter AA, Koza RA, Kozak LP. Genetic variability affects the development of brown adipocytes in white fat but not in interscapular brown fat. J Lipid Res. 2007;48(1):41-51.
26. Lasar D, Julius A, Fromme T, Klingenspor M. Browning attenuates murine white adipose tissue expansion during postnatal development. Biochim Biophys Acta. 2013;1831(5):960-8.
27. Birnbacher L, Maurer S, Scheidt K, Herzen J, Pfeiffer F, Fromme T. Electron Density of Adipose Tissues Determined by Phase-Contrast Computed Tomography Provides a Measure for Mitochondrial Density and Fat Content. Front Physiol. 2018;9:707.
28. Baars A, Oosting A, Engels E, Kegler D, Kodde A, Schipper L, et al. Milk fat globule membrane coating of large lipid droplets in the diet of young mice prevents body fat accumulation in adulthood. Br J Nutr. 2016;115(11):1930-7.
29. Kodde A, van der Beek EM, Phielix E, Engels E, Schipper L, Oosting A. Supramolecular structure of dietary fat in early life modulates expression of markers for mitochondrial content and capacity in adipose tissue of adult mice. Nutr Metab (Lond). 2017;14:37.
30. Bouwman LMS, Fernandez-Calleja JMS, Swarts HJM, van der Stelt I, Oosting A, Keijer J, et al. No Adverse Programming by Post-Weaning Dietary Fructose of Body Weight, Adiposity, Glucose Tolerance, or Metabolic Flexibility. Molecular nutrition & food research. 2018;62(2).
31. Fernandez-Calleja JMS, Bouwman LMS, Swarts HJM, Oosting A, Keijer J, van Schothorst EM. Direct and Long-Term Metabolic Consequences of Lowly vs. Highly-Digestible Starch in the Early Post-Weaning Diet of Mice. Nutrients. 2018;10(11).
32. Reeves PG, Nielsen FH, Fahey GC, Jr. AIN-93 purified diets for laboratory rodents: final report of the American Institute of Nutrition ad hoc writing committee on the reformulation of the AIN-76A rodent diet. J Nutr. 1993;123(11):1939-51.
33. Vanhoutvin SA, Troost FJ, Hamer HM, Lindsey PJ, Koek GH, Jonkers DM, et al. Butyrate-induced transcriptional changes in human colonic mucosa. PLoS One. 2009;4(8):e6759.
34. Hellemans J, Mortier G, De Paepe A, Speleman F, Vandesompele J. qBase relative quantification framework and software for management and automated analysis of real-time quantitative PCR data. Genome Biol. 2007;8(2):R19.

35. Shepherd D, Garland PB. The kinetic properties of citrate synthase from rat liver mitochondria. Biochem J. 1969;114(3):597-610.
36. Meex RC, Phielix E, Schrauwen-Hinderling V, Moonen-Kornips E, Schaart G, Schrauwen P, et al. The use of statins potentiates the insulin-sensitizing effect of exercise training in obese males with and without Type 2 diabetes. Clin Sci. 2010;119(7):293-301.
37. Kaaman M, Sparks LM, van Harmelen V, Smith SR, Sjolin E, Dahlman I, et al. Strong association between mitochondrial DNA copy number and lipogenesis in human white adipose tissue. Diabetologia. 2007;50(12):2526-33.
38. Gesta S, Tseng YH, Kahn CR. Developmental origin of fat: tracking obesity to its source. Cell. 2007;131(2):242-56.
39. Boeuf S, Klingenspor M, Van Hal NL, Schneider T, Keijer J, Klaus S. Differential gene expression in white and brown preadipocytes. Physiol Genomics. 2001;7(1):15-25.
40. Timmons JA, Wennmalm K, Larsson O, Walden TB, Lassmann T, Petrovic N, et al. Myogenic gene expression signature establishes that brown and white adipocytes originate from distinct cell lineages. Proc Natl Acad Sci U S A. 2007;104(11):4401-6.
41. Ding WX, Yin XM. Mitophagy: mechanisms, pathophysiological roles, and analysis. Biol Chem. 2012;393(7):547-64.
42. Novak M, Hahn P, Penn D, Monkus E, Kirby L. Metabolism of subcutaneous adipose tissue in the immediate postnatal period of human newborns. Developmental changes in some cytoplasmic enzymes. Biol Neonate. 1973;23(1):19-24.
43. Prunet-Marcassus B, Moulin K, Carmona MC, Villarroya F, Penicaud L, Casteilla L. Inverse distribution of uncoupling proteins expression and oxidative capacity in mature adipocytes and stromal-vascular fractions of rat white and brown adipose tissues. FEBS Lett. 1999;464(3):184-8.
44. Deveaud C, Beauvoit B, Salin B, Schaeffer J, Rigoulet M. Regional differences in oxidative capacity of rat white adipose tissue are linked to the mitochondrial content of mature adipocytes. Mol Cell Biochem. 2004;267(1-2):157-66.
45. Wu J, Bostrom P, Sparks LM, Ye L, Choi JH, Giang AH, et al. Beige adipocytes are a distinct type of thermogenic fat cell in mouse and human. Cell. 2012;150(2):366-76.
46. Obregon MJ, Jacobsson A, Kirchgessner T, Schotz MC, Cannon B, Nedergaard J. Postnatal recruitment of brown adipose tissue is induced by the cold stress experienced by the pups. An analysis of mRNA levels for thermogenin and lipoprotein lipase. Biochem J. 1989;259(2):341-6.
47. Chabowska-Kita A, Trabczynska A, Korytko A, Kaczmarek MM, Kozak LP. Low ambient temperature during early postnatal development fails to cause a permanent induction of brown adipocytes. FASEB J. 2015;29(8):3238-52.
48. Yam KY, Naninck EFG, Abbink MR, la Fleur SE, Schipper L, van den Beukel JC, et al. Exposure to chronic early-life stress lastingly alters the adipose tissue, the leptin system and changes the vulnerability to western-style diet later in life in mice. Psychoneuroendocrinology. 2017;77:186-95.
49. Altshuler-Keylin S, Shinoda K, Hasegawa Y, Ikeda K, Hong H, Kang Q, et al. Beige Adipocyte Maintenance Is Regulated by Autophagy-Induced Mitochondrial Clearance. Cell Metab. 2016;24(3):402-19.
50. Lu X, Altshuler-Keylin S, Wang Q, Chen Y, Sponton CH, Ikeda K, et al. Mitophagy controls beige adipocyte maintenance through a Parkin-dependent and UCP1-independent mechanism. Science Signaling. 2019;11(527):1-21.
51. Forner F, Kumar C, Luber CA, Fromme T, Klingenspor M, Mann M. Proteome differences between brown and white fat mitochondria reveal specialized metabolic functions. Cell Metab. 2009;10(4):324-35.

52. Wilson-Fritch L, Burkart A, Bell G, Mendelson K, Leszyk J, Nicoloro S, et al. Mitochondrial biogenesis and remodeling during adipogenesis and in response to the insulin sensitizer rosiglitazone. Mol Cell Biol. 2003;23(3):1085-94.
53. Zimmermann M, Reichert AS. How to get rid of mitochondria: crosstalk and regulation of multiple mitophagy pathways. Biol Chem. 2017;399(1):29-45.
54. Hales CN, Barker DJ. The thrifty phenotype hypothesis. Br Med Bull. 2001;60:5-20.
55. Gluckman PD, Hanson MA. The developmental origins of the metabolic syndrome. Trends Endocrinol Metab. 2004;15(4):183-7.
56. Hanson MA, Gluckman PD. Early developmental conditioning of later health and disease: physiology or pathophysiology? Physiol Rev. 2014;94(4):1027-76.

Supplementary material Chapter 3

Supplementary methods: LC3 protein levels

Protein levels of LC3 as marker for mitophagy, were measured with western blot (1). Briefly, 15 µg of total protein per sample was used for SDS-PAGE, transfer to a PVDF membrane was done using the Pierce Power Blot (Thermo Fisher Scientific). Blots were blocked with 5% Protifar (Nutricia, Zoetermeer, The Netherlands), incubated with goat anti mouse LC3 (Nanotools, Teningen, Germany) as primary antibody and HRP conjugated anti mouse IgG (R&D systems) as a secondary antibody. LC3 protein levels were detected with Supersignal West Femto (Thermo Fisher Scientific) and were related to total protein levels as analyzed by Coomassie brilliant blue staining. Protein levels were detected with the Chemidoc XRS and analyzed by Quantity One (Biorad). Results and a representative Western blot stained for LC3 and the corresponding Coomassie brilliant blue stained blot is shown in Supplementary figure 5.

Supplementary Table 1: Expression of transcripts belonging to mitochondrial dysfunction pathway as determined with mRNA sequencing and data analyzed with ingenuity Pathway Analysis (Qiagen Bioinformatics, Aarhus, Denmark). Difference between postnatal day 21 over 98.

Gene ID	Ensembl ID	p-value	FDR	FC
Acox2	ENSMUST00000126352	0,047	0,226	-2,00
Aph1a	ENSMUST00000015894	0,009	0,131	-1,50
Aph1b	ENSMUST00000034934	0,011	0,140	1,66
App	ENSMUST00000005406	0,049	0,228	1,74
Atp5a1	ENSMUST00000114748	0,004	0,100	-2,00
Atp5b	ENSMUST00000125992	0,029	0,192	-4,30
Atp5d	ENSMUST00000105366	0,019	0,167	-1,90
Atp5e	ENSMUST00000149191	0,001	0,048	-2,20
Atp5g1	ENSMUST00000107684	0,035	0,205	-1,70
Atp5g3	ENSMUST00000131045	0,048	0,227	-1,50
Atp5h	ENSMUST00000138779	0,026	0,185	-1,70
Atp5o	ENSMUST00000023677	0,006	0,117	-2,60
Bace2	ENSMUST00000047275	0,021	0,172	-3,00
Cat	ENSMUST00000028610	0,001	0,062	2,24
Cox10	ENSMUST00000049091	0,002	0,074	-2,10
Cox11	ENSMUST00000020851	0,003	0,083	-2,10
Cox15	ENSMUST00000045562	0,021	0,173	-1,60
Cox4i2	ENSMUST00000010020	0,043	0,220	-2,00
Cox5a	ENSMUST00000000090	0,040	0,215	-2,00
Cox6b2	ENSMUST00000182272	0,020	0,168	-2,60
Cox7a1	ENSMUST00000098594	0,015	0,154	-5,60
Cyb5a	ENSMUST00000025549	0,002	0,072	2,19
Cyc1	ENSMUST00000023210	0,042	0,219	-1,80

Supplementary Table 1: Continued

Gene ID	Ensembl ID	p-value	FDR	FC
Glrx2	ENSMUST00000152435	0,016	0,159	-1,80
Gpx7	ENSMUST00000030332	0,049	0,228	-1,80
Htra2	ENSMUST00000113962	0,032	0,198	-1,50
Maoa	ENSMUST00000026013	0,002	0,075	1,97
Maob	ENSMUST00000040820	0,023	0,177	1,67
Ndufa3	ENSMUST00000108644	0,049	0,229	-1,80
Ndufa11	ENSMUST00000002452	0,035	0,205	-1,80
Ndufb5	ENSMUST00000122290	0,045	0,222	-1,80
Ndufb10	ENSMUST00000141324	0,026	0,186	-2,30
Ndufs7	ENSMUST00000155523	0,033	0,200	-1,60
Ndufs8	ENSMUST00000075092	0,017	0,161	-1,90
Pdha1	ENSMUST00000156531	0,029	0,192	-3,30
Pink1	ENSMUST00000030536	0,000	0,024	2,66
Rhot2	ENSMUST00000043897	0,045	0,223	-1,50
Sdhb	ENSMUST00000010007	0,045	0,223	-1,90
Sdhd	ENSMUST00000000175	0,047	0,226	-1,80
Surf1	ENSMUST00000150776	0,007	0,121	3,54
Txn2	ENSMUST00000174468	0,014	0,152	-4,00
Uqcr11	ENSMUST00000141683	0,048	0,227	-3,50
Uqcrfs1	ENSMUST00000042834	0,046	0,224	-1,90
Xdh	ENSMUST00000024866	0,004	0,101	1,84

FC: Fold change; FDR: Fold discovery rate

Supplementary Table 2: Regulation of genes selective for brown or white (pre)adipocytes over time, analysed with mRNA sequencing. Gene list derived from (2) and expression levels of transcripts with p<0.05 included in table. Expression reported as fold changes between postnatal day 21 over 98. Up regulated values red and down regulated values green, empty cells indicate that these genes were not significantly regulated.

Preadipocyte markers:		**Adipocyte markers**	
Gene	**Time**	**Gene**	**Time**
Brown adipose tissue		*Brown adipose tissue*	
Acta1		*Acaa2*	
Actc1		*Acss1*	
Actn4		*Cidea*	
Adam15		*Cox7a1*	-5.6
Cd83		*Cox8b*	
Chrna1		*Cpn2*	-9.0
Cldn5		*Cpt1b*	
Fn1	-2.3	*Dio2*	
Hdlbp		*Elovl3*	
Icam2		*Elovl6*	
Maged2	-4.7	*Esrrg*	
Mme	2.3	*Fgf16*	
Myh3		*Gpd2*	
Myl1	3.6	*Hoxa1*	
Mylpf	4.7	*Hoxc4*	
Myog		*Mpzl2*	
Ndn	-2.6	*Ntrk3*	
Snrpa	-1.4	*Otop1*	
Tnnc1		*Ppara*	
Tnni1		*Ppargc1a*	-2.2
Tnnt3	12.6	*S100b*	-1.9
		Sirt3	
		Ucp1	-7.3
White adipose tissue		*White adipose tissue*	
C2		*Aldh1a1*	3.5
C3		*App*	1.7
Cfb	2.0	*Ccl6*	
Fads2		*Dpt*	
		Fads3	3.4
		Fbn1	-3.3
		Hmgn3	
		Hoxa4	
		Hoxa7	
		Hoxc8	
		Lep	4.7
		Nrip1	
		Psat1	
		Retn	
		Retnla	
		Serpina3k	5.1
		Sphk1	

Supplementary Table 3: Functional categorization of genes downregulated at postnatal day 98 compared to 21, with strong support of mitochondrial localization. Expression of transcripts analyzed with mRNA sequence, of the transcripts with p<0.05 genes encoding proteins with strong support of mitochondrial localization (Mouse MitoCarta 2.0, Broad institute) were selected and functional categorized with Nextprot (SIB Swiss institute for bioinformatics)

Functional Category	Symbol	EnsemblGeneID	FC	P.Value
Cell death	*Prelid1*	ENSMUSG00000021486	-7,5	0,002
Cell death	***Endog***	ENSMUSG00000015337	-2	0,030
Cell death	*Fkbp8*	ENSMUSG00000019428	-1,8	0,032
Cell death	*Alkbh7*	ENSMUSG00000002661	-1,8	0,036
Cell death	*Aifm2*	ENSMUSG00000020085	-1,4	0,017
Dynamics/Morphology	***Stoml2***	ENSMUSG00000028455	-1,4	0,038
Dynamics/Morphology	***Opa1***	ENSMUSG00000038084	-2,4	0,023
Dynamics/Morphology	*Mul1*	ENSMUSG00000041241	-1,9	0,019
Dynamics/Morphology	***Rab24***	ENSMUSG00000034789	-1,8	0,018
Dynamics/Morphology	***Atad3a***	ENSMUSG00000029036	-1,8	0,017
Dynamics/Morphology	*Cisd2*	ENSMUSG00000028165	-1,7	0,016
Dynamics/Morphology	***Letm1***	ENSMUSG00000005299	-1,6	0,040
Dynamics/Morphology	***Poldip2***	ENSMUSG00000001100	-1,6	0,015
Dynamics/Morphology	***Opa3***	ENSMUSG00000052214	-1,5	0,026
Dynamics/Morphology	***Mcu***	ENSMUSG00000009647	-1,4	0,022
FA oxidation	***Etfb***	ENSMUSG00000004610	-2,3	0,027
FA oxidation	***Etfdh***	ENSMUSG00000027809	-2,2	0,002
FA oxidation	***Acadl***	ENSMUSG00000026003	-2,1	0,036
FA oxidation	*Slc25a29*	ENSMUSG00000021265	-1,7	0,024
FA oxidation	*Tysnd1*	ENSMUSG00000020087	-1,6	0,015
FA oxidation	***Lactb***	ENSMUSG00000032370	-1,4	0,022
Fe/FeS/Heme	***Nfu1***	ENSMUSG00000029993	-120,5	0,037
Fe/FeS/Heme	***Cisd3***	ENSMUSG00000078695	-2,2	0,018
Fe/FeS/Heme	***Alas1***	ENSMUSG00000032786	-1,9	0,021
Fe/FeS/Heme	***Fxn***	ENSMUSG00000059363	-1,8	0,026
Fe/FeS/Heme	***Isca1***	ENSMUSG00000044792	-1,7	0,025
Fe/FeS/Heme	***Ppox***	ENSMUSG00000062729	-1,7	0,021
Fe/FeS/Heme	*Slc25a37*	ENSMUSG00000034248	-1,7	0,036
Fe/FES/Heme	*Rsad1*	ENSMUSG00000039096	-1,6	0,017
Fe/FeS/Heme	***Iba57***	ENSMUSG00000049287	-1,5	0,044
Metabolic regulation	*Sirt4*	ENSMUSG00000029524	-2,8	0,003
Metabolic regulation	***Agk***	ENSMUSG00000029916	-1,7	0,012
Metabolic regulation	***Agpat5***	ENSMUSG00000031467	-1,6	0,017
Metabolic regulation	***Gadd45gip1***	ENSMUSG00000033751	-1,6	0,047
Metabolic regulation	*Rdh11*	ENSMUSG00000066441	-1,5	0,025
Metabolic regulation	*Pick1*	ENSMUSG00000068206	-1,5	0,031
Metabolite transport	***Slc25a10***	ENSMUSG00000025792	-5000	0,003
Metabolite transport	***Slc25a42***	ENSMUSG00000002346	-4,3	0,002
Metabolite transport	***Slc25a45***	ENSMUSG00000024818	-3	0,028
Metabolite transport	***Slc25a35***	ENSMUSG00000018740	-2,6	0,008

Supplementary Table 3: Continued

Functional Category	Symbol	EnsemblGeneID	FC	P.Value
Metabolite transport	***Slc25a19***	ENSMUSG00000020744	-2,6	0,013
Metabolite transport	***Slc25a3***	ENSMUSG00000061904	-1,9	0,016
Metabolite transport	***Slc25a5***	ENSMUSG00000016319	-1,7	0,011
Metabolite transport	*Slc16a1*	ENSMUSG00000032902	-1,7	0,018
Non mitochondrial	*Rpl10a*	ENSMUSG00000037805	-3	0,002
Non mitochondrial	*Tcirg1*	ENSMUSG00000001750	-3	0,032
Non mitochondrial	***Lamc1***	ENSMUSG00000026478	-2,2	0,007
Non mitochondrial	*Rps15a*	ENSMUSG00000008683	-2,2	0,048
Non mitochondrial	*Rpia*	ENSMUSG00000053604	-1,9	0,002
Non mitochondrial	*Rpl34*	ENSMUSG00000062006	-1,8	0,040
Non mitochondrial	***Rps18***	ENSMUSG00000008668	-1,4	0,026
Nucleotide metabolism	*Apex2*	ENSMUSG00000025269	-2,9	0,001
Nucleotide metabolism	***Dut***	ENSMUSG00000027203	-2,6	0,002
Nucleotide metabolism	*Nt5c*	ENSMUSG00000020736	-2,6	0,012
Nucleotide metabolism	***Nme4***	ENSMUSG00000024177	-2,1	0,026
Other	*Nt5dc2*	ENSMUSG00000071547	-6,2	0,000
Other	***Glod4***	ENSMUSG00000017286	-3,3	0,008
Other	***Hdhd3***	ENSMUSG00000038422	-3	0,006
Other	***Tha1***	ENSMUSG00000017713	-2,6	0,000
Other	***Abhd11***	ENSMUSG00000040532	-2,5	0,009
Other	***1700021F05Rik***	ENSMUSG00000019797	-2,1	0,028
Other	***2010107E04Rik***	ENSMUSG00000021290	-1,8	0,028
Other	***2310061I04Rik***	ENSMUSG00000050705	-1,8	0,016
Other	***Abhd10***	ENSMUSG00000033157	-1,5	0,022
Other	*Xrcc6bp1*	ENSMUSG00000025436	-1,4	0,025
Other	***Dhrs1***	ENSMUSG00000002332	-1,4	0,026
Other	*Rcc1l*	ENSMUSG00000061979	-1,3	0,048
OXPHOS	***Sdhc***	ENSMUSG00000058076	-8,4	0,000
OXPHOS	***Cox7a1***	ENSMUSG00000074218	-5,6	0,015
OXPHOS	***Uqcr11***	ENSMUSG00000020163	-3,5	0,048
OXPHOS	***Cmc2***	ENSMUSG00000014633	-3,5	0,001
OXPHOS	*Cep89*	ENSMUSG00000023072	-3,1	0,029
OXPHOS	***Uqcc1***	ENSMUSG00000005882	-2,6	0,024
OXPHOS	*Cox6b2*	ENSMUSG00000051811	-2,6	0,020
OXPHOS	***Atp5k***	ENSMUSG00000050856	-2,6	0,004
OXPHOS	***Cox7c***	ENSMUSG00000017778	-2,3	0,010
OXPHOS	***Ndufb10***	ENSMUSG00000040048	-2,2	0,010
OXPHOS	***Atp5e***	ENSMUSG00000016252	-2,2	0,001
OXPHOS	***Fmc1***	ENSMUSG00000019689	-2,2	0,018
OXPHOS	*Cox10*	ENSMUSG00000042148	-2,1	0,002
OXPHOS	***Adck4***	ENSMUSG00000003762	-2,1	0,050
OXPHOS	*Atp5sl*	ENSMUSG00000057229	-2	0,001
OXPHOS	***Tomm5***	ENSMUSG00000078713	-2	0,013

Supplementary Table 3: Continued

Functional Category	Symbol	EnsemblGeneID	FC	P.Value
OXPHOS	***Coa7***	ENSMUSG00000048351	-2	0,001
OXPHOS	***Cox5a***	ENSMUSG00000000088	-2	0,040
OXPHOS	***Cox4i2***	ENSMUSG00000009876	-2	0,043
OXPHOS	***Atp5b***	ENSMUSG00000025393	-2	0,000
OXPHOS	***Atp5a1***	ENSMUSG00000025428	-2	0,004
OXPHOS	***Tbrg4***	ENSMUSG00000000384	-2	0,013
OXPHOS	*Fastk*	ENSMUSG00000028959	-2	0,006
OXPHOS	***Hccs***	ENSMUSG00000031352	-1,9	0,007
OXPHOS	***Ndufs1***	ENSMUSG00000025968	-1,9	0,010
OXPHOS	***Ndufs8***	ENSMUSG00000059734	-1,9	0,017
OXPHOS	***Sdhb***	ENSMUSG00000009863	-1,9	0,045
OXPHOS	***Uqcrfs1***	ENSMUSG00000038462	-1,9	0,046
OXPHOS	*Coa4*	ENSMUSG00000044881	-1,9	0,020
OXPHOS	***Atp5d***	ENSMUSG00000003072	-1,9	0,019
OXPHOS	***Atpif1***	ENSMUSG00000054428	-1,9	0,025
OXPHOS	***Cyc1***	ENSMUSG00000022551	-1,8	0,042
OXPHOS	***Ndufb5***	ENSMUSG00000027673	-1,8	0,044
OXPHOS	*Ndufc1*	ENSMUSG00000037152	-1,8	0,047
OXPHOS	***Ndufa3***	ENSMUSG00000035674	-1,8	0,049
OXPHOS	***Sdhd***	ENSMUSG00000000171	-1,8	0,047
OXPHOS	***Uqcrh***	ENSMUSG00000063882	-1,8	0,037
OXPHOS	***Lace1***	ENSMUSG00000038302	-1,8	0,047
OXPHOS	***Ndufaf4***	ENSMUSG00000028261	-1,7	0,038
OXPHOS	***Ndufc2***	ENSMUSG00000030647	-1,7	0,040
OXPHOS	***Minos1***	ENSMUSG00000050608	-1,7	0,030
OXPHOS	***Coq4***	ENSMUSG00000026798	-1,7	0,042
OXPHOS	*Atp5g1*	ENSMUSG00000006057	-1,7	0,035
OXPHOS	*Pdss2*	ENSMUSG00000038240	-1,6	0,048
OXPHOS	***Ndufb11***	ENSMUSG00000031059	-1,6	0,004
OXPHOS	***Ndufs7***	ENSMUSG00000020153	-1,6	0,033
OXPHOS	***Atp5c1***	ENSMUSG00000025781	-1,6	0,004
OXPHOS	***Acad9***	ENSMUSG00000027710	-1,5	0,023
OXPHOS	***Coa3***	ENSMUSG00000017188	-1,5	0,032
OXPHOS	***Atp5f1***	ENSMUSG00000000563	-1,5	0,043
OXPHOS	*Atp5g3*	ENSMUSG00000018770	-1,5	0,048
OXPHOS	***Ttc19***	ENSMUSG00000042298	-1,5	0,045
OXPHOS	***Noa1***	ENSMUSG00000036285	-1,5	0,004
Protein import and folding	*Dnajc4*	ENSMUSG00000024963	-3	0,002
Protein import and folding	***Ppif***	ENSMUSG00000021868	-2,8	0,001
Protein import and folding	***Timm13***	ENSMUSG00000020219	-2,4	0,000
Protein import and folding	***Timm8a1***	ENSMUSG00000045455	-2,2	0,002
Protein import and folding	***Timm17b***	ENSMUSG00000031158	-1,9	0,004
Protein import and folding	***Tomm40***	ENSMUSG00000002984	-1,9	0,009

Supplementary Table 3: Continued

Functional Category	Symbol	EnsemblGeneID	FC	P.Value
Protein import and folding	***Mtx1***	ENSMUSG00000064068	-1,9	0,008
Protein import and folding	***Timm50***	ENSMUSG00000003438	-1,8	0,030
Protein import and folding	***Hspd1***	ENSMUSG00000025980	-1,8	0,014
Protein import and folding	***Tmem14c***	ENSMUSG00000021361	-1,7	0,019
Protein import and folding	***Oxa1l***	ENSMUSG00000000959	-1,7	0,004
Protein import and folding	***Tomm22***	ENSMUSG00000022427	-1,5	0,014
Protein import and folding	***Tmem186***	ENSMUSG00000043140	-1,4	0,012
Protein import and folding	*Abcb9*	ENSMUSG00000029408	-1,4	0,027
Protein import and folding	*Grpel2*	ENSMUSG00000024580	-1,4	0,032
Redox	***Txn2***	ENSMUSG00000005354	-4	0,014
Redox	***Prdx4***	ENSMUSG00000025289	-2,2	0,006
Redox	***Ptges2***	ENSMUSG00000026820	-1,9	0,024
Redox	*Glrx2*	ENSMUSG00000018196	-1,8	0,016
Redox	***Selo***	ENSMUSG00000035757	-1,7	0,009
Redox	*Txndc12*	ENSMUSG00000028567	-1,5	0,027
TCA/TCA associated	***Pdha1***	ENSMUSG00000031299	-3,3	0,029
TCA/TCA associated	***Gls***	ENSMUSG00000026103	-3	0,003
TCA/TCA associated	*Mmadhc*	ENSMUSG00000026766	-2,8	0,036
TCA/TCA associated	***Mecr***	ENSMUSG00000028910	-2,4	0,043
TCA/TCA associated	***Suclg1***	ENSMUSG00000052738	-2,1	0,019
TCA/TCA associated	***Aco2***	ENSMUSG00000022477	-2	0,047
TCA/TCA associated	***Sucla2***	ENSMUSG00000022110	-2	0,036
TCA/TCA associated	***Got2***	ENSMUSG00000031672	-1,9	0,002
TCA/TCA associated	***Me2***	ENSMUSG00000024556	-1,8	0,044
TCA/TCA associated	***Pck2***	ENSMUSG00000040618	-1,6	0,037
TCA/TCA associated	***Nit2***	ENSMUSG00000022751	-1,6	0,021
TCA/TCA associated	***Idh3g***	ENSMUSG00000002010	-1,4	0,044
TCA/TCA associated	*Gls2*	ENSMUSG00000044005	-1,4	0,050
TCA/TCA associated	***Slc25a11***	ENSMUSG00000014606	-1,4	0,035
Transcription	***Mterfd3***	ENSMUSG00000049038	-2	0,019
Transcription	***Supv3l1***	ENSMUSG00000020079	-1,9	0,030
Transcription	***Polrmt***	ENSMUSG00000020329	-1,8	0,028
Transcription	*Ptcd2*	ENSMUSG00000021650	-1,8	0,004
Translation	***Rmnd1***	ENSMUSG00000019763	-3,7	0,001
Translation	*Fkbp10*	ENSMUSG00000001555	-3,7	0,002
Translation	*Hemk1*	ENSMUSG00000032579	-3,4	0,007
translation	*Alkbh1*	ENSMUSG00000079036	-2,9	0,014
Translation	*Gtpbp3*	ENSMUSG00000007610	-2,6	0,029
Translation	***Fastkd2***	ENSMUSG00000025962	-2,5	0,004
Translation	***Qrsl1***	ENSMUSG00000019863	-2,3	0,000
Translation	***Mrps28***	ENSMUSG00000040269	-2,3	0,006
Translation	***Dap3***	ENSMUSG00000068921	-2,2	0,015
Translation	***Elac2***	ENSMUSG00000020549	-2,2	0,007

Supplementary Table 3: Continued

Functional Category	Symbol	EnsemblGeneID	FC	P.Value
Translation	***Mrps12***	ENSMUSG00000045948	-2,1	0,000
Translation	***Mrps36***	ENSMUSG00000061474	-2,1	0,011
Translation	***Mrpl12***	ENSMUSG00000039640	-2,1	0,018
Translation	***Mrps2***	ENSMUSG00000035772	-2,1	0,018
Translation	***C1qbp***	ENSMUSG00000018446	-2,1	0,009
Translation	***Ict1***	ENSMUSG00000018858	-2	0,006
Translation	***Vars2***	ENSMUSG00000038838	-2	0,004
Translation	***Mrpl47***	ENSMUSG00000037531	-2	0,022
Translation	***Mrpl21***	ENSMUSG00000024829	-1,9	0,006
Translation	***Mrps22***	ENSMUSG00000032459	-1,9	0,008
Translation	***Mrps16***	ENSMUSG00000049960	-1,9	0,019
Translation	***Mrpl34***	ENSMUSG00000034880	-1,9	0,026
Translation	***Mrpl23***	ENSMUSG00000037772	-1,9	0,034
Translation	***Trmu***	ENSMUSG00000022386	-1,8	0,004
Translation	***Tsfm***	ENSMUSG00000040521	-1,8	0,014
Translation	*Trmt2b*	ENSMUSG00000067369	-1,8	0,021
Translation	***Mrpl19***	ENSMUSG00000030045	-1,8	0,027
Translation	*Mrpl38*	ENSMUSG00000020775	-1,8	0,040
Translation	***Pdf***	ENSMUSG00000078931	-1,8	0,019
Translation	*Rpusd3*	ENSMUSG00000051169	-1,8	0,035
Translation	***Mrps5***	ENSMUSG00000027374	-1,7	0,004
Translation	*Mtg2*	ENSMUSG00000039069	-1,7	0,005
Translation	***Mrpl18***	ENSMUSG00000057388	-1,7	0,015
Translation	***Mrpl15***	ENSMUSG00000033845	-1,7	0,022
Translation	***Mrpl24***	ENSMUSG00000019710	-1,7	0,022
Translation	***Mrps33***	ENSMUSG00000029918	-1,7	0,041
Translation	***Mars2***	ENSMUSG00000046994	-1,7	0,015
Translation	***Guf1***	ENSMUSG00000029208	-1,7	0,026
Translation	***Mrps17***	ENSMUSG00000034211	-1,6	0,005
Translation	***Mrps23***	ENSMUSG00000023723	-1,6	0,030
Translation	***Mrps18b***	ENSMUSG00000024436	-1,6	0,033
Translation	*Thg1l*	ENSMUSG00000011254	-1,6	0,010
Translation	*Mtrf1l*	ENSMUSG00000019774	-1,5	0,007
Translation	***Mtif2***	ENSMUSG00000020459	-1,5	0,016
Translation	***Yars2***	ENSMUSG00000022792	-1,5	0,017
Translation	***Mrpl4***	ENSMUSG00000003299	-1,5	0,017
Translation	*Trmt10c*	ENSMUSG00000044763	-1,5	0,030
Translation	***Mrpl46***	ENSMUSG00000030612	-1,5	0,030
Translation	***Ears2***	ENSMUSG00000030871	-1,5	0,031
Translation	***Mrpl22***	ENSMUSG00000020514	-1,5	0,032
Translation	***Mrpl28***	ENSMUSG00000024181	-1,5	0,044
Translation	*Tars*	ENSMUSG00000022241	-1,4	0,009
Translation	***Mrpl3***	ENSMUSG00000032563	-1,4	0,015

Supplementary Table 3: Continued

Functional Category	Symbol	EnsemblGeneID	FC	P.Value
Translation	***Mrpl43***	ENSMUSG00000025208	-1,4	0,020
Translation	***Aars2***	ENSMUSG00000023938	-1,4	0,026
Translation	***Mrpl45***	ENSMUSG00000018882	-1,4	0,032
Translation	***Gars***	ENSMUSG00000029777	-1,4	0,034
Translation	***Kars***	ENSMUSG00000031948	-1,4	0,047
Translation	*Rars*	ENSMUSG00000018848	-1,4	0,021
Translation	*Secisbp2*	ENSMUSG00000035139	-1,4	0,027
Translation	*Ftsj2*	ENSMUSG00000029557	-1,4	0,041
Uncoupling	***Ucp1***	ENSMUSG00000031710	-7,3	0,042
Unknown	***Acyp2***	ENSMUSG00000060923	-1,7	0,037
Unknown	***Ccdc58***	ENSMUSG00000075229	-1,5	0,024
Various metabolism	***Gk***	ENSMUSG00000025059	-3,1	0,004
Various metabolism	*Shmt1*	ENSMUSG00000020534	-2,8	0,016
Various metabolism	***Akr1b10***	ENSMUSG00000061758	-2,2	0,025
Various metabolism	***Carkd***	ENSMUSG00000031505	-2,1	0,000
Various metabolism	***Comtd1***	ENSMUSG00000021773	-1,7	0,019
Various metabolism	***Acad8***	ENSMUSG00000031969	-1,4	0,019
Various metabolism	***Pycr1***	ENSMUSG00000025140	-9,2	0,000
Various metabolism	*Mthfd2*	ENSMUSG00000005667	-4,8	0,001

Bold symbols are of genes which mitochondrial localization is proven for the white adipose tissue.

Supplementary Table 4: Functional categorization of genes upregulated at postnatal day 98 compared to 21, with strong support of mitochondrial localization. Expression of transcripts analyzed with mRNA sequence, of the transcripts with p<0.05 genes encoding proteins with strong support of mitochondrial localization (Mouse MitoCarta 2.0, Broad institute) were selected and functional categorized with Nextprot (SIB Swiss institute for bioinformatics)

Functional Category	Symbol	EnsemblGeneID	FC	P.Value
Apoptosis	*Bcl2l2*	ENSMUSG00000089682	1,7	0,006
Apoptosis	***Ghitm***	ENSMUSG00000041028	1,8	0,050
Apoptosis	***Mtch1***	ENSMUSG00000024012	2,0	0,008
Apoptosis	***Fhit***	ENSMUSG00000060579	3,3	0,004
BCAA/SCFA metabolism	***Aldh6a1***	ENSMUSG00000021238	1,4	0,026
BCAA/SCFA metabolism	***Pcca***	ENSMUSG00000041650	1,4	0,048
BCAA/SCFA metabolism	***Prdx6***	ENSMUSG00000026701	1,5	0,029
BCAA/SCFA metabolism	***Auh***	ENSMUSG00000021460	1,5	0,022
BCAA/SCFA metabolism	***Ivd***	ENSMUSG00000027332	1,6	0,008
BCAA/SCFA metabolism	***Lyplal1***	ENSMUSG00000039246	2,0	0,006
BCAA/SCFA metabolism	***Gpt2***	ENSMUSG00000031700	2,1	0,003
BCAA/SCFA metabolism	***Abat***	ENSMUSG00000057880	3,2	0,021
BCAA/SCFA metabolism	*Sugct*	ENSMUSG00000055137	3,6	0,008
BCAA/SCFA metabolism	***Mccc1***	ENSMUSG00000027709	33217	0,002
Dynamics/Morphology	***Slc25a46***	ENSMUSG00000024259	1,9	0,001
FA metabolism	***Acsl1***	ENSMUSG00000018796	1,8	0,044
FA oxidation	***Echdc2***	ENSMUSG00000028601	2,1	0,002
FA oxidation	***Acox1***	ENSMUSG00000020777	2,9	0,000
FA oxidation	***Hsd17b4***	ENSMUSG00000024507	1,7	0,008
FA oxidation	***Abcd2***	ENSMUSG00000055782	2,1	0,002
FA oxidation	***Acad11***	ENSMUSG00000090150	3,3	0,001
FA oxidation	***Pccb***	ENSMUSG00000032527	2,0	0,016
FA synthesis	***Acss3***	ENSMUSG00000035948	5,2	0,000
FA synthesis	***Acsm3***	ENSMUSG00000030935	5,3	0,032
FA synthesis	***Acsm5***	ENSMUSG00000030972	5,3	0,000
Fe/FeS	***Iscu***	ENSMUSG00000025825	1,5	0,011
Fe/FeS	*Sfxn4*	ENSMUSG00000063698	2,5	0,035
Fe/FeS	***Bola1***	ENSMUSG00000015943	2,9	0,022
Fe/FeS	*Ndor1*	ENSMUSG00000006471	1,4	0,031
Metabolic signalling	***Aldh1a7***	ENSMUSG00000024747	2,0	0,011
Metabolic signalling	*Ncoa4*	ENSMUSG00000056234	1,8	0,003
Metabolite transport	***Slc25a26***	ENSMUSG00000045100	1,4	0,028
Metabolite transport	*Slc22a4*	ENSMUSG00000020334	2,4	0,001
Mitochondrial replication	***Tk2***	ENSMUSG00000035824	1,5	0,034
Mitophagy	*Stx17*	ENSMUSG00000061455	1,8	0,003
Mitophagy	*Kif1b*	ENSMUSG00000063077	2,3	0,002
Mitophagy	*Pink1*	ENSMUSG00000028756	2,7	0,000
Mitophagy	***Bnip3***	ENSMUSG00000078566	2,7	0,000
Mitophagy	*Bnip3l*	ENSMUSG00000022051	299,3	0,011
Non mitochondrial	*Dmpk*	ENSMUSG00000030409	2,3	0,004
Non mitochondrial	*Ttc7b*	ENSMUSG00000033530	1,7	0,007
Non mitochondrial	***Tkt***	ENSMUSG00000021957	2,2	0,045
Non mitochondrial	***Ephx2***	ENSMUSG00000022040	2,2	0,008

Supplementary Table 4: Continued

Functional Category	Symbol	EnsemblGeneID	FC	P.Value
Other	*Prepl*	ENSMUSG00000024127	1,5	0,044
Other	***Pxmp2***	ENSMUSG00000029499	2,7	0,020
Other	***Pxmp4***	ENSMUSG00000000876	1,4	0,046
OXPHOS	***Atp5h***	ENSMUSG00000034566	1,5	0,025
OXPHOS	***Surf1***	ENSMUSG00000015790	3,5	0,007
OXPHOS	*Cox19*	ENSMUSG00000045438	3,9	0,017
Protein import and folding	***Clpb***	ENSMUSG00000001829	1,5	0,046
Protein import and folding	*Nrd1*	ENSMUSG00000053510	1,6	0,016
Protein import and folding	***Tomm40l***	ENSMUSG00000005674	3,0	0,019
Protein import and folding	***Chchd4***	ENSMUSG00000034203	2,8	0,000
Redox	***Msra***	ENSMUSG00000054733	1,5	0,016
Redox	***Gpx1***	ENSMUSG00000063856	1,7	0,029
Redox	***Mgst1***	ENSMUSG00000008540	2,1	0,000
Redox	***Cat***	ENSMUSG00000027187	2,2	0,001
Redox	***Fam213a***	ENSMUSG00000021792	2,7	0,004
Redox	***Htatip2***	ENSMUSG00000039745	2,7	0,000
Redox	***Mgst3***	ENSMUSG00000026688	2,9	0,002
Sterol metabolism	***Cyp27a1***	ENSMUSG00000026170	1,5	0,003
Sterol metabolism	*Serac1*	ENSMUSG00000015659	2,4	0,001
Sterol metabolism	***Cyb5r3***	ENSMUSG00000018042	1,7	0,006
Transcription	***Lrpprc***	ENSMUSG00000024120	224,9	0,009
Translation	***Trnt1***	ENSMUSG00000013736	1,6	0,030
Translation	*Mtg1*	ENSMUSG00000039018	1,6	0,015
Translation	***Mrps6***	ENSMUSG00000039680	1,7	0,038
Translation	***Mrpl41***	ENSMUSG00000036850	1,8	0,014
Translation	***Hrsp12***	ENSMUSG00000022323	3,7	0,002
Unknown	***Tmem205***	ENSMUSG00000040883	308,5	0,010
Various metabolism	*Asah2*	ENSMUSG00000024887	1,5	0,028
Various metabolism	***Mdh1***	ENSMUSG00000020321	1,6	0,013
Various metabolism	***Pdp1***	ENSMUSG00000049225	5,3	0,022
Various metabolism	***Dhrs7b***	ENSMUSG00000042569	1,5	0,045
Various metabolism	***Sqrdl***	ENSMUSG00000005803	1,6	0,012
Various metabolism	***Maob***	ENSMUSG00000040147	1,7	0,023
Various metabolism	***Dglucy***	ENSMUSG00000021185	1,7	0,008
Various metabolism	***Acad12***	ENSMUSG00000042647	1,9	0,018
Various metabolism	***Maoa***	ENSMUSG00000025037	2,0	0,002
Various metabolism	***Car5b***	ENSMUSG00000031373	2,0	0,027
Various metabolism	***Fahd2a***	ENSMUSG00000027371	2,1	0,011
Various metabolism	***Cyb5***	ENSMUSG00000024646	2,2	0,002
Various metabolism	*Sdsl*	ENSMUSG00000029596	2,2	0,006
Various metabolism	*Chpt1*	ENSMUSG00000060002	2,3	0,005
Various metabolism	***Aldh2***	ENSMUSG00000029455	2,4	0,001
Various metabolism	***Ldhd***	ENSMUSG00000031958	2,6	0,015
Various metabolism	***Gldc***	ENSMUSG00000024827	4,5	0,000
Various metabolism	***Crat***	ENSMUSG00000026853	1,9	0,027

Bold symbols are of genes which mitochondrial localization is proven for the white adipose tissue.

References:

1 Meng L, Jan SZ, Hamer G, van Pelt AM, van der Stelt I, Keijer J, et al. Preantral follicular atresia occurs mainly through autophagy, while antral follicles degenerate mostly through apoptosis. *Biol Reprod* (2018) 99(4):853-63. doi: 10.1093/biolre/ioy116. PubMed PMID: 29767707.

2 Gesta S, Tseng YH, Kahn CR. Developmental origin of fat: tracking obesity to its source. *Cell* (2007) 131(2):242-56. doi: 10.1016/j.cell.2007.10.004. PubMed PMID: 17956727.

Supplementary Figures

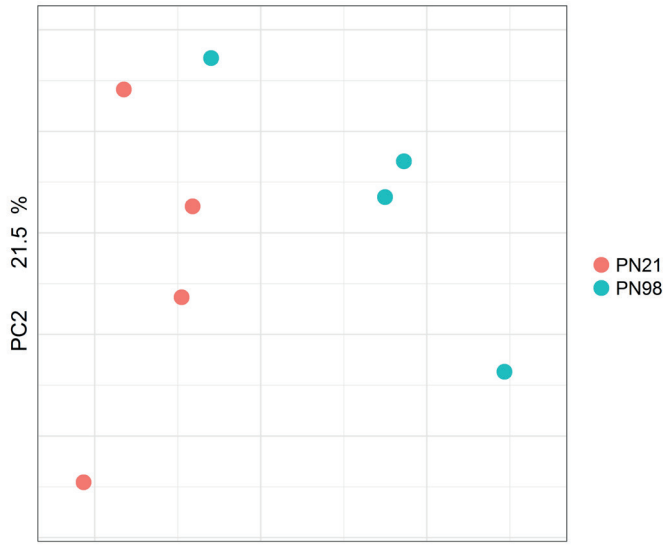

Supplementary Figure 1: Principal component analyses plot of the RNA sequence data. Transcripts were included when FPKM > 0 for all samples and average FPKM > 2 at PN21 or 98.

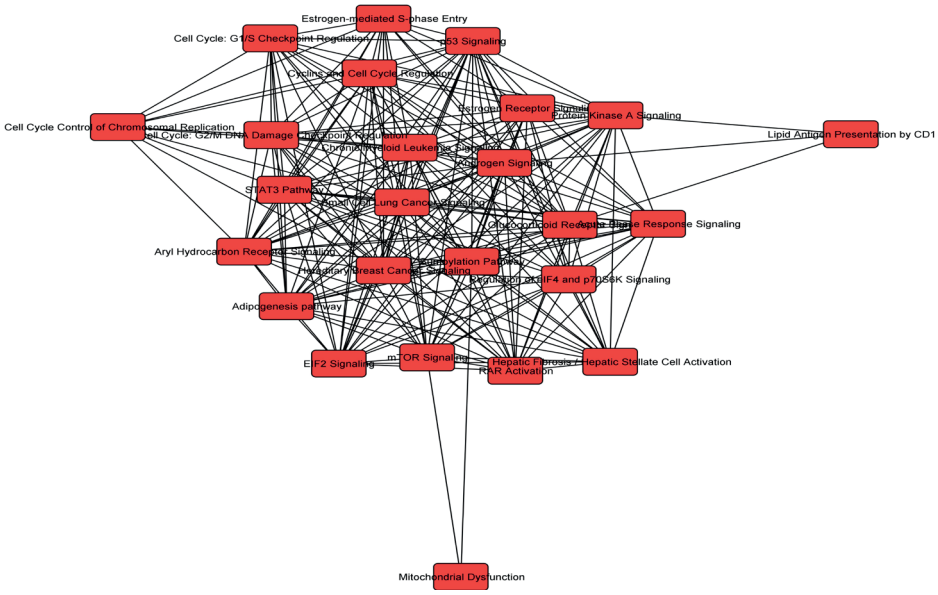

Supplementary Figure 2: Plot of overlapping canonical pathways in IPA analyses.

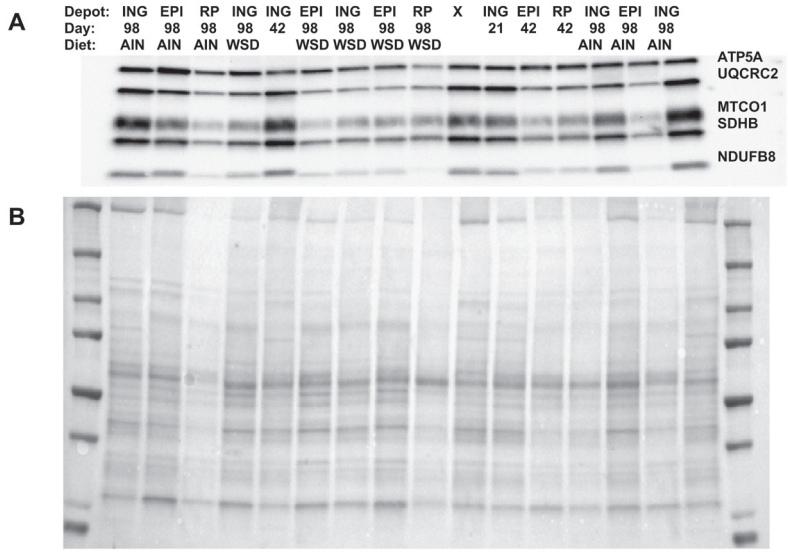

Supplementary Figure 3: Representative western blot (**A**) and corresponding Coomassie stained blot (**B**), used for total protein correction. Five subunits representing the five oxidative phosphorylation complexes were stained. ING: Inguinal; EPI: epididymal, RP: retroperitoneal, Days: days after birth; Diet: adult diet (from day 42-98); AIN: American Institute of Nutrition-93M; WSD: western style diet.

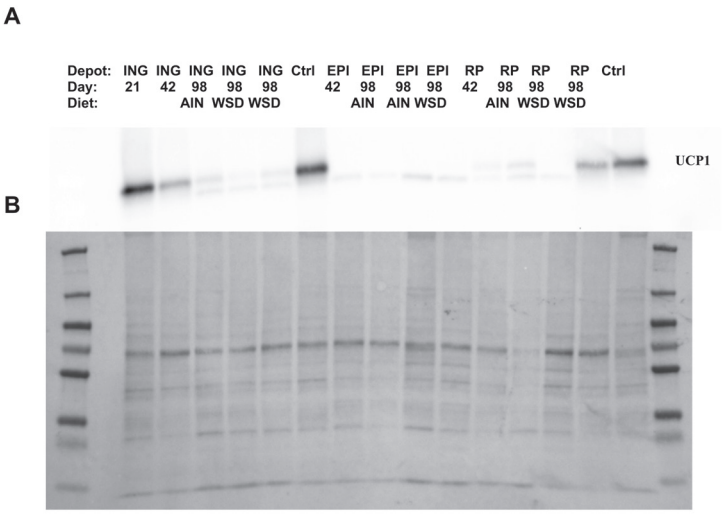

Supplementary Figure 4: Representative UCP1 western blot with UCP1 staining in inguinal (ING), epididymal (EPI) and retroperitoneal (RP) (**A**) and corresponding Coomassie stained blot (**B**), used for total protein correction. Groups are indicated above the western blot and are similar for the Coomassie stain. Two control samples (ctrl) were included to check for inter-gel differences in staining intensity, both were from ING PN42. Days: days after birth; Diet: adult diet (from day 42-98); AIN: American Institute of Nutrition-93M; WSD: western style diet.

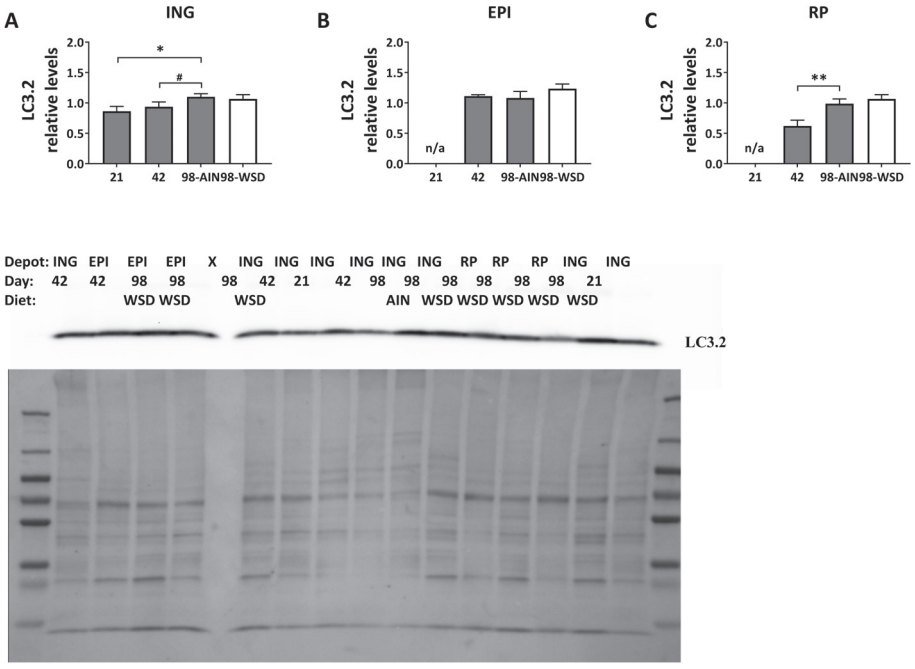

Supplementary Figure 5: Changes in LC3.2 protein levels between postnatal day 21 and 98 in **A**) inguinal (ING), **B**) epididymal (EPI) and **C**) retroperitoneal (RP) white adipose tissue. **D**) a representative blot with corresponding Coomassie staining, used for total protein correction. AIN: American Institute of Nutrition-93M; WSD: western style diet. Data expressed as mean expression levels corrected for total protein expression + SEM, n = 8 for PN21 and PN42 and n = 11 for PN98, no data available (n/a) for EPI and RP WAT at PN21. Time and WSD effects were analysed separately; time effect: *p<0.05; **p<0.01; $^{\#}$0.05<p<0.1.

[1] Danone Nutricia Research, Utrecht, The Netherlands; [2] Department of Pediatrics, University Medical Center Groningen - University of Groningen, Groningen, The Netherlands; [3] Human and Animal Physiology, Wageningen University, Wageningen, The Netherlands.

Chapter 4

Exploring mechanisms in a mouse model for nutritional programming: the impact of dietary lipid droplet structure on white adipose tissue in young mice

Andrea Kodde[1], Eline M. van der Beek[2], Sebastian Tims[1], Marieke Abrahamse[1] and Jaap Keijer[3]

In preparation

Abstract

The metabolic function of white adipose tissue (WAT) in obesity is associated with type 2 diabetes (T2D) and non-alcoholic fatty liver disease (NAFLD) risk. The perinatal diet, including, but not limited to, maternal under- and overnutrition has a demonstrated programming effect on WAT function. Previously, in a mouse model for nutritional programming, postnatal feeding a diet with large, (milk)phospholipid coated lipid droplets (Concept) increased WAT mitochondrial density and oxidative capacity markers following a Western style diet (WSD) in adulthood. The current study aims to determine whether the Concept diet already impacts mitochondrial density and oxidative capacity markers during early life i.e., immediately following the postnatal dietary intervention period.

C57BL/6j mice were fed the Concept diet or a control (CTRL) diet from postnatal day (PN)16, while they were also allowed to drink with their mothers and continued on the diets after weaning (PN21) until PN42. Expression of oxidative phosphorylation (OXPHOS) protein, mitochondrial (mt)DNA and citrate synthase (CS) were analyzed in epididymal (EPI), retroperitoneal (RP) and inguinal (ING) WAT at PN42. Further, DNA methylation and mRNA sequencing (RNAseq) of EPI WAT were performed as exploratory readouts to better understand potential mechanisms involved.

Following the postnatal intervention with the Concept diet, body weight and WAT weight were comparable to that of control animals. Interestingly, several subunits of OXPHOS were reduced in EPI and RP WAT (EPI: SDHB, ATP5A and a trend for NDUFB8, RP: UQCRC2 and a trend for ATP5A) and increased in ING WAT (NDUFB8 and a trend for SDHB), without affecting mtDNA and citrate synthase levels. The Concept diet reduced expression and increased methylation of pathways involved in growth and development of cells and tissues in EPI WAT and WAT innervation and changed the phospholipases pathway and expression of NAD synthase and salvage pathways.

In summary, the Concept diet had WAT depot-specific effects on OXPHOS protein expression but did not affect mitochondrial density markers. Our exploratory analyses indicated that the Concept may have changed growth and development of the EPI WAT, suggesting a difference in energy flow to this WAT depot that may underly the observed lower adiposity following a subsequent WSD challenge.

Introduction

The prevalence of obesity has increased worldwide over the last decades. Although numbers are stabilizing in some countries, prevalence is still increasing globally in adults, children and adolescents, affecting a large proportion of people across life stages (1). Although there is debate to which extent obesity may be a disease in its own right (2, 3), obesity is a risk factor for, and contributes to, the development of other metabolic diseases, like type 2 diabetes (T2D), cardiovascular disease and non-alcoholic fatty liver disease (NAFLD), especially when the onset is in childhood or adolescence (4, 5).

The metabolic function of white adipose tissue (WAT) i.e., WAT health, is an important link between obesity and T2D and NAFLD (6-8). Impaired WAT health in obesity and the associated WAT insulin resistance drives ectopic fat deposition in other organs such as liver and skeletal muscle, an important step in the development of NAFLD and T2D (7, 9). The location of WAT depots defines the contribution to whole-body energy metabolism; visceral fat mass (in the abdominal cavity) inversely correlates to whole-body insulin sensitivity, while subcutaneous WAT (under the skin) displays a higher oxidative capacity and its WAT mass only weakly correlates to insulin sensitivity measures (10, 11).

Mitochondrial oxidative capacity is strongly correlated to WAT health, as illustrated by the reduced mitochondrial density and oxygen consumption in white adipocytes in obesity and T2D (9, 12-14). Interestingly, WAT mitochondrial dysfunction is seen independent of glucose intolerance, indicating that WAT mitochondrial dysfunction may precede insulin resistance (9). WAT mitochondrial density and oxidative capacity can also respond to nutritional changes, such as five days high fat feeding, caloric restriction, or specific fatty acids like n-3 poly-unsaturated fatty acids or milk-derived phospholipids (15-19). These results indicate that nutritional interventions have the potential to improve mitochondrial oxidative capacity in WAT adipocytes and, possibly, whole-body energy metabolism.

Several observational and experimental studies showed that nutrition during the perinatal period, for instance maternal under- or over nutrition, can alter the risk for metabolic disturbances in later life in the offspring, so-called nutritional programming (20-23). Interestingly, the postnatal diet may also contribute to improved adult metabolic health outcomes, as illustrated by the observed reduced later life overweight and obesity risk associated with prolonged breastfeeding (24). Moreover, in experimental settings, several postnatal diets showed to reduce adult adiposity in a mouse model for postnatal programming i.e., a diet high in n-3 poly-unsaturated fatty acids, a diet with galactose, or a diet with an adapted lipid droplet structure (25-27). The programming of WAT growth, the distribution of WAT over different depots and mitochondrial density

may explain some of the effects of the perinatal diet on adult metabolic health (22, 23, 25, 27-29). In rodents, WAT develops in the second trimester of pregnancy, and development continues after birth, via growth in cell number and size (hyperplasia and hypertrophy) and via functional changes, like transient browning and subsequent whitening (30-33). Indeed, expression of markers for mitochondrial density and oxidative capacity and WAT browning decreases substantially over time in the postnatal period in a depot specific manner, establishing a window for the programming of WAT health during the postnatal period (34).

Mechanisms underlying the long-term consequences of perinatal nutrition are adaptations to tissue function and structure, cellular aging, and epigenetic alterations (35). The latter is defined as 'structural adaptations to chromosomal regions as to register, signal or perpetuate an altered activity state' (36). These changes can be long lasting, often arise during development, and include histone modifications, DNA methylation and altered expression of non-coding RNAs (35). During DNA methylation, a methyl group is added to (most often) a cytosine in a GpC island, and when this occurs in the promotor region of a gene, gene expression is often silenced (35). Studies in humans and rodents showed changes in DNA methylation upon dietary changes in the lactation period, possibly linking the postnatal diet to the adult metabolic phenotype (37, 38).

We previously investigated the programming effect of a postnatal diet with large, (milk) phospholipid coated lipid droplets (Concept), that closely resembles the human milk fat globule structure. Compared to a control diet with small, non-coated lipid droplets, resembling the lipid droplets in standard infant milk formula (IMF), a postnatal diet with Concept prevented adult, obesogenic diet-induced adiposity, and insulin resistance in a mouse model for nutritional programming (26, 39, 40). Interestingly, mice fed the Concept diet postnatally showed higher mitochondrial density and protein expression of the oxidative phosphorylation (OXPHOS) in visceral WAT in adulthood, following a WSD challenge, which may have been a contributing factor to the observed reduced adiposity (41). To investigate this, we examined in the current study the effect of postnatal Concept feeding on markers for mitochondrial density and β-oxidation as well as OXPHOS proteins directly at the end the postnatal dietary intervention and analyzed genome wide transcriptomics and DNA methylation to explore possible associated mechanisms.

Results

The effect of postnatal Concept feeding on bodyweight, WAT weight and mRNA expression of metabolic markers

C57BL/6jOlaHsd mice were fed a Control diet (CTRL) or a diet containing Concept (Concept) from postnatal day (PN)15 to PN42 i.e., postnatally for 28 days until the end of the study, see study design **Figure 1** and dietary composition **Table 1**.

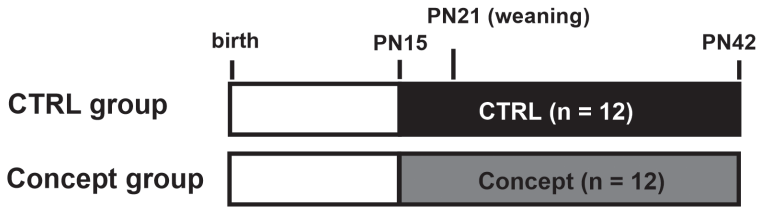

Figure 1: Study design. Concept and CTRL mice were fed a Concept-IMF or CTRL-IMF based diet from PN15 until PN42. n=12 per group. CTRL: control; PN: postnatal.

At PN42, no differences in body weight or WAT weight were found between CTRL and Concept groups (**Figure 2A and B**). mRNA expression of markers for adiposity and metabolic function was analyzed by quantitative-real time RT-PCR (qPCR) in epididymal (EPI) and inguinal (ING) WAT to identify eventual changes in WAT expansion and the metabolic profile of the visceral and subcutaneous WAT. mRNA expression of the adiposity marker *Leptin* and the adipocyte expansion marker mesoderm specific transcript (*Mest;* also known as *Peg1*) was higher in EPI WAT compared to ING WAT (*Leptin*, 1.819±0.271 *vs.* 0.550±0.109; *Mest*, 3.076±0.465 *vs.* 0.333±0.073; $p<0.01$). Also, expression of carnitine palmitoyltransferase 1a (*Cpt1a*), responsible for transport of fatty acids over the inner mitochondrial membrane, was higher in EPI WAT compared to ING WAT (1.469±0.133 *vs.* 0.690±0.088; $p<0.001$). mRNA expression of the pyruvate dehydrogenase kinase 4 (*Pdk4*), part of the glucose oxidative pathway and uncoupling protein 3 (*Ucp3*) were lower in EPI compared to ING WAT (*Pdk4*, 0.498±0.097 *vs.* 5.408±0.898; *Ucp3*, 0.806±0.112 *vs.* 1.992±0.380; $p<0.05$) but expression of the glucose transporter 4 (*Glut4)* was comparable between EPI and ING WAT (0.941±0.124 vs. 1.320±0.228). No differences were observed between the CTRL and Concept groups in mRNA expression of any of the measured metabolic markers in EPI WAT or ING WAT (**Figure 2C and D**).

Table 1: Dietary composition

Diet		**CTRL**	**Concept**
Carbohydrates	(g/kg)	643.7	643.7
Sugars [a]	(g/kg)	236.1	236.1
Polysaccharides [b]	(g/kg)	407.6	407.6
Protein	(g/kg)	178.6	178.6
Fat	(g/kg)	70	70
Saturated fatty acids	(g/kg)	30.2	30.2
Monounsaturated fatty acids	(g/kg)	27.9	27.9
Polyunsaturated fatty acids	(g/kg)	11.6	11.6
Phospholipids [c]	(g/kg)	0.1	1.1
Cholesterol	(g/kg)	-	0.03
Fiber	(g/kg)	47.5	47.5
Vitamin & mineral mix	(g/kg)	45	45

a) Total sugars, including lactose, glucose, and sucrose; b) including starch and maltodextrin; c) Phospholipids derived from bovine milk; CTRL: control diet; Concept: Concept diet.

The effect of postnatal Concept feeding on mitochondrial density and oxidative capacity markers in different WAT depots

Mitochondrial density, assessed as citrate synthase (CS) activity in EPI, retroperitoneal (RP) and ING WAT and as mitochondrial DNA (mtDNA) copy number in EPI WAT, was not different between both intervention groups (**Table 2**), nor was the activity of hydroxyacyl-CoA dehydrogenase (HADH), reflecting β-oxidation.

Expression of subunits of OXPHOS complexes, as markers for mitochondrial oxidative capacity, were assessed on Western blots using antibodies against NDUFB8 (complex I), SDHB (complex II), UQCRC2 (complex III), MTCOI (complex IV) and ATP5A (complex V). In general, compared to the CTRL group, mice in the Concept group had reduced levels of OXPHOS subunits in visceral WAT, a decrease that reached significance for SDHB and ATP5A in EPI WAT and for UQCRC2 in RP WAT, with a trend for NDUFB8 in EPI WAT and ATP5A in RP WAT (**Figure 3A, B**). In contrast, the levels of OXPHOS subunits were elevated in subcutaneous WAT of Concept compared to CTRL mice, resulting in significantly higher NDUFB8 expression and a tendency towards higher SDHB expression in Concept mice for ING WAT (**Figure 3C**). The contrasting response to the Concept diet observed between visceral and subcutaneous depots became more evident when the relative ratio of expression levels between ING and EPI WAT was calculated. The relative ratio was consistently higher for all OXPHOS proteins in the Concept compared to the CTRL group (**Figure 3D**), indicating that the difference in oxidative capacity between ING and EPI WAT, which was higher in the subcutaneous (ING) WAT, was enhanced by postnatal Concept feeding.

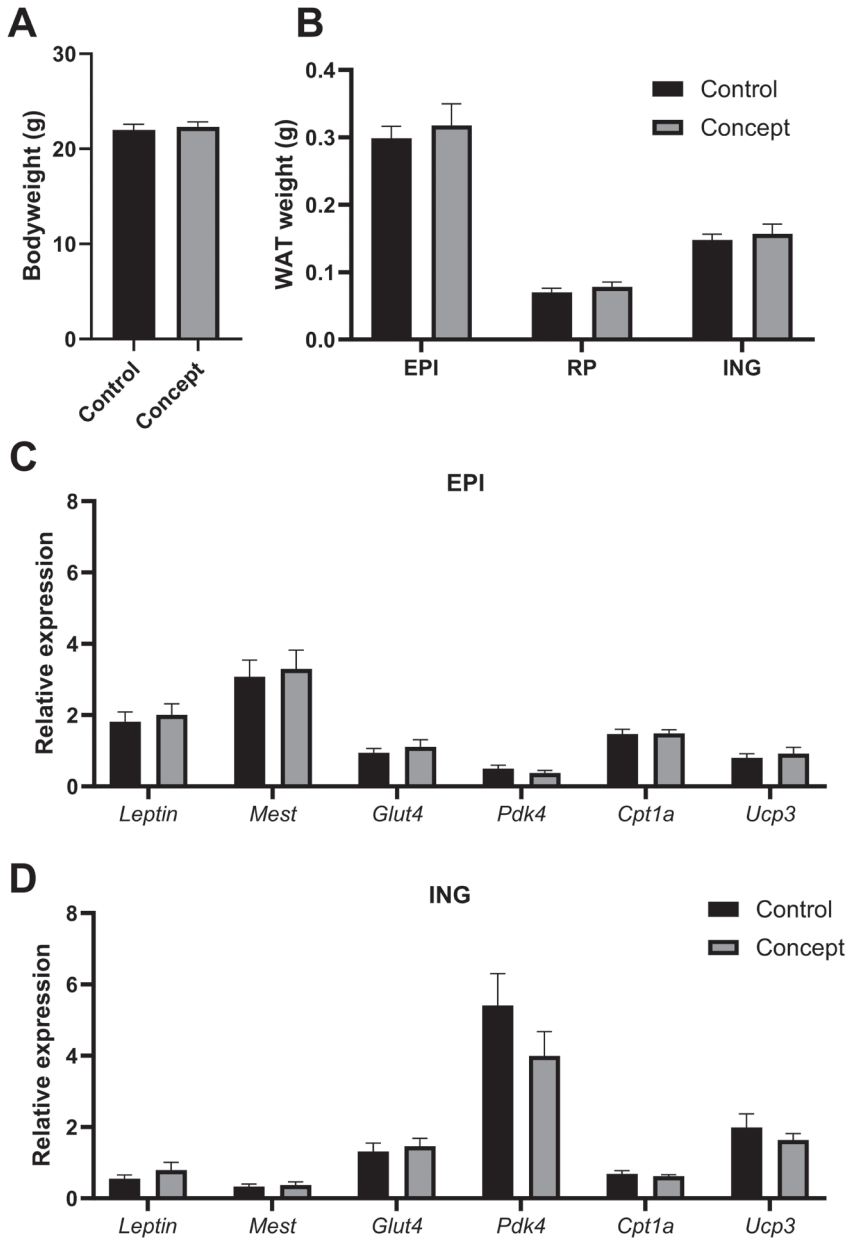

Figure 2: Bodyweight (**A**), WAT weight (**B**) and mRNA expression of metabolic genes in EPI (**C**) and ING (**D**) WAT. Bodyweight and WAT weight expressed as mean + SEM and n=12 per group. mRNA expression was n=12 for EPI WAT and n=8 for the CTRL and n=10 for the Concept group in ING WAT. Data expressed as mean expression normalized for the mean expression of the two reference genes (*Rpl19* and *Rps29*) and scaled to the mean expression per gene + SEM. Tested for statistical differences with unpaired ttest. CTRL: black bars; Concept: gray bars. EPI: epididymal; ING: inguinal; WAT: white adipose tissue.

Table 2: The effect of Concept feeding on levels of mitochondrial density and β-oxidation markers.

Group	CTRL	Concept
mtDNA (copy number)	535.0 ± 74.3	573.2 ± 91.3
CS activity (U/g protein):		
EPI	272.9 ± 45.4	241.7 ± 32.2
RP	334.9 ± 37.7	329.7 ± 41.9
ING	636.8 ± 48.01	615.3 ± 49.4
HADH activity (U/g protein):		
EPI	124.7 ± 15.8	148.2 ± 13.1
RP	83.3 ± 10.1	75.9 ± 8.3
ING	344.2 ± 21.9	283.7 ± 22.7

CS: citrate synthase; EPI: epididymal; HADH: hydroxyacyl-CoA dehydrogenase; ING: inguinal; mtDNA: mitochondrial DNA; RP: retroperitoneal.

The effect of postnatal Concept feeding on mRNA expression of the OXPHOS pathway.

To explore possible effects of postnatal feeding the Concept on mitochondrial function in WAT, mRNA sequencing (RNAseq) was performed in EPI WAT of a subset of 5 animals per group as an exploratory readout. To reduce the potential confounding impact of mice being litter mates, the samples were selected from mice from different litters, taking the quality and quantity of the available RNA samples into consideration for the final selection.

RNAseq analyses resulted in 91970 different transcripts. Of the identified transcripts, 91638 had a known identity, of which 3455 transcripts were differentially expressed in EPI WAT of Concept compared to CTRL mice ($p<0.05$). These 3455 transcripts were used for Ingenuity Pathway Analyses (IPA). The pathway mostly reflecting mitochondrial function, named “mitochondrial dysfunction”, was downregulated in the EPI WAT of the Concept compared to CTRL group (Z-score -0.429; $p<0.01$). More specifically, only genes from complex I and V of OXPHOS were present in the list of differentially expressed genes for this pathway (full list of genes in **Supplementary Table 1**). Some of those genes were upregulated, but in line with the OXPHOS protein expression patterns in EPI WAT, the general trend (as concluded by IPA) was a downregulation of those complexes in EPI WAT in the Concept compared to the CTRL group.

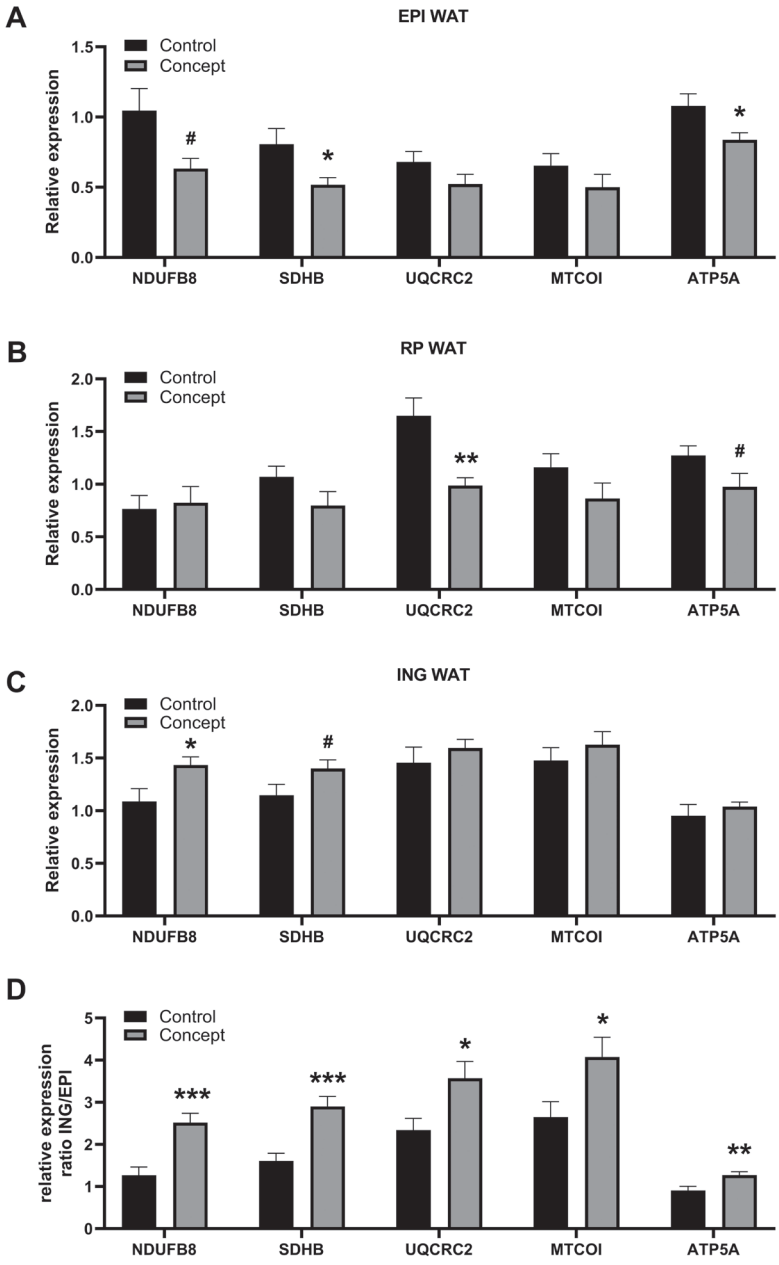

Figure 3: Changes in protein expression of OXPHOS subunits upon Concept feeding. NDUFB8 (complex I), SDHB (complex II), UQCRC2 (complex III), MTCOI (complex IV) and ATP5A (complex V) in **A**) EPI, **B**) RP and **C**) ING WAT and **D**) the ratio of those subunits between ING and EPI WAT. CTRL: black bars, Concept: gray bars. Data expressed as mean expression corrected for total protein concentration and inter-gel calibrators + SEM, n = 12 per group, except for RP WAT with n = 9 per group. Unpaired ttest; * p<0.05; ** p<0.01; ***p<0.001, # p<0.1. CTRL: control; EPI: epididymal; ING: inguinal; OXPHOS: oxidative phosphorylation; RP: retroperitoneal; WAT: white adipose tissue.

The effect of postnatal Concept feeding on DNA methylation of OXPHOS genes

Previous studies indicated that changes in DNA methylation may underlie adult consequences of postnatal nutrition (37, 38). Therefore, whole genome DNA methylation was assessed as an exploratory readout to investigate if postnatal Concept feeding changed DNA methylation of genes of the mitochondrial function pathway and the association of DNA methylation with mRNA and protein expression levels. In addition, DNA methylation changes may explain previously observed increased mitochondrial density and oxidative capacity marker levels in adult mice fed Concept in early postnatal life (41).

DNA methylation analysis of EPI WAT was performed, using methyl-CpG-binding (MBD) sequencing in DNA samples of the same animals as used for RNAseq analysis (n=5 per group). A total of 633327 unique methylated regions were identified; 43826 within 2500 base pairs of a known gene and 1336 thereof (3%) being differentially methylated between Concept and CTRL mice ($p<0.05$). The 1336 differentially methylated regions were used for IPA pathway analyses which revealed that DNA methylation of the mitochondrial dysfunction pathway was not differentially affected by Concept feeding, neither was the methylation of specific OXPHOS subunits genes.

The effect of postnatal Concept feeding on mRNA expression and DNA methylation – Pathway analyses

Association of DNA methylation and RNAseq: More extensive data analyses were executed with the mRNA sequence and DNA methylation data. First, differentially expressed transcripts and methylated regions were compared to explore association between DNA methylation and gene expression of specific genes. Unique genes differentially expressed between Concept and CTRL mice (3454 transcripts leading to 5190 unique genes, some transcripts overlapping with more than one gene region, $p<0.05$) and unique genes located near differentially methylated regions (within 2500 bp, 1829 regions linking to 1485 unique genes, $p<0.05$) were compared for similarities, resulting in 312 genes appearing in both lists. Subsequently, these 312 common genes were tested for significance with bootstrapping, resulting in a mean background distribution of 232.2 ± 14.51 genes and Z-score: 5.49, $p<0.001$, indicating that part of overlap is expected to result from biology, not a random effect.

Methylation of promotor regions of genes is reported to often result in downregulation of expression of those genes (35). Therefore, the correlation between methylation and expression of the 312 genes, with overlap in the differentially expressed and methylated list, was calculated. However, no correlation between DNA methylation and

gene expression of the same gene (r=-0.081; p=0.245) was found. Also, no correlation was observed when focussing on the methylated regions located in known promotor regions (8 genes only, r=-0.270; p=0.518).

Visualization of the methylation data showed in general a higher methylation in the Concept compared to CTRL mice (**Figure 4**). Of the genes which were differentially methylated between groups 55% had an increased methylation in the Concept compared to the CTRL group. The Concept group also showed an overall reduction in gene expression with 60% of the significant regulated genes being downregulated in the Concept compared to the CTRL group. Thus, although correlation analyses did not show a correlation between methylation and mRNA expression of the same gene, there was a general trend towards increased methylation and reduced gene expression in the Concept group.

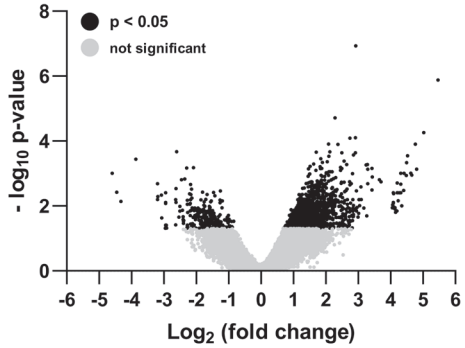

Figure 4: Volcano Plot of the DNA methylation data. Log_2 of the fold change is plotted against the $-Log_{10}$ of the p-value, each dot representing a methylated region, gray for the non-significant changed and black in case of p<0.05.

RNAseq: IPA Pathway analyses of RNAseq data resulted in 189 pathways regulated by the Concept (p<0.05), 117 with a negative z-score, 31 with a positive z-score and 41 with no z-score or a z-score of zero (**Supplementary Table 2**). The pathways were subsequently clustered according to their function as depicted in **Figure 5**, which showed a high abundance of pathways involved in growth and development of cells and tissues in EPI WAT (boxed), like organism growth and development, biosynthesis, growth factor signalling, cell cycle regulation and cellular growth, proliferation and development. A general down regulation of those pathways was seen in the mice of the Concept group. The most regulated pathway cluster was “neurotransmitters and other nervous system signalling”, including the opioid signalling, endocannabinoid neuronal synapse, synaptogenesis signalling and circadian rhythm signalling pathways among others,

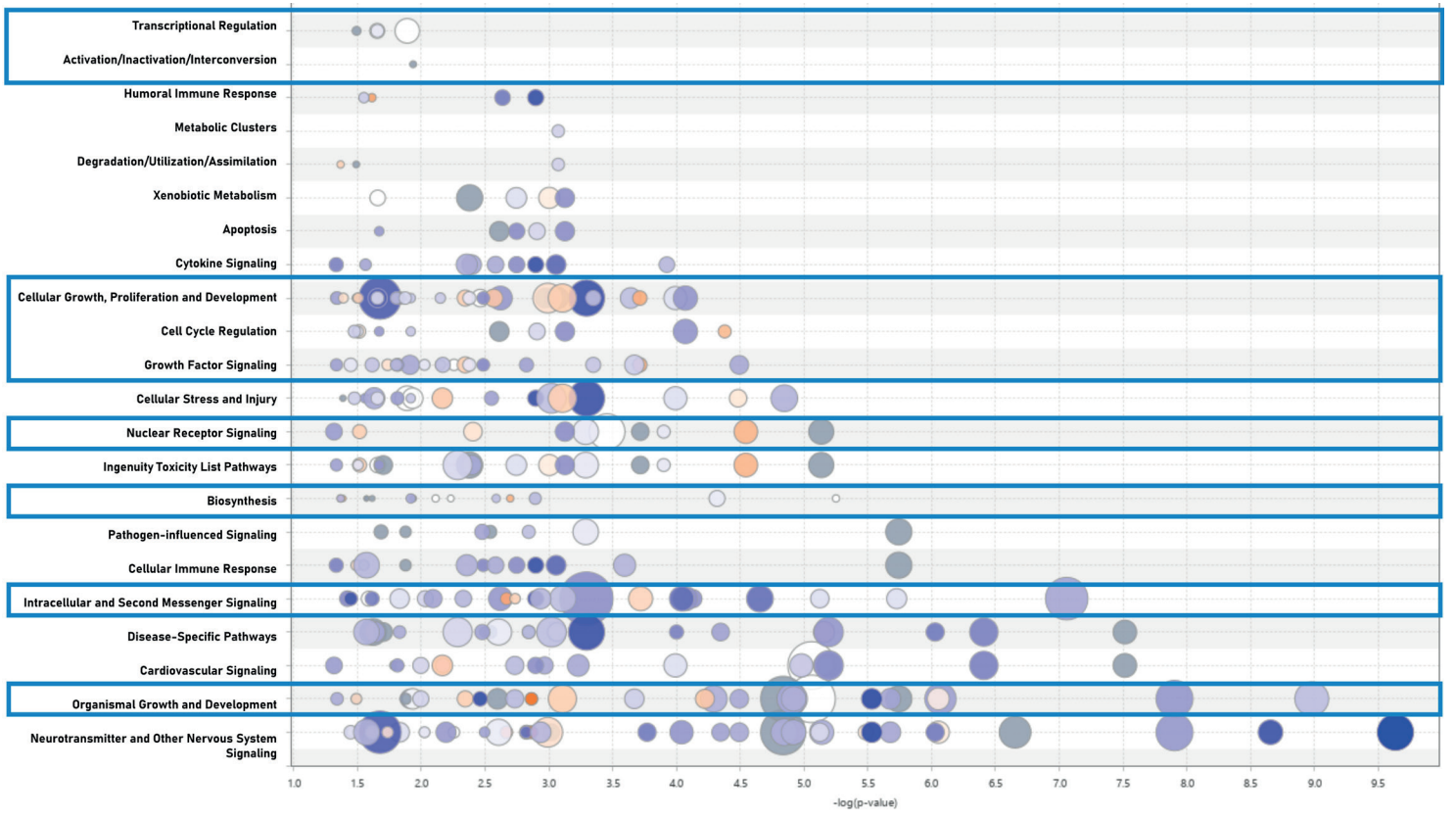

Figure 5: Functional clusters of pathways differentially expressed upon postnatal Concept feeding. Clusters as defined in IPA and chart generated by IPA (62). Color of the bubbles are defined by the z-score, blue: negative z-score, red: positive z-score, white: zero value, gray: no activity pattern and the size by the number of genes in the pathway which are changed. IPA: ingenuity pathway analyses.

which were mostly downregulated in Concept. The changes in the neurotransmitters and other nervous system signalling clusters can indicate differences in neuronal outgrowth in WAT i.e., WAT innervation, a process that is regulated by the binding of semaphorins (Sema) to Neuropilin-1 (Nrp1) and Plexin (Plxn) (42). Indeed the "Semaphorin Neuronal Repulsive Signalling Pathway" was affected by Concept feeding and has a slightly positive Z-score (Z-score: 0.174, p>0.001; Supplementary Table 2). The correlation between expression of Sema, Nrp1 and Plxn subtypes (selected based on IPA pathway) and OXPHOS was calculated, as WAT innervation can be regulated by energy balance (42), and results are depicted in a heatmap (**Figure 6A**). Protein expression of complex IV of OXPHOS (MTCOI) correlated to mRNA expression of *Sema6a* (r=0.750, p=0.012), *Nrp1* (r=0.702, p=0.024) and *Plxna2* (r=0.779, p=0.008) and tended to correlate to *Sema6d* (r=0.595, p=0.070) and *Plxna1* (r=0.579, p=0.080). Protein expression of complex III of OXPHOS (UQCRC2) tended to correlate to *Sema6a* (r=0.591, p=0.072) and *Plxna2* (r=0.589, p=0.073). No correlations between *Sema3a, Sema6c* and *Plxna3* and OXPHOS complexes were found (Figure 6A). The cluster analysis also showed that the metabolic cluster only consisted of one pathway, phospholipases.

DNA methylation: Similar trends in regulated pathways were seen in the IPA analysis of the DNA methylation data. DNA methylation of genes from 171 pathways was changed by postnatal Concept feeding, 134 showed increased methylation, 6 showed reduced methylation and 31 had no z-score or a z-score of zero (**Supplementary Table 3**). When clustered into functional categories, again a high abundance of pathways related to growth of cells and tissues in EPI WAT was found i.e., cellular growth, proliferation, development, organismal growth and development, growth factor signalling and cell cycle regulation, boxed in **Figure 7**. Methylation of most of those pathways was increased, as shown by the higher abundance of red coloured bubbles in Figure 7. The cluster "neurotransmitters and other nervous system signalling" was also differentially methylated in the Concept group, showing mostly increased methylation of genes in those pathways. Pathways present in this cluster are, among others, the myelination signalling, synaptic long-term depression, oxytocin in brain signalling and synaptogenesis signalling pathway. Methylation of the semaphorin neuronal repulsive signalling pathway was increased by Concept (Z-score: 0.832, p=0.003, Supplementary Table 3), methylation of *Sema6d* being increased by Concept, but none of the other above-mentioned genes. The metabolic cluster again only consisted of the phospholipases pathway.

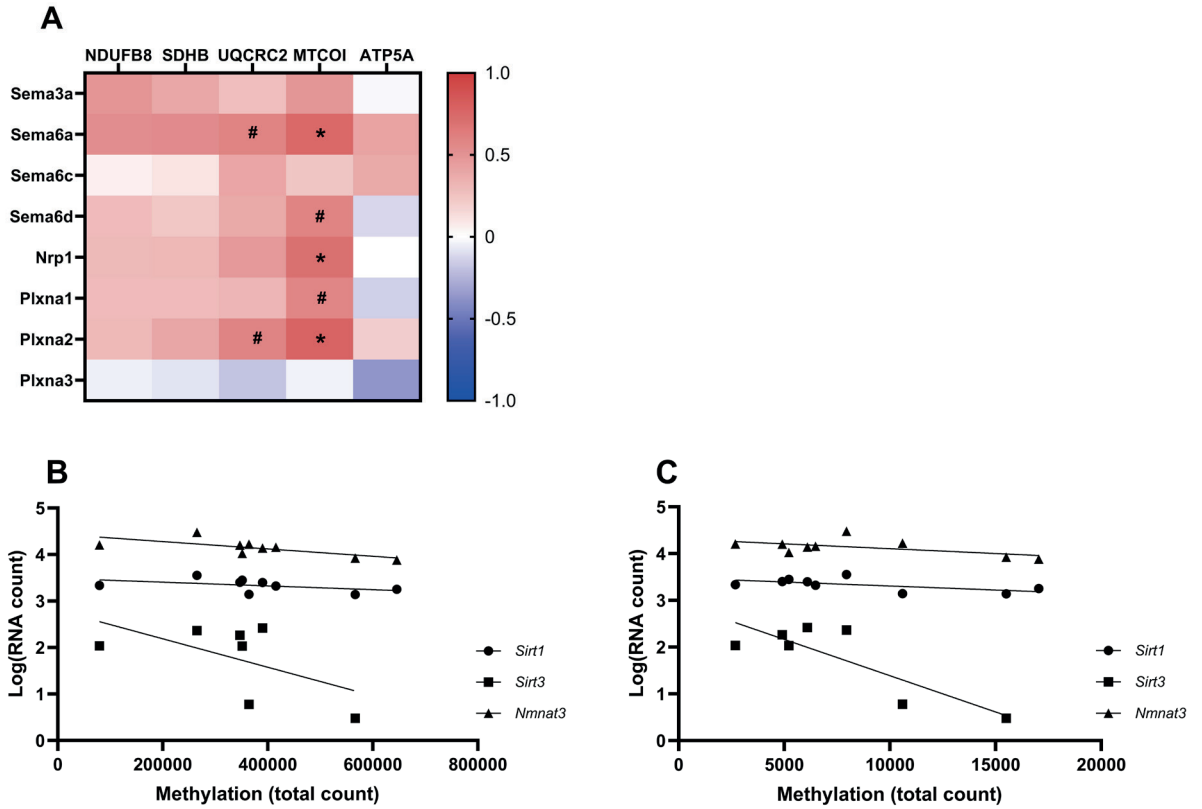

Figure 6: Correlation between mRNA expression of WAT innervation genes and OXPHOS and whole genome methylation and expression of *Sirt1*, *Sirt3* and *Nmnat3* in EPI WAT. The logarithm transformed mRNA sequence count of **A**) genes involved in WAT innervation was correlated to OXPHOS protein expression and depicted in a heatmap; and of *Sirt1*, *Sirt3* and *Nmnat3* was correlated to the sum of **B**) the total methylation count and **C**) the total methylation count of all differentially methylated regions. The heatmap shows the Pearson r for the correlation between the indicated genes and OXPHOS complexes with significant correlated shown as *p<0.05; # p<0.1. Nrp1: Neuropilin 1; OXPHOS: oxidative phosphorylation; Plxn: Plexin; Sema: semaphorin; Sirt: sirtuin; Nmnat: Nicotinamide Nucleotide Adenylyltransferase; EPI: epididymal; WAT: white adipose tissue.

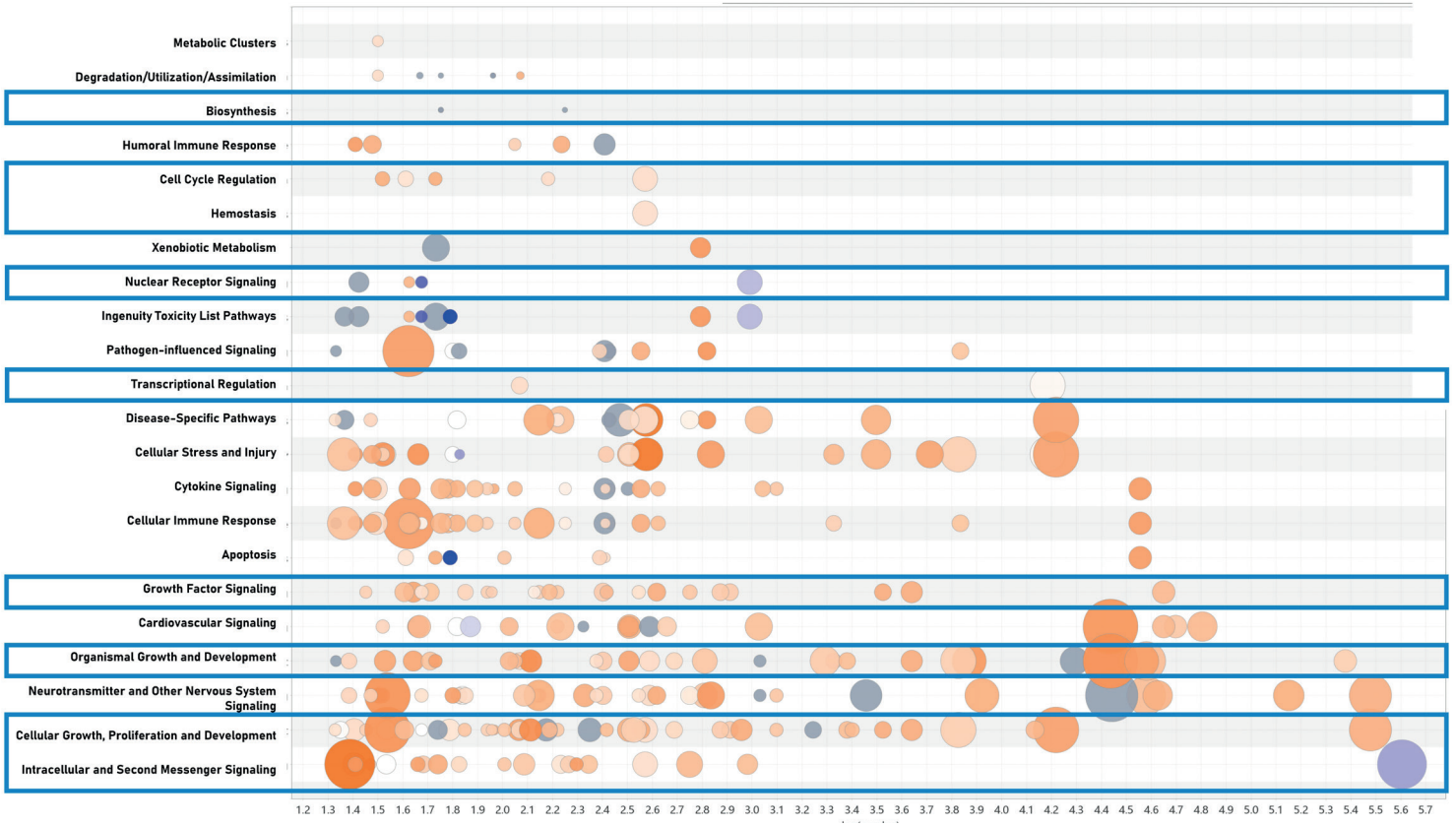

Figure 7: Functional clusters of pathways differentially methylated upon postnatal Concept feeding. Clusters as defined in IPA and chart generated by IPA (62). Color of the bubbles are defined by the z-score, blue: negative z-score, red: positive z-score, white: zero value, gray: no activity pattern and the size by the number of genes in the pathway which are changed. IPA: ingenuity pathway analyses.

Metabolic pathways: To explore changes in metabolic pathways, the results of the RNAseq and DNA methylation pathway analyses were filtered for "metabolic pathways" (**Table 3**). The expression and DNA methylation of pathways changed by Concept related to phospholipid biosynthesis and degradation. Interestingly, expression of the phosphatidylcholine synthesis pathway was increased in EPI WAT of Concept compared to the CTRL mice and expression of genes involved in degradation of phospholipids decreased and DNA methylation of those genes increased. Another metabolic pathway changed by the Concept was the mitochondrial L-carnitine shuttle pathway, which was more highly methylated (Table 3). Although mRNA expression of this pathway was affected, the direction of the change at pathway level was unclear. mRNA expression of genes of several pathways related to nicotinamide adenine dinucleotide (NAD^+) synthesis and degradation were changed by Concept feeding, including NAD^+ biosynthesis II (from tryptophan), NAD^+ biosynthesis from 2-amino-3-carboxymuconate semialdehyde, NAD^+ salvage pathway II and tryptophan degradation X (mammalian, via tryptamine). NAD^+ is a co-substrate in the deacylation of histones by the sirtuins (43). Acylation is an epigenetic process in which an acyl group, mostly an acetyl, is attached to the core or tail of a histone, changing the histone conformation. In contrast to DNA methylation, which in general silences gene expression by reducing accessibility of DNA for transcription factors, acylation in general activates gene expression by enhancing DNA accessibility for transcription factors. DNA methylation and histone acylation are tightly coupled, and thus, the increased genome wide methylation seen in EPI WAT of the Concept mice, may be linked to reduced acylation. DNA acylation was not analysed, but to investigate a possible link between the regulation of the NAD^+ pathway and the increased DNA methylation in the Concept mice, the expression of three NAD^+ related genes and their correlation to total DNA methylation were analyzed. Expression of nicotinamide nucleotide adenylyltransferase 3 (*Nmnat3*), a key enzyme in both the NAD^+ biosynthesis and salvage pathway, was downregulated by the Concept (logFC: -4.927; $p<0.001$) and inversely correlated to total methylation ($r=-0.719$, $p=0.029$), but not to the total methylation count of the differentially methylated regions ($r=-0.569$, $p=0.180$; **Figure 6B, C**). Expression of the sum of three transcripts of the mitochondrial sirtuin *Sirt3* (logFC: -10.172, 8.936, -6.019; each $p<0.01$), was inversely correlated to methylation of differentially methylated regions ($r=-0.837$, $p=0.019$). The expression of *Sirt1* (LogFC: -8.496; $p<0.001$), with a primarily cytoplasmic and nuclear distribution, tended to inversely correlate to methylation of differentially methylated regions ($r=-0.616$, $p=0.077$; Figure 6B, C). The correlations between *Sirt3* or *Sirt1* and whole genome methylation did not reach significance ($r=-0.561$, $p=0.191$ and $r=-0.478$, $p=0.193$ respectively). Poly (ADP-ribose) polymerase (PARP) is a major NAD^+ consumer

and inhibition of PARPs activity by NAD^+ depletion leads to DNA hypermethylation (43). *Parp* mRNA expression was not changed by the Concept ($p>0.1$), nor was its expression correlated to DNA methylation ($r=-0.367$, $p=0.332$).

Table 3: IPA pathway analyses, selection of metabolic pathways regulated by the Concept, mRNA expression and DNA methylation

Ingenuity Canonical Pathways	p-value	z-score	Genes
mRNA sequencing			
Phosphatidylcholine Biosynthesis I	5.62E-06	0	CEPT1, CHKB, CHPT1, PCYT1A, PCYT1B, PHKA1
Salvage Pathways of Pyrimidine Ribonucleotides	4.79E-05	-0.209	AK1, AK4, APOBEC1, APOBEC3B, ARAF, CDK1, CMPK1, DMPK, DYRK1A, GRK6, IRAK1, MAK, MAP2K2, MAP2K4, MAP2K6, MAP3K6, NME2, PAK3, PAK5, SGK1, UCKL1, UPP1, UPP2
Phospholipases	8.51E-04	-0.5	ABHD3, PLA2G2E, PLA2G4A, PLA2G4E, PLA2G5, PLA2G6, PLA2G7, PLB1, PLCB2, PLCB4, PLCD3, PLCG1, PLCH1, PLCH2, PLCZ1, PLD3
Pyridoxal 5'-phosphate Salvage Pathway	1.29E-03	-0.775	ARAF, CDK1, DMPK, DYRK1A, GRK6, IRAK1, MAK, MAP2K2, MAP2K4, MAP2K6, MAP3K6, PAK3, PAK5, PDXK, SGK1
Choline Biosynthesis III	2.00E-03	0.816	CEPT1, CHPT1, PCYT1A, PCYT1B, PHKA1, PLD3
D-myo-inositol (1,4,5)-Trisphosphate Biosynthesis	2.57E-03	-0.707	PIP5K1C, PLCB2, PLCB4, PLCD3, PLCG1, PLCH1, PLCH2, PLCZ1
NAD biosynthesis II (from tryptophan)	5.89E-03	0	KMO, NADSYN1, NMNAT1, Nmnat3, TDO2
γ-linolenate Biosynthesis II (Animals)	7.76E-03	0	ACSF2, ACSL4, ACSL6, ACSM1, FADS1, SLC27A2
Fatty Acid Activation	1.17E-02	NaN	ACSF2, ACSL4, ACSL6, ACSM1, SLC27A2
tRNA Splicing	1.20E-02	-1	MPPED2, PDE10A, PDE12, PDE1A, PDE1C, PDE2A, PDE4B, PDE8B, PDE9A, TULP2
NAD Biosynthesis from 2-amino-3-carboxymuconate Semialdehyde	2.40E-02	NaN	NADSYN1, NMNAT1, Nmnat3
Hypusine Biosynthesis	2.69E-02	NaN	DHPS, EIF5A
Geranylgeranyldiphosphate Biosynthesis	2.69E-02	NaN	FNTB, GGPS1
Mitochondrial L-carnitine Shuttle Pathway	3.24E-02	NaN	ACSF2, ACSL4, ACSL6, ACSM1, SLC27A2
Colanic Acid Building Blocks Biosynthesis	4.17E-02	1	GALK2, GMDS, GMPPA, UGP2
NAD Salvage Pathway II	4.27E-02	-0.816	ACP1, Acp5, NMNAT1, Nmnat3, NT5C3B, PXYLP1
Tryptophan Degradation X (Mammalian, via Tryptamine)	4.27E-02	0.447	Akr1b7, ALDH3A1, ALDH3A2, ALDH7A1, DDC, SMOX

Table 3: Continued

Ingenuity Canonical Pathways	p-value	z-score	Genes
Phosphatidylglycerol Biosynthesis II (Non-plastidic)	4.27E-02	0.816	AGPAT3, LPCAT1, LPGAT1, PGS1, TAFAZZIN, TAMM41
DNA methylation			
Biotin-carboxyl Carrier Protein Assembly	5.62E-03	NaN	ACACB, HLCS
Mitochondrial L-carnitine Shuttle Pathway	8.51E-03	2	CPT1A, CPT1C, SLC27A1, SLC27A2
Phenylethylamine Degradation I	1.10E-02	NaN	ALDH3A2, AOC2
Citrulline-Nitric Oxide Cycle	1.78E-02	NaN	ASS1, NOS1
Phenylalanine Degradation IV (Mammalian, via Side Chain)	2.14E-02	NaN	ACSF3, ALDH3A2, SLC27A2
Phospholipases	3.16E-02	0.816	ABHD3, PLA2G2C, PLA2G4D, PLA2G5, PLA2G6, PLCL2, PNPLA2

NaN: not a number

Discussion

In the present study, we show that postnatal feeding of a diet with large, (milk) phospholipid coated lipid droplets reduced OXPHOS protein and gene expression in visceral WAT depots, without affecting DNA methylation of OXPHOS complexes. In contrast, OPXHOS protein levels in the subcutaneous depot were higher in the mice fed the Concept compared to the CTRL in postnatal life. Overall, OXPHOS protein levels were higher in ING versus EPI WAT and this difference was augmented in the Concept group. Further exploratory analyses of RNAseq and DNA methylation in EPI WAT showed a higher methylation by postnatal Concept feeding. Reduced mRNA expression and increased methylation was seen for pathways involved in growth and development of cells and tissues in EPI WAT, WAT innervation and the phospholipases pathways. Additionally, mRNA expression of NAD^+-biosynthesis and salvage pathways was altered. Previously, we found that postnatal feeding with the Concept increased levels of mitochondrial density markers and OXPHOS protein levels in RP WAT after a later life (PN42-98) WSD challenge (41). In the present study, we examined if those changes were already present directly after the postnatal diet intervention, prior to adipose tissue accumulation following the WSD challenge. The reduced expression of OXPHOS proteins and unchanged levels of mitochondrial density markers in both visceral WAT depots and absence of DNA methylation of OXPHOS complexes in EPI WAT at PN42 suggests that mitochondrial density and oxidative capacity in visceral WAT were not programmed by the Concept. At least OXPHOS protein expression and mitochondrial density were not permanently i.e., into later life, increased by the Concept. Yet, programming of

mitochondrial oxidative capacity via upstream regulators and via different epigenetic mechanisms, like histone modification or non-coding RNA's, cannot be excluded. Targeted analyses of promotor region methylation of OXPHOS genes and upstream regulators and additional functional analyses are needed to draw more definitive conclusions about programming of mitochondrial oxidative capacity.

Interestingly OXPHOS protein levels in the ING WAT were increased by postnatal Concept feeding. ING WAT has been shown to have a higher oxidative capacity and a brown-like phenotype, especially at younger ages, compared to visceral WAT (11, 34). The higher OXPHOS protein expression in the ING WAT may therefore reflect an increase in number of brown adipocytes or browning of adipocytes and a higher oxidative capacity in the ING WAT of Concept mice, potentially leading to a reduced energy flow towards the visceral depots. Indeed, exposure of adult mice to different milk-derived phospholipids has been shown to increase WAT browning and oxidative capacity in subcutaneous depots (19, 44). However, the unchanged WAT weight in the present study showed that differences in oxidative capacity did not result in differences in lipid storage, although a difference in maximum oxidative capacity may only become evident in case of subsequent (dietary) challenges. Furthermore, histological analysis of ING WAT is needed to confirm possible effects of the Concept on WAT browning.

The exploratory analyses of mRNA expression and DNA methylation in EPI WAT gave more insight into potentially implicated mechanisms. First, the marked reduction in expression of pathways involved in growth and development of cells and tissues in EPI WAT and the in general higher methylation of those pathways in the Concept mice supports the notion that the energy flow to the EPI WAT may be reduced in Concept mice. This is further supported by the changes in NAD^+ pathways and the correlation between *Nmnat3* and total methylation. NAD^+ is a known regulator of the energy metabolism and a co-substrate in epigenetic modifications, like DNA methylation and histone acylation, and in this way it regulates gene expression (43). *Nmnat3* is a key enzyme in NAD^+ synthesis and salvage pathways, and a reduced expression of *Nmnat3* in EPI WAT of Concept mice may be the consequence of increased NAD^+/NADH ratio, resulting from the lower energy influx. An increased NAD^+/NADH ratio may also explain the higher methylation in Concept, as NAD+ is a co-substrate in deacylation of histones by sirtuins (43). However, the inverse correlation between *Sirt3* and total methylation count of differentially methylated genes is inconsistent with this hypothesis. The feeding status of the mice may explain this inconsistency, as mice were not fasted before the dissection and *Sirt3* is known to be upregulated by fasting (45), suggesting that the inverse correlation between *Sirt3* and methylation of the differentially methylated genes may be caused by indirect mechanisms.

Another interesting finding was the reduced mRNA expression and increased DNA methylation of the neurotransmitter and other nervous system signaling cluster, potentially indicating a difference in neuronal outgrowth in EPI WAT upon Concept feeding. *Sema3a,* suggested to be crucial in WAT innervation, is shown to be present in smooth muscle cells of arteries and adipocytes in WAT (42, 46). The role of *Sema6a* in WAT innervation is not confirmed but in the brain Sema6a together with Plxna2, are shown to be essential for neuronal guidance (47). The positive correlation between MTCOI protein and *Sema6a*, *Plxna2* and *Nrp1* gene expression suggests that the regulation of neuronal migration is associated with the metabolic capacity of WAT. This association is supported by the literature which shows that WAT innervation is responsive to changes in energy status, like fasting or a cafeteria diet (46, 48, 49). Nervous activation of energy expenditure in brown adipose tissue or skeletal muscle may suggest that the reverse, a reduced innervation resulting in reduced OXPHOS levels, may exist (50, 51). Another consequence of changes in level of WAT innervation may be enhanced WAT browning and although in general browning of visceral depots is low compared to subcutaneous depots, histological analyses of these depots may give more insight into possible changes in cell population and WAT innervation upon Concept feeding (52). Altogether, decreased expression of markers for WAT innervation in the Concept group is associated with a reduced OXPHOS activity. However, further research is needed on cause and consequence and on the effect of the Concept on WAT innervation and eventual programming thereof under different dietary conditions, including the role of Sema6a in WAT.

The present study had several limitations. First, the number of samples used for RNAseq and DNA methylation analyses was too limited to generate conclusive evidence and was included in the study design only as an exploratory readout and considered sufficient for hypothesis generation. Hence, since several methylated gene regions and RNA transcripts showed high inter-group variation, it is crucial to include a larger number of samples per group in follow up studies. Second, in the present study, DNA methylation was only analyzed at one time point i.e., at PN42. To find long-lasting changes in DNA methylation potentially explaining programming of WAT health, samples from different time points should be analyzed, ideally including a baseline sample taken at the start of the dietary intervention, and a sample shortly after start of the dietary intervention, in addition to samples from later timepoints. Such an approach would also make it possible to link changes to functional outcomes later in life. Third, the animals used for the present analyses were not fasted before dissections and therefore may have been at different postprandial states which can affect gene expression and DNA

methylation. Furthermore, RNAseq and methylation was performed on EPI WAT, as more literature is available for this depot and the previous effects of the Concept on OXPHOS and mitochondrial density had been described in visceral WAT (41). However, retrospectively, in view of the OXPHOS protein expression data, ING WAT may have been the preferred depot for RNAseq and DNA methylation analyses. Finally, the contradictory results on OXPHOS protein expression, being decreased in visceral WAT and increased in subcutaneous WAT, shows that (programming) effects can be WAT depot-specific. Analyzing DNA methylation and RNAseq in multiple WAT depots in one study is therefore advised.

In conclusion, postnatal Concept feeding changed OXPHOS protein expression in WAT in a depot specific pattern without affecting WAT weight. Exploratory RNAseq and DNA methylation analyses suggested changed growth and development of EPI WAT and WAT innervation. The latter may illustrate a reduced energy flow towards EPI WAT in Concept mice that may elicit beneficial effects when facing dietary challenges in later life.

Methods

Study design

Animal procedures were performed according to the principles of good laboratory animal care and approved by an external, independent Animal Experimental Committee (DEC consult, Soest, The Netherlands), in compliance with the EU directive for the use of animals for scientific purposes. In addition, the study was co-reviewed by the local Ethics Committee of the executing facility (DEC NVI, Bilthoven, The Netherlands), endorsing the previously obtained positive advice from DEC consult. In the current study *ex vivo* analyses were performed with tissues collected in a larger study focusing on the effect of the Concept on brain fatty acid composition, the design of the study and the ethical approval was based on this primary outcome, the results of this main outcomes are not published (yet). C57BL/6jOlaHsd mice (Envigo, Horst, The Netherlands) were kept under a 12h light - 12h dark cycle (lights on at 06:00 hours) with room temperature and humidity at a constant level (21 ± 2°C and 50 ± 5% respectively), in standard cages (Macrolon II) with appropriate cage enrichment (wood chips, nesting material and shelter) and under conventional conditions with *ad libitum* access to food and (tap)water. Male breeder mice were kept individual and female breeder mice in pairs, until start of breeding which was time mated and as described (53). Breeder mice were fed a semi-synthetic American Institute of Nutrition 93 G (AIN93G) diet before and during the breeding (54). Two breeding cohorts were used and male, but not female, breeder mice were re-used in both breeding cohorts. Dams were continued on the AIN93G diet throughout

pregnancy and lactation and housed individually when visibly pregnant, around day 14 of pregnancy. The day the litters were found (checked daily) was marked as PN0. At PN2 sex of the pups was determined, and the pups were culled, randomized and assigned to one of the dams; 4 males and 2 females per litter, except for one litter with 4 males and 1 female due to the total number of females/male ration of the offspring born. At PN16 dams and litters were assigned to either one of the study groups, being the CTRL or the Concept diet (Figure 1) and the intervention diets were introduced as a dough in a petri dish at the level of the bedding of the cage and refreshed daily. Until weaning, at PN21, the pups were also allowed to drink with their mothers and had therefore a mixed diet from PN16 until PN21. Weight of the litters were assessed as one nest once a week from PN2-PN21 and after weaning (PN21) offspring were weighted individually twice a week. At weaning (PN21) dams and female pups were sacrificed and male pups were housed in sibling pairs and continued on their respective diets until end of the study (at PN42) when males were sacrificed, n = 12 per dietary group. Males were selected to reduce the numbers of animals per study arm and because the effects of sex on the primary outcome was unknown. For more details on the animal experimental procedures and missing values of the analyses, check the **Supplementary methods and Supplementary Table 4**. The EPI, ING and RP WAT were weighed, snap frozen in liquid nitrogen and stored at -80 until further analyses. The mice were not fasted before the dissections.

Animal diets

The intervention diets as provided to the dams and offspring from PN16 onwards were IMF based. The IMF powder used for the CTRL diet was a commercially available IMF for children 0-6 months of age and produced following Good Manufacturer Procedures (ISO 22000; Danone Nutricia Research, Utrecht, The Netherlands). To produce the Concept IMF powder, milk fat globule membrane fragments of bovine milk origin (Fonterra, Auckland, New Zealand) were added (0.5 g/l) during the production process with the aim to produce large (3-5µm) lipid droplets surrounded by (milk)phospholipids (55). The lipid droplets of the Concept IMF had a mode diameter based on volume of 4.3 µm and the CTRL IMF a mode diameter of 0.4 µm. The IMF powders were used to produce a semi-synthetic rodent diet (Research Diets Services) containing 28.2% (w/w) of the IMF powders. The animal diets were iso-caloric and had a similar macronutrient composition (Table 1) and macro- and micronutrient composition was according to AIN93G (54). To this end, only proteins, carbohydrates, vitamins and minerals were added, and the total lipid fraction originated from the IMF powders.

Homogenization of WAT samples

Samples were taken from the -80°C freezer and immediately crushed with the Cell Crusher (Cellcrusher, Cork, Ireland), homogenized and divided over different tubes for the separate analyses. RP WAT was too small to complete all analyses and was therefore only used for enzyme activity and Western blot analyses, ING WAT was also not large enough to also complete the DNA isolations.

Enzyme activity

CS and HADH activity was measured as described (41, 56).

Western blot:

Protein expression of five subunits of the five different OXPHOS complexes were analyzed with Western blot using the Total OXPHOS rodent WB antibody cocktail (Abcam, Cambridge, UK) as previously described (41). Shortly, homogenized samples were dissolved in RIPA buffer (ThermoFisher, Landsmeer, The Netherlands) with added protease inhibitors (Roche diagnostics, Almere, The Netherlands). Protein concentrations were measured using the BCA protein assay kit (Thermofisher) according to manufacturer's instructions. For the Western blot 7.5 ug total protein was used for RP WAT and 8 ug for EPI and ING WAT. EPI and ING WAT samples were analyzed in the same run over different gels, but with inter-run calibrators to allow comparisons between the depots. For the electrophoresis and blotting, a criterion 4-15% gradient gel and trans-blot turbo midi PVDF transfer package and system were used (all from Bio-Rad, Veenendaal, The Netherlands) and ECL anti mouse IgG as secondary antibody. Protein expression was visualized using the ECL kit (ThermoFisher) and the ChemiDoc XRS (BioRad). Data was adjusted for total protein expression as assessed by a Coomassie brilliant blue staining of the blots. Inter-gel calibrators were used to correct for differences in staining intensity between blots. OXPHOS subunits expression ratios between ING and EPI WAT depots were calculated as representative for the ratios between subcutaneous and visceral WAT. Samples of EPI and ING WAT, but not RP WAT, were analyzed in the same experiment, spread over multiple blots.

DNA and RNA isolation

RNA of EPI and ING tissues was isolated as described (57). Shortly, tissues were, directly from the -80°C freezer, added to a tube containing a pre-heated mixture of Trizol/β-mercaptoethenol and homogenized using the FastPrep-24 (Bio-connect, Huissen, The

Netherlands). After a chloroform extraction, the water phase was further purified with a RNeasy kit (Qiagen, Venlo, The Netherlands). DNA of EPI WAT was isolated using the QIAamp DNA kit (Qiagen). The isolated DNA was further precipitated with 3M sodium acetate and 100% ethanol (ratio of 1:0.1:2.2) and purified with a QIAamp stool kit (Qiagen) to remove the lipid residues from the samples. RNA and DNA quantity and quality were assessed with the Nanodrop (Thermofisher).

mtDNA

The mtDNA copy number of EPI WAT was assessed with a qPCR using 90 ng DNA and primers for the mitochondrial marker *Nd1* and nuclear marker *Lpl* (**Supplementary Table 5**) as described (41). The threshold cycle (Ct)-value of Nd1 was divided by the Ct-value of LPL and the resulting value returned to copy numbers (2^x).

qPCR

Relative expression of *Lep*, *Mest*, *Cpt1a*, *Pdk4*, *Glut4* and *Ucp3* was assessed with qPCR. 500 ng RNA of EPI and ING WAT was used as input for cDNA synthesis (iScriptcDNA synthesis kit, Biorad) and 12.5 ng cDNA was used as input for the qPCR reactions (5x Hot FirePol Evagreen, Bio-connect), using the Quantstudio 6 Flex Real PCR system (Life Technologies Europe), with primers for *Leptin, Mest, Glut4, Pdk4, Cpt1a* and *Ucp3*, as listed in Supplementary Table 5 and previously described (41). Several reference genes were checked for stability with qbase+ (Biogazell, Genth, Belgium), and Rpl19 and Rps29 were selected being most stable between conditions and samples (Supplementary Table 5). Expression of target genes was normalized for the mean expression of the reference genes (58) and scaled to the mean expression per gene with qbase+ (Biogazelle).

mRNA sequencing

RNA from EPI WAT was used for mRNA sequence analyses (Nxt-Dx, Gent, Belgium; n = 5 per diet group group). RNA quantity and quality was assessed with the Bioanalyzer, using the Agilent Eukaryote Total RNA Pico assay (Agilent, Santa Clara, US). Ribosomal RNA was removed using biotinylated, target specific oligonucleotides in combination with Ribo-Zero rRNA removal beads (Illumina, Eindhoven, The Netherlands). The RNA samples were subsequently fragmented (with divalent cations under elevated temperature) and copied into first strand cDNA (with reverse transcriptase and random primers), after which second strand cDNA was synthesized (with DNA polymerase I and RNase H). After further purification and enrichment with PCR the quality of the created cDNA library

was checked using the Agilent 2100 HS DNA chip and concentrations and degradation with smear analyses (Agilent 2000). The cDNA was subsequently sequenced (single end, 49 bp) on an Illumina Hi-Seq sequencer (Illumina). The Illumina Casava pipeline 1.8.2 was used to generate the FASTQ sequences. Quality assessment was done with the Chastity filter and the FASTQC quality control tool version 0.10.0. Sequences were mapped with the STAR RNA Aligner 2.3.0 on the mouse reference genome mm10 and analyzed with Cufflinks v2.1.1 on Ensemble Mus musculus annotation v74.

DNA methylation

DNA from EPI WAT (n=5 per dietary group; same samples as used for RNAseq) was used for MBD based genome wide methylation sequencing analyses (Nxt-Dx). After DNA quantification (Quant-iTTM Picogreen dsDNA assay kit, Invitrogen, Merelbeke, Belgium), DNA was fragmented to an average length of 200 bp using a Covaris S2 Ultra-sonicator (Covaris S2, Covaris Ltd, Woodingdean, UK; 10% duty cycle, 200 cycles per burst, 190 seconds, intensity 5), samples were concentrated (rotary evaporator) and fragment distribution checked (high sensitivity DNA chip) and quality checked with the Bioanalyzer (Agilent). Methylated DNA was captured (MethylCap kit, Diagenode, Belgium) and concentrations determined (Quant-iTTM Picogreen dsDNA assay kit). 250 ng fragmented DNA was used as input for the library preparation with the Apollo 324 (PrepX-DNA Library kit, Illumina). The library was subsequently amplificated according to the multiplexed paired end ChIP protocol including the indexes of the Multiplexing Sample Preparation Oligo kit (Illumina). Smaller fragments were removed via gel electrophorese (2% agarose gel, Low range Ultra, Biorad, 2h, 120V) and a 300 +/- 50 bp fragment was extracted and eluted (Qiagen Gel Extraction Kit Column, Qiagen), followed by concentration and smear analyses with the Agilent 2100. The samples were subsequently sequenced (paired end, 51 bp) on an Illumina Hi-Seq sequencer (Illumina). The Illumina Casava pipeline 1.8.0 was used to generate the FASTQ sequences, quality assessment based on the data passing the Illumina Chasity filter, reads containing adaptors and or Phix control signal were removed, and a second quality assessment done using the FASTQC quality control tool version 0.10.0. Sequences were mapped using Bowtie v2.3.5.1 and samtools v1.10 on the mouse reference genome mm39 as being single end reads, as for two samples one of the data files was damaged with data transport and original data was lost. Duplicate reads were removed. Peak calling was done as follows: a coverage profile was created for each sample, defined as all genomic regions covered by two or more reads, genomic regions present in three or more coverage profiles were combined to form a set of preliminary methylation regions

and regions in each other's proximity (<400 bp) merged as one region. Regions with a length of 10bp less were removed. Regions with an average coverage of <10 over all samples were removed. Subsequently, reads are mapped to the methylation regions resulting in a read count matrix and regions were annotated using Ensembl biomart v108 to obtain gene names. Methylation calls located within 2500 bp from a gene were annotated to that gene.

Data analyses mRNA sequencing and DNA methylation data

Normalization and different abundance analyses for the mRNA expression (read count base) and DNA methylation data (peak height) were performed with EdgeR (59-61). DNA methylation data was normalized for the total count per samples and differences between groups for RNAseq and DNA methylation data detected using an exact test, as default in EdgeR. The sample size was too small to find differences when corrected for multiple testing (Benjamini-Hochberg), therefore, data was analyzed on pathway level with Ingenuity Pathway Analyses (IPA, Qiagen, (62)) using $p<0.05$ as threshold for the analyses. The first Ensemble ID per transcript or region was used for pathway analyses in case of several hits, to avoid double use of the same transcript or region in the pathway analyses. The overlap between differentially expressed genes and differentially methylated genes was tested for significance with a Bootstrapping procedure. Therefore, 3454 random transcripts (identical to the number of unique differentially expressed genes) were sampled from the expression data set and 1829 random regions (identical to the number of unique differentially methylated genes) from the DNA methylation data set and the overlap between the two sets of associated genes calculated. This procedure was repeated 500 times, yielding 500 overlaps, representing a background distribution. Data analyses, except for the IPA analyses, were performed by BISC Global (Schiphol, The Netherlands). Cancer pathways were unselected for the pathway analyses as not being relevant in the context of the study. Correlations between total DNA methylation and RNA expression of specific genes were calculated as follows: the sum of all methylation counts were calculated per sample and the sum of all methylation count of regions which were differentially methylated between groups and those values were correlated to the logarithmically transformed total mRNA count of *Sirt1*, *Sirt3* and *Nmnat3*, for which the sum of all transcripts per gene were calculated for each sample. Correlations between RNA expression of Sema3a, Sema6a, Sema6c, Sema6d, Nrp1, Plxna1, Plxna2 and Plxna3 and OXPHOS protein expression was calculated using the logarithmically transformed total mRNA count of all transcripts per gene present in the data file. Logarithmic transformation was needed because of the exponential nature of the mRNA sequence data.

Statistics

The power calculation for the *in vivo* study was based on the primary readout of the study, brain FA composition, which is not part of the presented data (see Supplementary Methods). The offspring were the experimental unit, n=12 per group, except for the mRNA sequence and DNA methylation analyses which had n=5 per group, missing data is reported with reason in **Supplementary Table 4**. No specific inclusion and exclusion criteria were defined for the animal experiment, but standard HEP (human endpoint) criteria were applicable. GraphPad Prism 9.4.1 was used for statistical testing, unless otherwise stated. Each parameter was tested with the Kolmogorov-Smirnov for Gaussian distribution and subsequently tested for significant differences with an Unpaired t-test or Mann-Whitney in case of non-normal distribution. Trends ($p<0.1$) were also reported.

Additional information

Acknowledgments

We thank Lidewij Schipper, Annemarie Baars and Eefje Engels for the execution of the animal experiment, Annemarie Oosting for organizing the funding for this study and Lennard Leman from BISC global for the analyses of the DNA methylation data.

References

1. Collaboration NCDRF. Worldwide trends in body-mass index, underweight, overweight, and obesity from 1975 to 2016: a pooled analysis of 2416 population-based measurement studies in 128.9 million children, adolescents, and adults. Lancet. 2017;390(10113):2627-42.
2. Obesity: preventing and managing the global epidemic. Report of a WHO consultation. World Health Organ Tech Rep Ser. 2000;894:i-xii, 1-253.
3. Steele M, Finucane FM. Philosophically, is obesity really a disease? Obes Rev. 2023;24(8):e13590.
4. Reilly JJ, Kelly J. Long-term impact of overweight and obesity in childhood and adolescence on morbidity and premature mortality in adulthood: systematic review. Int J Obes (Lond). 2011;35(7):891-8.
5. Conway B, Rene A. Obesity as a disease: no lightweight matter. Obes Rev. 2004;5(3):145-51.
6. Hammarstedt A, Graham TE, Kahn BB. Adipose tissue dysregulation and reduced insulin sensitivity in non-obese individuals with enlarged abdominal adipose cells. Diabetol Metab Syndr. 2012;4(1):42.
7. Azzu V, Vacca M, Virtue S, Allison M, Vidal-Puig A. Adipose tissue-liver cross talk in the control of whole-body metabolism: implications in non-alcoholic fatty liver disease. Gastroenterology. 2020.
8. Bodis K, Roden M. Energy metabolism of white adipose tissue and insulin resistance in humans. Eur J Clin Invest. 2018;48(11):e13017.
9. Schottl T, Kappler L, Fromme T, Klingenspor M. Limited OXPHOS capacity in white adipocytes is a hallmark of obesity in laboratory mice irrespective of the glucose tolerance status. Mol Metab. 2015;4(9):631-42.
10. Pouliot MC, Despres JP, Nadeau A, Moorjani S, Prud'Homme D, Lupien PJ, et al. Visceral obesity in men. Associations with glucose tolerance, plasma insulin, and lipoprotein levels. Diabetes. 1992;41(7):826-34.
11. Schottl T, Kappler L, Braun K, Fromme T, Klingenspor M. Limited mitochondrial capacity of visceral versus subcutaneous white adipocytes in male C57BL/6N mice. Endocrinology. 2015;156(3):923-33.
12. Yin X, Lanza IR, Swain JM, Sarr MG, Nair KS, Jensen MD. Adipocyte mitochondrial function is reduced in human obesity independent of fat cell size. J Clin Endocrinol Metab. 2014;99(2):E209-16.
13. Wilson-Fritch L, Nicoloro S, Chouinard M, Lazar MA, Chui PC, Leszyk J, et al. Mitochondrial remodeling in adipose tissue associated with obesity and treatment with rosiglitazone. J Clin Invest. 2004;114(9):1281-9.
14. Choo HJ, Kim JH, Kwon OB, Lee CS, Mun JY, Han SS, et al. Mitochondria are impaired in the adipocytes of type 2 diabetic mice. Diabetologia. 2006;49(4):784-91.
15. Voigt A, Agnew K, van Schothorst EM, Keijer J, Klaus S. Short-term, high fat feeding-induced changes in white adipose tissue gene expression are highly predictive for long-term changes. Molecular nutrition & food research. 2013;57(8):1423-34.
16. Derous D, Kelder T, van Schothorst EM, van Erk M, Voigt A, Klaus S, et al. Network-based integration of molecular and physiological data elucidates regulatory mechanisms underlying adaptation to high-fat diet. Genes Nutr. 2015;10(4):470.
17. Nisoli E, Tonello C, Cardile A, Cozzi V, Bracale R, Tedesco L, et al. Calorie restriction promotes mitochondrial biogenesis by inducing the expression of eNOS. Science. 2005;310(5746):314-7.
18. Flachs P, Horakova O, Brauner P, Rossmeisl M, Pecina P, Franssen-van Hal N, et al. Polyunsaturated fatty acids of marine origin upregulate mitochondrial biogenesis and induce beta-oxidation in white fat. Diabetologia. 2005;48(11):2365-75.

19. Li T, Du M, Wang H, Mao X. Milk fat globule membrane and its component phosphatidylcholine induce adipose browning both in vivo and in vitro. The Journal of nutritional biochemistry. 2020;81:108372.
20. de Rooij SR, Painter RC, Roseboom TJ, Phillips DI, Osmond C, Barker DJ, et al. Glucose tolerance at age 58 and the decline of glucose tolerance in comparison with age 50 in people prenatally exposed to the Dutch famine. Diabetologia. 2006;49(4):637-43.
21. Ravelli AC, van Der Meulen JH, Osmond C, Barker DJ, Bleker OP. Obesity at the age of 50 y in men and women exposed to famine prenatally. Am J Clin Nutr. 1999;70(5):811-6.
22. Bruce KD, Cagampang FR, Argenton M, Zhang J, Ethirajan PL, Burdge GC, et al. Maternal high-fat feeding primes steatohepatitis in adult mice offspring, involving mitochondrial dysfunction and altered lipogenesis gene expression. Hepatology. 2009;50(6):1796-808.
23. Jousse C, Muranishi Y, Parry L, Montaurier C, Even P, Launay JM, et al. Perinatal protein malnutrition affects mitochondrial function in adult and results in a resistance to high fat diet-induced obesity. PLoS One. 2014;9(8):e104896.
24. Harder T, Bergmann R, Kallischnigg G, Plagemann A. Duration of breastfeeding and risk of overweight: a meta-analysis. Am J Epidemiol. 2005;162(5):397-403.
25. Oosting A, Kegler D, Boehm G, Jansen HT, van de Heijning BJ, van der Beek EM. N-3 long-chain polyunsaturated fatty acids prevent excessive fat deposition in adulthood in a mouse model of postnatal nutritional programming. Pediatr Res. 2010;68(6):494-9.
26. Oosting A, van Vlies N, Kegler D, Schipper L, Abrahamse-Berkeveld M, Ringler S, et al. Effect of dietary lipid structure in early postnatal life on mouse adipose tissue development and function in adulthood. Br J Nutr. 2014;111(2):215-26.
27. Bouwman LMS, Fernandez-Calleja JMS, van der Stelt I, Oosting A, Keijer J, van Schothorst EM. Replacing Part of Glucose with Galactose in the Postweaning Diet Protects Female But Not Male Mice from High-Fat Diet-Induced Adiposity in Later Life. J Nutr. 2019;149(7):1140-8.
28. Lecoutre S, Deracinois B, Laborie C, Eberle D, Guinez C, Panchenko PE, et al. Depot- and sex-specific effects of maternal obesity in offspring's adipose tissue. J Endocrinol. 2016;230(1):39-53.
29. Thompson N, Huber K, Bedurftig M, Hansen K, Miles-Chan J, Breier BH. Metabolic programming of adipose tissue structure and function in male rat offspring by prenatal undernutrition. Nutr Metab (Lond). 2014;11(1):50.
30. Poissonnet CM, LaVelle M, Burdi AR. Growth and development of adipose tissue. J Pediatr. 1988;113(1 Pt 1):1-9.
31. Birsoy K, Berry R, Wang T, Ceyhan O, Tavazoie S, Friedman JM, et al. Analysis of gene networks in white adipose tissue development reveals a role for ETS2 in adipogenesis. Development. 2011;138(21):4709-19.
32. DiGirolamo M, Fine JB, Tagra K, Rossmanith R. Qualitative regional differences in adipose tissue growth and cellularity in male Wistar rats fed ad libitum. Am J Physiol. 1998;274(5 Pt 2):R1460-7.
33. Lasar D, Julius A, Fromme T, Klingenspor M. Browning attenuates murine white adipose tissue expansion during postnatal development. Biochim Biophys Acta. 2013;1831(5):960-8.
34. Kodde A, Engels E, Oosting A, van Limpt K, van der Beek EM, Keijer J. Maturation of White Adipose Tissue Function in C57BL/6j Mice From Weaning to Young Adulthood. Front Physiol. 2019;10:836.
35. Sutton EF, Gilmore LA, Dunger DB, Heijmans BT, Hivert MF, Ling C, et al. Developmental programming: State-of-the-science and future directions-Summary from a Pennington Biomedical symposium. Obesity (Silver Spring). 2016;24(5):1018-26.
36. Bird A. Perceptions of epigenetics. Nature. 2007;447(7143):396-8.

37. Obermann-Borst SA, Eilers PH, Tobi EW, de Jong FH, Slagboom PE, Heijmans BT, et al. Duration of breastfeeding and gender are associated with methylation of the LEPTIN gene in very young children. Pediatr Res. 2013;74(3):344-9.
38. Butruille L, Marousez L, Pourpe C, Oger F, Lecoutre S, Catheline D, et al. Maternal high-fat diet during suckling programs visceral adiposity and epigenetic regulation of adipose tissue stearoyl-CoA desaturase-1 in offspring. Int J Obes (Lond). 2019;43(12):2381-93.
39. Oosting A, Kegler D, Wopereis HJ, Teller IC, van de Heijning BJ, Verkade HJ, et al. Size and phospholipid coating of lipid droplets in the diet of young mice modify body fat accumulation in adulthood. Pediatr Res. 2012;72(4):362-9.
40. Baars A, Oosting A, Engels E, Kegler D, Kodde A, Schipper L, et al. Milk fat globule membrane coating of large lipid droplets in the diet of young mice prevents body fat accumulation in adulthood. Br J Nutr. 2016;115(11):1930-7.
41. Kodde A, van der Beek EM, Phielix E, Engels E, Schipper L, Oosting A. Supramolecular structure of dietary fat in early life modulates expression of markers for mitochondrial content and capacity in adipose tissue of adult mice. Nutr Metab (Lond). 2017;14:37.
42. Qian X, Meng X, Zhang S, Zeng W. Neuroimmune regulation of white adipose tissues. The FEBS journal. 2022;289(24):7830-53.
43. Xie N, Zhang L, Gao W, Huang C, Huber PE, Zhou X, et al. NAD(+) metabolism: pathophysiologic mechanisms and therapeutic potential. Signal Transduct Target Ther. 2020;5(1):227.
44. Li T, Gao J, Du M, Song J, Mao X. Milk Fat Globule Membrane Attenuates High-Fat Diet-Induced Obesity by Inhibiting Adipogenesis and Increasing Uncoupling Protein 1 Expression in White Adipose Tissue of Mice. Nutrients. 2018;10(3).
45. Hirschey MD, Shimazu T, Goetzman E, Jing E, Schwer B, Lombard DB, et al. SIRT3 regulates mitochondrial fatty-acid oxidation by reversible enzyme deacetylation. Nature. 2010;464(7285):121-5.
46. Giordano A, Cesari P, Capparuccia L, Castellucci M, Cinti S. Sema3A and neuropilin-1 expression and distribution in rat white adipose tissue. J Neurocytol. 2003;32(4):345-52.
47. Limoni G, Niquille M. Semaphorins and Plexins in central nervous system patterning: the key to it all? Curr Opin Neurobiol. 2021;66:224-32.
48. Giordano A, Frontini A, Murano I, Tonello C, Marino MA, Carruba MO, et al. Regional-dependent increase of sympathetic innervation in rat white adipose tissue during prolonged fasting. J Histochem Cytochem. 2005;53(6):679-87.
49. Chaves VE, Frasson D, Martins-Santos ME, Boschini RP, Garofalo MA, Festuccia WT, et al. Glyceroneogenesis is reduced and glucose uptake is increased in adipose tissue from cafeteria diet-fed rats independently of tissue sympathetic innervation. J Nutr. 2006;136(10):2475-80.
50. Morrison SF, Madden CJ. Central nervous system regulation of brown adipose tissue. Compr Physiol. 2014;4(4):1677-713.
51. Gavini CK, Jones WC, 2nd, Novak CM. Ventromedial hypothalamic melanocortin receptor activation: regulation of activity energy expenditure and skeletal muscle thermogenesis. J Physiol. 2016;594(18):5285-301.
52. Murano I, Barbatelli G, Giordano A, Cinti S. Noradrenergic parenchymal nerve fiber branching after cold acclimatisation correlates with brown adipocyte density in mouse adipose organ. J Anat. 2009;214(1):171-8.
53. Jelenik T, Kodde A, Pesta D, Phielix E, Oosting A, Rohbeck E, et al. Dietary lipid droplet structure in postnatal life improves hepatic energy and lipid metabolism in a mouse model for postnatal programming. Pharmacol Res. 2022:106193.
54. Reeves PG. Components of the AIN-93 diets as improvements in the AIN-76A diet. J Nutr. 1997;127(5 Suppl):838S-41S.

55. Gallier S, Vocking K, Post JA, Van De Heijning B, Acton D, Van Der Beek EM, et al. A novel infant milk formula concept: Mimicking the human milk fat globule structure. Colloids and surfaces B, Biointerfaces. 2015;136:329-39.
56. Shepherd D, Garland PB. The kinetic properties of citrate synthase from rat liver mitochondria. Biochem J. 1969;114(3):597-610.
57. Vanhoutvin SA, Troost FJ, Hamer HM, Lindsey PJ, Koek GH, Jonkers DM, et al. Butyrate-induced transcriptional changes in human colonic mucosa. PLoS One. 2009;4(8):e6759.
58. Hellemans J, Mortier G, De Paepe A, Speleman F, Vandesompele J. qBase relative quantification framework and software for management and automated analysis of real-time quantitative PCR data. Genome Biol. 2007;8(2):R19.
59. Chen Y, Lun AT, Smyth GK. From reads to genes to pathways: differential expression analysis of RNA-Seq experiments using Rsubread and the edgeR quasi-likelihood pipeline. F1000Res. 2016;5:1438.
60. Robinson MD, McCarthy DJ, Smyth GK. edgeR: a Bioconductor package for differential expression analysis of digital gene expression data. Bioinformatics. 2010;26(1):139-40.
61. McCarthy DJ, Chen Y, Smyth GK. Differential expression analysis of multifactor RNA-Seq experiments with respect to biological variation. Nucleic Acids Res. 2012;40(10):4288-97.
62. Kramer A, Green J, Pollard J, Jr., Tugendreich S. Causal analysis approaches in Ingenuity Pathway Analysis. Bioinformatics. 2014;30(4):523-30.

Supplementary Material

Supplementary Methods

Animal experiment, further details:

Primary readout: Brain fatty acid composition

Exploratory readouts: WAT mitochondrial function markers and mRNA and methylation analyses

Power calculation: The sample-size calculation was based on the primary readout (brain fatty acid composition) and on the hypothesis that the DHA content of the brain would increase upon feeding the Concept diet in postnatal life. Therefore, a one-sided sample-size calculation was performed using Power calculation, v1.02, an estimated variation (σ) of 7.5% and maximal effect size (μ) of 10%, type 1 error (α) 2.5%, power (π) 80%, based on results of previous experiments of our own lab. Considering this, 6 animals per dietary group were sufficient to detect differences between groups. But to allow fatty acid analyses in whole brain as well as in specific brain regions 12 animals per dietary groups were used, with a total of 24 animals for the study.

General Humane Endpoint criteria: disease symptoms, fatigue, reduction in body weight of more than 20% over two days, reduced water and food intake for two days (compared to other animals). No animals were removed from the experiment based on those criteria.

Blinding: The study was not blinded.

Randomization: The pups were culled, randomized and assigned to one of the dams at PN2, 4 males and 2 females per litter, except for one litter with 4 males and 1 female due to the total number of females/male ration of the offspring born. Litters with dams were subsequently divided over the different intervention groups in a way to spread the groups evenly over the different breeding cohorts. No further randomization was used.

Marking of the animals: The mice were marked with ear punches at PN21.

Acclimatization protocol: Breeders were acclimated for 1 week on a semi-synthetic American Institute of Nutrition 93 G (AIN93G) diet upon arrival from the breeder.

Housing conditions: Conventional, in standard cages (Macrolon II) with appropriate cage enrichment (wood chips, nesting material and shelter).

Baseline characteristics: No baseline data is available. Body weight of the offspring was not individually assessed before weaning, to avoid stress of the separation in the lactation phase.

Breeding cohorts and litters: Animals were bred in two cohorts, each of the cohorts resulting in 3 litters, assigned to the different dietary groups (cohort 1: 2 CTRL, 1 Concept; cohort 2: 1 CTRL, 2 Concept).

Age range start of the dietary intervention: PN15 – 17, while still with the dam

Age range of dissection: PN 41 - 43

Method of euthanasia: Breeders and female offspring were euthanized under isoflurane anaesthesia (5% by volume in a gas mixture of 30% oxygen, 0.4L/min), followed by cervical dislocation. Male offspring were anaesthetized with isoflurane (5% by volume in a gas mixture of 30% oxygen, 0.4L/min) and euthanized by heart puncture and cervical dislocation.

Randomization analyses: Mitochondrial measures were assessed in all available tissues. For DNA methylation and mRNA sequence analyses, animals from different litters were selected and those with the highest RNA and DNA quantity and quality.

Missing values: see Supplementary Table 4

Supplementary Table 1: Differentially regulated genes in the mitochondrial dysfunction pathway as analyzed with IPA.

Symbol	Entrez Gene Name	Ensembl ID	Expression Log Ratio	Expression p-value
ATF2	activating transcription factor 2	ENSMUSG00000027104	12.494	3.03E-04
ATP5MC3	ATP synthase membrane subunit c locus 3	ENSMUSG00000018770	9.882	1.07E-02
ATP5PD	ATP synthase peripheral stalk subunit d	ENSMUSG00000034566	-8.901	2.82E-02
ATP5PF	ATP synthase peripheral stalk subunit F6	ENSMUSG00000022890	-9.937	1.21E-02
ATP5PO	ATP synthase peripheral stalk subunit OSCP	ENSMUSG00000022956	10.779	5.14E-03
BCL2	BCL2 apoptosis regulator	ENSMUSG00000057329	-6.393	6.39E-03
CACNA1A	calcium voltage-gated channel subunit alpha1 A	ENSMUSG00000034656	6.89	4.82E-02
CACNA1B	calcium voltage-gated channel subunit alpha1 B	ENSMUSG00000004113	9.01	1.95E-02
CACNA1H	calcium voltage-gated channel subunit alpha1 H	ENSMUSG00000024112	-8.5	3.95E-03
CACNA1S	calcium voltage-gated channel subunit alpha1 S	ENSMUSG00000026407	-6.829	4.16E-02
CACNB2	calcium voltage-gated channel auxiliary subunit beta 2	ENSMUSG00000057914	-10.517	2.36E-04
CACNB4	calcium voltage-gated channel auxiliary subunit beta 4	ENSMUSG00000017412	5.647	3.69E-02
CACNG3	calcium voltage-gated channel auxiliary subunit gamma 3	ENSMUSG00000066189	-9.18	2.07E-02
CACNG5	calcium voltage-gated channel auxiliary subunit gamma 5	ENSMUSG00000040373	-6.665	1.97E-02
CAMK2B	calciumcalmodulin dependent protein kinase II beta	ENSMUSG00000057897	-10.795	1.43E-03
CAMK2D	calciumcalmodulin dependent protein kinase II delta	ENSMUSG00000053819	-10.573	7.20E-03
CAPN1	calpain 1	ENSMUSG00000024942	11.721	3.45E-05
CAPN5	calpain 5	ENSMUSG00000035547	-6.983	3.83E-02
CAPN11	calpain 11	ENSMUSG00000058626	7.19	2.65E-02
GPD2	glycerol-3-phosphate dehydrogenase 2	ENSMUSG00000026827	-5.398	4.37E-02
GPX5	glutathione peroxidase 5	ENSMUSG00000004344	7.105	9.70E-04
GPX6	glutathione peroxidase 6	ENSMUSG00000004341	6.977	4.03E-02
GSTM2	glutathione S-transferase mu 2	ENSMUSG00000004035	-8.564	3.24E-02
MAP2K4	mitogen-activated protein kinase kinase 4	ENSMUSG00000033352	10.155	6.61E-03
MAP2K7	mitogen-activated protein kinase kinase 7	ENSMUSG00000002948	6.722	2.65E-02
MAPK10	mitogen-activated protein kinase 10	ENSMUSG00000046709	-12.172	2.81E-04
MAPT	microtubule associated protein tau	ENSMUSG00000018411	-10.01	3.84E-03
MDM2	MDM2 proto-oncogene	ENSMUSG00000020184	7.677	1.97E-02
MGST2	microsomal glutathione S-transferase 2	ENSMUSG00000074604	12.23	4.06E-09

Supplementary Table 1: Coninued

Symbol	Entrez Gene Name	Ensembl ID	Expression Log Ratio	Expression p-value
NDUFA7	NADH:ubiquinone oxidoreductase subunit A7	ENSMUSG00000041881	-10.309	3.83^{E}-04
NDUFAF1	NADH:ubiquinone oxidoreductase complex assembly factor 1	ENSMUSG00000027305	-6.911	2.15^{E}-02
NDUFV1	NADH:ubiquinone oxidoreductase core subunit V1	ENSMUSG00000037916	7.644	1.34^{E}-02
NOS1	nitric oxide synthase 1	ENSMUSG00000029361	-8.405	3.62^{E}-02
NRF1	nuclear respiratory factor 1	ENSMUSG00000058440	10.403	5.46^{E}-03
PIK3CD	phosphatidylinositol-4,5-bisphosphate 3-kinase catalytic subunit delta	ENSMUSG00000039936	10.424	5.99^{E}-03
PIK3CG	phosphatidylinositol-4,5-bisphosphate 3-kinase catalytic subunit gamma	ENSMUSG00000020573	-5.552	1.60^{E}-02
PIK3R6	phosphoinositide-3-kinase regulatory subunit 6	ENSMUSG00000046207	-8.228	5.59^{E}-03
PPP3CB	protein phosphatase 3 catalytic subunit beta	ENSMUSG00000021816	-8.63	3.42^{E}-02
PRKAG2	protein kinase AMP-activated non-catalytic subunit gamma 2	ENSMUSG00000028944	-6.866	7.07^{E}-03
PRKAR1A	protein kinase cAMP-dependent type I regulatory subunit alpha	ENSMUSG00000020612	8.737	7.82^{E}-03
PRKAR1B	protein kinase cAMP-dependent type I regulatory subunit beta	ENSMUSG00000025855	8.874	2.20^{E}-02
PRKAR2A	protein kinase cAMP-dependent type II regulatory subunit alpha	ENSMUSG00000032601	-6.956	3.83^{E}-02
PSEN2	presenilin 2	ENSMUSG00000010609	12.097	8.23^{E}-07
PSENEN	presenilin enhancer, gamma-secretase subunit	ENSMUSG00000036835	6.972	3.41^{E}-04
RAPGEF3	Rap guanine nucleotide exchange factor 3	ENSMUSG00000022469	-7.595	8.29^{E}-03
SIRT1	sirtuin 1	ENSMUSG00000020063	-8.496	1.52^{E}-02
SIRT3	sirtuin 3	ENSMUSG00000025486	-10.173	5.86^{E}-04
SURF1	SURF1 cytochrome c oxidase assembly factor	ENSMUSG00000015790	7.083	2.97^{E}-02
TP53	tumor protein p53	ENSMUSG00000059552	-3.693	4.44^{E}-02

Supplementary Table 2: Pathways up- or down-regulated by the Concept, as analyzed with IPA

Ingenuity Canonical Pathways	p-value	z-score
Opioid Signaling Pathway	0.0000	-3.434
Sperm Motility	0.0000	-0.756
Endocannabinoid Neuronal Synapse Pathway	0.0000	-2.466
Synaptogenesis Signaling Pathway	0.0000	-1.291
Cellular Effects of Sildenafil (Viagra)	0.0000	NaN
Protein Kinase A Signaling	0.0000	-1.069
Circadian Rhythm Signaling	0.0000	NaN
Role of NFAT in Cardiac Hypertrophy	0.0000	-1.64
Insulin Secretion Signaling Pathway	0.0000	-1.155
Semaphorin Neuronal Repulsive Signaling Pathway	0.0000	0.174
Neuropathic Pain Signaling In Dorsal Horn Neurons	0.0000	-1.732
Clathrin-mediated Endocytosis Signaling	0.0000	NaN
G Beta Gamma Signaling	0.0000	-0.365
SNARE Signaling Pathway	0.0000	-1.061
Reelin Signaling in Neurons	0.0000	-2.828
Melatonin Signaling	0.0000	0.229
Phosphatidylcholine Biosynthesis I	0.0000	0
Thrombin Signaling	0.0000	-1.915
Cardiac Hypertrophy Signaling	0.0000	-1.298
Dilated Cardiomyopathy Signaling Pathway	0.0000	0.408
GNRH Signaling	0.0000	-0.928
RAR Activation	0.0000	NaN
GPCR-Mediated Nutrient Sensing in Enteroendocrine Cells	0.0000	-0.378
Cardiac Hypertrophy Signaling (Enhanced)	0.0000	0
Cardiac β-adrenergic Signaling	0.0000	-0.655
Ephrin Receptor Signaling	0.0000	-0.898
Oxytocin Signaling Pathway	0.0000	-0.98
Neurovascular Coupling Signaling Pathway	0.0000	-0.905
Axonal Guidance Signaling	0.0000	NaN
cAMP-mediated signaling	0.0000	-1.897
PPARα/RXRα Activation	0.0000	0.784
Endocannabinoid Developing Neuron Pathway	0.0000	-1.043
Antioxidant Action of Vitamin C	0.0000	0.218
GADD45 Signaling	0.0000	0.728
Amyotrophic Lateral Sclerosis Signaling	0.0000	-1.147
Salvage Pathways of Pyrimidine Ribonucleotides	0.0000	-0.209
Actin Cytoskeleton Signaling	0.0001	-0.962
White Adipose Tissue Browning Pathway	0.0001	0.557
Gαs Signaling	0.0001	-1.342
Integrin Signaling	0.0001	-1.333
Calcium Signaling	0.0001	-1.89
Synaptic Long Term Depression	0.0001	-1.333

Supplementary Table 2: Continued

Ingenuity Canonical Pathways	p-value	z-score
Leptin Signaling in Obesity	0.0001	-1.633
Adrenomedullin signaling pathway	0.0001	-0.343
IL-1 Signaling	0.0001	-0.832
PXR/RXR Activation	0.0001	-0.243
Synaptic Long Term Potentiation	0.0002	-1.732
RHOGDI Signaling	0.0002	0.426
FXR/RXR Activation	0.0002	NaN
FGF Signaling	0.0002	0.894
Relaxin Signaling	0.0002	-0.535
Ribonucleotide Reductase Signaling Pathway	0.0002	-0.707
Leukocyte Extravasation Signaling	0.0003	-0.87
Estrogen Receptor Signaling	0.0003	0
Melanocyte Development and Pigmentation Signaling	0.0004	-0.655
Hepatic Fibrosis Signaling Pathway	0.0005	-2.449
G-Protein Coupled Receptor Signaling	0.0005	-1.429
LPS/IL-1 Mediated Inhibition of RXR Function	0.0005	-0.243
Endothelin-1 Signaling	0.0006	-1.029
Aryl Hydrocarbon Receptor Signaling	0.0007	-1.414
Signaling by Rho Family GTPases	0.0008	-0.73
Senescence Pathway	0.0008	0.48
Phospholipases	0.0009	-0.5
Gap Junction Signaling	0.0009	NaN
CXCR4 Signaling	0.0009	-2.041
Type II Diabetes Mellitus Signaling	0.0009	0
Sertoli Cell-Sertoli Cell Junction Signaling	0.0009	NaN
Pulmonary Fibrosis Idiopathic Signaling Pathway	0.0010	-0.714
GABA Receptor Signaling	0.0010	NaN
Xenobiotic Metabolism PXR Signaling Pathway	0.0010	0.174
Myelination Signaling Pathway	0.0010	0.283
P2Y Purigenic Receptor Signaling Pathway	0.0011	-1.043
Germ Cell-Sertoli Cell Junction Signaling	0.0011	NaN
Dopamine-DARPP32 Feedback in cAMP Signaling	0.0011	-0.816
14-3-3-mediated Signaling	0.0012	-0.426
p38 MAPK Signaling	0.0013	-2.524
Nitric Oxide Signaling in the Cardiovascular System	0.0013	-1.414
Pyridoxal 5'-phosphate Salvage Pathway	0.0013	-0.775
Netrin Signaling	0.0014	-0.5
Ephrin B Signaling	0.0014	1.732
Role of MAPK Signaling in Inhibiting the Pathogenesis of Influenza	0.0014	-0.728
Maturity Onset Diabetes of Young (MODY) Signaling	0.0014	NaN
Glutamate Receptor Signaling	0.0015	-1.89

Supplementary Table 2: Continued

Ingenuity Canonical Pathways	p-value	z-score
ERBB Signaling	0.0015	-1.147
IL-15 Production	0.0018	-1.46
Xenobiotic Metabolism CAR Signaling Pathway	0.0018	-0.354
Factors Promoting Cardiogenesis in Vertebrates	0.0019	-0.784
Apelin Muscle Signaling Pathway	0.0019	0.447
Choline Biosynthesis III	0.0020	0.816
GPCR-Mediated Integration of Enteroendocrine Signaling Exemplified by an L Cell	0.0021	1
Fc Epsilon RI Signaling	0.0023	-1.706
AMPK Signaling	0.0024	-1.279
Tight Junction Signaling	0.0025	NaN
Huntington's Disease Signaling	0.0025	-0.2
Regulation of the Epithelial-Mesenchymal Transition Pathway	0.0025	NaN
D-myo-inositol (1,4,5)-Trisphosphate Biosynthesis	0.0026	-0.707
CCR3 Signaling in Eosinophils	0.0026	-1
Epithelial Adherens Junction Signaling	0.0027	0.577
UVA-Induced MAPK Signaling	0.0028	-1.155
Role of MAPK Signaling in the Pathogenesis of Influenza	0.0029	NaN
Amyloid Processing	0.0032	-1.134
IL-7 Signaling Pathway	0.0033	-1.5
Role of MAPK Signaling in Promoting the Pathogenesis of Influenza	0.0033	-1.091
Paxillin Signaling	0.0035	-2.668
Corticotropin Releasing Hormone Signaling	0.0035	0
Androgen Signaling	0.0040	0.243
Acute Phase Response Signaling	0.0041	-1
PDGF Signaling	0.0042	-0.243
Xenobiotic Metabolism Signaling	0.0042	NaN
IL-8 Signaling	0.0044	-0.962
HGF Signaling	0.0046	0.471
Insulin Receptor Signaling	0.0047	-0.853
Mitochondrial Dysfunction	0.0051	-0.429
ERBB4 Signaling	0.0055	0
NAD biosynthesis II (from tryptophan)	0.0059	0
Oxytocin In Brain Signaling Pathway	0.0065	-1.257
Renin-Angiotensin Signaling	0.0068	-0.688
HIF1α Signaling	0.0068	0.539
EGF Signaling	0.0071	-0.577
γ-linolenate Biosynthesis II (Animals)	0.0078	0
Gαq Signaling	0.0081	-1.091
Gαi Signaling	0.0093	-0.471
ERB2-ERBB3 Signaling	0.0095	-0.277

Supplementary Table 2: Continued

Ingenuity Canonical Pathways	p-value	z-score
Apelin Endothelial Signaling Pathway	0.0102	-0.471
Autophagy	0.0117	0
Fatty Acid Activation	0.0117	NaN
tRNA Splicing	0.0120	-1
DNA damage-induced 14-3-3σ Signaling	0.0120	-0.632
Apelin Pancreas Signaling Pathway	0.0120	-0.632
Regulation Of The Epithelial Mesenchymal Transition By Growth Factors Pathway	0.0123	-1.043
CLEAR Signaling Pathway	0.0129	0
Caveolar-mediated Endocytosis Signaling	0.0132	NaN
Regulation of Cellular Mechanics by Calpain Protease	0.0135	-0.378
RANK Signaling in Osteoclasts	0.0148	-1
Inhibition of Angiogenesis by TSP1	0.0148	-0.707
Gustation Pathway	0.0148	-0.365
VEGF Signaling	0.0155	-1.291
Apelin Cardiomyocyte Signaling Pathway	0.0155	-1.213
VEGF Family Ligand-Receptor Interactions	0.0158	-0.775
nNOS Signaling in Skeletal Muscle Cells	0.0162	NaN
Neurotrophin/TRK Signaling	0.0182	0.277
Hepatic Cholestasis	0.0200	NaN
CREB Signaling in Neurons	0.0209	-2.216
Virus Entry via Endocytic Pathways	0.0209	NaN
MYC Mediated Apoptosis Signaling	0.0214	-1.265
Cell Cycle: G2/M DNA Damage Checkpoint Regulation	0.0214	-1.265
ILK Signaling	0.0219	-2.041
Sumoylation Pathway	0.0219	-0.277
Xenobiotic Metabolism General Signaling Pathway	0.0219	0
STAT3 Pathway	0.0224	0
Osteoarthritis Pathway	0.0234	-1
Sphingosine-1-phosphate Signaling	0.0240	-1.698
NGF Signaling	0.0240	-0.688
Cleavage and Polyadenylation of Pre-mRNA	0.0240	NaN
Role of Macrophages, Fibroblasts and Endothelial Cells in Rheumatoid Arthritis	0.0240	NaN
NAD Biosynthesis from 2-amino-3-carboxymuconate Semialdehyde	0.0240	NaN
BER (Base Excision Repair) Pathway	0.0245	-0.333
Complement System	0.0245	1
RAC Signaling	0.0257	0
Neuroinflammation Signaling Pathway	0.0269	-0.822
Hypusine Biosynthesis	0.0269	NaN
Geranylgeranyldiphosphate Biosynthesis	0.0269	NaN
UVB-Induced MAPK Signaling	0.0275	-1.265

Supplementary Table 2: Continued

Ingenuity Canonical Pathways	p-value	z-score
FLT3 Signaling in Hematopoietic Progenitor Cells	0.0275	-1.069
CD40 Signaling	0.0282	-0.577
LXR/RXR Activation	0.0302	0.471
CDK5 Signaling	0.0309	0.243
Cell Cycle: G1/S Checkpoint Regulation	0.0316	-0.302
Remodeling of Epithelial Adherens Junctions	0.0316	0.447
Macropinocytosis Signaling	0.0324	0.333
Role of OCT4 in Mammalian Embryonic Stem Cell Pluripotency	0.0324	NaN
Mitochondrial L-carnitine Shuttle Pathway	0.0324	NaN
ATM Signaling	0.0339	-0.535
Agrin Interactions at Neuromuscular Junction	0.0347	-0.632
PAK Signaling	0.0355	-2.324
Neuregulin Signaling	0.0355	-0.277
nNOS Signaling in Neurons	0.0363	-2.236
α-Adrenergic Signaling	0.0363	1
NAD Signaling Pathway	0.0380	-1.528
Thrombopoietin Signaling	0.0407	0.302
Colanic Acid Building Blocks Biosynthesis	0.0417	1
DNA Double-Strand Break Repair by Homologous Recombination	0.0417	NaN
NAD Salvage Pathway II	0.0427	-0.816
Tryptophan Degradation X (Mammalian, via Tryptamine)	0.0427	0.447
Phosphatidylglycerol Biosynthesis II (Non-plastidic)	0.0427	0.816
Mouse Embryonic Stem Cell Pluripotency	0.0457	-1
IL-6 Signaling	0.0468	-1.606
TGF-β Signaling	0.0468	-1.155
Aldosterone Signaling in Epithelial Cells	0.0479	-1.213

Supplementary Table 3: Pathways with a changed DNA methylation upon Concept feeding, as analyzed with IPA

Ingenuity Canonical Pathways	p-value	z-score
Protein Kinase A Signaling	0.00000	-0.756
Myelination Signaling Pathway	0.00000	2.058
Paxillin Signaling	0.00000	1.155
Synaptic Long Term Depression	0.00001	2.132
Endothelin-1 Signaling	0.00002	1.789
Nitric Oxide Signaling in the Cardiovascular System	0.00002	1.387
Renin-Angiotensin Signaling	0.00002	1.732
Oxytocin In Brain Signaling Pathway	0.00002	1.964
Synaptogenesis Signaling Pathway	0.00003	1.671
Sperm Motility	0.00003	2.496
IL-15 Production	0.00003	2.668
Insulin Secretion Signaling Pathway	0.00003	1.4
Cardiac Hypertrophy Signaling (Enhanced)	0.00004	2.92
Axonal Guidance Signaling	0.00004	NaN
Regulation of the Epithelial-Mesenchymal Transition Pathway	0.00005	NaN
Hepatic Fibrosis Signaling Pathway	0.00006	2.502
CLEAR Signaling Pathway	0.00007	0.192
PEDF Signaling	0.00007	1.732
Opioid Signaling Pathway	0.00012	2.132
Oxytocin Signaling Pathway	0.00013	2.746
Senescence Pathway	0.00015	1.177
NF-κB Activation by Viruses	0.00015	1.508
Pulmonary Healing Signaling Pathway	0.00019	2.4
HGF Signaling	0.00023	2.111
VEGF Family Ligand-Receptor Interactions	0.00030	2.111
Osteoarthritis Pathway	0.00032	2
Circadian Rhythm Signaling	0.00035	NaN
Thrombopoietin Signaling	0.00040	1.667
Regulation Of The Epithelial Mesenchymal Transition In Development Pathway	0.00042	1.667
Macropinocytosis Signaling	0.00047	1.134
GP6 Signaling Pathway	0.00047	1.807
Actin Cytoskeleton Signaling	0.00051	1.291
Regulation of Cellular Mechanics by Calpain Protease	0.00058	NaN
CNTF Signaling	0.00079	1.414
FLT3 Signaling in Hematopoietic Progenitor Cells	0.00091	1.667
Role of NFAT in Cardiac Hypertrophy	0.00093	1.606
Ephrin A Signaling	0.00093	NaN
PPARα/RXRα Activation	0.00102	-0.535
RAC Signaling	0.00105	1.667
Corticotropin Releasing Hormone Signaling	0.00110	2.138

Supplementary Table 3: Continued

Ingenuity Canonical Pathways	p-value	z-score
Melanocyte Development and Pigmentation Signaling	0.00123	1.265
VEGF Signaling	0.00135	1.265
Neurovascular Coupling Signaling Pathway	0.00145	2.683
Role of MAPK Signaling in Promoting the Pathogenesis of Influenza	0.00151	2.887
Ephrin Receptor Signaling	0.00155	1.414
Xenobiotic Metabolism General Signaling Pathway	0.00162	2.84
Amyotrophic Lateral Sclerosis Signaling	0.00178	0.333
GDNF Family Ligand-Receptor Interactions	0.00178	1.414
Calcium Signaling	0.00178	1.732
Mouse Embryonic Stem Cell Pluripotency	0.00204	0.905
P2Y Purigenic Receptor Signaling Pathway	0.00219	1.155
IL-3 Signaling	0.00240	1.667
NGF Signaling	0.00240	2.111
Semaphorin Neuronal Repulsive Signaling Pathway	0.00257	0.832
Cellular Effects of Sildenafil (Viagra)	0.00257	NaN
Pulmonary Fibrosis Idiopathic Signaling Pathway	0.00263	3.922
Role Of Osteoblasts In Rheumatoid Arthritis Signaling Pathway	0.00269	0.447
Integrin Signaling	0.00269	0.728
Role of Osteoblasts, Osteoclasts and Chondrocytes in Rheumatoid Arthritis	0.00269	NaN
ERBB4 Signaling	0.00282	0.707
Th1 Pathway	0.00282	2.111
mTOR Signaling	0.00295	1.069
Type II Diabetes Mellitus Signaling	0.00309	0.707
Adrenomedullin signaling pathway	0.00309	2
Factors Promoting Cardiogenesis in Vertebrates	0.00309	2.309
Role of JAK1 and JAK3 in γc Cytokine Signaling	0.00316	NaN
Role of Macrophages, Fibroblasts and Endothelial Cells in Rheumatoid Arthritis	0.00339	NaN
IL-23 Signaling Pathway	0.00372	1.134
Role of MAPK Signaling in the Pathogenesis of Influenza	0.00372	NaN
UVA-Induced MAPK Signaling	0.00380	1.265
Growth Hormone Signaling	0.00380	1.667
IL-9 Signaling	0.00389	0.816
Th1 and Th2 Activation Pathway	0.00389	NaN
Endocannabinoid Developing Neuron Pathway	0.00398	1.265
LPS-stimulated MAPK Signaling	0.00407	1
Netrin Signaling	0.00417	0.707
nNOS Signaling in Neurons	0.00417	NaN
Sertoli Cell-Sertoli Cell Junction Signaling	0.00447	NaN
G Beta Gamma Signaling	0.00457	1.508
GNRH Signaling	0.00468	2.111

Supplementary Table 3: Continued

Ingenuity Canonical Pathways	p-value	z-score
nNOS Signaling in Skeletal Muscle Cells	0.00479	NaN
ERK5 Signaling	0.00501	2.646
PAK Signaling	0.00537	1.134
IL-2 Signaling	0.00562	0.378
Biotin-carboxyl Carrier Protein Assembly	0.00562	NaN
Fc Epsilon RI Signaling	0.00575	2.111
Gα12/13 Signaling	0.00589	0.577
Cardiac Hypertrophy Signaling	0.00589	1.606
Leptin Signaling in Obesity	0.00603	0.447
Angiopoietin Signaling	0.00603	1.342
IGF-1 Signaling	0.00646	1.667
Antiproliferative Role of Somatostatin Receptor 2	0.00661	0.816
Gap Junction Signaling	0.00661	NaN
Neurotrophin/TRK Signaling	0.00708	1.134
Neuroinflammation Signaling Pathway	0.00708	2.132
ERB2-ERBB3 Signaling	0.00741	0.378
Human Embryonic Stem Cell Pluripotency	0.00776	3.153
White Adipose Tissue Browning Pathway	0.00794	0.905
Dopamine-DARPP32 Feedback in cAMP Signaling	0.00813	1.387
Role of NANOG in Mammalian Embryonic Stem Cell Pluripotency	0.00851	0.816
Mitochondrial L-carnitine Shuttle Pathway	0.00851	2
MicroRNA Biogenesis Signaling Pathway	0.00871	2.5
CD40 Signaling	0.00891	1.134
Prolactin Signaling	0.00891	1.667
Apelin Endothelial Signaling Pathway	0.00933	1.732
JAK/STAT Signaling	0.00977	1.414
Oncostatin M Signaling	0.01072	2
EGF Signaling	0.01096	1.134
Phenylethylamine Degradation I	0.01096	NaN
GM-CSF Signaling	0.01148	1.134
fMLP Signaling in Neutrophils	0.01288	1.508
Cardiac β-adrenergic Signaling	0.01349	-0.333
Neuregulin Signaling	0.01413	0.816
PDGF Signaling	0.01413	1.414
Endocannabinoid Neuronal Synapse Pathway	0.01445	0
Apelin Pancreas Signaling Pathway	0.01479	-0.816
GPCR-Mediated Nutrient Sensing in Enteroendocrine Cells	0.01479	0.905
Virus Entry via Endocytic Pathways	0.01479	NaN
Dilated Cardiomyopathy Signaling Pathway	0.01514	0
CCR3 Signaling in Eosinophils	0.01514	1.897
MSP-RON Signaling In Macrophages Pathway	0.01585	0
Cholecystokinin/Gastrin-mediated Signaling	0.01585	2.53

Supplementary Table 3: Continued

Ingenuity Canonical Pathways	p-value	z-score
Apoptosis Signaling	0.01622	-2.121
ILK Signaling	0.01622	0.577
CXCR4 Signaling	0.01660	1.941
IL-33 Signaling Pathway	0.01778	1.807
Citrulline-Nitric Oxide Cycle	0.01778	NaN
Gαq Signaling	0.01820	2.138
Germ Cell-Sertoli Cell Junction Signaling	0.01820	NaN
Ceramide Signaling	0.01862	2.121
BMP signaling pathway	0.01862	2.449
Xenobiotic Metabolism Signaling	0.01862	NaN
Relaxin Signaling	0.01950	1.508
VDR/RXR Activation	0.02089	-1.342
IL-7 Signaling Pathway	0.02089	0
Insulin Receptor Signaling	0.02089	1.265
ERBB Signaling	0.02138	0.707
Thrombin Signaling	0.02138	1.604
Phenylalanine Degradation IV (Mammalian, via Side Chain)	0.02138	NaN
α-Adrenergic Signaling	0.02188	2.449
HIF1α Signaling	0.02188	3
Regulation Of The Epithelial Mesenchymal Transition By Growth Factors Pathway	0.02291	2.324
PXR/RXR Activation	0.02344	1.89
IL-8 Signaling	0.02344	2.496
Leukocyte Extravasation Signaling	0.02399	1.807
Phagosome Formation	0.02399	2.655
14-3-3-mediated Signaling	0.02455	0.632
Erythropoietin Signaling Pathway	0.02455	1.604
CREB Signaling in Neurons	0.02884	3
Regulation of eIF4 and p70S6K Signaling	0.02951	0
Autophagy	0.02951	2.324
Apelin Cardiomyocyte Signaling Pathway	0.03020	1
CDK5 Signaling	0.03020	2.121
Wound Healing Signaling Pathway	0.03020	2.828
Phospholipases	0.03162	0.816
Synaptic Long Term Potentiation	0.03162	2.333
IL-12 Signaling and Production in Macrophages	0.03236	0.728
HMGB1 Signaling	0.03311	2.111
Neuropathic Pain Signaling In Dorsal Horn Neurons	0.03388	1
Eicosanoid Signaling	0.03388	1.342
FGF Signaling	0.03548	1.134
RAR Activation	0.03802	NaN
p38 MAPK Signaling	0.03890	2.646

Supplementary Table 3: Continued

Ingenuity Canonical Pathways	p-value	z-score
AMPK Signaling	0.03981	0.832
G-Protein Coupled Receptor Signaling	0.04074	4.111
Reelin Signaling in Neurons	0.04169	1
Hepatic Cholestasis	0.04266	NaN
Neutrophil Extracellular Trap Signaling Pathway	0.04365	1.569
Epithelial Adherens Junction Signaling	0.04467	0
RANK Signaling in Osteoclasts	0.04677	0.707
Caveolar-mediated Endocytosis Signaling	0.04677	NaN

Supplementary Table 4: Missing values of the analyses

Parameter	N (per group)	Missing values	Reason
Body weight	12	0	
WAT weight	12	0	
CS activity			
RP WAT	CTRL: 12 Concept: 11	1	Whole sample used for Western blot
EPI WAT	12	0	
ING WAT	12	0	
HADH activity			
RP WAT	CTRL: 12 Concept: 11	1	Whole sample used for Western blot
EPI WAT	12	0	
ING WAT	12	0	
mtDNA	CTRL: 12 Concept: 9	3	2 samples: pipet error; 1 sample: no sample left for this analysis
OXPHOS			
RP WAT	9	6	Technical error scanning one of the blots
EPI WAT	12	0	
ING WAT	12	0	
qPCR			
EPI WAT	12	0	
ING WAT	CTRL: 8 Concept: 10	6	No sample left for this analysis
mRNA sequencing	5	0	
DNA methylation	5	0	

Supplementary Table 5: Primer sequences

Gene name	NCBI reference number	Forward primer (5'- 3')	Reverse primer (3'- 5')
DNA primers			
Lpl	NM_008509	tcctgatgacgctgattttg	atgtcaacatgccctactgg
Nd1	NC_005089.1	accaatacgccctttaacaac	aatgggtgtggtattggtagg
RNA Primers			
Leptin	NM_008509.2	cacttgtcatctcattcctggatt	ccgttaccgtccatccatg
Mest	NM_008590.1	tcagtgacaagccgagacca	gttgattctgcggttctggag
Pdk4	NM_013743.2	aagagctggtatatccagagcctg	ttgaccagcgtgtctacaaactc
Glut4	NM_009204.2	cggatgctatgggtccttacg	aacgtccggcctctggttt
Cpt1a	NM_013495.2	gcccatgttgtacagcttcc	tcatcagtggcctcacagac
Ucp3	NM_009464.3	aacgctcccctaggcaggta	gcagaaaggagggcacaaatc
Rpl19	NM_009078.2	ttgcctctagtgtcctccgc	cttcctgatctgctgacggg
Rps29	NM_009093.2	agtcacccacggaagttcgg	gtccaacttaatgaagcctatgtcctt

[1] Institute for Clinical Diabetology, German Diabetes Center, Leibniz Center for Diabetes Research at Heinrich-Heine University, Düsseldorf, Germany; [2] German Center for Diabetes Research, Partner Düsseldorf, Germany; [3] Danone Nutricia Research, Utrecht, The Netherlands; [4] Institute of Aerospace Medicine, German Aerospace Center (DLR), Cologne, Germany; [5] Center for Endocrinology, Diabetes and Preventive Medicine (CEDP), University Hospital Cologne, Cologne, Germany; [6] Cologne Excellence Cluster on Cellular Stress Responses in Aging-Associated Diseases (CECAD), Cologne, Germany; [7] Department of Nutrition and Movement Sciences, School for Nutrition and Translational Research in Metabolism, Maastricht University Medical Center, Maastricht, The Netherlands; [8] Department of Pharmacology and Toxicology, Faculty of Pharmacy, Tanta University, Tanta, Egypt; [9] Human and Animal Physiology, Wageningen University, Wageningen, The Netherlands; [10] Department of Pediatrics, University Medical Centre Groningen, University of Groningen, Groningen, The Netherlands; [11] Department of Endocrinology and Diabetology, Medical Faculty and University Hospital, Heinrich-Heine University, Düsseldorf, Germany

Chapter 5

Dietary lipid droplet structure in postnatal life improves hepatic energy and lipid metabolism in a mouse model for postnatal programming

Tomas Jelenik[1,2], Andrea Kodde[3], Dominik Pesta[1,2,4,5,6], Esther Phielix[7], Annemarie Oosting[3], Elisabeth Rohbeck[1,2], Bedair Dewidar[1,2,8], Lucia Mastrototaro[1,2], Sandra Trenkamp[1,2], Jaap Keijer[9], Eline M. van der Beek[10], Michael Roden[1,2,11]

Pharmacological Research, 2022: 106193
DOI: 10.1016/j.phrs.2022.106193

Abstract

Early-life diets may have a long-lasting impact on metabolic health. This study tested the hypothesis that an early-life diet with large, phospholipid-coated lipid droplets (Concept) induces sustained improvements of hepatic mitochondrial function and metabolism. Young C57BL/6j mice were fed Concept or control (CTRL) diet from postnatal day 15 (PN15) to PN42, followed by western style (WSD) or standard rodent diet (AIN) until PN98. Measurements comprised body composition, insulin resistance (HOMA-IR), tricarboxylic acid (TCA) cycle- and β-oxidation-related hepatic oxidative capacity using high-resolution respirometry, mitochondrial dynamics, mediators of insulin resistance (diacylglycerols (DAG) or ceramides) in subcellular compartments as well as systemic oxidative stress. Concept feeding increased TCA cycle-related respiration by 33% and mitochondrial fusion protein-1 by 65% at PN42 (both<p 0.05). At PN98, CTRL, but not Concept, mice developed hyperinsulinemia (CTRL/AIN 0.22 ± 0.44 vs. CTRL/WSD 1.49 ± 0.53 nmol/l, p<0.05 and Concept/AIN 0.20 ± 0.38 vs. Concept/WSD 1.00 ± 0.29 nmol/l, n.s.) and insulin resistance after WSD (CTRL/AIN 107 ± 23 vs. CTRL/WSD 738 ± 284, p<0.05 and Concept/AIN 109 ± 24 vs. Concept/WSD 524 ± 157, n.s.). WSD-induced liver weight was 18% lower in adult Concept-fed mice and β-oxidation-related respiration was 69% higher (p<0.05; Concept/WSD vs. Concept/AIN) along with lower plasma lipid peroxides (CTRL/AIN 4.85 ± 0.28 vs. CTRL/WSD 5.73 ± 0.47 µmol/l, p<0.05 and Concept/AIN 4.49 ± 0.31 vs. Concept/WSD 4.42 ± 0.33 µmol/l, n.s.) and were in part protected from WSD-induced increase in hepatic cytosolic DAG C16:0/C18:1. Early-life feeding of Concept partly protected from WSD-induced insulin resistance and systemic oxidative stress, potentially via changes in specific DAG and mitochondrial function, highlighting the role of early life diets on metabolic health later in life.

Keywords: Early life programming, mitochondrial function, supramolecular structure of lipid droplets, milk fat globule membrane, insulin resistance, diacylglycerol

Introduction

The prevalence of childhood obesity keeps increasing (1) and contributes to the global rise in the incidence of type 2 diabetes (T2D), cardiovascular diseases and non-alcoholic fatty liver disease (NAFLD) (2,3). Consumption of hypercaloric fat- and carbohydrate-rich diets contributes to this pandemic, by promoting ectopic lipid deposition, which is related to insulin resistance, and key to the development of T2D (4). Excessive lipid deposition can lead to adaptation of hepatic mitochondrial function as demonstrated in mouse models of insulin resistance, obesity or lipodystrophy (5–7). In addition, subcellular accumulation of bioactive lipids, such as diacylglycerols (DAG) and ceramides (CER), have a major role in mediating lipid-induced insulin resistance by interfering with the insulin signalling pathway (4). Both the quantity and quality of dietary lipids affect metabolic function. Dietary lipids can either exert beneficial metabolic effects, as reported for n-3 polyunsaturated fatty acids- and monounsaturated fatty acids-enriched diets (8,9), or may promote inflammation and insulin resistance, as reported for saturated fats (10). In addition to these direct effects, dietary lipid quality, particularly during pre- and (early) postnatal life, was shown to have sustained effects on offspring metabolic health. Moreover, a high saturated fat intake during pregnancy impaired insulin sensitivity (11,12), as well as hepatic and skeletal muscle mitochondrial function (13,14) in adult offspring. Interestingly, postnatal dietary modulations can attenuate the metabolic consequences of an adverse maternal diet for the offspring (15). Postnatal feeding of a diet rich in n-3 long-chain polyunsaturated fatty acids prevented adult adiposity in rodents exposed to an obesogenic environment (16). Observational studies demonstrated that breastfeeding associates with a reduced risk of overweight and obesity (17,18), and it is postulated that besides fatty acid composition also the physical characteristics of human milk may contribute to these beneficial effects. Lipid droplets of human milk are larger compared to those of infant milk formula and are surrounded by a milk fat globule membrane, consisting of phospholipids, glycolipids, cholesterol and membrane proteins (19,20). To mimic the supramolecular structure of human milk lipid droplets, an infant milk formula with large lipid droplets, coated with phospholipids (Nuturis®) was developed (21). Previous studies in mice demonstrated that postnatal feeding with a diet containing Nuturis® (Concept) protects, at least in part, from western style diet (WSD)-induced lipid accumulation, adipocyte hypertrophy and insulin resistance (22,23). Although the underlying mechanisms remain elusive, there is evidence that Concept may enhance expression of genes regulating mitochondrial content and oxidative function in murine adipose tissue (24). Of note, current paradigms indicate that adipose tissue dysfunction will alter hepatic energy metabolism, ultimately leading to T2D and NAFLD (4). Hepatic mitochondrial functionality is important for the regulation of lipid metabolism and indeed Concept has been shown to enhance expression of

hepatic mitochondrial markers, directly after postnatal exposure, suggesting increased lipid oxidation (25). However, the long-term effects of the early life Concept exposure on hepatic mitochondrial function, biogenesis and dynamics as well as lipid composition and content has not been investigated. To this end, we examined the effects of postnatal Concept feeding on key features of hepatic mitochondrial function, biogenesis, dynamics, efficiency and oxidative stress, as well as hepatic lipid content and composition (i) after postnatal exposure and (ii) after subsequent exposure to standard chow diet or WSD in adult mice. We hypothesized that early postnatal Concept feeding improves hepatic mitochondrial function and lipid metabolism, thereby protecting from WSD-induced metabolic deterioration later in life.

Materials and methods

Animals

All experiments were performed according to the guidelines for the care and use of animals (GV-SOLAS [Society for Laboratory Animal Science], Freiburg, Germany) and approved by the local council of animal care in line with the requirements of the German Animal Protection Act and compliant to EU Directive 2010/63/EU. Male (n = 36) and female (n = 36) C57BL/6JOlaHsd breeder mice (9 weeks old at arrival, Envigo, Horst, The Netherlands) were maintained on a 12-h light-dark cycle in standard cages under conventional conditions, regularly checked for pathogens and received all diets and water ad libitum. Upon arrival, breeder mice were housed with 1 per cage (Macrolon type 3 cages, floor area 800 cm2 , height 150 mm, equipped with poplar bedding, nest material made of hemp fibers, wooden blocks for gnawing and red shelter mouse houses), and were allowed to acclimatize for one week, receiving a grain-based diet (2018S, Teklad Global 18% Protein Rodent Diet, Envigo, The Netherlands) as provided by the breeder and subsequently adapted to a semi-synthetic American Institute of Nutrition 93 G (growth) diet (AIN93G, Research Diet Services) (26) for two weeks. Breeders were time-mated (see **Supplementary Material** for more information) and provided with the AIN93G during breeding, pregnancy and until day 15 of lactation. At PN2, pups were randomly assigned to a dam to reduce between-litter variability and avoid litter effects, and culled to four male and two female pups per dam, except one litter who consisted of three males and three females and another litter which consisted of two males and four females, respectively, due to the sex-ratio and total offspring born. On PN15, dam and litters were assigned to either Concept or CTRL groups and fed with respective diets (see below), while pups were also allowed to drink milk from the dams (**Figure 1**). Concept and CTRL diets were provided daily as a dough on the floor of the cage. After weaning on PN21, male offspring were housed in pairs (with littermate) in Macrolon type 3 cages identical to the breeder mice and continued their respective diets until PN42. At PN42, males were

either dissected or switched to an AIN-93M (AIN) diet or to a WSD (20 w/w % fat) challenge until PN98 (Figure 1). The study comprised the following six groups: PN 42: CTRL (n = 13) and Concept (n = 10) and PN98: CTRL/AIN (n = 10), CTRL/WSD (n = 12), Concept/AIN (n = 12) and Concept/WSD (n = 16) (for power calculation see Supplementary Material). Group sizes were different as one litter (n = 4 males) was incorrectly assigned to the Concept group, but these 4 animals were kept in the study after consultation with the Animal Welfare Officer, as the animals could not be used for other experiments given their exposure to the diet. The extra male in the litter with 3 males and 3 females was kept in the study for the same reason and housed with the two littermates until the end of the study. To further reduce litter effects, offspring of the same litter were per pair divided over different groups i.e., either sacrificed at PN42 or assigned to WSD vs. AIN group. Body weight was measured twice a week from PN21 onwards, and food intake once a week from PN42 onwards. Food intake was assessed per cage by weighing the metal cage top with food per 24 h. Body composition was monitored by using nuclear magnetic resonance (Whole Body Composition Analyzer; Echo NRI, Houston, Texas, USA) at PN42 and PN98 (27). All animal procedures were performed in the light phase. At PN42 or PN98, mice were fasted for 3 h, anesthetized (isoflurane/N2O/O2) and killed by cervical incision, while trunk blood was obtained for EDTA plasma. Fresh pieces of liver were immediately transferred to biopsy preservation solution on ice for analysis of mitochondrial function using high-resolution respirometry within 2 h. The remaining tissues were snap-frozen and stored at -80°C for later analysis.

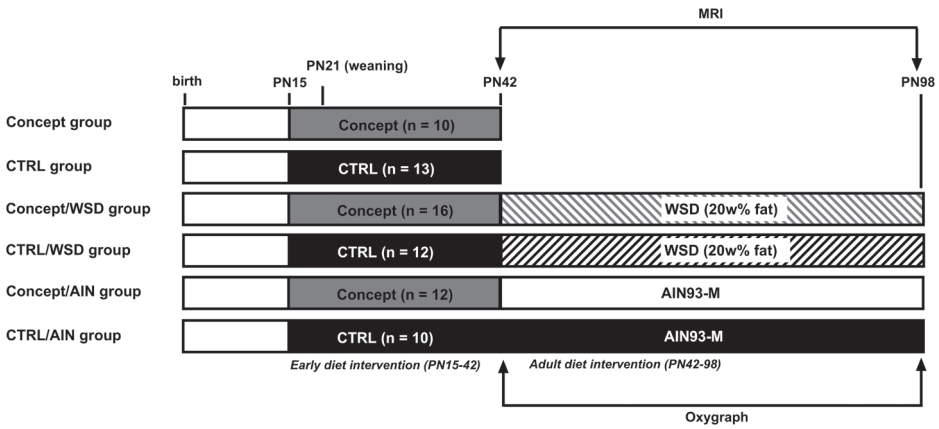

Figure 1: Study design. Mice were assigned to one of the 6 experimental groups and exposed to either CTRL or Concept diet from PN15 to 42. At PN42, CTRL- and Concept-fed mice were sacrificed and liver and skeletal muscle tissue was used for respirometry. Mice of the other groups were fed AIN93M or WSD until PN98. At PN98, remaining mice were sacrificed, and liver and skeletal muscle tissue was used for respirometry. Body composition was assessed with MRI at PN42 and PN98. AIN: AIN93M: American Institute of Nutrition rodent diet 93-maintenance, CTRL: control, MRI: magnetic resonance imaging, PN: postnatal day; WSD: western style diet.

Diets

The postnatal diets are semi-synthetic diets (Research Diets Services), containing 28.2% (w/w) CTRL or Concept infant milk formula (IMF) powder, are iso-caloric and contain similar amounts of macronutrients. To establish appropriate rodent macro- and micronutrient composition according to AIN-93G standards (26) only proteins, carbohydrates, vitamins and minerals were added i.e., the lipid portions of the diets were entirely derived from the IMFs. The CTRL IMF powder was a commercially available IMF manufactured per good manufacturing practices (ISO 22000) and intended for use of 0−6 months old infants (Danone Nutricia Research, Utrecht, The Netherlands). To produce Concept IMF (Nuturis®, Danone Nutricia Research, Utrecht, The Netherlands), 0.5 g/l milk phospholipid concentrate of bovine origin (Lipamin M20, Lecico, Hamburg, Germany) was added to the recipe and the processing adapted to generate larger lipid droplets surrounded with phospholipids (21,22). The mode diameter based on volume of the lipid droplet was 3.13 µm for Concept compared to 0.47 µm for CTRL. The composition of the diets is given in **Table 1**.

Hepatic and skeletal muscle mitochondrial function

Mitochondrial respiration (O_2 flux) and reactive oxygen species (ROS) emission were measured in freshly permeabilized liver and soleus muscle samples using the Oxygraph-2k (Oroboros Instruments, Innsbruck, Austria) as described (28). Defined respiratory states were obtained by employing the following protocols: (i) TCA-linked respiration, by consecutive addition of 2 mM malate, 10 mM pyruvate (complex I, state 2 respiration also termed as LEAK), 2.5 mM ADP, 10 mM glutamate and (complex I, state 3 also termed as OXPHOS (oxidative phosphorylation)), 10 mM succinate (complex I+II, state 3 (OXPHOS)), 10 µM cytochrome C (mitochondrial membrane integrity check), 5 nM oligomycin (complex I+II, state 4o also termed as LEAKomy), carbonyl cyanide-p-trifluoromethoxyphenylhydrazone (FCCP; stepwise titrations of 0.25 µM up to the final concentration of max. 1.25 µM) in order to obtain maximal electron transfer capacity (ETC) and 2.5 µM antimycin A (non-mitochondrial respiration); as well as (ii) β-oxidation-linked respiration, successive addition of 2 mM malate, 1 mM octanoyl-carnitine (complex I + electron-transferring flavoprotein complex (CETF), state 2 (LEAK)), 2.5 mM ADP (complex I + CETF, state 3 (OXPHOS)), 10 µM cytochrome C, 5 nM oligomycin (complex I + CETF, state 4o (LEAKomy)), FCCP to obtain maximal ETC (stepwise titrations of 0.25 µM up to the final concentration of max. 1.25 µM, state u) and 2.5 µM antimycin A. Addition of cytochrome C did not significantly increase oxygen consumption, indicating integrity of the mitochondrial outer membrane after saponin

permeabilization. Respiratory control ratio (RCR), reflecting mitochondrial coupling, was calculated for each protocol from the respective ratio of state 3 (OXPHOS):state 4o (LEAKomy) (28,29). Leak control ratio (LCR), reflecting mitochondrial proton leakage, was calculated using state 4o (LEAKomy):ETC ratios (28). Rates of hepatic ROS emission at state 4o were quantified by fluorometric measurement of H_2O_2 concentration by the O2k-Fluorescence module (Oroboros Instruments) as described (30). Citrate synthase activity (CSA) was assessed spectrophotometrically (Citrate Synthase Assay kit, Sigma-Aldrich, St. Louis, MO). Mitochondrial respiration and H_2O_2 emission were normalized for individual CSA values to account for any differences in mitochondrial content.

Circulating hormones and metabolites

Plasma glucose was measured using the Glucose Assay Kit (Calbiochem®, Merck, KGaA, Darmstadt) and plasma insulin using the Mercodia Mouse Insulin ELISA (Mercodia AB, Uppsala, Sweden). Plasma levels of thiobarbituric acid reactive substances (TBARS), as markers of lipid peroxidation, were measured fluorometrically (BioTek, Bad Friedrichshall, Germany) as reported previously (31). Plasma non-esterified fatty acid (NEFA) levels were measured using the Free Fatty Acids Kit (Cell Biolabs, INC., San Diego, USA).

Table 1: Dietary composition of the early life diets (g per kg powder).

Diet	**Programming diet**	
	CTRL	**Concept**
Carbohydrates	655	655
Sugars [a]	189	189
Polysaccharides [b]	420	420
Protein	203	203
Fat	70	70
Saturated fatty acids	31	31
Monounsaturated fatty acids	27	27
Polyunsaturated fatty acids	12	12
Phospholipids [c]	0.1	1.1
Cholesterol	-	0.03
Fiber	45.2	45.2
Vitamin & mineral mix	45	45

a) Total sugars, including lactose, glucose and sucrose; b) including starch and maltodextrin;
c) Phospholipids derived from bovine milk; CTRL: control diet; Concept: Concept diet.

Hepatic lipid analysis

Hepatic triglyceride concentration was measured colorimetrically (Triglyceride Quantification Colorimetric/Fluorometric Kit, BioVision, California, US). For the rapid and simultaneous quantification of DAG and ceramide species in liver tissue, we used a liquid chromatography triple quadrupole mass spectrometry (LC-MS/MS)-method as described before (32). After immediate freezing of the samples in liquid nitrogen, lipids were extracted and purified from ~50 mg of liver and muscle tissue each. For extraction, fractionation and purification of bioactive lipids, liver tissue was homogenized in 500 µl of buffer A (20 mM Tris/HCL, 1 mM EDTA 0.25 mM EGTA, 250 mM Sucrose, PIC) using an IKA T10 basic Ultra Turrax (IKA; NC, USA) and a tight-fitting glass homogenizer (Wheaton, UK) (32). Lipids of three subcellular compartment i.e., lipid droplet, cytosol and membrane fractions were obtained by centrifugation. Briefly, samples were transferred to centrifuge tubes, overlaid with 150 µl Buffer A and centrifuged for 1 h, 100,000 * g, 4°C. The floating lipid droplet layer was separated from the underlying cytosol fraction using a slicer (Beckman Coulter, Brea, CA, USA). Subsequently, the cytosol fraction was transferred to a fresh tube, while the membrane fraction remained as a pellet in the centrifuge tube. Internal standards were added and lipids of lipid droplet, cytosol and membrane fraction were extracted according to Folch et al. (33), followed by solid phase extraction (Sep Pak Diol Cartridges; Waters, MA, USA). The resulting lipid phase was dried under a gentle flow of nitrogen, resuspended in 400 µl methanol and then analysed by LC−MS/MS (32). In brief, the chromatographic separation of analytes was conducted using an Infinity 1290 Ultra-High Performance Liquid Chromatography system (Agilent Technologies Inc., Santa Clara, CA, USA) and a reversed-phase Luna Omega C18 column, 50 × 2.1 mm, 1.6 µm (Phenomenex, Torrance, CA, USA) operated at 50°C. A binary gradient was used consisting of 5 mM ammonium formate in water (Solvent A) and 5 mM ammonium formate in 90% methanol/10% i-propanol (solvent B) at the flow rate of 0.4 ml/min. The analytes were measured as ammonium adducts (DAGs) or protonated adducts (CERs) using electrospray ionization (ESI) and detected by multiple reaction monitoring (MRM) on a triplequadrupole mass spectrometer (MS, Agilent 6495; Agilent Technologies, CA, USA) operated in positive ion mode.

Immunoblotting

Immunoblotting of proteins was performed according to a previously described protocol (34). Proteins were extracted from approximately 30 mg of liver tissue, homogenized in 300 µl of lysis buffer (25 mM trisaminomethane-hydrochloride (Tris-HCl), pH 7.4, 150 mM NaCl, 0.20% Nonidet P-40, 1 mM ethylenediaminetetraacetic acid (EDTA) and

0.1% sodium dodecyl sulfate (SDS), supplemented with a Protease Inhibitor Cocktail and the Phosphatase Inhibitor Cocktail II (Roche, Mannheim, Germany) and loaded onto SDS polyacrylamide gradient gels (4–20% Mini-PROTEAN® TGX™ Precast Protein Gels, Biorad, Hercules, CA, USA). An inter-run calibrator (IRC) was loaded to each gel to account for between-run differences. Prior to immunoblotting, the stain-free gels were UV-activated for 1 min and pictures were taken using the ChemiDoc MP imaging system (Biorad). Proteins were transferred to a polyvinylidene difluoride (PVDF) membrane using the Trans-Blot Turbo Transfer System (Biorad), imaged using the ChemiDoc MP and quantified using Image LabTM 6.0.1 software (Bio-Rad 199 Laboratories) for normalization. The PVDF membrane was blocked with 5% non-fat milk in Tris-buffered saline with Tween 20 (TBST buffer: 10 mM Tris, pH 8.0, 150 mM NaCl, and 0.5% Tween 20) for 2 h at room temperature. Afterwards, the membranes were incubated overnight with primary antibodies at 4°C and then with horseradish peroxidase (HRP)-conjugated secondary antibodies for 1h at room temperature. Finally, membranes were coated with Immobilon Western Chemiluminescent HRP Substrate (Merck Millipore, Darmstadt, Germany) and proteins were detected using a ChemiDoc imaging system in combination with the software ImageLab 6.0.1 (Biorad) for densitometric analysis. Data are expressed in arbitrary units and normalized to voltage-dependent anion channel (VDAC) protein to normalize for mitochondrial content. The dynamin related protein (DRP) 1 (5391) and phospho-DRP1 Ser616 (3455) antibodies were purchased from Cell Signaling Technology; peroxisome proliferator-activated receptor gamma coactivator (PGC) 1-α from Millipore (ST1202); mitochondrial transcription factor A (TFAM) from Santa Cruz Biotechnology (sc-166965); other primary antibodies were purchased from Abcam: Mitofusin1 (MFN1) (ab57602), Mitofusin2 (MFN2) (ab56889) and VDAC (ab14734).

qPCR

Quantitative real-time-PCR (RT-PCR) was performed as described previously (35). Briefly, total RNA was isolated from 10 mg of frozen liver using the RNeasy Mini Kit (Qiagen, Düsseldorf, Germany), cDNA was transcribed from 1000 ng total RNA with the QuantiTect Reverse Transcription Kit (Qiagen, Cat. No.205311) and used for RT-PCR with QuantiTect SYBR® Green PCR Kit (Qiagen, Cat. No.204145) in a StepOnePlus RT-PCR System (Applied Biosystems, Waltham, MA USA) using QuantiTect Primer Assays (Qiagen, Düsseldorf, Germany). The following primers were purchased from Qiagen: TFAM (QT00154413), PGC1a (QT02524242); hypoxanthine-guanine phosphoribosyltransferase (QT00166768), Peptidylprolyl isomerase A (QT00247709) and β2-microglobulin (QT01149547) were

used as endogenous reference genes. Ct values were first normalized to geometric mean of Ct of the 3 reference genes, then to Ct of IRC to obtain the expression fold-change following the ΔΔCt method (35). A melting curve was created to ensure primer specificity. Each sample was measured in triplicate.

Calculations and statistics

As a surrogate of insulin resistance, HOMA-IR was calculated from 3- h fasting insulin (mlU/l) * fasting glucose (mmol/l)/22.5 (36,37). Statistical analyses were performed using GraphPad Prism (8.0.0) except for changes in body weight and body composition over time, which were analysed using SPSS (19.0.0). Data are expressed as mean ± SEM. The effects of early-life diet (Concept vs. CTRL) at PN42 were compared using the unpaired t-test. At PN98, effects of the early (Concept vs. CTRL) and adult diet (AIN vs. WSD) and the interaction between those, were analysed using two-way ANOVA and Sidak's multiple comparisons test in case of an overall early or adult diet effect. Data was tested for normal distribution by the Kolmogorov-Smirnov test and when data did not show a Gaussian distribution, analysed with a Mann-Whitney or Kruskall-Wallis test. Changes in body weight and body composition over time were analysed using repeated measure ANOVA. Differences were considered significant when $p<0.05$, $p<0.01$ and $p<0.001$.

Results

Direct effects of postnatal Concept feeding at PN42

The direct effects of the early-life dietary intervention, as defined by the 4 weeks from PN15 to PN42, were studied at PN42. Body weight was similar between Concept and CTRL (**Figure 2A**). However, Concept fed mice had a higher lean body mass (**Figure 2B**), while total body fat mass tended to be lower compared to CTRL (p=0.06). Consequently, relative body fat mass was lower after Concept feeding compared to CTRL (**Figure 2C, D**).

The differences in body composition did not affect organ weights (**Supplementary Table 1**).

In the liver, maximum uncoupled TCA cycle-linked respiration was 33% higher (p=0.05) after Concept feeding compared to CTRL (**Figure 3A**). No differences were observed for other parameters of TCA-cycle-linked respiration, including LCR and RCR (**Supplementary Figure 1A, B**). The parameters of β-oxidation-linked respiration, including LCR and RCR and CSA activities did not differ between Concept and CTRL (**Figure 3B, C and**

Supplementary Figure 1C, D). Also, hepatic mitochondrial ROS production, expressed as H_2O_2 emission, was similar between both groups (**Figure 3D**). Mitochondrial function and content as well as oxidative stress of the soleus muscle were not different between groups (**Supplementary Figure 2A-D**).

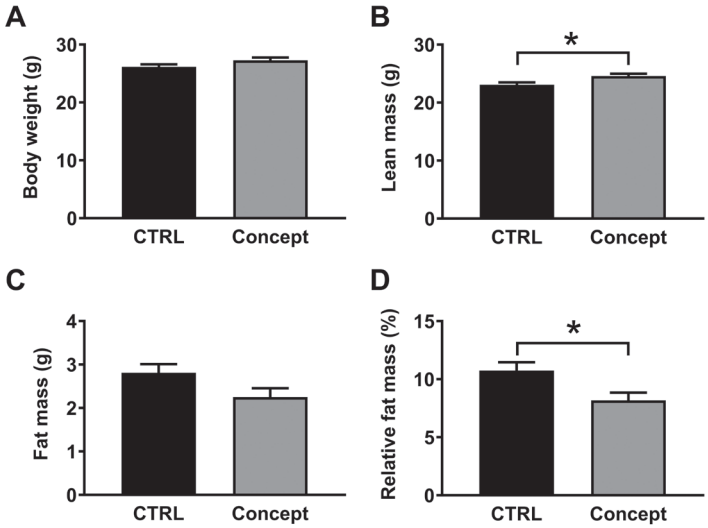

Figure 2: Direct effects of Concept vs CTRL on body weight and body composition. (**A**) Body weight at PN42. (**B-D**) Body composition at PN42. Data are shown as mean ±SEM, CTRL: n = 13; Concept: n = 10. Unpaired t-test; *p<0.05. CTRL: control.

Protein content of the biomarkers of mitochondrial biogenesis, PGC-1α and TFAM, was not different between Concept and CTRL at PN42 (**Figure 4A, B**). However, there was a 65% increase in MFN1 protein, indicating higher mitochondrial fusion after Concept feeding (p=0.03) (**Figure 4C, D**). DRP1 protein and the ratio of DRP1 to phospho-DRP1 (Ser616), as biomarkers of mitochondrial fission, were not different between the groups (**Figure 4E, F**).

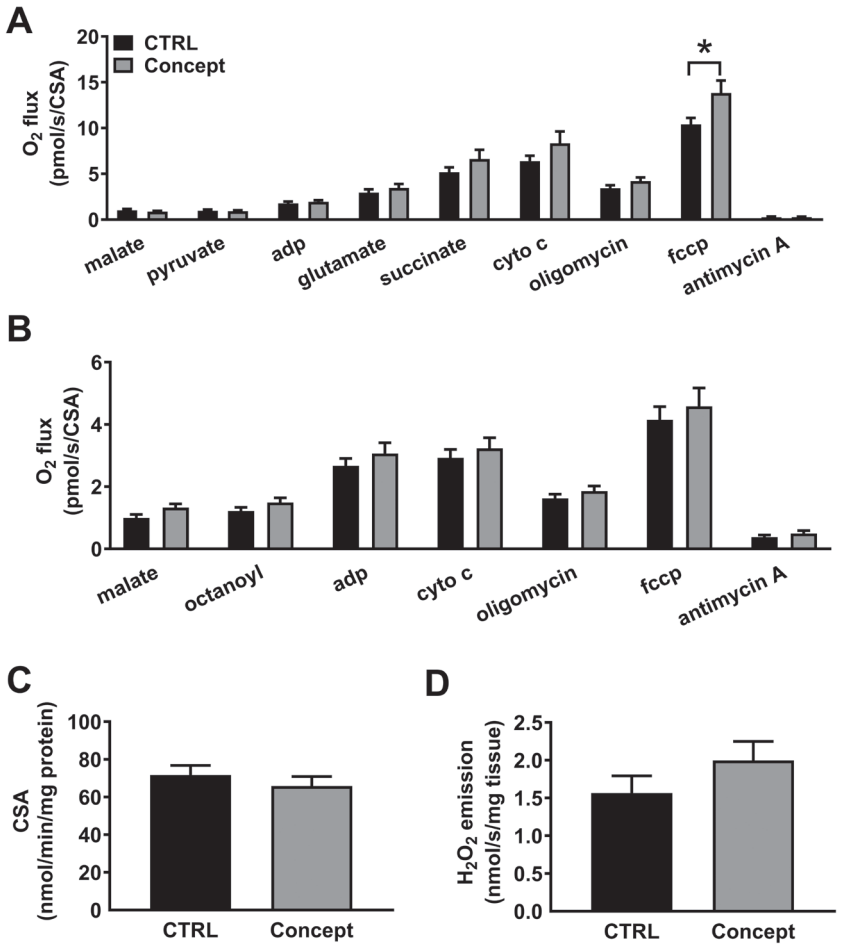

Figure 3: Direct effects of the Concept diet on mitochondrial function of the liver at PN42. Mitochondrial respiration [O_2 flux normalized to CSA] was measured with substrates supporting TCA cycle (**A**) and β-oxidation (**B**). Mitochondrial content (**C**) was assessed by CSA normalized to protein concentration. Oxidative stress (**D**) was measured as the rate of malate-stimulated H_2O_2 emission. Data are shown as mean±SEM, CTRL: n = 13; Concept: n = 10. Multiple t-test (A, B) or unpaired t-test (C,D); *p<0.05. CSA: citrate synthase activity, CTRL: control; cyto C: cytochrome c; fccp: carbonyl cyanide-p-trifluoromethoxyphenylhydrazone; TCA: tricarboxylic acid.

After 3 h of fasting, there were no differences in plasma glucose, insulin, HOMA-IR, as well as plasma TBARS and NEFA (**Supplementary Figure 3A-F**). Liver weight and liver triglycerides were comparable between Concept and CTRL at PN42 (**Figure 5A, B**). Cytoplasmic DAGs (cDAG), lipid droplet DAGs (ldDAG) and most membrane DAGs (mDAG) as measured in liver tissue, were not affected by Concept compared to CTRL. However, C20, C22 and C24 mCER were higher in Concept compared to CTRL mice (**Figure 5C and Supplementary Figure 4A-E**).

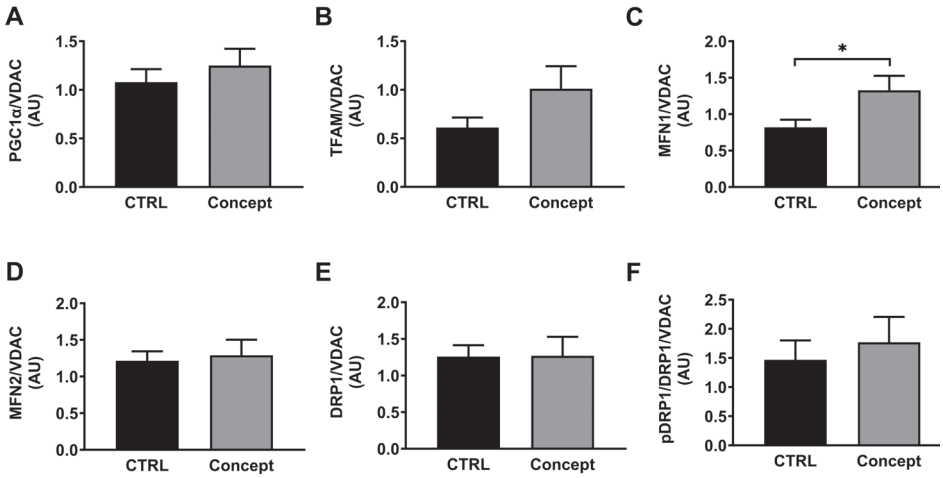

Figure 4: Direct effects of Concept and CTRL on protein markers of mitochondrial biogenesis and dynamics at PN42. PGC-1α (**A**), TFAM (**B**), MFN1 (**C**), MFN2 (**D**), DRP1 (**E**) and pDRP1/DRP1 (**F**). Data are shown as mean±SEM, CTRL: n = 13; Concept: n = 10. Unpaired t-test, *p<0.05. CTRL: control; PGC-1α: peroxisome proliferator-activated receptor gamma coactivator 1-α; TFAM: mitochondrial transcription factor A; MFN1 or 2: mitofusion 1 or 2; DRP1: dynamin-related protein 1, VDAC: voltage-dependent anion channel.

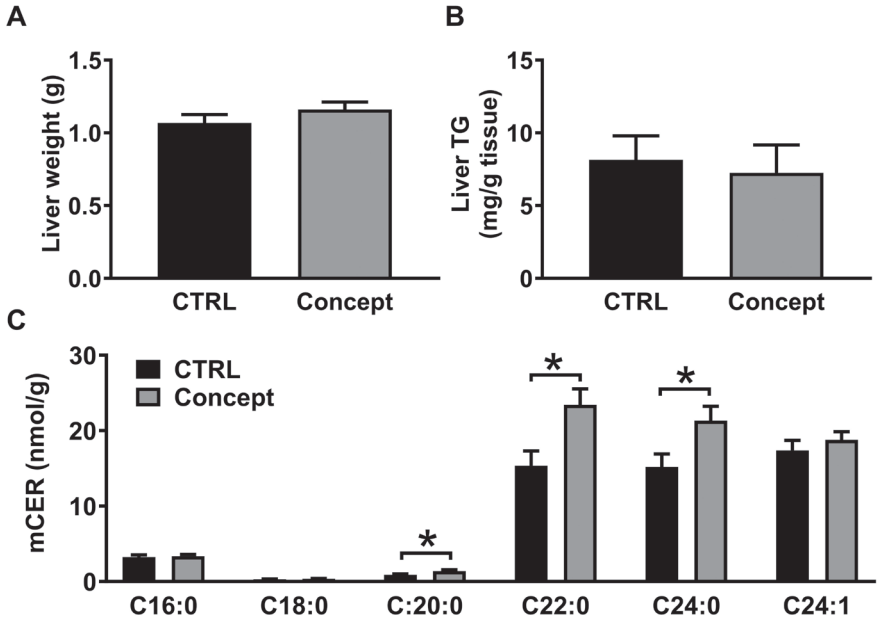

Figure 5: Direct effects of Concept and CTRL on liver weight and hepatic lipids at PN42. Liver weight (**A**), liver TG (**B**) and mCER (**C**). Data are shown as mean±SEM, CTRL: n = 13; Concept: n = 10 for liver weight; CTRL: n = 12; Concept: n = 10 for liver TG and mCER. Unpaired t-test, *p<0.05. CTRL: control; mCER: ceramides in membranes, TG: triglycerides.

Effects of postnatal Concept feeding in adult mice

At PN98, the effect of the early-life feeding with Concept vs CTRL was assessed upon a WSD challenge. Compared to AIN, WSD exposure increased body weight and lean mass over time (PN42–98) to a similar extent in the Concept/WSD and CTRL/WSD groups, also when corrected for the respective baseline values (**Figure 6A, B and Supplementary Figure 5A, B**). Concept/WSD showed a somewhat lower increase in (relative) body fat mass over time than CTRL/WSD, which was statistically different compared to CTRL/WSD, when corrected for baseline values (**Figure 6C, D and Supplementary Figure 5C and D**).

Neither early nor adult diets affected fasting plasma glucose and NEFA levels (**Figure 6E, I**). Plasma insulin and HOMA-IR significantly worsened in CTRL/WSD compared to CTRL/AIN, but not in Concept/WSD compared to Concept/ AIN (**Figure 6F-G**). Plasma TBARS levels were increased in CTRL/WSD compared to CTRL/AIN, but not in Concept/WSD mice (**Figure 6H**).

In order to assess long-term effects of postnatal Concept feeding on mitochondrial biogenesis and dynamics, we assessed protein levels of PGC-1α, TFAM, MFN1, MFN2, DRP1 and the ratio of DRP1 to phosphor-DRP1 (Ser616). Neither early nor adult diets affected these biomarkers of mitochondrial biogenesis and dynamics (**Figure 8A-F**) or the differences of the mitochondrial protein between PN42 and PN98 (**Supplementary Figure 8A-F**).

In contrast to CTRL/WSD, liver weight of the Concept/WSD group did not increase upon WSD challenge and was lower compared to that of CTRL/WSD (**Figure 9A**). The WSD-induced increase in weight of any other tissue or organ studied was not affected by the early-life Concept diet (**Supplemental Table 2**). Hepatic triglyceride levels increased upon WSD feeding in both the CTRL/WSD and the Concept/WSD (**Figure 9B**). When assaying subcellular fractions to study bioactive lipids in more detail, we found that the WSD challenge increased hepatic cDAG and mDAG species containing C18:1 mainly in CTRL/WSD compared to CTRL/AIN, which only reached significance for cDAG C16:0/C18:1 (**Figure 9C, D and Supplementary Figure 9A, C, E**). Neither the WSD, nor the early Concept feeding had an effect on CER species in the different subcellular fractions (**Supplementary Figure 9B, D and F**).

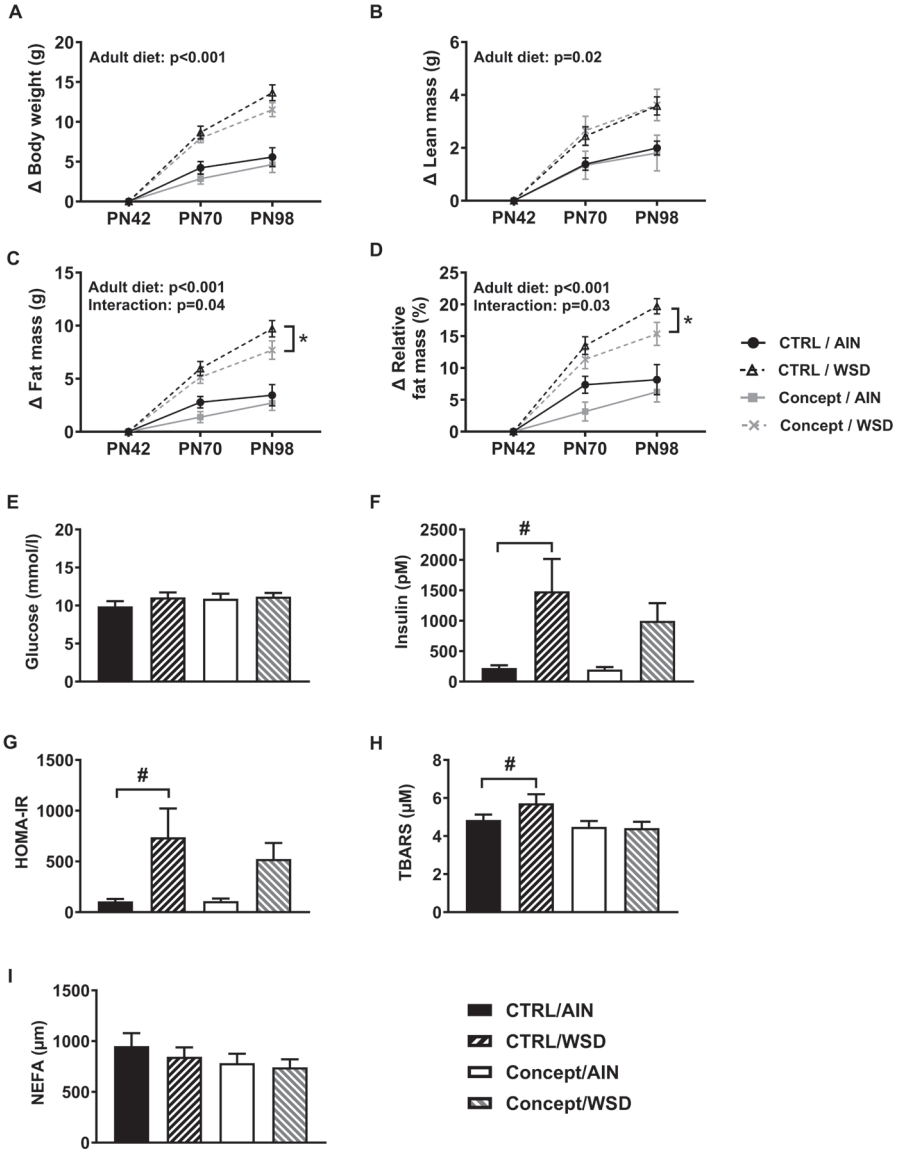

Figure 6: Long-term effects of postnatal Concept feeding on changes in body weight, body composition and glucose metabolism. Development of body weight (**A**), lean mass (**B**), fat mass (**C**) and relative fat mass (**D**, % of body weight) from PN42 to PN98 as corrected for baseline. Fasted (3 h) plasma glucose (**E**), plasma insulin (**F**), HOMA-IR (**G**) TBARS (**H**), and NEFA (**I**). Data are shown as mean±SEM, CTR/AIN: n = 10; CTRL/WSD: n = 12; Concept/AIN: n = 12; Concept/WSD: n = 16, except for the glucose, HOMA-IR which had n = 9 for the CTRL/AIN and n = 11 for the Concept/AIN. For body weight and composition, repeated measures ANOVA with two factors (early and adult diet) was used and in case of existing interaction between factors, separate factors were tested. *p<0.05 Concept/WSD different from CTRL/WSD. Glucose and insulin data were tested with two-way ANOVA. #p<0.01 WSD effect in groups fed the same early-life diet. AIN: American Institute of Nutrition rodent diet; CTRL: control; NEFA: non-esterified fatty acids; PN: postnatal day; TBARS: thiobarbituric acid reactive substances; WSD: western style diet.

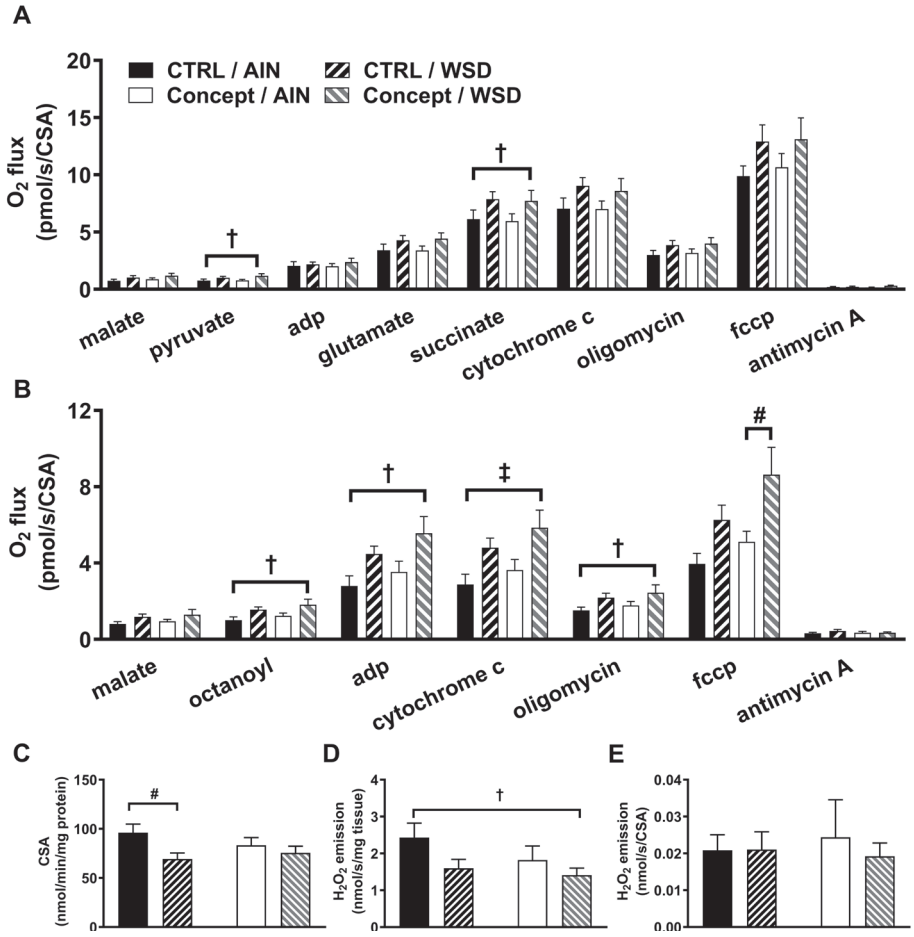

Figure 7: Long-term effects of postnatal Concept feeding on mitochondrial function in the liver at PN98. Mitochondrial respiration [O_2 flux normalized to citrate synthase activity (CSA)] was measured with substrates supporting TCA cycle (**A**) and β-oxidation (**B**). Mitochondrial content (**C**) was assessed by CSA activity normalized to protein concentration. Oxidative stress was measured as the rate of malate-stimulated H_2O_2 emission and displayed per mg tissue (**D**) and per CSA (**E**). Data are shown as mean±SEM, CTRL/AIN: n = 10; CTRL/WSD: n = 12; Concept/AIN: n = 12; Concept/WSD: n = 16. Two-way ANOVA; †p<0.05; ‡ p<0.01: overall WSD effect; #p<0.05: WSD effect in groups fed the same early-life diet. AIN: American Institute of Nutrition rodent diet; CSA: citrate synthase activity, CTRL: control; cyto c: cytochrome c; fccp: carbonyl cyanide-p-trifluorom ethoxyphenylhydrazone; TCA: tricarboxylic acid; WSD: western style diet.

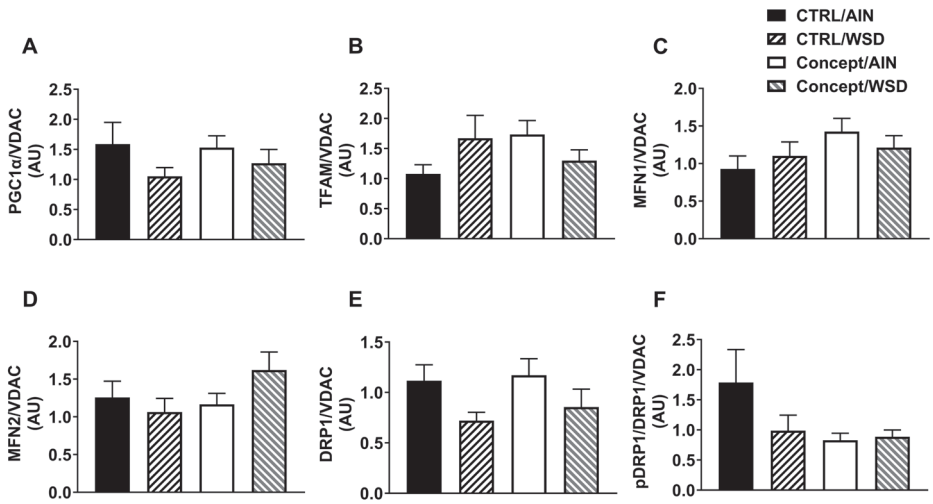

Figure 8: Long-term effects of postnatal Concept feeding on liver-specific markers of mitochondrial biogenesis and dynamics at PN98. PGC-1α (**A**), TFAM (**B**), MFN1 (**C**), MFN2 (**D**), DRP1 (**E**) and pDRP1/DRP1 (**F**). Data are shown as mean±SEM, two-way ANOVA; CTRL/AIN: n = 10; CTRL/WSD: n = 12; Concept/AIN: n = 12; Concept/WSD: n = 14. PGC-1α: peroxisome proliferator-activated receptor gamma coactivator 1-α; TFAM: mitochondrial transcription factor A; MFN1 or 2: mitofusion protein 1 or 2; DRP1: dynamin-related protein 1, VDAC: voltage.

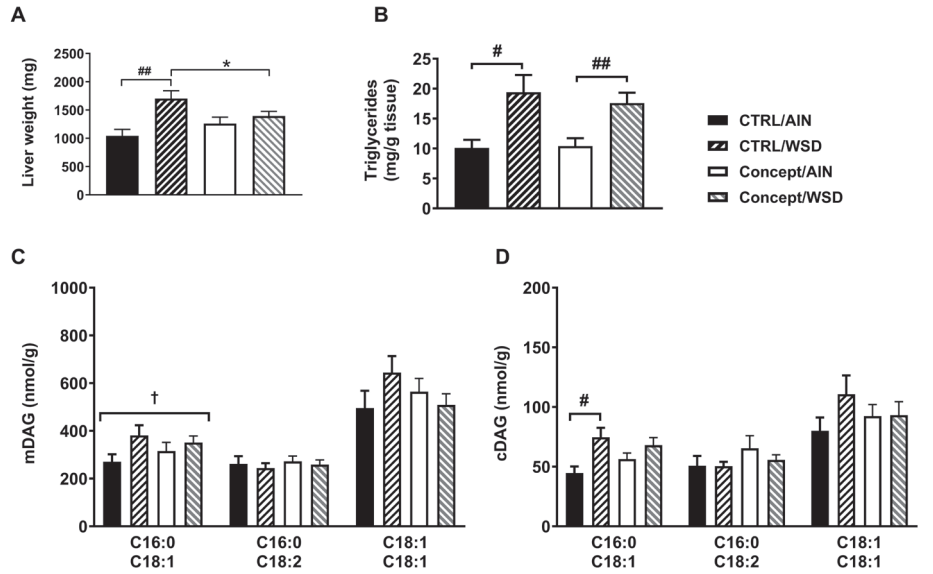

Figure 9: Long-term effects of postnatal Concept feeding on liver weight and liver lipids on PN98. Liver weight (**A**), liver TG (**B**), mDAG (**C**) and cDAG (**D**). Data are shown as mean±SEM, CTRL/AIN: n = 10; CTRL/WSD: n = 12; Concept/AIN: n = 12 for all; Concept/WSD: n = 16 for liver weight, n = 12 for liver TG and n = 14 for mDAG and cDAG. Two-way ANOVA; †p< 0.05; overall WSD effect; #p<0.05; ##p<0.01: WSD effect in groups fed the same early-life diet; *p<0.05 early diet effect in groups fed the same adult diet. AIN: American institute of nutrition diet; cDAG: diacylglycerols in cytoplasm; CTRL: control; mDAG: diacylglycerols in membranes, TG: triglycerides; WSD: western style diet.

Correlation analyses

Energy expenditure can best be correlated to lean mass (38), due to significant weight contribution but low metabolic activity of white adipose tissue (39). Indeed, at PN98, the lean body mass of CTRL groups (CTRL/AIN and CTRL/WSD together) correlated to hepatic mitochondrial respiration from different substrates (Malate r=0.490; Octanoyl-carnitine r=0.436; Oligomycin r=0.476; Antimycin r=0.453; $p<0.05$ for all; **Supplementary Table 3**). However, in Concept fed groups, no such correlations were found. As for AIN and WSD animals at PN98, we observed a correlation between lean body mass and respiration rate after ADP (r=−0.548), cytochrome c (r=−0.523) and FCCP titration (r=−0.403), $p<0.05$ for all (**Supplementary Table 4**).

Discussion

This diet intervention study showed that early-life exposure to a diet comprising large, phospholipid-coated lipid droplets (Concept) affects various features of mitochondrial function and lipid metabolism in rodent liver, but not skeletal muscle. Concept feeding not only directly enhanced maximum hepatic TCA-cycle-linked mitochondrial oxidative capacity and mitochondrial fusion at PN42, but also potentiated β-oxidation-linked oxidative capacity later in life, at PN98. Furthermore, postnatal exposure to the Concept diet at least partially protected against WSD-induced hyperinsulinemia, insulin resistance, body fat accumulation, cytosolic and membrane DAG accumulation and systemic oxidative stress.

Early-life environment can affect metabolic health and specifically liver function either adversely e.g., by foetal over- or undernutrition (40,41), or beneficially e.g., by breastfeeding (42). Several rodent and piglet studies suggested that altered hepatic mitochondrial function and ROS production may be associated with this so-called programming of metabolic health (13,43,44). In those studies, intrauterine growth restricted piglets (43) and rodents born to obese dams (13,44) showed reduced hepatic mitochondrial content, oxidative capacity and increased production of ROS and/or expression of its markers. Early-life feeding with the Concept diet for several weeks increased maximum uncoupled TCA-cycle-linked respiration directly after exposure and maximum uncoupled β-oxidation-linked respiration later in WSD-fed adult mice. These findings suggest that the Concept diet induces programming of hepatic mitochondrial function, increasing maximum oxidative capacity. Interestingly, in the current study, hepatic mitochondrial ROS emission remained unchanged between Concept/WSD and CTRL/WSD, while plasma lipid peroxides (TBARS) increased only in CTRL/WSD, but not in Concept/WSD. The absence of a rise in ROS production in the face of higher oxidative

capacity hints at an improved antioxidant activity and/or altered lipid metabolism, maybe due to preferred β-oxidation or decreased VLDL secretion from the liver of Concept/WSD mice.

Mitochondrial dynamics i.e., fission and fusion events, are closely related to intact mitochondrial function. One of the factors contributing to NAFLD development is the inadequate mitochondrial quality control (45). While mitochondrial fusion positively correlates with oxidative phosphorylation capacity (46), mitochondrial fission has a role in the development of hepatic steatosis and metabolic deterioration (47,48). The present study found evidence for higher mitochondrial fusion upon normalization to mitochondrial content in mice receiving Concept during early life, supporting the contention of an association with the improvement of mitochondrial function in these mice (46). While there were no long-term effects of postnatal Concept feeding on liver-specific mitochondrial biogenesis and dynamics, we cannot exclude longer-lasting effects on hepatic metabolism, maybe occurring via epigenetic alterations associated with fetal programming (49).

Fat droplets of concept diet are composed of a mixture of phospholipids, proteins and cholesterol, mimicking largely the structure and composition of human fat globules (50). Although exact mechanisms are still under investigation, the specific structure of Concept may enhance intestinal lipolysis and postprandial lipemia in a way that postprandial responses and bioavailability of ingested fatty acids exert possible longer-term consequences on hepatic bioenergetics.

The WSD intervention increased hepatic oxidative capacity from several mitochondrial substrates. Recent studies demonstrated that hepatic mitochondria can adapt their activity to short-term as well as long-term changes of substrate availability. Specifically, increased lipid availability leads to adaptive increases in mitochondrial oxidative capacity, indicating “mitochondrial flexibility” in both humans and murine obesity, at least during the early course of NAFLD (29). In the present study, the Concept/WSD mice featured higher hepatic mitochondrial function from different substrates independent of WSD-induced changes in lean body mass, in line with a sustained effect of early life Concept exposure. This effect is likely not related to improved mitochondrial biogenesis, as Concept did not affect hepatic CSA, reflecting mitochondrial content or mass. Collectively, these findings point towards a protective effect of Concept in early life from WSD-induced impairment of hepatic lipid metabolism in later life (22, 23).

The long-term effects of Concept on hepatic mitochondrial respiration may result from different mechanisms. Previously, we showed that Concept increases postprandial glucose concentrations (51). One might speculate that higher glucose levels may have

stimulated TCA-cycle-linked respiration and de novo lipogenesis and lipid export at PN42. Subsequently, the increased β-oxidation-linked respiration in Concept/WSD at PN98 observed in the current study, may result from adaptation of hepatic mitochondria to several weeks of higher lipid exposure. Early Concept diet could thereby lead to improved handling of lipid overloads by improved "mitochondrial flexibility" for oxidation of the lipid surplus instead of storing it, supported by the observation of a lower fat mass gain in Concept/WSD. Notably, Concept feeding did not impact skeletal muscle mitochondrial function, content or oxidative stress. Nutrient overload, induced by high-fat feeding, can result in exhaustion of adipose tissue storage capacities and subsequent "spillover" of lipids into other tissues such as skeletal muscle or liver (52,53), potentially impairing mitochondrial function (54). Although we cannot infer general effects of the WSD on skeletal muscle mitochondrial function, we conclude that Concept at least did not result in improved mitochondrial function in soleus muscle.

Of note, Concept feeding prevented a WSD-induced increase in mDAG and cDAG, key bioactive lipids interfering with proximal insulin signalling. Particularly, C18-containing mDAG are known to activate PKCε, which then phosphorylates threonine residues of the insulin receptor kinase and thereby impairs insulin signalling (4,55). In contrast, sequestration of DAGs into neutral cellular lipid storage sites such as lipid droplets is considered protective towards metabolic derangements (56). Concept feeding therefore seems to favour cellular lipid re-distribution with a profile favouring protection from hepatic insulin resistance. Moreover, the lower DAG lipid profile after Concept feeding could explain higher mitochondrial respiration, as it has recently been shown that C18-containing DAG reduced state 3 mitochondrial respiration in vitro in a dose-dependent manner (57). In addition, to exert effects via DAGs, early life exposure to Concept feeding may cause epigenetic changes to genes involved in lipid metabolism and/or mitochondrial function as reported for body mass-induced changes in skeletal muscle and liver in humans (58,59). Indeed, a recent study has revealed a novel role of phospholipids as a methyl sink and important regulator of histone methylation (60). Elevated ceramides, particularly C16, C18, C22 and C24 species, have been associated with fatty liver disease and impaired mitochondrial function after feeding high-fat diets ranging from 45% to 60% fat content (61,62). Early life diets, mimicking human breast milk, are also naturally rich in fat (70%, see Table 1 for composition). As there are no differences regarding key metabolic outcomes (Supplementary Figure 2), we conclude that elevated CER at this point do not associate with metabolic impairments. Furthermore, the milk phospholipid concentrate used to coat the lipid droplets in the Concept diet also contained ceramides, which may have a direct effect on ceramide levels in blood and membranes, as shown for phosphatidylcholines (63,64). With regard

to longer-term effects, it is important to note that feeding a WSD did not differentially affect CTRL or Concept mice, as shown in Supplementary Figure 6.

Despite the significant improvements in hepatic lipid oxidation and circulating lipid peroxides, the effects of Concept on fasting glycemia, NEFA and insulin sensitivity were relatively modest. The relative short exposure to the WSD (8 weeks) may be explanatory as the effect of Concept on fasting plasma glucose, lipids, leptin, resistin and total body fat mass were more pronounced after longer (12 weeks) exposure to WSD in Concept treated mice (22). On the other hand, exact quantification of hepatic insulin sensitivity would have required clamp tests, as HOMA-IR was assessed only upon a rather short duration of fasting (3 h), based on ethical considerations for animal well-being. Concept treated animals did respond to the obesogenic diet, but Concept feeding, even when challenged for a longer period with WSD, protected animals from development of hyperinsulinemia. Elevated plasma insulin results from higher insulin secretion or lower insulin clearance (65). In humans, insulin clearance is not necessarily related to liver fat content (66), whereas a high-fat diet may impair insulin clearance in mice (67). In our study, hyperinsulinemia could therefore originate from both compensatory increased insulin secretion or decreased insulin clearance. As C-peptide clearance by the liver is negligible, this parameter is used to estimate insulin secretion rate (68) or to obtain a crude measure of hepatic insulin fractional extraction from the C-peptide:insulin molar ratio (69). However, we could not assess C-peptide in this study due to limited plasma availability.

This study has some limitations we need to address. We cannot conclude whether the effects of Concept on mitochondrial oxidative activity and lipid metabolism are due to the increased size of dietary lipid droplets, the phospholipid coating of these droplets or its combined effects. Previous studies showed, however, that both an increase in lipid droplet size and phospholipid coating are required for the phenotypic Concept effects (70). Also monitoring of mitochondrial ATP concentration and/or synthesis, which is affected by lipid diets, diabetes and NAFLD in humans (71–73) would have been of interest, but was not possible due experimental limitations. Furthermore, to uncover subtle metabolic changes, detailed analysis of tissue-specific insulin sensitivity using hyperinsulinemic clamp tests with isotopic dilution methods (74) would be required.

In conclusion, early-life feeding with a diet containing large, phospholipid coated lipid droplets (Nuturis®) was shown to improve hepatic oxidative capacity, mitochondrial fusion and lipid profiles, directly after exposure, which persisted into later in life under an obesogenic environment in a mouse model for nutritional programming. Thus, this study highlights the role of an early life diet containing specific phospholipids mimicking human breast milk on metabolic health later in life.

Additional information

Sources of support

This study was sponsored in part by Danone/Nutricia as well as by the Ministry of Culture and Science of the State of North Rhine-Westfalia (MKW NRW), the German Federal Ministry of Health (BMG) as well as by a grant of the Federal Ministry for Research (BMBF) to the German Center for Diabetes Research (DZD e. V.), the German Research Foundation (DFG, CRC 1116/2) as well as the Schmutzler-Stiftung.

Credit author statement

TJ, AK, AO, EP, EvdB and MR designed research; TJ, AK, DP, ER, ST, LM and BD conducted research; TJ, AK, and ER analysed data; TJ, AK, DP, EP, LM, JK, EvdB and MR interpret the data; TJ, AK, DP and MR wrote the paper; MR had primary responsibility for final content. All authors read and approved the final manuscript.

Declaration of Competing interest

TJ: none; AK, AO: are employees of Danone Nutricia Research, EvdB: was an employee of Danone Nutricia Research at the time of the study conduct and analyses; DP none; EP: none; ER: none; BD: none; ST: none; JK: none; MR: none.

Data availability

Data supporting the conclusions of this manuscript are available upon reasonable request from the corresponding author.

Acknowledgements

Assistance: We wish to thank Ilka Rokitta and Fariba Zivehe for expert help with performing experiments and analyses, Eefje Engels for her advice for conduct of the study and Dennis Acton for contribution to data interpretation.

Grants: This study was sponsored in part by Danone Nutricia Research as well as by the Ministry of Culture and Science of the State of North Rhine-Westfalia (MKW NRW), the German Federal Ministry of Health (BMG) as well as by a grant of the Federal Ministry for Research (BMBF) to the German Center for Diabetes Research (DZD e. V.), the German Research Foundation (DFG, CRC 1116/2) as well as the Schmutzler-Stiftung. Danone Nutricia Research provided the animal diets and was involved in discussions on study design, data interpretation and writing of the manuscript.

References

1. Ng M, Fleming T, Robinson M, Thomson B, Graetz N, Margono C, et al. Global, regional, and national prevalence of overweight and obesity in children and adults during 1980-2013: a systematic analysis for the Global Burden of Disease Study 2013. Lancet. 2014;384(9945):766-81.
2. Sinha R, Fisch G, Teague B, Tamborlane WV, Banyas B, Allen K, et al. Prevalence of impaired glucose tolerance among children and adolescents with marked obesity. N Engl J Med. 2002;346(11):802-10.
3. Reilly JJ, Kelly J. Long-term impact of overweight and obesity in childhood and adolescence on morbidity and premature mortality in adulthood: systematic review. Int J Obes (Lond). 2011;35(7):891-8.
4. Roden M, Shulman GI. The integrative biology of type 2 diabetes. Nature. 2019;576(7785):51-60.
5. Arruda AP, Pers BM, Parlakgul G, Guney E, Inouye K, Hotamisligil GS. Chronic enrichment of hepatic endoplasmic reticulum-mitochondria contact leads to mitochondrial dysfunction in obesity. Nat Med. 2014;20(12):1427-35.
6. Gancheva S, Jelenik T, Alvarez-Hernandez E, Roden M. Interorgan Metabolic Crosstalk in Human Insulin Resistance. Physiol Rev. 2018;98(3):1371-415.
7. Jelenik T, Kaul K, Sequaris G, Flogel U, Phielix E, Kotzka J, et al. Mechanisms of Insulin Resistance in Primary and Secondary Nonalcoholic Fatty Liver. Diabetes. 2017;66(8):2241-53.
8. Lombardo YB, Hein G, Chicco A. Metabolic syndrome: effects of n-3 PUFAs on a model of dyslipidemia, insulin resistance and adiposity. Lipids. 2007;42(5):427-37.
9. Gillingham LG, Harris-Janz S, Jones PJ. Dietary monounsaturated fatty acids are protective against metabolic syndrome and cardiovascular disease risk factors. Lipids. 2011;46(3):209-28.
10. Kennedy A, Martinez K, Chuang CC, LaPoint K, McIntosh M. Saturated fatty acid-mediated inflammation and insulin resistance in adipose tissue: mechanisms of action and implications. J Nutr. 2009;139(1):1-4.
11. Oben JA, Mouralidarane A, Samuelsson AM, Matthews PJ, Morgan ML, McKee C, et al. Maternal obesity during pregnancy and lactation programs the development of offspring non-alcoholic fatty liver disease in mice. J Hepatol. 2010;52(6):913-20.
12. Samuelsson AM, Matthews PA, Argenton M, Christie MR, McConnell JM, Jansen EH, et al. Diet-induced obesity in female mice leads to offspring hyperphagia, adiposity, hypertension, and insulin resistance: a novel murine model of developmental programming. Hypertension. 2008;51(2):383-92.
13. Bruce KD, Cagampang FR, Argenton M, Zhang J, Ethirajan PL, Burdge GC, et al. Maternal high-fat feeding primes steatohepatitis in adult mice offspring, involving mitochondrial dysfunction and altered lipogenesis gene expression. Hepatology. 2009;50(6):1796-808.
14. Pileggi CA, Hedges CP, Segovia SA, Markworth JF, Durainayagam BR, Gray C, et al. Maternal High Fat Diet Alters Skeletal Muscle Mitochondrial Catalytic Activity in Adult Male Rat Offspring. Front Physiol. 2016;7:546.
15. Jorgensen W, Gam C, Andersen JL, Schjerling P, Scheibye-Knudsen M, Mortensen OH, et al. Changed mitochondrial function by pre- and/or postpartum diet alterations in sheep. Am J Physiol Endocrinol Metab. 2009;297(6):E1349-57.
16. Oosting A, Kegler D, Boehm G, Jansen HT, van de Heijning BJ, van der Beek EM. N-3 long-chain polyunsaturated fatty acids prevent excessive fat deposition in adulthood in a mouse model of postnatal nutritional programming. Pediatr Res. 2010;68(6):494-9.
17. Harder T, Bergmann R, Kallischnigg G, Plagemann A. Duration of breastfeeding and risk of overweight: a meta-analysis. Am J Epidemiol. 2005;162(5):397-403.

18. Owen CG, Martin RM, Whincup PH, Smith GD, Cook DG. Effect of infant feeding on the risk of obesity across the life course: a quantitative review of published evidence. Pediatrics. 2005;115(5):1367-77.
19. Gallier S, Gragson D, Jimenez-Flores R, Everett D. Using confocal laser scanning microscopy to probe the milk fat globule membrane and associated proteins. J Agric Food Chem. 2010;58(7):4250-7.
20. Michalski MC, Briard V, Michel F, Tasson F, Poulain P. Size distribution of fat globules in human colostrum, breast milk, and infant formula. J Dairy Sci. 2005;88(6):1927-40.
21. Gallier S, Vocking K, Post JA, Van De Heijning B, Acton D, Van Der Beek EM, et al. A novel infant milk formula concept: Mimicking the human milk fat globule structure. Colloids and surfaces B, Biointerfaces. 2015;136:329-39.
22. Oosting A, Kegler D, Wopereis HJ, Teller IC, van de Heijning BJ, Verkade HJ, et al. Size and phospholipid coating of lipid droplets in the diet of young mice modify body fat accumulation in adulthood. Pediatr Res. 2012;72(4):362-9.
23. Oosting A, van Vlies N, Kegler D, Schipper L, Abrahamse-Berkeveld M, Ringler S, et al. Effect of dietary lipid structure in early postnatal life on mouse adipose tissue development and function in adulthood. Br J Nutr. 2014;111(2):215-26.
24. Kodde A, van der Beek EM, Phielix E, Engels E, Schipper L, Oosting A. Supramolecular structure of dietary fat in early life modulates expression of markers for mitochondrial content and capacity in adipose tissue of adult mice. Nutr Metab (Lond). 2017;14:37.
25. Ronda O, van de Heijning BJM, Martini I, Gerding A, Wolters JC, van der Veen YT, et al. Effects of an early life diet containing large phospholipid-coated lipid globules on hepatic lipid metabolism in mice. Scientific reports. 2020;10(1):16128.
26. Reeves PG, Nielsen FH, Fahey GC, Jr. AIN-93 purified diets for laboratory rodents: final report of the American Institute of Nutrition ad hoc writing committee on the reformulation of the AIN-76A rodent diet. J Nutr. 1993;123(11):1939-51.
27. Nixon JP, Zhang M, Wang C, Kuskowski MA, Novak CM, Levine JA, et al. Evaluation of a quantitative magnetic resonance imaging system for whole body composition analysis in rodents. Obesity (Silver Spring). 2010;18(8):1652-9.
28. Pesta D, Gnaiger E. High-resolution respirometry: OXPHOS protocols for human cells and permeabilized fibers from small biopsies of human muscle. Methods Mol Biol. 2012;810:25-58.
29. Koliaki C, Szendroedi J, Kaul K, Jelenik T, Nowotny P, Jankowiak F, et al. Adaptation of hepatic mitochondrial function in humans with non-alcoholic fatty liver is lost in steatohepatitis. Cell Metab. 2015;21(5):739-46.
30. Doerrier C, Garcia-Souza LF, Krumschnabel G, Wohlfarter Y, Meszaros AT, Gnaiger E. High-Resolution FluoRespirometry and OXPHOS Protocols for Human Cells, Permeabilized Fibers from Small Biopsies of Muscle, and Isolated Mitochondria. Methods Mol Biol. 2018;1782:31-70.
31. Jelenik T, Flogel U, Alvarez-Hernandez E, Scheiber D, Zweck E, Ding Z, et al. Insulin Resistance and Vulnerability to Cardiac Ischemia. Diabetes. 2018;67(12):2695-702.
32. Preuss C, Jelenik T, Bodis K, Mussig K, Burkart V, Szendroedi J, et al. A New Targeted Lipidomics Approach Reveals Lipid Droplets in Liver, Muscle and Heart as a Repository for Diacylglycerol and Ceramide Species in Non-Alcoholic Fatty Liver. Cells. 2019;8(3).
33. Folch J, Lees M, Sloane Stanley GH. A simple method for the isolation and purification of total lipides from animal tissues. J Biol Chem. 1957;226(1):497-509.
34. Apostolopoulou M, Mastrototaro L, Hartwig S, Pesta D, Straßburger K, de Filippo E, et al. Metabolic responsiveness to training depends on insulin sensitivity and protein content of exosomes in insulin-resistant males. Science advances. 2021;7(41):eabi9551.
35. Livak KJ, Schmittgen TD. Analysis of relative gene expression data using real-time quantitative PCR and the 2(-Delta Delta C(T)) Method. Methods. 2001;25(4):402-8.

36. Haffner SM, Miettinen H, Stern MP. The homeostasis model in the San Antonio Heart Study. Diabetes Care. 1997;20(7):1087-92.
37. Tang Q, Li X, Song P, Xu L. Optimal cut-off values for the homeostasis model assessment of insulin resistance (HOMA-IR) and pre-diabetes screening: Developments in research and prospects for the future. Drug Discov Ther. 2015;9(6):380-5.
38. Cannon B, Nedergaard J. Nonshivering thermogenesis and its adequate measurement in metabolic studies. J Exp Biol. 2011;214(Pt 2):242-53.
39. Wang Z, Ying Z, Bosy-Westphal A, Zhang J, Heller M, Later W, et al. Evaluation of specific metabolic rates of major organs and tissues: comparison between nonobese and obese women. Obesity (Silver Spring). 2012;20(1):95-100.
40. Mingrone G, Manco M, Mora ME, Guidone C, Iaconelli A, Gniuli D, et al. Influence of maternal obesity on insulin sensitivity and secretion in offspring. Diabetes Care. 2008;31(9):1872-6.
41. Modi N, Murgasova D, Ruager-Martin R, Thomas EL, Hyde MJ, Gale C, et al. The influence of maternal body mass index on infant adiposity and hepatic lipid content. Pediatr Res. 2011;70(3):287-91.
42. Nobili V, Bedogni G, Alisi A, Pietrobattista A, Alterio A, Tiribelli C, et al. A protective effect of breastfeeding on the progression of non-alcoholic fatty liver disease. Arch Dis Child. 2009;94(10):801-5.
43. Liu J, Yu B, Mao X, He J, Yu J, Zheng P, et al. Effects of intrauterine growth retardation and maternal folic acid supplementation on hepatic mitochondrial function and gene expression in piglets. Arch Anim Nutr. 2012;66(5):357-71.
44. Borengasser SJ, Lau F, Kang P, Blackburn ML, Ronis MJ, Badger TM, et al. Maternal obesity during gestation impairs fatty acid oxidation and mitochondrial SIRT3 expression in rat offspring at weaning. PLoS One. 2011;6(8):e24068.
45. Sheldon RD, Meers GM, Morris EM, Linden MA, Cunningham RP, Ibdah JA, et al. eNOS deletion impairs mitochondrial quality control and exacerbates Western diet-induced NASH. Am J Physiol Endocrinol Metab. 2019;317(4):E605-e16.
46. Yao CH, Wang R, Wang Y, Kung CP, Weber JD, Patti GJ. Mitochondrial fusion supports increased oxidative phosphorylation during cell proliferation. eLife. 2019;8.
47. Galloway CA, Lee H, Brookes PS, Yoon Y. Decreasing mitochondrial fission alleviates hepatic steatosis in a murine model of nonalcoholic fatty liver disease. American journal of physiology Gastrointestinal and liver physiology. 2014;307(6):G632-G41.
48. Wang L, Ishihara T, Ibayashi Y, Tatsushima K, Setoyama D, Hanada Y, et al. Disruption of mitochondrial fission in the liver protects mice from diet-induced obesity and metabolic deterioration. Diabetologia. 2015;58(10):2371-80.
49. Wang Y, Wang X, Long Q, Liu Y, Yin T, Sirota I, et al. Reducing embryonic mtDNA copy number alters epigenetic profile of key hepatic lipolytic genes and causes abnormal lipid accumulation in adult mice. The FEBS journal. 2021;288(23):6828-43.
50. Gallier S, Vocking K, Post JA, Van De Heijning B, Acton D, Van Der Beek EM, et al. A novel infant milk formula concept: Mimicking the human milk fat globule structure. Colloids and Surfaces B: Biointerfaces. 2015;136:329-39.
51. Baumgartner S, van de Heijning BJM, Acton D, Mensink RP. Infant milk fat droplet size and coating affect postprandial responses in healthy adult men: a proof-of-concept study. Eur J Clin Nutr. 2017;71(9):1108-13.
52. Sarabhai T, Koliaki C, Mastrototaro L, Kahl S, Pesta D, Apostolopoulou M, et al. Dietary palmitate and oleate differently modulate insulin sensitivity in human skeletal muscle. Diabetologia. 2021.
53. Lettner A, Roden M. Ectopic fat and insulin resistance. Curr Diab Rep. 2008;8(3):185-91.
54. Koliaki C, Roden M. Alterations of Mitochondrial Function and Insulin Sensitivity in Human Obesity and Diabetes Mellitus. Annu Rev Nutr. 2016;36:337-67.

55. Lyu K, Zhang Y, Zhang D, Kahn M, Ter Horst KW, Rodrigues MRS, et al. A Membrane-Bound Diacylglycerol Species Induces PKCε-Mediated Hepatic Insulin Resistance. Cell Metab. 2020;32(4):654-64.e5.
56. Cantley JL, Yoshimura T, Camporez JP, Zhang D, Jornayvaz FR, Kumashiro N, et al. CGI-58 knockdown sequesters diacylglycerols in lipid droplets/ER-preventing diacylglycerol-mediated hepatic insulin resistance. Proc Natl Acad Sci U S A. 2013;110(5):1869-74.
57. Perreault L, Newsom SA, Strauss A, Kerege A, Kahn DE, Harrison KA, et al. Intracellular localization of diacylglycerols and sphingolipids influences insulin sensitivity and mitochondrial function in human skeletal muscle. JCI Insight. 2018;3(3).
58. Gancheva S, Ouni M, Jelenik T, Koliaki C, Szendroedi J, Toledo FGS, et al. Dynamic changes of muscle insulin sensitivity after metabolic surgery. Nat Commun. 2019;10(1):4179.
59. Ahrens M, Ammerpohl O, von Schonfels W, Kolarova J, Bens S, Itzel T, et al. DNA methylation analysis in nonalcoholic fatty liver disease suggests distinct disease-specific and remodeling signatures after bariatric surgery. Cell Metab. 2013;18(2):296-302.
60. Ye C, Sutter BM, Wang Y, Kuang Z, Tu BP. A Metabolic Function for Phospholipid and Histone Methylation. Mol Cell. 2017;66(2):180-93 e8.
61. Zalewska A, Maciejczyk M, Szulimowska J, Imierska M, Błachnio-Zabielska A. High-Fat Diet Affects Ceramide Content, Disturbs Mitochondrial Redox Balance, and Induces Apoptosis in the Submandibular Glands of Mice. Biomolecules. 2019;9(12):877.
62. Kasumov T, Li L, Li M, Gulshan K, Kirwan JP, Liu X, et al. Ceramide as a mediator of non-alcoholic Fatty liver disease and associated atherosclerosis. PloS one. 2015;10(5):e0126910.
63. He X, Parenti M, Grip T, Domellof M, Lonnerdal B, Hernell O, et al. Metabolic phenotype of breast-fed infants, and infants fed standard formula or bovine MFGM supplemented formula: a randomized controlled trial. Scientific reports. 2019;9(1):339.
64. Kodde A, Mischke M, Rakhshandehroo M, Voggel J, Fink G, Nusken E, et al. The effect of dietary lipid quality in early life on serum LysoPC(18:2) levels and their association with adult blood glucose levels in intrauterine growth restricted rats. Nutr Metab (Lond). 2021;18(1):101.
65. Jung SH, Jung CH, Reaven GM, Kim SH. Adapting to insulin resistance in obesity: role of insulin secretion and clearance. Diabetologia. 2018;61(3):681-7.
66. Utzschneider KM, Kahn SE, Polidori DC. Hepatic Insulin Extraction in NAFLD Is Related to Insulin Resistance Rather Than Liver Fat Content. The Journal of clinical endocrinology and metabolism. 2019;104(5):1855-65.
67. Foley KP, Zlitni S, Duggan BM, Barra NG, Anhê FF, Cavallari JF, et al. Gut microbiota impairs insulin clearance in obese mice. Molecular Metabolism. 2020;42:101067.
68. Van Cauter E, Mestrez F, Sturis J, Polonsky KS. Estimation of insulin secretion rates from C-peptide levels. Comparison of individual and standard kinetic parameters for C-peptide clearance. Diabetes. 1992;41(3):368-77.
69. Lebowitz MR, Blumenthal SA. The molar ratio of insulin to C-peptide. An aid to the diagnosis of hypoglycemia due to surreptitious (or inadvertent) insulin administration. Arch Intern Med. 1993;153(5):650-5.
70. Baars A, Oosting A, Engels E, Kegler D, Kodde A, Schipper L, et al. Milk fat globule membrane coating of large lipid droplets in the diet of young mice prevents body fat accumulation in adulthood. Br J Nutr. 2016;115(11):1930-7.
71. Sarabhai T, Kahl S, Szendroedi J, Markgraf DF, Zaharia OP, Barosa C, et al. Monounsaturated fat rapidly induces hepatic gluconeogenesis and whole-body insulin resistance. JCI Insight. 2020;5(10).
72. Kupriyanova Y, Zaharia OP, Bobrov P, Karusheva Y, Burkart V, Szendroedi J, et al. Early changes in hepatic energy metabolism and lipid content in recent-onset type 1 and 2 diabetes mellitus. Journal of hepatology. 2021;74(5):1028-37.

73. Schmid AI, Szendroedi J, Chmelik M, Krssak M, Moser E, Roden M. Liver ATP synthesis is lower and relates to insulin sensitivity in patients with type 2 diabetes. Diabetes Care. 2011;34(2):448-53.
74. Philippaert K, Roden M, Lisak D, Bueno D, Jelenik T, Radyushkin K, et al. Bax inhibitor-1 deficiency leads to obesity by increasing Ca(2+)-dependent insulin secretion. J Mol Med (Berl). 2020;98(6):849-62.

Supplementary Material

Supplementary methods:

Breeding protocol and weaning:

Two days before the start of mating, bedding of male breeders was transferred into cages of the female breeders to let females getting acquainted to the scent of the males and synchronizes the oestrus cycle which will improve breeding results. On breeding day 0, female breeders were introduced into cages with male breeders (1:1). After three days of mating, males were sacrificed and females housed in pairs. When visible pregnant (around day 14 of pregnancy) females where housed individually and were visually examined twice a day around the day litters were expected (day 19-23 of pregnancy). The day when litters were born was marked as postnatal day 0 (PN0). On PN2, litter size and sex were determined by shortly separating the dams in their home cage while pups were kept on a heated pad. Litters (ideally born on a same day) were culled to 4:2 males:females (ratio 3:3 with 2:4 also acceptable when not enough males were available) which were weighted and randomly assigned to a dam. On PN16, the dietary intervention (CTRL vs Concept diets) started and fresh dough balls prepared 3 times a week (Mo, We and Fri). At weaning (PN21), males were weighed and caged in pairs (or 3 with odd group sizes), while dams and female offspring was sacrificed. Nesting material from mother's cage were added to the cage of the weaned males to reduce stress and diets were continued until PN42 (CTRL or Concept).

Further details of animal experiment:

Age of breeders at arrival: 9 weeks of age

Acclimatization protocol: After arrival from the breeder animals were acclimated 1 week on grain-based chow (Envigo, Teklad Global 2018S) and subsequently for 2 weeks on AIN before mating.

Diet of the breeders: AIN93G

Cages: Macrolon type 3 cages, floor area 800 cm2, height 150 mm

Housing conditions: Conventional

Bedding material: poplar, 3-6 mm (Altromin Spezialfutter GmbH & Co. KG, Germany)

Nesting material: hemp fibers (Altromin Spezialfutter GmbH & Co. KG, Germany)

Cage enrichment: wooden blocks for gnawing (Sniff-Spezialdiäten, Germany) and 1 red polycarbonate shelter house (Techniplast Deutschland GmbH, Germany)

Blinding: the study was not blinded

Randomization: the study was not randomized other than that pups were randomized at PN2 as described above and groups per cohort divided over different dietary groups. At the day of the measurements animals of the groups were randomly taken for the measurements in a way to reduce time effects per group.

Exclusion criteria: According to animal welfare regulation animals were scored on bodyweight (body weight loss), general health status (fur, cramps, muscle tone, eyes) and social behavior and excluded when a set threshold value was reached. No animals were excluded in this study.

Method of euthanasia: Breeders and female offspring were euthanized under Isoflurane anaesthesia (5% by volume in a gas mixture of 30% oxygen, 0.4 /min) by cervical dislocation. Male offspring sacrificed at PN42 and PN98 were anaesthetized with Isoflurane, 5% by volume in a gas mixture of 30% oxygen (0.4 /min) and euthanized by cervical incision and cervical dislocation.

Marking of the animals: Ear holes by ear punch device. Mice had either no, one left, one right or left and right ear holes.

Range of dissection: PN42: range of 1 week. PN98: range of 1,5 week. 2-3 animals per day were sacrificed due to limited capacity of respiratory measurements.

Sample calculation: Two-sided power calculations were performed prior to the start of the study, based on indirect calorimetry analyses as the main parameter performed at DDZ with C57BL/6 mice using the online computer program www.statisticalsolutions.net. Considering these data, and assuming a standard deviation of the respiratory coefficient of 18% and an effect size of 15% change of the respiratory coefficient after feeding with WSD, including 12 animals per group would be sufficient to detect differences. In total, 73 animals were investigated (1 animal more than calculated for reasons that are explained in the Materials & Methods section of the main manuscript). Individual offspring animals were taken as the experimental unit.

Primary outcome: mitochondrial respiration as assessed by Oxygraph and body composition.

Secondary outcome: glucose, insulin levels and organ weights

Exploratory outcome: H_2O_2 emission, TBARS, NEFA, liver TG levels and diacylglycerol and ceramide levels in liver tissue

Supplementary Tables

Supplemental Table 1: Organ weight of CTRL and Concept animals at PN42

Weight (g)	CTRL	Concept
Liver	1.068 ± 0.057	1.160 ± 0.052
White adipose tissue		
Epididymal	0.458 ± 0.029	0.415 ± 0.036
Inguinal	0.240 ± 0.014	0.206 ± 0.024
Retroperitoneal	0.105 ± 0.008	0.091 ± 0.013
Muscle		
Gastrocnemius	0.246 ± 0.008	0.242 ± 0.012
Quadriceps	0.284 ± 0.015	0.294 ± 0.017
Brown adipose tissue	0.111 ± 0.008	0.099 ± 0.008
Heart	0.150 ± 0.006	0.150 ± 0.004
Kidney	0.355 ± 0.009	0.357 ± 0.009

CTRL: control. CTRL: n=13; Concept: n=10.

Supplemental Table 2: Organ weight of animals at PN98

Weight (g)	CTRL/AIN	CTRL/WSD	Concept/AIN	Concept/WSD	WSD effect	Concept effect
White adipose tissue						
Epididymal	996.0 ± 143.1	1661.9 ± 98.0	939.7 ± 113.7	1787.3 ± 135.6	p<0.001	p=0.937
Inguinal	388.3 ± 78.9	847.1 ± 112.4	371.9 ± 62.6	700.8 ± 70.9	p<0.001	p=0.338
Retroperitoneal	250.7 ± 39.7	536.4 ± 23.9	268.6 ± 32.4	476.6 ± 35.8	p<0.001	p=0.547
Muscle						
Gastrocnemius	258.0 ± 11.4	283.8 ± 9.0	272.6 ± 11.8	280.7 ± 10.8	p=0.132	p=0.607
Quadriceps	328.1 ± 11.5	347.7 ± 9.9	345.4 ± 9.2	340.7 ± 9.8	p=0.473	p=0.618
Brown adipose tissue	156.8 ± 22.8	250.4 ± 27.2	144.3 ± 20.5	220.9 ± 24.3	p<0.01	p=0.400
Heart	142.4 ± 4.3	150.6 ± 4.6	140.9 ± 4.6	155.3 ± 5.1	p<0.05	p=0.741
Kidney	328.7 ± 13.2	357.7 ± 10.5	331.7 ± 10.8	382.2 ± 11.6	p<0.05	p=0.249

AIN: American institute of nutrition diet; CTRL: control; WSD: Western style diet. Effects of the respective early (CTRL vs. Concept) and adult (AIN vs. WSD) diets were tested with two-way ANOVA and results shown in the last columns. CTRL/AIN: n=10; CTRL/WSD: n=12; Concept/AIN: n=12; Concept/WSD: n=16.

Supplementary Table 3: Pearson correlations between lean body mass and hepatic mitochondrial respiration linked to β-oxidation in CTRL and Concept animals at PN98.

	CTRL		Concept	
	r	***P***	***r***	***p***
Malate	0.490	0.024	-0.175	0.372
Octanoyl-carnitine	0.436	0.048	-0.137	0.485
ADP	0.113	0.625	-0.183	0.351
Cytochrome c	0.122	0.598	-0.168	0.391
Oligomycin	0.476	0.029	-0.159	0.419
FCCP	0.156	0.500	-0.158	0.421
Antimycin	0.453	0.040	0.092	0.643

CTRL: control; FCCP: carbonyl cyanide-p-trifluoromethoxyphenylhydrazone. Correlations with p<0.05 are in bold. CTRL: n= 21; Concept: n= 28.

Supplementary Table 4: Pearson correlations between lean body mass and hepatic mitochondrial respiration linked to β-oxidation in AIN and WSD animals at PN98.

	AIN		WSD	
	r	***p***	***r***	***p***
Malate	0.320	0.147	-0.285	0.142
Octanoyl- carnitine	0.159	0.490	-0.314	0.104
ADP	0.012	0.957	-0.548	0.003
Cytochrome c	-0.019	0.936	-0.523	0.004
Oligomycin	0.112	0.630	-0.251	0.199
FCCP	-0.018	0.938	-0.403	0.034
Antimycin	0.376	0.093	0.101	0.608

AIN: AIN93M; WSD: Western style diet; FCCP: carbonyl cyanide-p-trifluoromethoxyphenylhydraz one. Correlations with p<0.05 are in bold. AIN: n= 21; WSD: n= 28.

Supplementary Figures

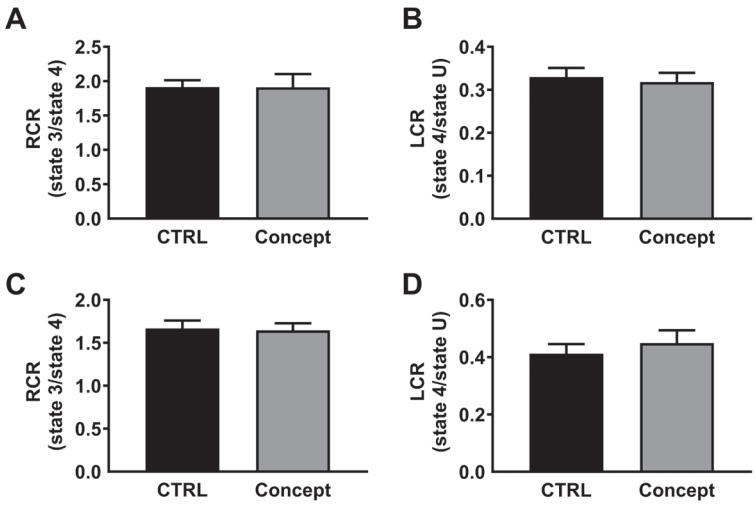

Supplementary Figure 1: Direct effects of postnatal Concept feeding on RCR and LCR. Mitochondrial RCR and LCR were measured on PN42 with substrates supporting TCA cycle (**A, B**) and β-oxidation (**C-D**). Data shown as mean±SEM, CTRL: n=13; Concept: n=10. Unpaired t-test. CTRL: control; LCR: leak control ratio; RCR: respiratory control ratio; TCA: tricarboxylic acid.

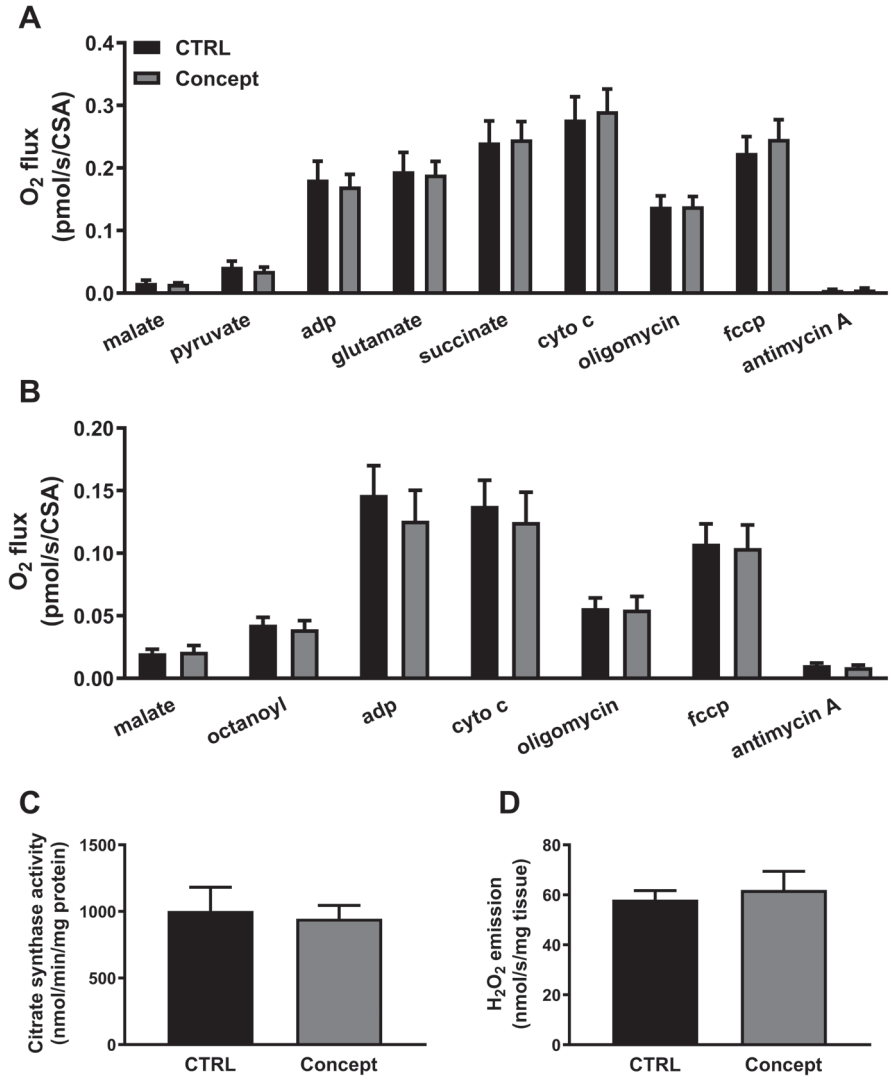

Supplementary Figure 2: Direct effects of the Concept diet on mitochondrial function of the skeletal muscle**.** Mitochondrial respiration [O_2 flux normalized to CSA] was measured with substrates supporting TCA cycle (**A**) and β-oxidation (**B**). Mitochondrial density (**C**) was assessed by CSA normalized to protein content. Oxidative stress (**D**) was measured as the rate of malate-stimulated H_2O_2 emission. Data are shown as mean±SEM, CTRL: n=13; Concept: n=10. Multiple t-test (A, B) or unpaired t-test (C,D); *p<0.05. CSA: citrate synthase activity, CTRL: control; cyto C: cytochrome c; fccp: carbonyl cyanide-p-trifluoromethoxyphenylhydrazone; TCA: tricarboxylic acid.

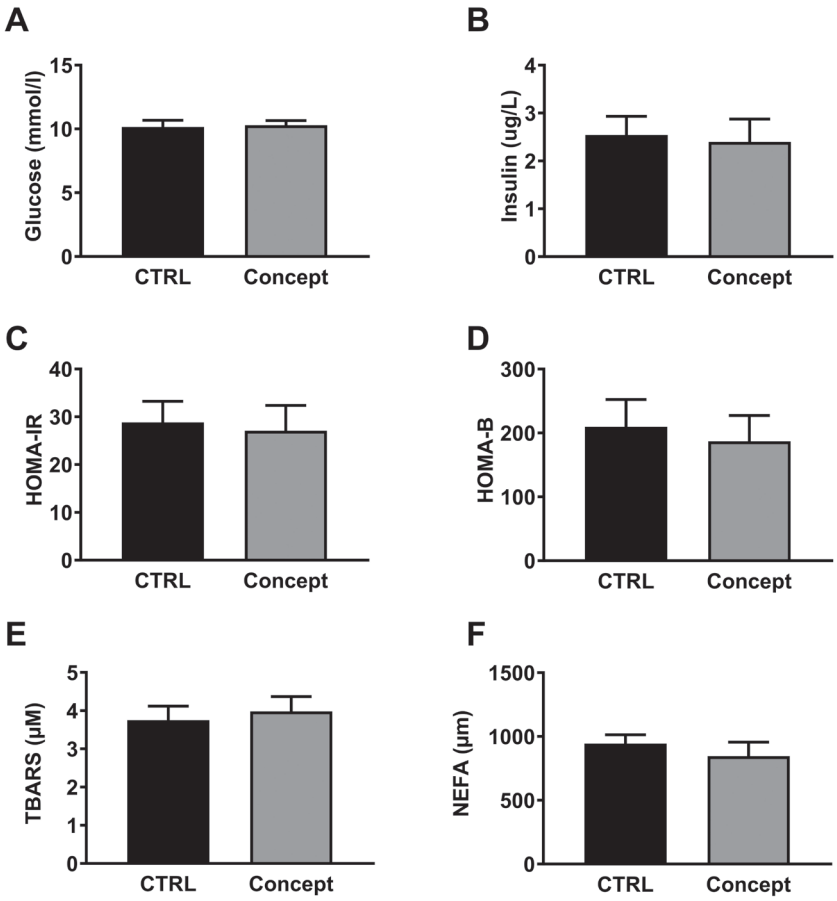

Supplementary Figure 3: Direct effects of postnatal Concept feeding on plasma parameters. Fasted (3 h) plasma glucose (**A**), insulin (**B**), HOMA-IR (**C**), HOMA-B (**D**), TBARS (**E**) and NEFA (**F**) were assessed on PN42. Data shown as mean±SEM, CTRL: n=13 except for TBARS and NEFA with n=12; Concept: n=10 except for TBARS with n=9. Unpaired t-test. CTRL: control; NEFA: non-essential fatty acids; TBARS: thiobarbituric acid reactive substances**.**

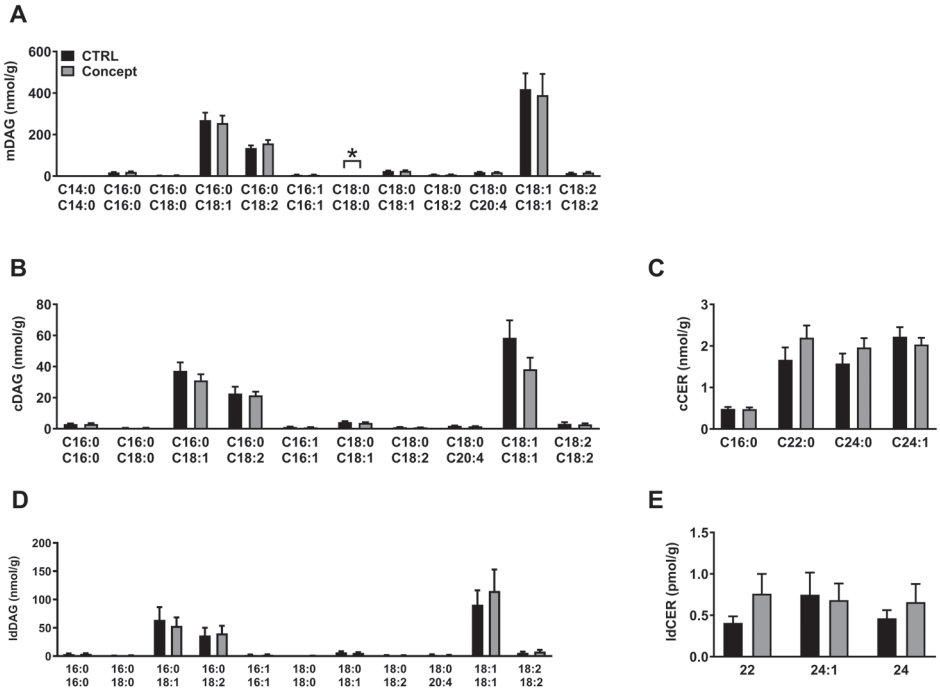

Supplementary Figure 4: Direct effects of postnatal Concept feeding on hepatic lipid species. mDAG (**A**), cDAG (**B**), cCER (**C**), ldDAG (**D**) and ldCER (**E**) levels assessed on PN42. Data shown as mean±SEM, CTRL: n=12; Concept: n=10. Unpaired t-test. *p<0.05. cCER: ceramides in cytoplasm; cDAG: diacylglycerols in cytoplasm; CTRL: control; ldCER: ceramides in lipid droplets; ldDAG: diacylglycerols in lipid droplets; mCER: ceramides in membranes; mDAG: diacylglycerols in membranes.

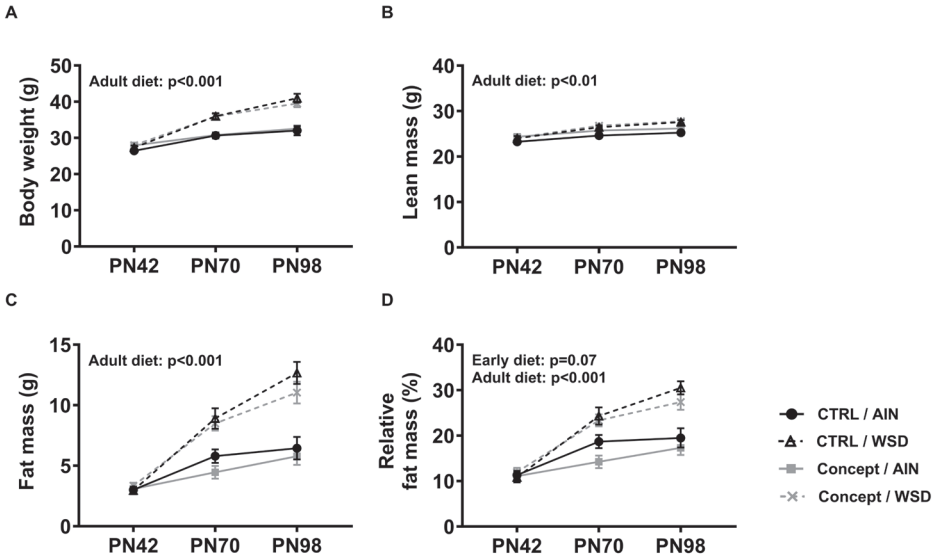

Supplementary Figure 5: Long-term effects of postnatal Concept feeding on body weight and body composition. Development of body weight (**A**), lean mass (**B**), fat mass (**C**) and relative fat mass (**D**, % of body weight) from PN42 to PN98. CTRL/AIN: n=10; CTRL/WSD: n=12; Concept/AIN: n=12; Concept/WSD: n=16. Repeated measures ANOVA with two factors (early and adult diet) was used and in case of found interaction between factors, separate factors were tested. AIN: American institute of nutrition diet; CTRL: control; PN: postnatal day; WSD: western style diet.

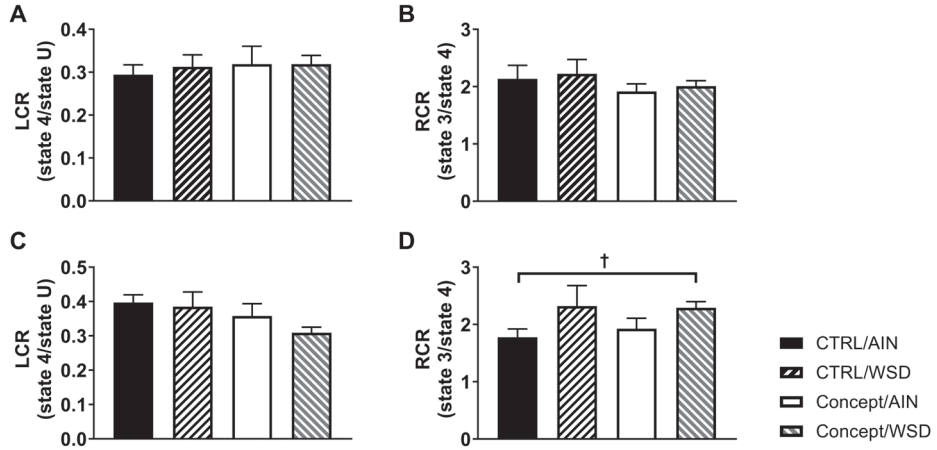

Supplementary Figure 6: Long-term effects of postnatal Concept feeding on RCR and LCR. Mitochondrial RCR and LCR were measured on PN98 with substrates supporting TCA cycle (**A, B**) and β-oxidation (**C-D**). Data shown as mean±SEM; CTRL/AIN: n=10; CTRL/WSD: n=12; Concept/AIN: n=12; Concept/WSD: n=16. Data were tested with two-way ANOVA. †p<0.05 overall WSD effect. AIN: American institute of nutrition diet; CTRL: control; LCR: leak control ratio; RCR: respiratory control ratio; TCA: tricarboxylic acid; WSD: western style diet.

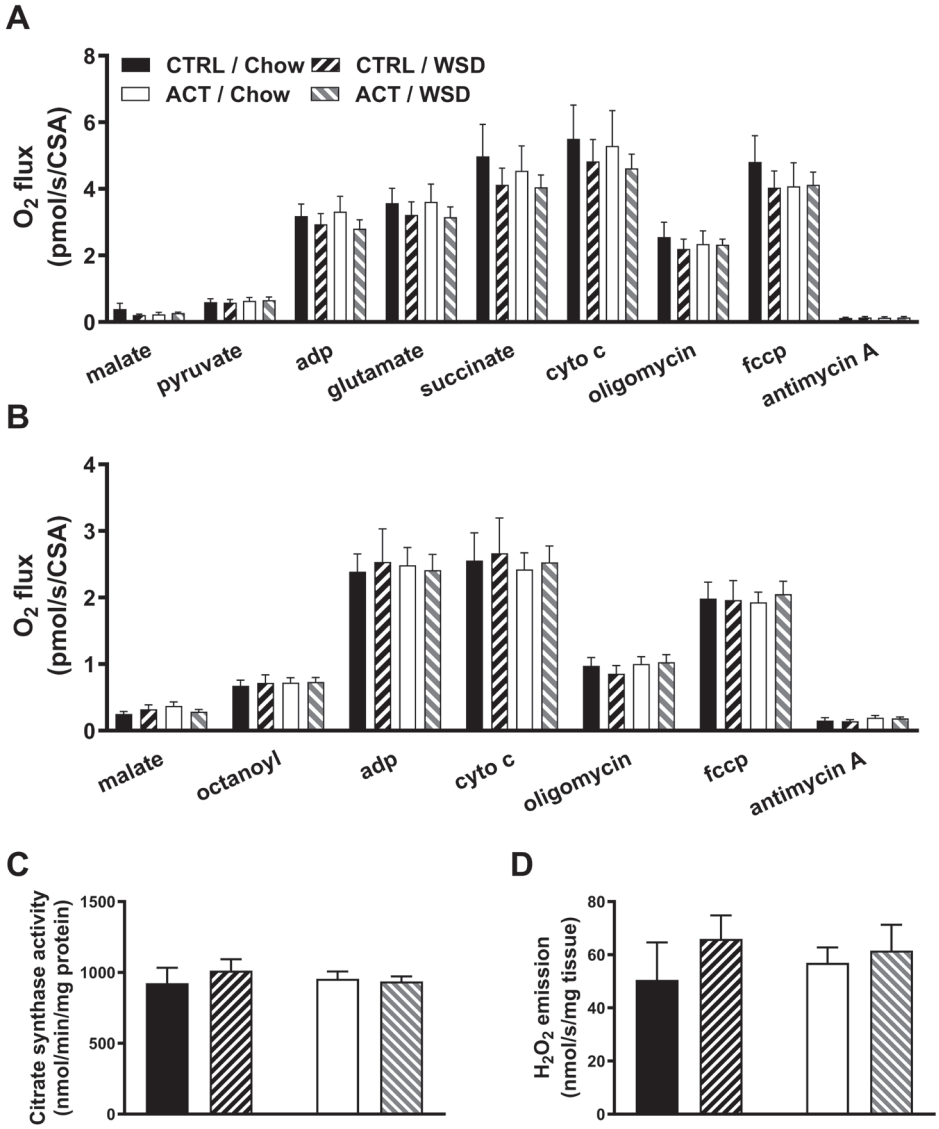

Supplementary Figure 7: Long-term effects of postnatal Concept feeding on mitochondrial function in skeletal muscle. Mitochondrial respiration [O_2 flux normalized to citrate synthase activity (CSA)] was measured with substrates supporting TCA cycle (**A**) and β-oxidation (**B**). Mitochondrial density (**C**) was assessed by CSA activity normalized to protein content. Oxidative stress (**D**) was measured as the rate of malate-stimulated H_2O_2 emission. Data are shown as mean±SEM, CTRL/AIN: n=10; CTRL/WSD: n=12; Concept/AIN: n=12; Concept/WSD: n=16. Two-way ANOVA. AIN: American Institute of Nutrition rodent diet; CSA: citrate synthase activity, CTRL: control; cyto c: cytochrome c; fccp: carbonyl cyanide-p-trifluoromethoxyphenylhydrazone; TCA: tricarboxylic acid; WSD: western style diet.

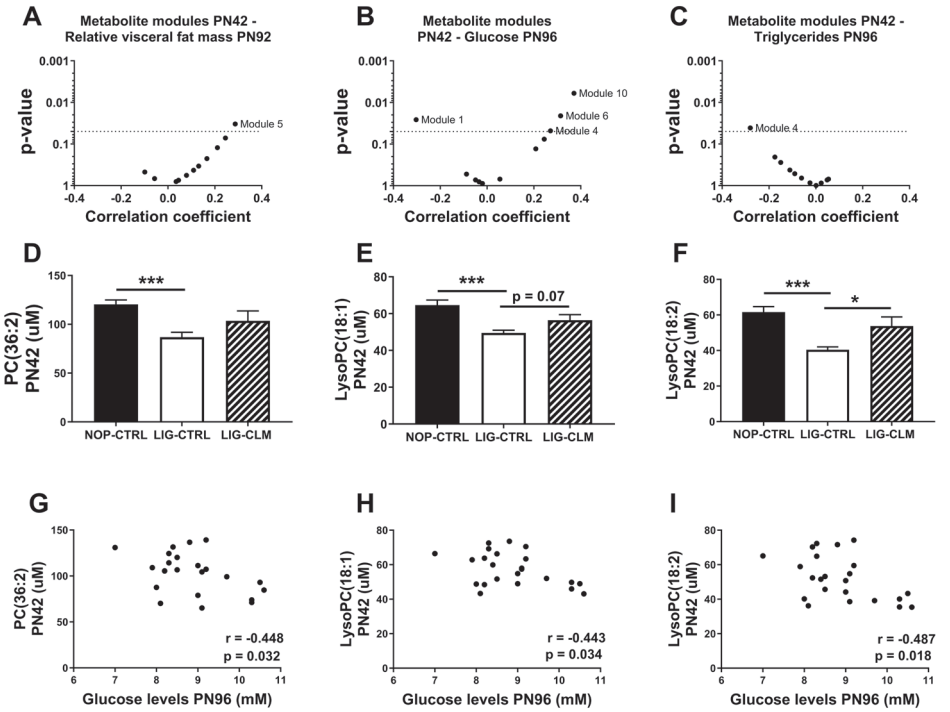

Supplementary Figure 8: Long-term effects of postnatal Concept feeding of differences between PN42 and PN98 on liver-specific markers of mitochondrial biogenesis and dynamics. PGC-1α (**A**), TFAM (**B**), MFN1 (**C**), MFN2 (**D**), DRP1 (**E**) and pDRP1/DRP1 (**F**). Data are shown as mean±SEM, two-way ANOVA; CTRL/AIN: n=10; CTRL/WSD: n=12; Concept/AIN: n=12; Concept/WSD: n=14. PGC-1α: peroxisome proliferator-activated receptor gamma coactivator 1-α; TFAM: mitochondrial transcription factor A; MFN1 or 2: mitofusion protein 1 or 2; DRP1: dynamin-related protein 1, VDAC: voltage-dependent anion channel.

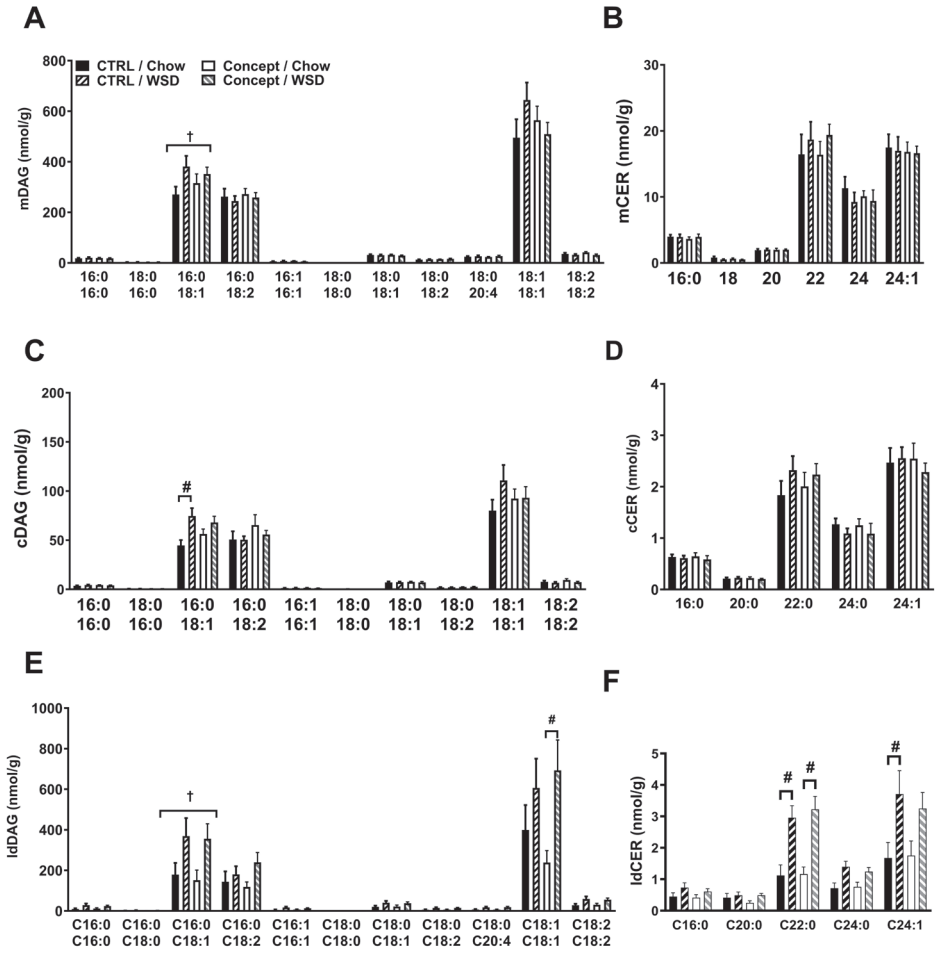

Supplementary Figure 9: Long-term effects of postnatal Concept feeding on hepatic lipid species. mDAG (**A**), mCER (**B**), cDAG (**C**), cCER (**D**), ldDAG (**E**) and ldCER (**F**) levels assessed on PN98. Data shown as mean±SEM, CTRL/AIN: n=10; CTRL/WSD: n=12; Concept/AIN: n=12; Concept/WSD: n=14. Two-way ANOVA; †p<0.05 overall WSD effect; #p<0.05 WSD effect in groups fed the same early-life diet. AIN: American institute of nutrition diet; cCER: ceramides in cytoplasm; cDAG: diacylglycerols in cytoplasm; CTRL: control; ldCER: ceramides in lipid droplets; ldDAG: diacylglycerols in lipid droplets; mCER: ceramides in membranes; mDAG: diacylglycerols in membranes; WSD: western style diet.

[1]Danone Nutricia Research, Utrecht, The Netherlands; [2]Department of Pediatrics and Adolescent Medicine, Medical Faculty, University Hospital Cologne, University of Cologne, Cologne, Germany; [3]Department of Pediatrics and Adolescent Medicine, University Hospital Erlangen, Erlangen, Germany; [4]Department of Pediatrics, University Medical Centre Groningen, University of Groningen, Groningen, The Netherlands

Chapter 6

The effect of dietary lipid quality in early life on serum LysoPC(18:2) levels and their association with adult blood glucose levels in intrauterine growth restricted rats

Andrea Kodde[1], Mona Mischke[1], Maryam Rakhshandehroo[1], Jenny Voggel[2], Gregor Fink[2], Eva Nüsken[2], Manfred Rauh[3], Eline M. van der Beek[4], Jörg Dötsch[2] and Kai-Dietrich Nüsken[2]

Nutrition & Metabolism, 2021, 18(1):101
DOI: 10.1186/s12986-021-00614-8

Abstract

Being born small-for-gestational-age, especially with subsequent catch-up growth, is associated with impaired metabolic health in later-life. We previously showed that a postnatal diet with an adapted lipid droplet structure can ameliorate some of the adverse metabolic consequences in intrauterine growth-restricted (IUGR) rats. The aim of the present work was to explore possible underlying mechanism(s) and potential biomarkers. To this end, serum metabolomics was performed in postnatal day (PN) 42 and PN96 samples of the above-mentioned rat offspring, born after uterine vasculature ligation. Blood samples were collected at PN42, directly after a postnatal dietary intervention with either complex lipid matrix (CLM) or control (CTRL) diet, and at PN96 after a subsequent western-style diet (WSD). Offspring of Non-operated (NOP) dams fed CTRL in early life were included as control group. In the PN42 metabolomics data, 11 co-abundance modules of metabolites were identified, of which four were significantly correlated to adult blood glucose levels at PN96. Further analyses showed that Lysophosphatidylcholine(18:2) (LysoPC(18:2)) levels were reduced by ligation ($p<0.01$) and restored in CLM fed animals ($p<0.05$). LysoPC(18:2) levels at PN42 correlated inversely with adult blood glucose levels. These data indicate that early-life LysoPC(18:2) blood levels may predict adult blood glucose levels and are affected by a postnatal diet with an adapted lipid droplet structure in IUGR offspring.

Keywords: Metabolomics, Lysophosphatidylcholine, Intrauterine growth restriction, Postnatal diet, Blood glucose, Diabetes susceptibility, Milk fat globule membrane

Introduction

The early-life environment is essentially linked to adult metabolic health and obesity risk, and potential underlying mechanisms are manifold (1). Low birth weight, specifically when followed by subsequent catch-up growth, is associated with increased risk for later-life obesity and impaired glucose tolerance (2–4). Intrauterine growth-restriction (IUGR) is a major cause of low birth weight (5). In line with this, rat offspring born after IUGR have a lower birthweight, accelerated postnatal growth, increased adiposity, and impaired glucose tolerance in adulthood (6). Nutritional interventions starting in early-life, before the onset of an adverse phenotype, may reduce the risk for later-life obesity and impaired glucose tolerance. Indeed, exposure in postnatal life to a diet with a so-called complex lipid matrix (CLM, Nuturis®), i.e. comprising large, (milk) phospholipid coated lipid droplets, has been shown to ameliorate some of the adverse metabolic consequences of IUGR, such as relative visceral adiposity, high blood glucose and triglyceride levels (7). The CLM is inspired by the architecture of human milk lipid droplets, which are larger compared to those in regular infant milk formula (IMF) and enveloped by a milk fat globule membrane (MFGM) (8).

Part of the beneficial effect of the CLM may be explained by differences in tissue fat handling and postprandial kinetics, as indicated by earlier experiments in healthy mice and men (9, 10). The aim of the present work was to further explore potential mechanisms and identify biomarkers underlying the beneficial effects of postnatal exposure to CLM on adult visceral adiposity, blood glucose and triglyceride levels in IUGR rats (7). We hypothesized that differences in adult adiposity, blood glucose and triglyceride levels might arise from or could be predicted by differences in metabolites directly after exposure to the CLM. Therefore, serum metabolites were analyzed, and comprehensive data analysis was performed on collected data.

Methods

Study design

Samples and data used for this study were collected as part of a larger study, of which the phenotypic and physiological data were published previously, including a detailed description of the complete animal study design (7). The design of the three groups, which were the focus of the present study was as follows, IUGR was induced by bilateral ligation (LIG) of uterine arteries and veins in pregnant Wistar HAN rats (Charles River Wiga Deutschland GmbH). Offspring of non-operated (NOP) dams was included as control group. All pups were nursed by NOP dams, which were fed American Institute

of Nutrition-93Growth (AIN-93G) diet until PN15 and then either the control (CTRL) or CLM diet until litters were weaned at PN21 (**Figure 1**). Weaned males continued their diet until PN42, followed by a Western-style diet (WSD) challenge (39 en% fat) until PN96. The resulting experimental groups which were the focus of this study were, NOP-CTRL (n=9), LIG-CTRL (n=7) and LIG-CLM (n=8). The early diets (PN15-42) contained 28.3% (w/w) CTRL or CLM infant formula powder and were provided as dough balls in the home cage as described before (7, 8); for dietary composition see **Supplementary Table 1**. The CLM diet contained large lipid droplets coated with milk-phospholipids (8).

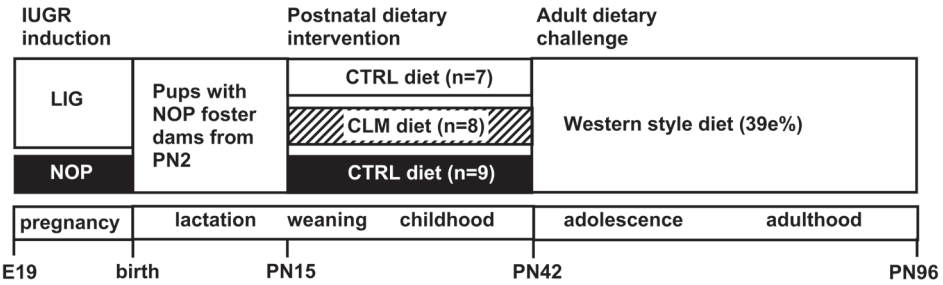

Figure 1: Study design. The group size was dependent on the available blood samples which was afected by the small amounts of the blood samples. The reported group size only included the animals of which all data was available. IUGR: intra-uterine growth restriction, LIG: ligated group, NOP: non-operated group, PN: postnatal day, E: embryonic day.

Physiological parameters

Whole blood was collected after an overnight fast at PN42 and PN96. Blood glucose levels were assessed using ABL 800 FLEX (Radiometer GmbH, Willich, Germany), serum triglyceride levels determined by routine clinical laboratory procedure, and visceral adiposity at PN92 by means of micro-computerized tomography (μCT, LaTeta LCT-100; Aloka Co. LTD., Tokyo, Japan), as described (7).

Metabolomics analyses

PN42 and PN96 serum metabolite profiles were determined with tandem mass spectrometry using a Metabolomics AbsoluteIDQ® p180 96 AB Sciex Edition Kit (Biocrates, Innsbruck, Austria) as described (11). Results below limit of detection (LOD) were set at LOD/2, results below lower limit of quantification (LLOQ) were set at (LOD+LLOQ)/2, results above upper limit of quantification (ULOQ) were set to ULOQ. Raw data are reported in the online data table **Additional file 2**.

Data analyses

Metabolites with>50% missing values or zero within-group variance for all groups were excluded. On the resulting metabolomics data set, weighted correlation network analysis (WGCNA) was performed for data reduction, leading to co-abundance modules of highly correlated metabolites (EdgeLeap B.V., Utrecht, The Netherlands, Additional file 1 for more details). Data of all experimental groups was used for the WGCNA analyses, including the groups which were not the focus of our research question (see **Supplementary Figure 1A** for details of all experimental groups). For each module an 'Eigenprofile' was calculated, representing overall abundance of the metabolites of the module. Biweight midcorrelations were calculated between 'Eigenprofiles' of the modules and physiological parameters at PN96 (PN92 for visceral adiposity). All analyses were performed in R 3.2.2 (2015-08-14) using the WGCNA package 1.46.

Statistics

Statistical differences between the focus groups were analyzed with GraphPad Prism 7.03 (GraphPad Software. Inc, San Diego, US), using unpaired t-tests for each comparison (NOP-CTRL vs. LIG-CTRL and LIG-CTRL vs. LIG-CLM). Gaussian distribution was tested with the Kolmogorov–Smirnov test. Pearson's correlations were calculated between individual metabolites and physiological outcomes. Sample size calculations were designed to detect differences in plasma glucose, triglyceride levels as well as differences in body composition in the larger study (7) and was set to at least n=8 per group. The group size was also dependent on the available blood samples which was affected by the small amounts of the blood samples. The metabolomics analyses are exploratory analyses in this study and as such not included in the power calculations.

Results

Since the primary aim was to explore potential mechanisms for and identify biomarkers connected to the nutritionally programmed improvements in IUGR on adult visceral adiposity, blood glucose and triglyceride levels (7), we focused on the PN42 metabolomics data, their correlation with adult visceral adiposity, blood glucose and triglyceride levels and compared results between the LIG-CTRL and LIG-CLM (CLM effect), and between NOP-CTRL and LIG-CTRL (LIG effect) groups.

Data analyses

Out of 192 serum metabolites detected at PN42, 170 met the indicated quality criteria and WGCNA resulted in 11 metabolite modules (**Supplementary Table 2 and 3**). Correlation

analysis between the 'Eigenprofiles' of the metabolite modules and later-life relative visceral fat mass, blood glucose and triglyceride levels showed significant correlations between module 5 and relative visceral fat mass (r=0.287, p=0.033), modules 1, 4, 6 and 10 and blood glucose levels (module 1: r=− 0.303, p=0.026; module 4: r=0.271, p=0.048; module 6: r=0.314, p=0.021 and module 10: r=0.371, p=0.006), and between module 4 and blood triglyceride levels (r=− 0.280, p=0.041; **Figure 2A–C**, **Supplementary Table 4**). All those metabolite modules (1, 4, 5, 6 and 10) were subsequently further analyzed.

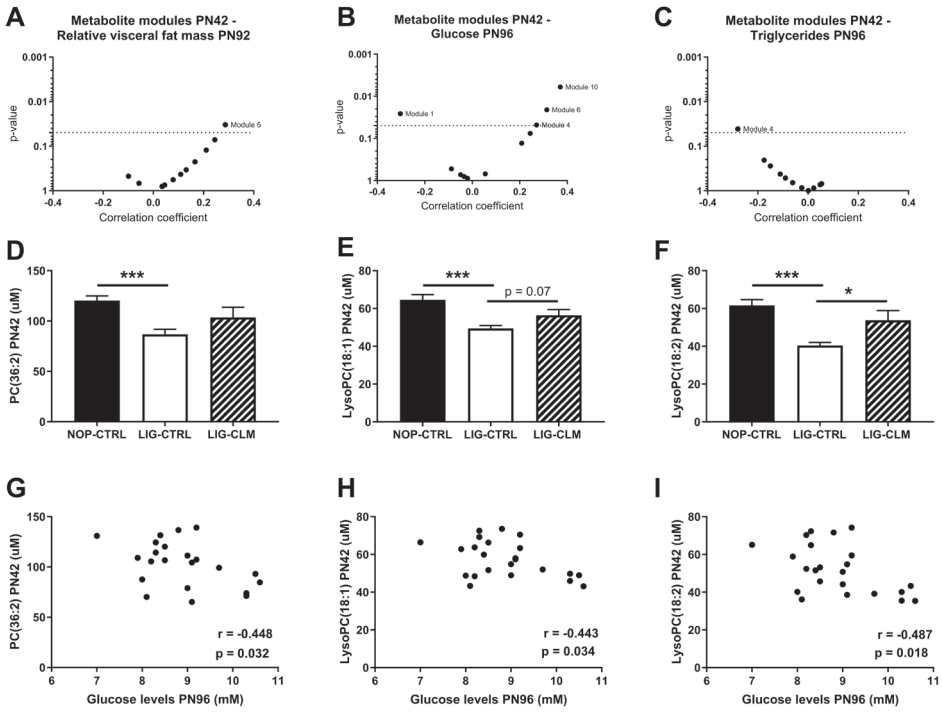

Figure 2: Serum metabolites at PN42 in relation to metabolic parameters at PN96. Correlation between metabolite co-abundance modules at PN42 and **A**) relative fat mass at PN92; **B**) plasma glucose levels at PN96 and **C**) plasma triglyceride levels at PN96; serum **D**) PC(36:2), **E**) LysoPC(18:1) and **F**) LysoPC(18:2) levels at PN42; correlations between glucose levels at PN96 and serum **G**) PC(36:2), **H**) LysoPC(18:1) and **I**) LysoPC(18:2) levels at PN42, with the correlation coefficient r and p-value depicted in the graphs. A–C biweight midcorrelations were based on the calculated 'Eigenprofiles' of a metabolite module and metabolic parameters, p-values were plotted against the correlation coefficient. Metabolite modules were determined by co-abundance analyses based on data from all groups (n=57). PC: phosphatidylcholine, PN: postnatal day. *p<0.05; **p<0.01; ***p<0.001.

Follow up data analyses

Serum levels of the individual metabolites from the indicated modules were tested for significant differences between the focus groups. Three metabolites of module 1, being phosphatidylcholine (PC(36:2)), LysoPC(18:1) and LysoPC(18:2), were decreased in the ligated compared to the non-operated group (LIG-CTRL v. NOP-CTRL: $p<0.01$, **Figure 2D–F**). In turn, levels of LysoPC(18:2) were higher in the LIG-CLM compared to the LIG-CTRL ($p<0.05$), while LysoPC(18:1) levels tended to be higher (LIG-CTRL v. LIG-CLM: $p=0.07$). Levels of these three metabolites at PN42 were individually correlated to the blood glucose levels at PN96 ($r=-0.4$ and $p<0.05$ for all metabolites, **Figure 2G–I**), but not to blood glucose levels at PN42 (**Supplementary Figure 1B-D**). Levels of these three metabolites in adulthood (PN96) were not correlated to blood glucose levels at PN96 (**Supplementary Figure 1E-G**).

Discussion

In the present study we showed that a diet containing large, milk phospholipid coated lipid droplets restored early-life LysoPC(18:2) levels in a rat model for IUGR. While early-life (PN42) LysoPC(18:2) levels showed no association with early-life glucose levels, we did find that early-life LysoPC(18:2) levels negatively correlated to adult (PN96) basal glucose levels.

In humans, reduced LysoPC(18:2) levels were found in insulin-resistant individuals and appeared years ahead of diagnosis for Type 2 diabetes mellitus (T2D) (12, 13). How the reduced LysoPC(18:2) levels link with T2D is unknown, but this may include disturbed hepatic phospholipid biosynthesis in the onset of insulin resistance (14). In the current study, low LysoPC(18:2) levels correlated to elevated adult fasting blood glucose levels in IUGR rats, which might indicate a (pre)diabetic phenotype in early adulthood of fetal growth restricted animals. A direct link between LysoPCs and blood glucose levels is supported by in vitro data showing increased glucose uptake by adipocytes exposed to specific, saturated LysoPCs (15). However, the absence of a direct correlation between LysoPC(18:2) levels and glucose levels at the same time point, both at PN42 and PN96, in our data does not support such a direct effect for LysoPC(18:2). Instead, the correlation between early-life LysoPC(18:2) levels and adult glucose levels as found in the present study, suggests that set points for adult glucose regulation may be established in early life, thus determining later-life susceptibility to impaired glucose tolerance. Further in vitro and in vivo experiments would be needed to confirm the role of LysoPC(18:2) in long-term regulation of blood glucose levels.

Interestingly, one recent clinical study showed that plasma LysoPC levels are affected by the early-life diet, as blood metabolome of infants fed either human milk, standard IMF or an IMF low in energy and protein, but supplemented with MFGM-fragments showed distinctly different LysoPC levels (16). In the present study we used a postnatal diet with large lipid globules, coated with milk phospholipids i.e., MFGM-fragments (8). Therefore, one might argue that the increased LysoPC(18:2) levels were simply a direct consequence of the higher phospholipid intake. Approximately 30% of phospholipids in the MFGM source used were PCs with a relatively high abundance of C18:2 (~10% of total fatty acids (17, 18)). Although a direct link between dietary PC levels and serum LysoPC(18:2) levels cannot be ruled out, the unchanged LysoPC(18:2) levels in the control groups fed CLM in early life (**Supplementary Table 5**), argues against this.

The study had some limitations e.g., the study was conducted in male offspring only while effects of early life nutrition on the metabolism are sex specific (19) and may therefore be different in female. Furthermore, the results reported are exploratory findings of a larger study, which was not powered for this readout specifically, and thus may be underpowered. Follow up research, preferably in a clinical setting, would be needed to confirm the data, and affirmation of the present results would render LysoPC(18:2) an interesting biomarker, which could also be useful for the clinical setting i.e., for risk assessment in children born small for gestational age.

Altogether, this study indicates that LysoPC(18:2) levels in early life may be a predictive biomarker for future glucose regulation and T2D risk in the IUGR population, and that these levels can be influenced by an early diet with large, phospholipid coated lipid droplets.

Additional information

Supplementary Information

The online version contains supplementary material available at https://doi.org/10.1186/s12986-021-00614-8.

Acknowledgements

We thank Dr. Inga Teller who was one of the initiators of this project and Dr. Annemarie Oosting for making the data available for our analyses. Authors' contributions AK, MM, MRak, EvdB, JD and KN designed the research; AK, MM, JV, GF, EN, MRauh and KN conducted the research; AK, MM, MRauh, and KN analysed the data; AK, MM, MRak, EvdB, JD and KN interpreted the data; AK, MM and MRak wrote the paper; all authors reviewed the paper.

Funding

Part of the work was funded by Danone Nutricia Research.

Availability of data and materials

The datasets used and/or analyzed during the current study are published as additional files or available from the corresponding author upon reasonable request.

Declarations

Ethics approval: Samples and data used for this study where collected as part of a larger animal study which was conducted in full compliance to the European Directive 2010/63/EU for the use of animals for scientific purposes and according to institutional guidelines as established by the Ethics Committee for Animal Experiments of the University of Cologne and the German Government (AZ 2011.A248).

Consent for publication: Not applicable.

Competing interests: AK, MM, and MR are employees of Danone Nutricia Research, or were (EvdB) at the time of study conduct.

References

1. Hanson MA, Gluckman PD. Early developmental conditioning of later health and disease: physiology or pathophysiology? Physiol Rev. 2014;94(4):1027-76.
2. Mericq V, Martinez-Aguayo A, Uauy R, Iniguez G, Van der Steen M, Hokken-Koelega A. Long-term metabolic risk among children born premature or small for gestational age. Nature reviews Endocrinology. 2017;13(1):50-62.
3. Milovanovic I, Njuieyon F, Deghmoun S, Chevenne D, Levy-Marchal C, Beltrand J. SGA children with moderate catch-up growth are showing the impaired insulin secretion at the age of 4. PLoS One. 2014;9(6):e100337.
4. Harder T, Rodekamp E, Schellong K, Dudenhausen JW, Plagemann A. Birth weight and subsequent risk of type 2 diabetes: a meta-analysis. Am J Epidemiol. 2007;165(8):849-57.
5. Blencowe H, Krasevec J, de Onis M, Black RE, An X, Stevens GA, et al. National, regional, and worldwide estimates of low birthweight in 2015, with trends from 2000: a systematic analysis. Lancet Glob Health. 2019;7(7):e849-e60.
6. Nusken KD, Dotsch J, Rauh M, Rascher W, Schneider H. Uteroplacental insufficiency after bilateral uterine artery ligation in the rat: impact on postnatal glucose and lipid metabolism and evidence for metabolic programming of the offspring by sham operation. Endocrinology. 2008;149(3):1056-63.
7. Teller IC, Hoyer-Kuhn H, Bronneke H, Nosthoff-Horstmann P, Oosting A, Lippach G, et al. Complex lipid globules in early-life nutrition improve long-term metabolic phenotype in intra-uterine growth-restricted rats. Br J Nutr. 2018;120(7):763-76.
8. Gallier S, Vocking K, Post JA, van de Heijning B, Acton D, Van Der Beek EM, et al. A novel infant milk formula concept: Mimicking the human milk fat globule structure. Colloids and surfaces B, Biointerfaces. 2015;136:329-39.
9. Kodde A, van der Beek EM, Phielix E, Engels E, Schipper L, Oosting A. Supramolecular structure of dietary fat in early life modulates expression of markers for mitochondrial content and capacity in adipose tissue of adult mice. Nutr Metab (Lond). 2017;14:37.
10. Baumgartner S, van de Heijning BJM, Acton D, Mensink RP. Infant milk fat droplet size and coating affect postprandial responses in healthy adult men: a proof-of-concept study. Eur J Clin Nutr. 2017;71(9):1108-13.
11. Steininger PA, Strasser EF, Ziehe B, Eckstein R, Rauh M. Change of the metabolomic profile during short-term mononuclear cell storage. Vox Sang. 2017;112(2):163-72.
12. Wang-Sattler R, Yu Z, Herder C, Messias AC, Floegel A, He Y, et al. Novel biomarkers for pre-diabetes identified by metabolomics. Mol Syst Biol. 2012;8:615.
13. Floegel A, Stefan N, Yu Z, Muhlenbruch K, Drogan D, Joost HG, et al. Identification of serum metabolites associated with risk of type 2 diabetes using a targeted metabolomic approach. Diabetes. 2013;62(2):639-48.
14. Chang W, Hatch GM, Wang Y, Yu F, Wang M. The relationship between phospholipids and insulin resistance: From clinical to experimental studies. J Cell Mol Med. 2019;23(2):702-10.
15. Yea K, Kim J, Yoon JH, Kwon T, Kim JH, Lee BD, et al. Lysophosphatidylcholine activates adipocyte glucose uptake and lowers blood glucose levels in murine models of diabetes. J Biol Chem. 2009;284(49):33833-40.
16. He X, Parenti M, Grip T, Domellof M, Lonnerdal B, Hernell O, et al. Metabolic phenotype of breast-fed infants, and infants fed standard formula or bovine MFGM supplemented formula: a randomized controlled trial. Scientific reports. 2019;9(1):339.
17. Jensen RG. The composition of bovine milk lipids: January 1995 to December 2000. J Dairy Sci. 2002;85(2):295-350.
18. MacGibbon AKH, Taylor MW. Composition and Structure of Bovine Milk Lipids. In: Fox PF, McSweeney PLH (eds) Advanced Dairy Chemistry Volume 2 Lipids Springer, Boston, MA 2006:1-42.

19. Dearden L, Bouret SG, Ozanne SE. Sex and gender differences in developmental programming of metabolism. Mol Metab. 2018;15:8-19.

Supplementary Material

Supplementary method WGCNA analyses

Weighted co-expression analyses (WGCNA) was applied to identify clusters of highly correlated metabolites. As the sample size of the study was not sufficient to do this analysis per group, all samples of the study were included in the analyses. Signed weighted correlation using biweight midcorrelation was used to construct the network (parameter maxPOutliers = 0.1), a robust version of Pearson correlation. A soft threshold power parameter was fitted based on the criterion of approximately scale-free topology (power parameter 4). The "blockwiseModules" function from the WCGNA package of R was used to obtain co-abundance modules. With the "blockwiseModules" function topological overlap matrix are constructed, this matrix is clustered using average agglomeration and resulting dendrogram is cut into separate modules using the R package "dynamicTreeCut" (version 1.62). Subsequently, modules are filtered for consistency and size and merged when similar. The "cutHeight" parameter was set to 0.98 for tree cutting and default settings for other parameters. Minimal module size of 5 metabolites was enforced.

Supplementary Table 1: Dietary composition

Diet		CTRL	CLM	WSD	AIN93M
Ingredients					
Casein	g/kg	168	168	200	140
CTRL-IMF	g/kg	283	-	-	-
CLM-IMF	g/kg	-	283	-	-
Cornstarch, pre-gelatinized	g/kg	300	300	100	466
Maltodextrin	g/kg	101	101	60	155
Sucrose	g/kg	70	70	330	100
Cellulose powder B800	g/kg	39	39	50	50
L-Cystine	g/kg	2.2	2.2	3	1.8
Vitamin premix	g/kg	7	7	10	10
Mineral & trace element premix	g/kg	28	28	35	35
Choline chloride	g/kg	1.9	1.9	2.5	2.2
Pork lard	g/kg	-	-	170	-
Soybean oil	g/kg	-	-	30	40
Nutritional composition					
Carbohydrates (total)	g/kg	500	500	437	567
Starch	g/kg	268	268	98	455
Sugar	g/kg	232	232	339	112
Protein (total)	g/kg	177	177	177	123
Fat (total)	g/kg	70	70	211	41
SFA	g/kg	28.7	29.7	41	5.9
MUFA	g/kg	26.5	26.1	42.3	10.3

Supplementary Table 1: Continued

Diet		CTRL	CLM	WSD	AIN93M
PUFA	g/kg	11.5	11	13.2	23.5
LA:ALA		5.4	5.3	9.5	7.5
Phospholipids	g/kg	0.09	1.13	-	-
Cholesterol	mg/kg	4.8	15.7	-	-
Fibre	g/kg	49	49	50	50
Ash	g/kg	33	33	31	30

Supplementary Table 2: Metabolites modules with eigenprofiles and number of metabolites per module.

Module:	Eigenprofile	Number of metabolites
Module 1	0,665	26
Module 2	0,603	18
Module 3	0,705	17
Module 4	0,767	13
Module 5	0,716	11
Module 6	0,584	11
Module 7	0,545	9
Module 8	0,641	8
Module 9	0,658	7
Module 10	0,520	6
Module 11	0,742	5

Supplementary Table 3: metabolite module membership of PN42 metabolomics data. Order of metabolites within a module by module membership score.

Module	Molecule	Molecule class	Module membership score	Module membership significance
Module 1	PC ae C36:3	glycerophospholipids	0.96	1.55E-32
Module 1	PC aa C36:2	glycerophospholipids	0.96	2.58E-31
Module 1	PC aa C36:3	glycerophospholipids	0.96	3.12E-31
Module 1	PC ae C36:2	glycerophospholipids	0.94	1.75E-27
Module 1	PC ae C38:2	glycerophospholipids	0.93	1.91E-25
Module 1	lysoPC a C18:1	glycerophospholipids	0.91	3.12E-22
Module 1	PC aa C34:2	glycerophospholipids	0.90	5.78E-22
Module 1	PC aa C42:2	glycerophospholipids	0.90	6.02E-22
Module 1	lysoPC a C18:2	glycerophospholipids	0.89	9.32E-21
Module 1	PC ae C34:2	glycerophospholipids	0.88	9.46E-20
Module 1	PC aa C38:3	glycerophospholipids	0.88	2.33E-19
Module 1	PC aa C34:3	glycerophospholipids	0.87	6.16E-19
Module 1	lysoPC a C20:3	glycerophospholipids	0.87	2.03E-18
Module 1	PC ae C42:2	glycerophospholipids	0.86	8.97E-18

Supplementary Table 3: Continued

Module	Molecule	Molecule class	Module membership score	Module membership significance
Module 1	PC aa C32:2	glycerophospholipids	0.85	7.00E-17
Module 1	PC aa C40:3	glycerophospholipids	0.83	1.40E-15
Module 1	PC aa C40:2	glycerophospholipids	0.82	8.68E-15
Module 1	PC aa C42:6	glycerophospholipids	0.79	4.51E-13
Module 1	PC aa C36:1	glycerophospholipids	0.78	8.31E-13
Module 1	PC ae C34:3	glycerophospholipids	0.76	9.11E-12
Module 1	PC ae C42:0	glycerophospholipids	0.66	2.61E-08
Module 1	Pro	aminoacids	0.60	6.89E-07
Module 1	PC aa C40:1	glycerophospholipids	0.60	8.57E-07
Module 1	lysoPC a C26:1	glycerophospholipids	0.50	7.91E-05
Module 1	C0	acylcarnitines	0.41	1.48E-03
Module 1	Cit:Arg ratio		0.36	5.39E-03
Module 2	PC ae C40:6	glycerophospholipids	0.91	2.51E-22
Module 2	PC ae C38:6	glycerophospholipids	0.90	6.20E-21
Module 2	PC ae C34:1	glycerophospholipids	0.87	6.17E-19
Module 2	PC aa C40:4	glycerophospholipids	0.84	3.10E-16
Module 2	PC aa C38:6	glycerophospholipids	0.80	6.85E-14
Module 2	PC aa C38:0	glycerophospholipids	0.80	1.13E-13
Module 2	PC ae C34:0	glycerophospholipids	0.79	3.53E-13
Module 2	PC aa C36:0	glycerophospholipids	0.79	3.79E-13
Module 2	PC ae C36:0	glycerophospholipids	0.79	4.60E-13
Module 2	PC aa C40:5	glycerophospholipids	0.77	2.63E-12
Module 2	PC ae C42:3	glycerophospholipids	0.75	1.88E-11
Module 2	PC aa C40:6	glycerophospholipids	0.74	3.46E-11
Module 2	PC aa C30:0	glycerophospholipids	0.73	1.20E-10
Module 2	PC aa C42:5	glycerophospholipids	0.69	3.04E-09
Module 2	PC ae C32:2	glycerophospholipids	0.68	4.39E-09
Module 2	lysoPC a C24:0	glycerophospholipids	0.67	1.33E-08
Module 2	PC ae C44:5	glycerophospholipids	0.62	3.19E-07
Module 2	PC ae C30:0	glycerophospholipids	0.57	4.00E-06
Module 3	PC ae C40:5	glycerophospholipids	0.95	8.78E-29
Module 3	PC ae C40:2	glycerophospholipids	0.92	1.78E-24
Module 3	PC ae C38:3	glycerophospholipids	0.89	8.14E-21
Module 3	PC ae C42:4	glycerophospholipids	0.89	3.73E-20
Module 3	PC ae C36:1	glycerophospholipids	0.85	8.35E-17
Module 3	PC ae C38:1	glycerophospholipids	0.83	1.52E-15
Module 3	PC ae C42:1	glycerophospholipids	0.80	8.38E-14
Module 3	PC ae C44:3	glycerophospholipids	0.80	1.06E-13
Module 3	PC aa C42:4	glycerophospholipids	0.78	6.68E-13
Module 3	PC ae C40:3	glycerophospholipids	0.78	7.09E-13

Supplementary Table 3: Continued

Module	Molecule	Molecule class	Module membership score	Module membership significance
Module 3	PC ae C44:4	glycerophospholipids	0.76	6.86E-12
Module 3	PC ae C42:5	glycerophospholipids	0.66	2.72E-08
Module 3	PC aa C42:1	glycerophospholipids	0.59	1.67E-06
Module 3	PC ae C30:2	glycerophospholipids	0.53	2.38E-05
Module 3	PC aa C42:0	glycerophospholipids	0.53	2.45E-05
Module 3	lysoPC a C26:0	glycerophospholipids	0.42	1.12E-03
Module 3	lysoPC a C28:1	glycerophospholipids	0.41	1.70E-03
Module 4	SM C16:0	sphingolipids	0.91	4.42E-23
Module 4	SM C24:0	sphingolipids	0.91	1.12E-22
Module 4	SM C18:1	sphingolipids	0.89	2.40E-20
Module 4	SM C16:1	sphingolipids	0.86	1.82E-17
Module 4	SM C24:1	sphingolipids	0.86	1.99E-17
Module 4	SM (OH) C16:1	sphingolipids	0.85	3.10E-17
Module 4	SM C18:0	sphingolipids	0.81	2.37E-14
Module 4	SM (OH) C22:1	sphingolipids	0.81	4.04E-14
Module 4	SM (OH) C22:2	sphingolipids	0.80	6.28E-14
Module 4	SM C26:1	sphingolipids	0.79	2.38E-13
Module 4	SM (OH) C24:1	sphingolipids	0.79	2.65E-13
Module 4	SM (OH) C14:1	sphingolipids	0.70	1.29E-09
Module 4	PC aa C28:1	glycerophospholipids	0.67	1.02E-08
Module 5	PC aa C32:1	glycerophospholipids	0.97	3.81E-35
Module 5	PC aa C36:5	glycerophospholipids	0.94	2.95E-27
Module 5	PC aa C34:1	glycerophospholipids	0.89	2.17E-20
Module 5	PC ae C38:0	glycerophospholipids	0.88	1.28E-19
Module 5	PC aa C36:6	glycerophospholipids	0.88	2.05E-19
Module 5	TotalPC		0.87	2.53E-18
Module 5	PC aa C38:5	glycerophospholipids	0.87	3.22E-18
Module 5	PC aa C34:4	glycerophospholipids	0.78	7.56E-13
Module 5	PC aa C32:3	glycerophospholipids	0.77	2.57E-12
Module 5	lysoPC a C16:1	glycerophospholipids	0.70	1.06E-09
Module 5	TotalPC:Total LysoPC ratio		0.59	1.36E-06
Module 6	PC aa C38:4	glycerophospholipids	0.91	3.21E-23
Module 6	PC ae C38:4	glycerophospholipids	0.89	1.40E-20
Module 6	PC aa C36:4	glycerophospholipids	0.89	4.43E-20
Module 6	lysoPC a C20:4	glycerophospholipids	0.81	2.14E-14
Module 6	PC ae C40:1	glycerophospholipids	0.75	2.13E-11
Module 6	(C16+C18):C0 ratio		0.74	3.39E-11
Module 6	(C2+C3):C0 ratio		0.73	8.68E-11
Module 6	Gln	aminoacids	0.70	1.13E-09
Module 6	C2	acylcarnitines	0.69	2.65E-09

Supplementary Table 3: Continued

Module	Molecule	Molecule class	Module membership score	Module membership significance
Module 6	PC ae C40:4	glycerophospholipids	0.69	3.07E-09
Module 6	H1	sugars	0.52	3.74E-05
Module 7	Ser	aminoacids	0.86	7.50E-18
Module 7	Arg	aminoacids	0.86	9.57E-18
Module 7	Met	aminoacids	0.84	1.78E-16
Module 7	Asp	aminoacids	0.74	4.99E-11
Module 7	Glu	aminoacids	0.73	1.08E-10
Module 7	Tyr	aminoacids	0.67	1.45E-08
Module 7	Lys	aminoacids	0.66	2.58E-08
Module 7	Thr	aminoacids	0.60	8.59E-07
Module 7	Taurine	biogenic amines	0.39	3.08E-03
Module 8	PC ae C38:5	glycerophospholipids	0.96	1.98E-31
Module 8	PC ae C36:5	glycerophospholipids	0.90	3.01E-21
Module 8	PC ae C36:4	glycerophospholipids	0.90	5.86E-21
Module 8	PC ae C32:1	glycerophospholipids	0.87	8.83E-19
Module 8	PC aa C32:0	glycerophospholipids	0.85	4.43E-17
Module 8	His	aminoacids	0.60	7.84E-07
Module 8	PC ae C44:6	glycerophospholipids	0.59	1.31E-06
Module 8	lysoPC a C28:0	glycerophospholipids	0.42	1.24E-03
Module 9	Ile	aminoacids	0.93	7.35E-25
Module 9	Val	aminoacids	0.92	8.69E-24
Module 9	Leu	aminoacids	0.91	3.08E-22
Module 9	Phe	aminoacids	0.87	2.70E-18
Module 9	Asn	aminoacids	0.72	4.13E-10
Module 9	Orn	aminoacids	0.69	2.02E-09
Module 9	Ala	aminoacids	0.68	7.28E-09
Module 10	alpha-AAA	biogenic amines	0.82	6.81E-15
Module 10	Spermidine	biogenic amines	0.82	9.13E-15
Module 10	Gly	aminoacids	0.81	4.13E-14
Module 10	Serotonin	biogenic amines	0.80	1.27E-13
Module 10	Spermine	biogenic amines	0.78	1.57E-12
Module 10	Putrescine	biogenic amines	0.66	2.02E-08
Module 11	lysoPC a C16:0	glycerophospholipids	0.96	2.14E-33
Module 11	Total LysoPC		0.95	6.45E-30
Module 11	lysoPC a C17:0	glycerophospholipids	0.86	8.08E-18
Module 11	lysoPC a C18:0	glycerophospholipids	0.84	6.52E-16
Module 11	lysoPC a C14:0	glycerophospholipids	0.64	8.34E-08

Supplementary Table 4: Correlations between relative fat mass, blood glucose and triglyceride levels at PN92-96 and metabolite modules at PN42.

Metabolite module PN42	Relative fat mass PN92		Glucose PN96		Triglyceride PN96	
	Correlation coefficient	p-value	Correlation coefficient	p-value	Correlation coefficient	p-value
Module 1	0,035	0,800	**-0,303**	**0,026**	-0,025	0,859
Module 2	0,211	0,123	0,055	0,692	-0,061	0,659
Module 3	0,166	0,225	-0,049	0,727	0,048	0,729
Module 4	0,131	0,340	**0,271**	**0,048**	**-0,280**	**0,041**
Module 5	**0,287**	**0,033**	-0,088	0,527	0,023	0,869
Module 6	0,244	0,071	**0,314**	**0,021**	-0,111	0,424
Module 7	-0,099	0,472	-0,034	0,808	0,054	0,697
Module 8	0,109	0,428	0,244	0,076	-0,175	0,206
Module 9	-0,057	0,678	0,208	0,130	0,001	0,993
Module 10	0,045	0,743	**0,371**	**0,006**	-0,090	0,518
Module 11	0,079	0,567	-0,020	0,883	-0,150	0,278

Significant values in bold. Correlation coefficients are biweighted midcorrelations.

Supplementary Table 5: Serum lysoPC(18:2) levels at PN42 in all groups.

(µM)	NOP-CTRL	SOP-CTRL	LIG-CTRL	NOP-CLM	SOP-CLM	LIG-CLM
LysoPC(18:2)	61.6 ± 9.3	54.6 ± 12.7	40.5 ± 4.1	54.8 ± 16.3	46.0 ± 9.3	53.8 ± 14.4

Supplementary Figure

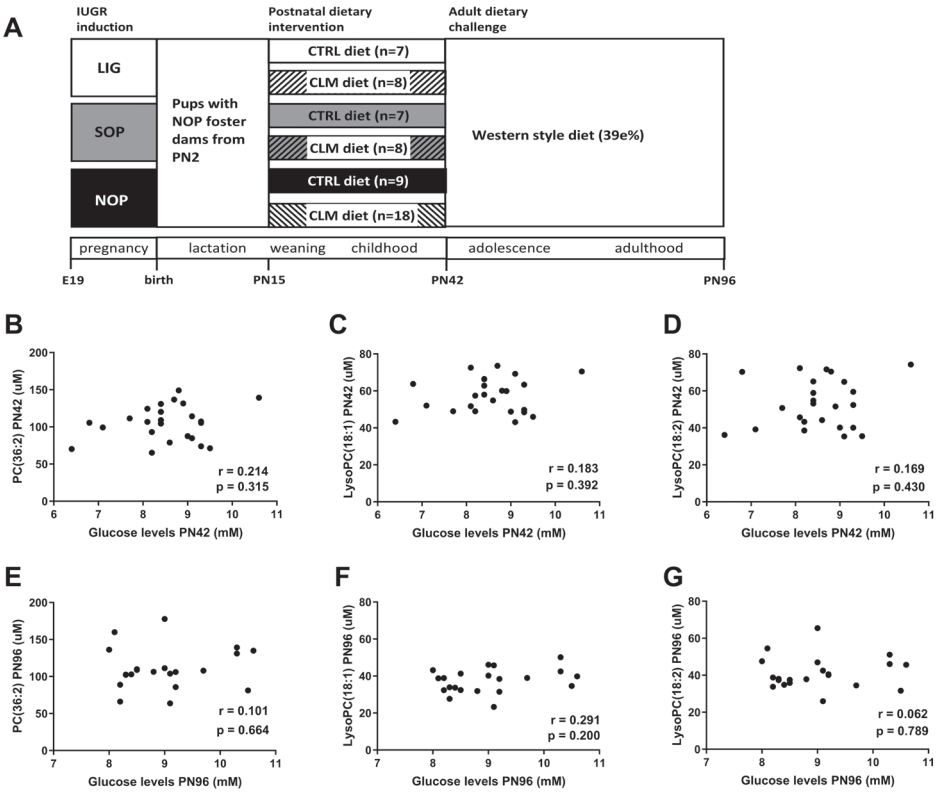

Supplementary Figure 1: Study design and correlation between serum metabolite and glucose levels. **A)** study design including all experimental groups used for the WGCNA. Intrauterine growth restriction (IUGR) was induced by bilateral ligation (LIG) in part of the dams, other dams were sham operated (SOP) or were not operated (NOP). 2 days after birth offspring was culled and assigned to NOP foster dams. From postnatal day (PN)15 onwards dams and litters were exposed to the different experimental diets. Offspring was weaned at PN21 and continued feeding the experimental diets until PN42 after which they were challenged with a western style diet. Correlations between plasma glucose and serum **B)** PC(36:2), **C)** LysoPC(18:1) and **D)** LysoPC(18:2) levels at PN42 and between plasma glucose and serum **E)** PC(36:2), **F)** LysoPC(18:1) and **G)** LysoPC(18:2) levels at PN98. E: embryonic day, PC: phosphatidylcholine, PN: postnatal day.

Chapter 7

General Discussion

Aim and outline

In this thesis, the effect of feeding a diet with large, (milk)phospholipid coated lipid droplets in early postnatal life was investigated, focusing on white adipose tissue (WAT) health and mitochondrial function in the liver, and potential predictors thereof. The broader scope was to investigate the processes underlying programming of adult metabolic health by the postnatal diet.

The potential impact of the maternal diet on offspring's later life metabolic health is well-established (1-4). There is also evidence showing that the postnatal diet has the potential to impact the long-term metabolic health of the offspring, although most evidence is from observational studies (5). We previously showed that feeding a postnatal diet with large, (milk)phospholipid (PL) coated lipid droplets (Concept) reduced adult adiposity development following a Western style diet (WSD) challenge, but the underlying processes were unclear (6-8). The sub aims of this thesis were 1) to investigate if the previous observed effects of the Concept on adiposity could be explained by (programmed) changes in mitochondrial function (markers) in WAT and liver; 2) to investigate the developmental trajectory of different WAT depots to gain insight in the potential window of opportunity for programming of WAT health; and 3) explore underlying processes for the observed programming of adult metabolic health. To this end, the effect of the Concept on (markers of) mitochondrial function in WAT and liver was assessed in **Chapters 2, 4 and 5**. In **Chapter 3** the developmental trajectory of different WAT depots was studied, and in **Chapters 4, 5 and 6** potential mechanisms involved in the programming of mitochondrial function and metabolic health were explored.

In this **Chapter 7**, I discuss and answer the research questions as presented in **Chapter 1** and formulate overall conclusions. I will first discuss the results on programming and development of WAT and WAT mitochondrial function. I will then discuss the effect of the Concept on hepatic lipid and energy metabolism and how this is connected to the observations in the WAT. I will next discuss programming of mitochondrial function as a proposed underlying process for risk of later life metabolic diseases. I will end this chapter with a discussion on the relevance of the research, provide proposals for follow up and finish with major overall conclusions.

The effect of the Concept on WAT health

WAT health is increasingly recognized as an important determinant for whole body metabolic health (9, 10). Safeguarding an optimal development of WAT in perinatal life may, therefore, provide opportunities to preventively reduce later life metabolic disease

risks. An important determinant of WAT health is WAT mitochondrial function. Although programming of WAT mitochondrial function is postulated to explain, at least partly, the effect of perinatal conditions on adult metabolic health, current evidence to support this notion is scarce. In **Chapter 2**, we showed that an early postnatal diet with large, (milk)phospholipid coated lipid droplets, fed from postnatal day (PN)16 until PN42, reduced adiposity and visceral WAT adipocyte size in adult mice exposed to a WSD from PN42 until PN98. In addition, postnatal Concept feeding increased levels of two markers for mitochondrial density, mitochondrial DNA (mtDNA) and citrate synthase (CS), in retroperitoneal (RP) WAT of the adult mice following the WSD challenge (**Chapter 2**), indicating an increased mitochondrial density in Concept fed mice (**Figure 1, box A**). Furthermore, protein expression of a subunit of complex 4 of oxidative phosphorylation (OXPHOS), indicative of mitochondrial oxidative capacity, was higher in RP WAT of the Concept fed mice. Together these findings may indicate an increased oxidative capacity in WAT of the adult mice challenged with a WSD after being fed Concept in postnatal life, potentially explaining the reduced adiposity observed. However, in **Chapter 4** we showed that WAT mitochondrial density, measured as mtDNA and CS levels, was not affected at PN42 i.e., directly after the postnatal intervention with Concept, a time point when still no changes in adiposity or WAT weight were seen (**Figure 1, box B**). Interestingly, the expression of OXPHOS subunits were reduced in RP and epididymal (EPI) WAT at this time point. The absence of increased mitochondrial density and oxidative capacity markers in visceral WAT directly after the postnatal intervention with Concept indicates that, although mice fed the Concept postnatally had increased the oxidative capacity upon the WSD challenge in adulthood, as shown in **Chapter 2**, this was not the consequence of consistent increases in expression of those markers from early life onwards. In other words, the effects of Concept on mitochondrial density and oxidative capacity seen in visceral WAT of adult mice, following the WSD challenge, were not due to an early increase in mitochondria oxidative capacity of the visceral WAT by postnatal Concept feeding that continued into adulthood. The increased levels of mitochondrial density and oxidative capacity markers in visceral WAT of Concept fed mice following the WSD challenge are therefore more likely to reflect preserved mitochondrial flexibility, leading to increased mitochondrial capacity following the WSD challenge. Mitochondria can increase their abundance and oxidative capacity upon dietary changes, like fasting or a carbohydrate load (11), and the ability of mitochondria to respond to a change in nutrient status is key for metabolic health (12).

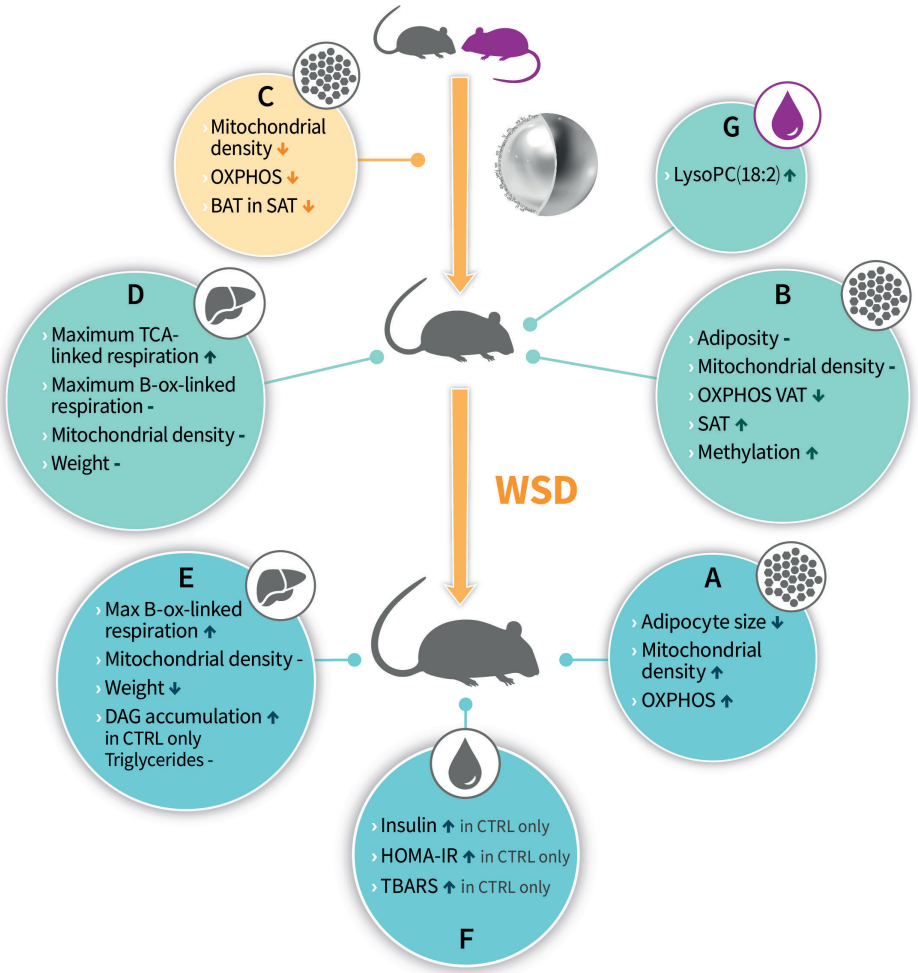

Figure 1: Graphic summary of the results of this thesis. Healthy mice (grey) or IUGR rats (purple) were fed either a control or Concept diet from PN16 until PN42. Some of those animals were subsequently challenged with a WSD challenge until PN98. The letters in the result boxes relate to the description of the results in Chapter 7. BAT: brown adipocyte tissue; B-ox: B-oxidation; CTRL: control diet fed group; DAG: diacylglycerol; HOMA-IR: homeostatic model assessment for insulin resistance; LysoPC: lysophosphatidylcholine; OXPHOS: oxidative phosphorylation; SAT: subcutaneous adipocyte tissue; TBARS: Thiobarbituric acid reactive substances; TCA: tricarboxylic acid cycle; VAT: visceral adipose tissue; WSD: Western style diet.

The capacity of mitochondria to respond to changes in nutrient supply can be impaired following dietary challenges, like a high fat diet (13, 14). This impairment in response to dietary changes by the mitochondria, rather than direct changes in mitochondrial density and oxidative capacity, may be counteracted by the Concept feeding. This is in line with patterns found in other programming studies showing a (more pronounced) effect of a maternal high fat diet, low protein diet or diabetes on body weight and

mitochondrial function markers in offspring over time or following a subsequent dietary challenge (15-17). Together, our data can be explained by postulating that postnatal Concept feeding preserved mitochondrial flexibility in visceral WAT, leading to increased levels of WAT mitochondrial function markers when challenged with a WSD. This increased mitochondrial flexibility may potentially explain the reduction in WSD-induced adiposity observed in Concept fed mice.

We showed in **Chapter 3** that levels of mitochondrial function markers were different between visceral and subcutaneous WAT, showing higher levels of mtDNA, CS activity and OXPHOS protein expression in the subcutaneous inguinal (ING) WAT compared to the two tested visceral depots, EPI and RP WAT (**Figure 1, box C**). Furthermore, in **Chapter 3** we also showed that CS levels were reduced from weaning (PN21) until adulthood (PN98) in all depots. This decline was most pronounced in ING WAT where it was paralleled by a decrease over time in protein expression of the OXPHOS subunits of complex I, II and III, indicating a strong decline in mitochondrial oxidative capacity from weaning (PN21) to young adulthood (PN42). The ING WAT also showed a reduction in brown adipocytes marker expression from weaning to young adulthood and showed whitening of this depot. The higher mitochondrial density and oxidative capacity in subcutaneous compared to visceral WAT has reported for rodents and can partly be explained by the higher abundance of the potential heat generating brown-in-white adipocytes in subcutaneous depots (18, 19). This in agreement with the correlation between uncoupling protein 1 (*Ucp1,* a brown adipocyte marker) mRNA expression and CS activity, mtDNA and OXPHOS protein levels in ING WAT, as observed in **Chapter 3**. Interestingly, we found in **Chapter 4** that postnatal Concept feeding, in contrast to the effect in visceral WAT, increased OXPHOS protein expression in the subcutaneous ING WAT and lead to a higher ratio of OXPHOS protein expression between ING and EPI WAT at PN42 (Figure 1, box B). This increased OXPHOS protein expression in ING WAT of Concept fed mice may reflect a difference in thermogenic activity in ING WAT of Concept fed mice. Indeed, previous studies indicated that feeding milk-fat globule membrane fragments, the ingredient used for the PL coating of the large lipid droplets of the Concept diet, to adult mice increased subcutaneous WAT browning (20, 21). However, the unchanged CS activity levels in ING WAT following Concept feeding, as seen in **Chapter 4**, argue against a difference in brown-in-white numbers in ING WAT, but may point towards a difference in intrinsic capacity of the mitochondria. An enhanced intrinsic capacity of mitochondria in WAT can coincide with increased WAT browning and is associated with increased insulin sensitivity (22). Histological analyses of ING WAT of Concept fed mice are needed to confirm if the changes in OXPHOS protein expression seen directly after the postnatal intervention are the consequence of differences in

WAT browning. Also, functional measurements in WAT depots of Concept fed animals directly after the postnatal dietary intervention and later in life may give insights into changes in intrinsic capacity of the mitochondria. Together, the substantial reduction in mitochondrial function markers and WAT browning from weaning to young adulthood suggests a window to program WAT browning, particularly in subcutaneous WAT. Yet measurements on WAT browning (markers) are needed to see if changes in WAT browning in subcutaneous WAT can explain the increased OXPHOS protein expression following postnatal Concept feeding in ING WAT.

Although *Ucp1* expression (as marker for WAT browning) in ING WAT of Concept fed mice was not measured, *Ucp1* mRNA expression was measured in the visceral RP WAT of postnatal Concept fed mice following the WSD challenge. *Ucp1* mRNA expression in those animals was not significantly changed by postnatal Concept feeding, as shown in **Chapter 2**. There was a tendency to a slightly increased mRNA expression of another browning marker, Cell Death Inducing DFFA Like Effector A (*Cidea*), but the limited effect size does not support the notion that a difference in RP WAT browning can explain the increase in mitochondrial density and OXPHOS expression in adult mice postnatal fed the Concept. Indeed, our analyses in **Chapter 3** showed that mitochondrial density and oxidative capacity are not correlated to *Ucp1* mRNA expression in RP WAT. However, a recent finding suggests that there is another brown cell population, especially present in visceral WAT (23). Those cells are *Ucp1* negative and have a thermogenic capacity which is associated with the futile creatine cycle. Thus, although no evidence was found for differences in subcutaneous or visceral WAT browning to explain the differences in adult mitochondrial density and oxidative capacity marker levels in Concept fed mice, further analyses are needed focusing on *Ucp1* negative thermogenic adipocytes.

In addition to differences in WAT browning, several alternative mechanisms may possibly explain the Concept-associated differences in mitochondrial density and oxidative capacity markers. There is some evidence showing that prenatal conditions i.e., gestational diabetes, and the postnatal diet i.e., a reduced n6 polyunsaturated fatty acids (PUFA) intake during lactation, can program adipocyte stem cells, resulting in impaired or improved mitochondrial functionality respectively upon differentiation to adipocytes (24, 25). This may explain why differences in mitochondrial function markers in **Chapter 3** and other studies only became evident later in life or upon dietary challenges, when new adipocytes are recruited from precursor cells (16, 26, 27). Another possible explanation for the programming of mitochondrial oxidative capacity can be via epigenetic mechanisms i.e., mechanisms regulating gene expression via structural adaptations to chromosomal regions (28). Examples of epigenetic mechanisms are alterations in DNA methylation, histone modifications (methylation, acetylation, and

others) and expression of non-coding RNAs. Long-lasting changes to DNA methylation of promotor regions of key genes involved in WAT development and health have been reported upon perinatal diet exposure in rodents, which may explain programming of WAT health (29, 30). For example, exposure to a maternal high fat diet during lactation resulted in methylation of the promotor region of stearoyl-CoA desaturase 1 (involved in fatty acid synthesis) in EPI WAT of mice offspring (29) and a maternal low protein diet increased DNA methylation of the promotor region of insulin growth factor 2 (a growth factor) in EPI WAT of rat offspring (30), suggesting programming of WAT growth and lipid storage capacity by DNA methylation. Studies in humans further showed associations between DNA methylation and the postnatal diet as well as DNA methylation at birth and later life adiposity in children (31, 32), suggesting that DNA methylation may be changed by the postnatal diet and be linked to later life adiposity. Indeed, in **Chapter 4** we showed, in an exploratory approach, that postnatal Concept feeding elevated total methylation in EPI WAT directly after the postnatal dietary period, with several pathways involved in growth and development of cells and tissues of EPI WAT showing an increased DNA methylation. Although these were only exploratory findings and the study design did not allow us to make a firm conclusion on long-term changes in DNA methylation and their correlation to functional outcomes, the study does provide some indications for possible mechanisms involved in the programming of adult metabolic health by the postnatal Concept feeding.

The Concept contains several features which distinguish it from the control diet. These are the larger size of the fat droplets (3-5 µm for the Concept versus 0.4 µm for the control) and the PL-rich ingredient (the bovine-derived milk fat globule membrane (MFGM) fragments) coating these large lipid droplets; both contribute to the effects of the Concept. For example, the higher total methylation seen in Concept fed mice may be linked to some of the PLs in the Concept diet. The milk-fat globule membrane fragments used to produce the Concept diet contain relative high levels of the PL phosphatidylcholine (PC). Choline can be used as donor for the one-carbon cycle, a series of pathways (including the folate and methionine pathways) involved in the transfer of methyl groups to different acceptors, including DNA methyltransferases, regulating DNA methylation (33). Thus, methylation in EPI WAT of Concept fed mice may be stimulated by the higher PC levels present in the diet, although further research is needed to see if this is indeed the case and, if so, whether those changes are long-lasting and can explain the observed beneficial impact on adult phenotype. As mentioned above, also WAT browning may also be linked to the PLs, as PL feeding to adult mice has shown to increase WAT browning (20, 21). Thus, this suggests that the PLs in the coating of the Concept may have been the dietary component that contributed to the observed

impact of the postnatal Concept feeding on WAT mitochondrial function markers and methylation profile.

How the other features of the Concept i.e., the larger size of the lipid droplets and the other components of the coating of the lipid droplets, may contribute to the beneficial effect of the Concept on WAT mitochondrial function is not clear. We previously showed that a combination of the larger lipid droplet size and its PL-rich, MFGM-derived coating is necessary to reduce adult adiposity, while the mere addition of PL-rich MFGM as a separated ingredient or applying the Concept coating to small lipid droplets is ineffective (8, 34). This may imply that also the effects of the Concept on mitochondrial function cannot be attributed to the PLs alone, at least when one postulates that the differences in WAT health are underlying the impact on later life adiposity. Changes in dietary lipid droplet size has been shown to alter gastric emptying, satiety regulation and fat digestion in humans (35, 36). Moreover, the combination of the large lipid droplets with the PL-rich coating as in the Concept diet showed to alter the absorption of carbohydrates and lipids in young healthy male subjects fed the Concept (37). Indeed, altered digestion and absorption of the Concept compared to a control product was also observed *in vitro* (38). Further, feeding the Concept in postnatal life affected later life postprandial kinetics in mice, suggesting programming of lipid handling by the Concept (39). Given the role of WAT in whole body metabolism, the differences in lipid handling and postprandial kinetics may also impact WAT and result in lasting differences in function. Another explanation may be that the location of the PL in the Concept, on the surface of the large lipid droplet, affects the absorption of the PL. To further investigate this, studies with labeled PL and different intermediate lipid droplet groups (small/large, coated/not coated) are needed. Thus, the location of the PLs in the diet i.e., on the surface of the lipid droplets, in combination with the size of the droplets are features of the Concept integral to its beneficial effects for later life metabolic health. Although the exact mechanism is still unrevealed, differences in postprandial kinetics are likely part of the explanation.

The effect of the Concept on hepatic lipid and energy metabolism

Impaired WAT health and consequent inadequate lipid storage in WAT leads to ectopic fat deposition in the liver and skeletal muscle, a step in the development of T2D and NAFLD. The improved mitochondrial oxidative capacity in WAT of postnatal Concept fed mice may therefore also affect hepatic lipid and energy metabolism. Hence, in **Chapter 5**, we investigated the effect of postnatal Concept feeding on mitochondrial function in liver tissue by functional analyses. We found that postnatal Concept feeding increased

maximum hepatic oxidative capacity linked to the TCA cycle direct after the postnatal dietary intervention. Moreover, the maximum oxidative capacity linked to β-oxidation was increased in Concept fed mice following a subsequent WSD challenge, indicating programming of the hepatic mitochondrial oxidative capacity by the Concept (**Figure 1, box D and E**). The differences in oxidative capacity described in **Chapter 5** only became evident when mitochondria were pushed towards maximum oxidative capacity, in this case by addition of the uncoupler carbonyl cyanide-p-trifluoromethoxyphenylhydrazone (FCCP) in the respiratory measurements. The adult WSD challenge may have provided a similar pressure on mitochondrial maximum capacity and with the Concept providing a higher capacity to oxidize the energy surplus, protecting the mice from metabolic derangements. Indeed, those Concept fed mice were partly protected from WSD-induced hyperinsulinemia and insulin resistance (**Figure 1, box F**).

Changes in mitochondrial function can affect production of reactive oxygen species (ROS), a term used for oxidants derived from oxygen. In non-inflamed conditions ROS are mainly produced in OXPHOS and have a role in normal cellular messaging. However, an imbalance between ROS production and antioxidant capacity results in oxidative stress and can lead to oxidative damage of lipids (lipid peroxidation), proteins and DNA. Oxidative damage is increased in T2D and NAFLD (40, 41) and has been suggested as a mechanism involved in programming of metabolic health and mitochondrial dysfunction (42-44). Increased oxidative damage is found in offspring that were exposed to adverse maternal conditions, which is suggested to be caused i) by enhanced ROS production in placenta's, ii) by mitochondrial dysfunction in the offspring or iii) by an impaired antioxidant capacity (42-44). To investigate if Concept feeding affected ROS production, we measured hydrogen peroxide (H_2O_2) emission in liver. As shown in **Chapter 5**, H_2O_2 emission was not affected by postnatal Concept feeding. Interestingly, systemic lipid peroxidation, measured as thiobarbituric acid reactive substances (TBARS), was not elevated after the WSD challenge in Concept fed mice, but was increased in control fed mice (Figure 1, box F). These findings may suggest an increased antioxidant capacity in Concept fed mice.

In **Chapter 5** we also showed that the WSD-linked hepatic cytosolic accumulation of C18:1 fatty acids containing diacylglycerols (DAG) was blunted in Concept fed mice (Figure 1, box E). Accumulation of DAGs interfere with proximal insulin signaling and especially C18 containing DAGs can impair insulin signaling via PKCε (45, 46). Although the effect of the Concept on DAG levels was moderate, the results may indicate that the Concept changed the hepatic lipid metabolism and prevented the adverse accumulation of lipid intermediates.

In addition to DAGs, PL levels are also disturbed in T2D and NAFLD, as indicated by altered hepatic and blood PL composition in T2D and NAFLD (47-50). Changes in blood PL levels may indicate disturbed PL metabolism in liver or skeletal muscle (51). In **Chapter 6** we showed that levels of LysoPC(18:2), a hydrolyzed PC, were reduced in serum of young IUGR rat offspring (at PN42) and that those levels were restored by postnatal Concept compared to control feeding (**Figure 1, box G**). The reduction in LysoPC(18:2) levels in IUGR rats is in line with the reduced LysoPC(18:2) levels that are seen in very low birth weight infants (52). The cause for the reduction in LysoPC(18:2) levels is unclear, but the lower levels in IUGR rats and low birth weight infants may be related to catch up growth seen in those populations, as LysoPCs can be used for the synthesis of PCs for incorporation in cellular membranes (53, 54). The restored LysoPC(18:2) levels in the Concept fed mice may be a direct consequence of feeding a diet rich in PL and specific PCs (55, 56). In **Chapter 6**, we also showed that LysoPC(18:2) levels in young IUGR rats correlated to adult blood glucose levels and serum LysoPC(18:2) levels may therefore reflect early alterations in the development of impaired glucose tolerance. This is in agreement with the results of a human cohort study in adults showing that reduced LysoPC(18:2) levels predicted impaired glucose tolerance and T2D years ahead of diagnosis (50, 57). LysoPC(18:2) may therefore be useful as predictive marker for later life impaired glucose tolerance. There are some indications for a direct effect of LysoPCs on the glucose metabolism. For example, exposure of perfused rat pancreases as well as a mouse pancreatic β-cell line to a mixture of different LysoPCs increased glucose stimulated insulin secretion via G-protein coupled receptor 119, and adipocyte glucose uptake was stimulated by specific LysoPCs (58, 59). How early life LysoPC(18:2) levels are mechanistically related to later life blood glucose levels is, however, still unclear and needs further research.

Programming of mitochondrial function by perinatal events

The results in this thesis indicate that a postnatal diet with large, (milk)phospholipid coated lipid droplets can adapt mitochondrial oxidative capacity later in life. Our research contributes to the previous findings of others describing that mitochondrial function can be programmed by (dietary) factors in prenatal, perinatal, and postnatal life (**Figure 2**). Currently, most evidence is from studies evaluating the impact of maternal factors, like a high fat diet (15, 60, 61), a low protein diet (17, 62-65), caloric restriction (61, 66-69), hypoxia (70-73) and intra-uterine growth restriction (43, 74-77), occasionally with maternal dietary interventions extending until weaning (78-82). Additionally, evidence exists for the programming of offspring mitochondrial function

by maternal health status, like obesity (83) and (gestational) diabetes (16, 24, 83) and maternal hormones levels, like testosterone (84, 85), glucocorticoids (86) and the stress hormone cortisol (87) as well as maternal stress (88) (Figure 2 and **Supplementary Table 1** for an overview). The number of studies investigating the sole effect of the early postnatal diet on mitochondrial function are, however, limited. Overfeeding during the lactation phase, by reducing the litter size, increased mitochondrial state 2 and 4 respiration when pups were subsequently exposed to caloric restriction in adulthood and increased OXPHOS protein expression independent of the adult diet (89). This, in combination with the results presented in this thesis, indicates that lactation is a period that allows programming of mitochondrial function.

Beneficial programming of mitochondrial function by the perinatal diet is occasionally investigated. Maternal fish oil feeding during pregnancy protected against maternal high fat diet induced mitochondrial damage and related mitochondrial dynamics in the offspring (90). Further, reduced n6/n3 PUFA intake during lactation increased palmitic acid stimulated respiration in adipose precursor cells, indicating enhance mitochondrial oxidative capacity (25). These two studies showed that improving the lipid quality of the early life diet could improve mitochondrial function. In **Chapter 2 and 5** we showed that the structure of the dietary lipid droplet can improve mitochondrial oxidative capacity in later life. With our studies, we therefore strengthened the evidence-base that the window for the programming of mitochondrial function is not restricted to the end of pregnancy or lactation but continues throughout early life.

Some of the above-mentioned studies on perinatal programming of mitochondrial function suggested that programming of mitochondrial function is tissue- and sex-specific. For example, in one study an effect of caloric restriction affected mitochondrial mRNA expression in liver, but not in WAT or skeletal muscle (68), whereas others have observed that a maternal low protein diet or maternal high testosterone levels resulted in tissue-specific effects on mitochondrial function markers (80, 91). Similarly, in **Chapter 5**, we showed that postnatal Concept feeding did not change mitochondrial function in the soleus muscle, indicating that programming of metabolic health by the Concept may be explained by changes in mitochondrial function specifically in liver and WAT, but not skeletal muscle. Next to being tissue-specific, programming of mitochondrial function may also be sex-specific, as several studies showed different effects in female compared to male offspring (70, 71, 73, 92). For example, changes in mitochondrial function of maternal hypoxia exposed offspring were only seen in males and not in females or even showed opposite changes between female and male offspring (70, 73). In our studies we used only male offspring and follow up studies in female offspring are needed to check for possible sex-specific effects of the Concept diet.

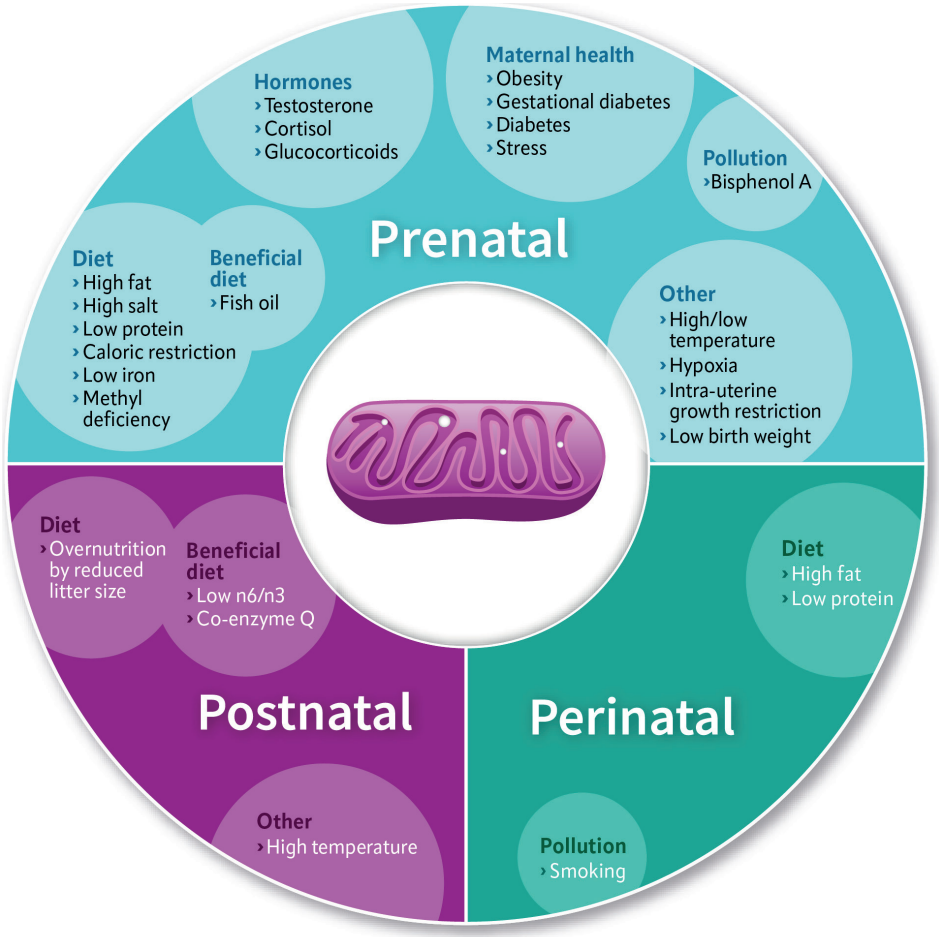

Figure 2: Programming of mitochondrial function by perinatal events. Overview of the results of a literature search, split to intervention period (prenatal, perinatal or postnatal) and categorized to intervention type (diet, maternal health, beneficial diet, hormones, pollution and other). Selection procedure of the publications: Pubmed search (date May 5th 2023): ((mitochondria[Title/Abstract]) OR (mitochondrial[Title/Abstract]) OR (mtDNA[Title/Abstract]) OR (oxidative phosphorylation[Title/Abstract])) AND (programming[Title/Abstract]) AND ((perinatal[Title/Abstract]) OR (prenatal[Title/Abstract]) OR (postnatal[Title/Abstract])), subsequently checked for appropriated readouts and timing. Studies with only direct effects (for example during fetal life) were excluded. Some extra studies were added based on past targeted searches: (24, 43, 75-77, 79, 81, 82).

Relevance and future directions

The data in this thesis strongly indicate that feeding a diet with large, (milk)phospholipid coated lipid droplets (Concept) in early postnatal life can improve adult mitochondrial oxidative capacity (**Chapter 2 and 5**). The improved mitochondrial oxidative capacity may (partly) explain previous described beneficial effects of postnatal Concept feeding

on adult adiposity and metabolic health outcomes (6-8). The Concept diet used for the postnatal dietary interventions in this thesis contains lipid droplets designed to closely resemble the lipid droplets as present in human milk (93, 94). The beneficial effects of breastfeeding are acknowledged and include reduction of infection risks (95, 96), but also a reduced overweight and obesity risk, especially with a longer duration of breastfeeding (97). Although explanations for this association between obesity risk and breastfeeding includes several factors, like behavioral and social-economic factors, the results presented in this thesis and previous papers on the effect of the Concept on adiposity and later life metabolic health (6-8), showed that the human milk lipid droplet structure is likely to contribute to the protective effect of breastfeeding. In addition to this effect of the milk lipid droplet structure, other milk-related factors may add to the beneficial effects of breastfeeding to adult metabolic health, since for example galactose, a monosaccharide almost exclusively present in milk as lactose, resulted in beneficial programming of metabolic health (98, 99). As breastfeeding, especially prolonged duration thereof, is not always possible, further research to understand the possible functional roles of various human milk components on later-life health is useful and can help to further improve infant milk formulas. In addition to functional effects, it is also important to obtain an understanding of the responsible mechanisms. This is needed for faithful verification in humans and to get a grip on possible modifying factors e.g., environmental factors that may enhance or diminish programming effects. Understanding the mechanisms of action can also help to predict the efficacy of future adaptations to infant milk formulae i.e., in the context of this thesis, to predict if mitochondrial function can potentially be changed by human milk constituents or food components. The data in this thesis contribute to our mechanistic understanding i.e., how Concept impacts on mitochondria, and this will ultimately contribute to further improvement of infant formula.

The study on WAT maturation as presented in **Chapter 3**, together with the data on the programming of WAT and liver mitochondrial function in **Chapters 2, 4 and 5** extended current knowledge on the window for programming of WAT health and mitochondrial function. The detrimental effect of factors during pregnancy, like a maternal high fat diet (60, 78, 79), (gestational) diabetes (16, 24, 83) as well as growth restriction of the fetus (43, 75, 76) on mitochondrial function and its associated metabolic sequela is well established. The data presented in this thesis show that mitochondrial function can be improved by the postnatal diet. This is useful, not only for infants born from complicated pregnancies, but also for healthy infants as they will nowadays have a higher likelihood to grow up in an obesogenic environment (100, 101) and they may be better protected when fed a beneficial postnatal diet. Improvement of the mitochondrial function by a

postnatal diet may also be important for infants with a compromised start in life due to a suboptimal fetal development i.e., those born with a low birth weight, exposed to (gestational diabetes) or maternal obesity, to provide them with a higher chance for a healthy life course. For the infants with a compromised start in life, detrimental effects of prenatal conditions may (partly) be ameliorated by a beneficial postnatal diet. Indeed, previous studies in IUGR rat showed that postnatal feeding Concept prevented visceral adiposity and improved glucose tolerance in adulthood (102). Although the effects of postnatal Concept feeding on mitochondrial function in the IUGR population needs further investigation, improved mitochondrial function may (partly) explain the metabolic phenotype.

The results described in this thesis are all based on animal research and follow up studies in humans are needed. Programming effects of the early postnatal diet are difficult to investigate in humans, as later life effects may not become evident before the subjects are, for example, 50 years old. Next to that, tissue analyses are challenging in the human population, and not possible in infants or young children. But the first clinical studies are executed and showed safety and adequate growth in Concept fed infants (103, 104). Follow up analyses on fat mass development and later childhood growth are ongoing, but have not been reported yet. Identification of biomarkers predictive for the later life phenotype would be useful to get insight into potential effectiveness in humans. As described in **Chapter 6** and discussed in the previous section, serum LysoPC(18:2) levels may predict the later life blood glucose levels in the IUGR population and may therefore be a useful candidate biomarker, but further validation in a clinical setting is needed. Indeed, plasma levels of several other LysoPCs at 3 months associated with visceral fat mass at 2 years of age in cohort study with health infants, further emphasizing that LysoPCs may be useful candidate biomarkers (105). There are clinical studies assessing programming of mitochondrial function, mostly by assessing mtDNA in whole blood or in specific cell populations i.e., peripheral blood monocular cells (88), which is relatively easy as only a small volume of blood is needed. Another option is to assess mitochondrial respiration in blood cells, but the relatively large volume of blood needed will likely not be available from infants and young children for ethical and legislative considerations.

Indications for several mechanisms and processes which may explain programming of mitochondrial function in postnatal life were obtained in this thesis. Those include changes in WAT browning, oxidative stress, and epigenetic mechanisms. Further research in animals is needed to confirm involvement of those mechanisms and processes. To understand the involvement of WAT browning, immunohistochemical analyses of UCP1, a marker for UCP1-linked thermogenesis, and alkaline phosphatase (ALPL or TNAP), a marker for the futile creatine cycle-linked thermogenesis, and possibly a complex IV

staining as a measure for OXPHOS protein levels, will be useful to identify possible increase of WAT browning by the Concept (23, 106). Ideally those analyses should be performed at different time points, before and after the intervention period and in adulthood, to investigate if potential differences in WAT browning are long-lasting from postnatal life onwards and preceding differences in adiposity.

In **Chapter 5**, we tested some indicators for oxidative stress to investigate the role of oxidative stress in the programming of metabolic health by the Concept. Measuring H_2O_2 emission in liver tissue during the respiratory analyses showed that the Concept did not change H_2O_2 emission, despite the increased respiration in those animals. The main source of H_2O_2 production is the oxidative phosphorylation, thus the unchanged H_2O_2 emission may indicate differences in antioxidant capacity. To investigate potential changes in antioxidant capacity by the Concept, analyzing total antioxidant capacity (by a colorimetric assay), enzymatic antioxidant defense (measuring levels of superoxide dismutase, catalase, glutathione peroxidases, glutathione-S-transferase or glucose-6-phosphate dehydrogenase activity) or levels of non-enzymatic antioxidants (reduced glutathione or the redox state (reduced/oxidized glutathione)) in liver or WAT tissues of Concept and control fed mice following the adult WSD challenge would be useful (63). The antioxidant capacity of breast milk is suggested to be different from infant milk formula (107, 108), but that did not lead to differences in systemic lipid peroxidation in preterm infants (109). Indeed, although we do not know the antioxidant capacity of the Concept diet compared to control, a direct effect of the Concept on oxidative damage is unlikely given the unchanged respiration and ROS emission in the liver tissue at PN42 as found in **Chapter 5**. Interestingly WSD-linked systemic lipid peroxidation was blunted by the Concept at PN98, thus next to potential differences in antioxidant capacity in tissues, also measuring systemic antioxidant capacity may be useful.

In **Chapter 4**, we analyzed whole genome DNA methylation direct after the postnatal dietary intervention with the Concept, in an exploratory setup. We showed that the Concept increased the total DNA methylation and methylation of pathways involved in growth and development of cells and tissues and WAT innervation. However, for a better understanding of epigenetic mechanisms in the programming of metabolic health and mitochondrial function, a better powered study in which DNA methylation or histone modification at different time points (before, after and in adulthood) will be assessed is required, preferably in several metabolic organs, like WAT, liver and skeletal muscle. As a start analyses of total DNA methylation and whole genome DNA methylation in a well-powered study, direct after the postnatal dietary intervention and later in life can be useful to further establish the results described in **Chapter 4**. When those DNA methylation analyses are performed in a study in which also the long-term metabolic outcome is

assessed i.e., adiposity, insulin sensitivity and mitochondrial function, correlation analyses may give further insight in how potential changes in epigenetic mechanisms are linked to the metabolic outcome. Targeted analyses of methylation of key genes of involved pathways would be needed to further establish the involvement of DNA methylation as potential exploratory mechanism in the programming of metabolic health by the Concept. Further insight in the role of epigenetic analyses can be obtained by analyses of histone modifications (acetylation and methylation). Specific histone modifications are seen with obesity and insulin resistance in WAT of human subjects (H3K4me3 and H3K9/14c) and with mitochondrial dysfunction (H3K9me2 and H3K27me2/3) and may be a good starting point to assess the effect of the Concept on histone modifications (110-112).

We described in **Chapter 4** that postnatal Concept feeding changed mRNA expression and DNA methylation of pathways involved in WAT innervation direct after the dietary intervention. Further assessing the effect of postnatal Concept feeding on the neuronal innervation in WAT will be useful to understand the involvement of this pathway in the programming effect of the Concept. Immunohistochemical staining of Neurolipin 1 and semaphorin (Sema)3a in WAT has shown that those proteins are essential in WAT innervation (113) and thus may be changed by Concept feeding. The semaphorin mostly affected by postnatal Concept feeding was Sema6a, but its role of in WAT innervation is not clear. Immunohistochemical staining can clarify the localization of Sema6a and confirm potential changes by the Concept.

To further explore potential drivers for the programming effect of the Concept on mitochondrial function we started some *in vitro* analyses which are not finalized yet. As described in Chapter 6, serum LysoPC(18:2) levels were changed following the postnatal Concept feeding in IUGR rat offspring and the early life LysoPC(18:2) levels correlated to later life blood glucose levels. The link between blood LysoPC(18:2) levels and regulation of insulin sensitivity is still unclear and we therefore aimed to investigate this in a cell culture model. To this end we exposed differentiated 3T3L1 adipocytes to different LysoPCs i.e., 14:0, 18:0, 18:1 and 18:2, for 6 days and assessed differences in cell numbers and lipid storage with the histological analyses. The different LysoPCs were included as different effects of LysoPCs are reported depending on the chain length and saturation of the attached fatty acid (59, 114). We also included several control groups with fatty acids of which the effects are more established in literature i.e., docosahexaenoic acid (DHA), linoleic acid (LA) and palmitic acid (PA). We found that LysoPC(18:2) increased the cells numbers per well, but not the lipid storage measured as lipid droplets per well or average size of the lipid droplets (**Figure 3A – C**). Further, the effect of LysoPC(18:2) was not specific, as similar effects were seen for LysoPC(14:0), (18:0) and (18:1). We aim to further investigate the role of LysoPC(18:2) on glucose uptake and mitochondrial function

and will measure cytokine levels in medium of the exposed adipocytes.

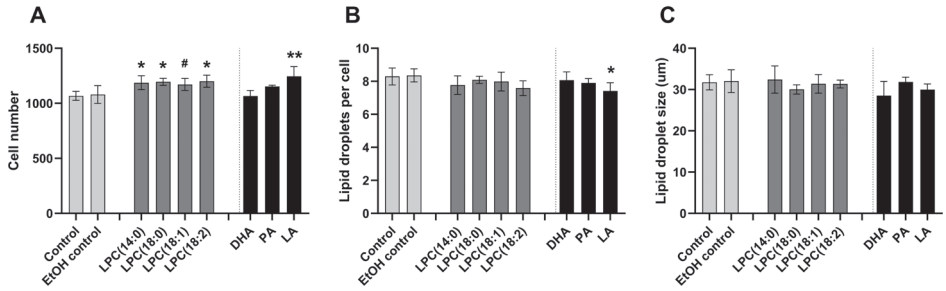

Figure 3: The effect of 6 days LysoPC(18:2) exposure of differentiated 3T3L1 cells on **A**) cell number, **B**) lipid droplets per cell and **C**) average lipid droplet size. Three days after growing to confluency, cells were differentiated to adipocytes by 24 hours incubation with 3 µM dexamethasone, 0.5 mM 3-isobutyl-1-methylxanthine and 10 µM prostaglandin I2. Cells were subsequently incubated with 20 µM LysoPCs in medium containing 1 µM insulin. Cell numbers were assessed using a Hoechst 33342 nuclei staining, and lipid storage was assessed with Bodipy. Cells were imaged using the Arrayscan (probes and arrayscan all Thermofisher, Nieuwegein, The Netherlands). Image J analyses software was used for quantification of the staining. The results of one experiment are shown, with n = 5 per condition. Differences between the EtOH-control and the different LysoPCs was tested separately from the effect of the reference fatty acids with an ANOVA. The results of two other experiments showed similar results. DHA: docosahexaenoic acid; EtOH: ethanol; LA: linoleic acid; LysoPC: lysophosphatidylcholine; PA: palmitic acid. *p<0.05; **p<0.01; # p<0.1.

Another further direction is analyzing respiration of differentiated 3T3L1 cells, a white adipocyte cell line, following 24 hours of exposure to plasma from Concept fed animals and control animals. The idea behind this approach is that bioactive components originating directly from the diet or from other tissues will be transported via the blood to the WAT, affecting WAT mitochondrial function. We performed one pilot experiment with a pooled plasma sample, but found that the model needs optimization. The measures were performed in a 96-well Bioanalyzer XF system, but the high density of the 3T3L1 cells resulted in hypoxia while measuring the maximum respiration. Using a system for 24-well plates may help to resolve this issue. Ones validated, the serum exposure setup may also be useful in clinical studies, especially when little blood sample is available.

Conclusions

In this thesis we investigated the effect of feeding a postnatal Concept diet with large, (milk)phospholipid coated lipid droplets on WAT health and on mitochondrial function in the liver, with as a broader scope to investigate the processes and mechanisms underlying programming of adult metabolic health by the postnatal diet.

The results described in this thesis show that postnatal feeding the Concept increased

levels of WAT mitochondrial function markers following an adult WSD challenge, but not directly after the early dietary intervention, indicating that WAT mitochondrial flexibility of Concept fed mice may have been preserved. Next to the effects in WAT, Concept also increased maximum respiration in the liver and partly prevented WSD-induced insulin resistance and oxidative damage. Together, the data indicated that early postnatal Concept feeding increased mitochondrial respiratory capacity in WAT and liver. These results may potentially explain (at least partly) the reduced WSD-induced adiposity in adult Concept fed mice. The results in this thesis further show that levels of mitochondrial function and WAT browning markers reduced from weaning to young adulthood in a depot-specific manner, being most pronounced in subcutaneous WAT. This data suggests that WAT health and browning is adapting in this period and may be programmed by the postnatal diet. Exploration of possible processes involved in programming showed that the Concept changed plasma LysoPC(18:2) levels in IUGR rats, what may result from differences in hepatic lipid metabolism. Further, exploratory DNA methylation and mRNA expression analyses pointed towards changes in growth and development of the WAT and changes in WAT innervation. However, follow up studies are needed to further confirm and unravel involved processes and underlying mechanisms in the programming of adult adiposity and mitochondrial function by the Concept. Ultimately such studies also include studies in humans.

References

1. Desclee de Maredsous C, Oozeer R, Barbillon P, Mary-Huard T, Delteil C, Blachier F, et al. High-Protein Exposure during Gestation or Lactation or after Weaning Has a Period-Specific Signature on Rat Pup Weight, Adiposity, Food Intake, and Glucose Homeostasis up to 6 Weeks of Age. J Nutr. 2016;146(1):21-9.
2. Lecoutre S, Deracinois B, Laborie C, Eberle D, Guinez C, Panchenko PE, et al. Depot- and sex-specific effects of maternal obesity in offspring's adipose tissue. J Endocrinol. 2016;230(1):39-53.
3. Jones AP, Simson EL, Friedman MI. Gestational undernutrition and the development of obesity in rats. J Nutr. 1984;114(8):1484-92.
4. Thompson N, Huber K, Bedurftig M, Hansen K, Miles-Chan J, Breier BH. Metabolic programming of adipose tissue structure and function in male rat offspring by prenatal undernutrition. Nutr Metab (Lond). 2014;11(1):50.
5. Owen CG, Martin RM, Whincup PH, Smith GD, Cook DG. Does breastfeeding influence risk of type 2 diabetes in later life? A quantitative analysis of published evidence. Am J Clin Nutr. 2006;84(5):1043-54.
6. Oosting A, Kegler D, Wopereis HJ, Teller IC, van de Heijning BJ, Verkade HJ, et al. Size and phospholipid coating of lipid droplets in the diet of young mice modify body fat accumulation in adulthood. Pediatr Res. 2012;72(4):362-9.
7. Oosting A, van Vlies N, Kegler D, Schipper L, Abrahamse-Berkeveld M, Ringler S, et al. Effect of dietary lipid structure in early postnatal life on mouse adipose tissue development and function in adulthood. Br J Nutr. 2014;111(2):215-26.
8. Baars A, Oosting A, Engels E, Kegler D, Kodde A, Schipper L, et al. Milk fat globule membrane coating of large lipid droplets in the diet of young mice prevents body fat accumulation in adulthood. Br J Nutr. 2016;115(11):1930-7.
9. Bodis K, Roden M. Energy metabolism of white adipose tissue and insulin resistance in humans. Eur J Clin Invest. 2018;48(11):e13017.
10. Azzu V, Vacca M, Virtue S, Allison M, Vidal-Puig A. Adipose tissue-liver cross talk in the control of whole-body metabolism: implications in non-alcoholic fatty liver disease. Gastroenterology. 2020.
11. Castro-Sepulveda M, Morio B, Tunon-Suarez M, Jannas-Vela S, Diaz-Castro F, Rieusset J, et al. The fasting-feeding metabolic transition regulates mitochondrial dynamics. FASEB J. 2021;35(10):e21891.
12. Tsilingiris D, Tzeravini E, Koliaki C, Dalamaga M, Kokkinos A. The Role of Mitochondrial Adaptation and Metabolic Flexibility in the Pathophysiology of Obesity and Insulin Resistance: an Updated Overview. Curr Obes Rep. 2021;10(3):191-213.
13. Sutherland LN, Capozzi LC, Turchinsky NJ, Bell RC, Wright DC. Time course of high-fat diet-induced reductions in adipose tissue mitochondrial proteins: potential mechanisms and the relationship to glucose intolerance. Am J Physiol Endocrinol Metab. 2008;295(5):E1076-83.
14. Crewe C, Kinter M, Szweda LI. Rapid inhibition of pyruvate dehydrogenase: an initiating event in high dietary fat-induced loss of metabolic flexibility in the heart. PLoS One. 2013;8(10):e77280.
15. Borengasser SJ, Faske J, Kang P, Blackburn ML, Badger TM, Shankar K. In utero exposure to prepregnancy maternal obesity and postweaning high-fat diet impair regulators of mitochondrial dynamics in rat placenta and offspring. Physiol Genomics. 2014;46(23):841-50.
16. Kamel MA, Helmy MH, Hanafi MY, Mahmoud SA, Abo Elfetooh H. Impaired peripheral glucose sensing in F1 offspring of diabetic pregnancy. J Physiol Biochem. 2014;70(3):685-99.

17. Oster M, Murani E, Metges CC, Ponsuksili S, Wimmers K. Transcriptional response of skeletal muscle to a low-protein gestation diet in porcine offspring accumulates in growth- and cell cycle-regulating pathways. Physiol Genomics. 2012;44(16):811-8.
18. Schottl T, Kappler L, Braun K, Fromme T, Klingenspor M. Limited mitochondrial capacity of visceral versus subcutaneous white adipocytes in male C57BL/6N mice. Endocrinology. 2015;156(3):923-33.
19. Barbatelli G, Murano I, Madsen L, Hao Q, Jimenez M, Kristiansen K, et al. The emergence of cold-induced brown adipocytes in mouse white fat depots is determined predominantly by white to brown adipocyte transdifferentiation. Am J Physiol Endocrinol Metab. 2010;298(6):E1244-53.
20. Li T, Du M, Wang H, Mao X. Milk fat globule membrane and its component phosphatidylcholine induce adipose browning both in vivo and in vitro. The Journal of nutritional biochemistry. 2020;81:108372.
21. Li T, Gao J, Du M, Song J, Mao X. Milk Fat Globule Membrane Attenuates High-Fat Diet-Induced Obesity by Inhibiting Adipogenesis and Increasing Uncoupling Protein 1 Expression in White Adipose Tissue of Mice. Nutrients. 2018;10(3).
22. Wilson-Fritch L, Nicoloro S, Chouinard M, Lazar MA, Chui PC, Leszyk J, et al. Mitochondrial remodeling in adipose tissue associated with obesity and treatment with rosiglitazone. J Clin Invest. 2004;114(9):1281-9.
23. Bertholet AM, Kazak L, Chouchani ET, Bogaczynska MG, Paranjpe I, Wainwright GL, et al. Mitochondrial Patch Clamp of Beige Adipocytes Reveals UCP1-Positive and UCP1-Negative Cells Both Exhibiting Futile Creatine Cycling. Cell Metab. 2017;25(4):811-22 e4.
24. Kim J, Piao Y, Pak YK, Chung D, Han YM, Hong JS, et al. Umbilical cord mesenchymal stromal cells affected by gestational diabetes mellitus display premature aging and mitochondrial dysfunction. Stem Cells Dev. 2015;24(5):575-86.
25. Varshney R, Das S, Trahan GD, Farriester JW, Mullen GP, Kyere-Davies G, et al. Neonatal intake of Omega-3 fatty acids enhances lipid oxidation in adipocyte precursors. iScience. 2023;26(1):105750.
26. Jo J, Gavrilova O, Pack S, Jou W, Mullen S, Sumner AE, et al. Hypertrophy and/or Hyperplasia: Dynamics of Adipose Tissue Growth. PLoS Comput Biol. 2009;5(3):e1000324.
27. Boque N, Campion J, Paternain L, Garcia-Diaz DF, Galarraga M, Portillo MP, et al. Influence of dietary macronutrient composition on adiposity and cellularity of different fat depots in Wistar rats. J Physiol Biochem. 2009;65(4):387-95.
28. Sutton EF, Gilmore LA, Dunger DB, Heijmans BT, Hivert MF, Ling C, et al. Developmental programming: State-of-the-science and future directions-Summary from a Pennington Biomedical symposium. Obesity (Silver Spring). 2016;24(5):1018-26.
29. Butruille L, Marousez L, Pourpe C, Oger F, Lecoutre S, Catheline D, et al. Maternal high-fat diet during suckling programs visceral adiposity and epigenetic regulation of adipose tissue stearoyl-CoA desaturase-1 in offspring. Int J Obes (Lond). 2019;43(12):2381-93.
30. Claycombe KJ, Uthus EO, Roemmich JN, Johnson LK, Johnson WT. Prenatal low-protein and postnatal high-fat diets induce rapid adipose tissue growth by inducing Igf2 expression in Sprague Dawley rat offspring. J Nutr. 2013;143(10):1533-9.
31. Obermann-Borst SA, Eilers PH, Tobi EW, de Jong FH, Slagboom PE, Heijmans BT, et al. Duration of breastfeeding and gender are associated with methylation of the LEPTIN gene in very young children. Pediatr Res. 2013;74(3):344-9.
32. Godfrey KM, Sheppard A, Gluckman PD, Lillycrop KA, Burdge GC, McLean C, et al. Epigenetic gene promoter methylation at birth is associated with child's later adiposity. Diabetes. 2011;60(5):1528-34.
33. Choi SW, Friso S. Epigenetics: A New Bridge between Nutrition and Health. Adv Nutr. 2010;1(1):8-16.

34. Oosting A, Harvey L, Ringler S, van Dijk G, Schipper L. Beyond ingredients: Supramolecular structure of lipid droplets in infant formula affects metabolic and brain function in mouse models. PLoS One. 2023;18(8):e0282816.
35. Armand M, Pasquier B, Andre M, Borel P, Senft M, Peyrot J, et al. Digestion and absorption of 2 fat emulsions with different droplet sizes in the human digestive tract. Am J Clin Nutr. 1999;70(6):1096-106.
36. Maljaars PW, van der Wal RJ, Wiersma T, Peters HP, Haddeman E, Masclee AA. The effect of lipid droplet size on satiety and peptide secretion is intestinal site-specific. Clin Nutr. 2012;31(4):535-42.
37. Baumgartner S, van de Heijning BJM, Acton D, Mensink RP. Infant milk fat droplet size and coating affect postprandial responses in healthy adult men: a proof-of-concept study. Eur J Clin Nutr. 2017;71(9):1108-13.
38. van den Braak C. Concept infant formula with large fat droplets coated with milk phospholipids modulates lipid digestion and absorption in vitro. ICBL; Zurich, 2017.
39. Ronda O, van de Heijning BJM, Martini IA, Koehorst M, Havinga R, Jurdzinski A, et al. An early-life diet containing large phospholipid-coated lipid globules programmes later-life postabsorptive lipid trafficking in high-fat diet- but not in low-fat diet-fed mice. Br J Nutr. 2021;125(9):961-71.
40. Burgos-Moron E, Abad-Jimenez Z, Maranon AM, Iannantuoni F, Escribano-Lopez I, Lopez-Domenech S, et al. Relationship Between Oxidative Stress, ER Stress, and Inflammation in Type 2 Diabetes: The Battle Continues. J Clin Med. 2019;8(9).
41. Chen Z, Tian R, She Z, Cai J, Li H. Role of oxidative stress in the pathogenesis of nonalcoholic fatty liver disease. Free Radic Biol Med. 2020;152:116-41.
42. Stangenberg S, Nguyen LT, Chen H, Al-Odat I, Killingsworth MC, Gosnell ME, et al. Oxidative stress, mitochondrial perturbations and fetal programming of renal disease induced by maternal smoking. Int J Biochem Cell Biol. 2015;64:81-90.
43. Simmons RA, Suponitsky-Kroyter I, Selak MA. Progressive accumulation of mitochondrial DNA mutations and decline in mitochondrial function lead to beta-cell failure. J Biol Chem. 2005;280(31):28785-91.
44. Barnes SK, Ozanne SE. Pathways linking the early environment to long-term health and lifespan. Prog Biophys Mol Biol. 2011;106(1):323-36.
45. Roden M, Shulman GI. The integrative biology of type 2 diabetes. Nature. 2019;576(7785):51-60.
46. Lyu K, Zhang Y, Zhang D, Kahn M, Ter Horst KW, Rodrigues MRS, et al. A Membrane-Bound Diacylglycerol Species Induces PKCε-Mediated Hepatic Insulin Resistance. Cell Metab. 2020;32(4):654-64 e5.
47. Tian Y, Mehta K, Jellinek MJ, Sun H, Lu W, Shi R, et al. Hepatic Phospholipid Remodeling Modulates Insulin Sensitivity and Systemic Metabolism. Adv Sci (Weinh). 2023;10(18):e2300416.
48. Preuss C, Jelenik T, Bodis K, Mussig K, Burkart V, Szendroedi J, et al. A New Targeted Lipidomics Approach Reveals Lipid Droplets in Liver, Muscle and Heart as a Repository for Diacylglycerol and Ceramide Species in Non-Alcoholic Fatty Liver. Cells. 2019;8(3).
49. van der Kolk BW, Vogelzangs N, Jocken JWE, Valsesia A, Hankemeier T, Astrup A, et al. Plasma lipid profiling of tissue-specific insulin resistance in human obesity. Int J Obes (Lond). 2018.
50. Floegel A, Stefan N, Yu Z, Muhlenbruch K, Drogan D, Joost HG, et al. Identification of serum metabolites associated with risk of type 2 diabetes using a targeted metabolomic approach. Diabetes. 2013;62(2):639-48.
51. Chang W, Hatch GM, Wang Y, Yu F, Wang M. The relationship between phospholipids and insulin resistance: From clinical to experimental studies. J Cell Mol Med. 2019;23(2):702-10.

52. Takatera A, Takeuchi A, Saiki K, Morioka I, Yokoyama N, Matsuo M. Blood lysophosphatidylcholine (LPC) levels and characteristic molecular species in neonates: prolonged low blood LPC levels in very low birth weight infants. Pediatr Res. 2007;62(4):477-82.
53. Halliday HL. Neonatal management and long-term sequelae. Best Pract Res Clin Obstet Gynaecol. 2009;23(6):871-80.
54. Nusken KD, Dotsch J, Rauh M, Rascher W, Schneider H. Uteroplacental insufficiency after bilateral uterine artery ligation in the rat: impact on postnatal glucose and lipid metabolism and evidence for metabolic programming of the offspring by sham operation. Endocrinology. 2008;149(3):1056-63.
55. Jensen RG. The composition of bovine milk lipids: January 1995 to December 2000. J Dairy Sci. 2002;85(2):295-350.
56. MacGibbon AKH, Taylor MW. Composition and Structure of Bovine Milk Lipids. In: Fox PF, McSweeney PLH (eds) Advanced Dairy Chemistry Volume 2 Lipids Springer, Boston, MA 2006:1-42.
57. Wang-Sattler R, Yu Z, Herder C, Messias AC, Floegel A, He Y, et al. Novel biomarkers for pre-diabetes identified by metabolomics. Mol Syst Biol. 2012;8:615.
58. Soga T, Ohishi T, Matsui T, Saito T, Matsumoto M, Takasaki J, et al. Lysophosphatidylcholine enhances glucose-dependent insulin secretion via an orphan G-protein-coupled receptor. Biochem Biophys Res Commun. 2005;326(4):744-51.
59. Yea K, Kim J, Yoon JH, Kwon T, Kim JH, Lee BD, et al. Lysophosphatidylcholine activates adipocyte glucose uptake and lowers blood glucose levels in murine models of diabetes. J Biol Chem. 2009;284(49):33833-40.
60. Khamoui AV, Desai M, Ross MG, Rossiter HB. Sex-specific effects of maternal and postweaning high-fat diet on skeletal muscle mitochondrial respiration. J Dev Orig Health Dis. 2018;9(6):670-7.
61. Theys N, Ahn MT, Bouckenooghe T, Reusens B, Remacle C. Maternal malnutrition programs pancreatic islet mitochondrial dysfunction in the adult offspring. The Journal of nutritional biochemistry. 2011;22(10):985-94.
62. Vidyadharan VA, Betancourt A, Smith C, Yallampalli C, Blesson CS. Prenatal Low-Protein Diet Affects Mitochondrial Structure and Function in the Skeletal Muscle of Adult Female Offspring. Nutrients. 2022;14(6).
63. Ferreira DJS, da Silva Pedroza AA, Braz GRF, da Silva-Filho RC, Lima TA, Fernandes MP, et al. Mitochondrial bioenergetics and oxidative status disruption in brainstem of weaned rats: Immediate response to maternal protein restriction. Brain Res. 2016;1642:553-61.
64. Tarry-Adkins JL, Fernandez-Twinn DS, Chen JH, Hargreaves IP, Neergheen V, Aiken CE, et al. Poor maternal nutrition and accelerated postnatal growth induces an accelerated aging phenotype and oxidative stress in skeletal muscle of male rats. Dis Model Mech. 2016;9(10):1221-9.
65. Aiken CE, Tarry-Adkins JL, Ozanne SE. Suboptimal nutrition in utero causes DNA damage and accelerated aging of the female reproductive tract. FASEB J. 2013;27(10):3959-65.
66. Jorgensen W, Gam C, Andersen JL, Schjerling P, Scheibye-Knudsen M, Mortensen OH, et al. Changed mitochondrial function by pre- and/or postpartum diet alterations in sheep. Am J Physiol Endocrinol Metab. 2009;297(6):E1349-57.
67. Stone V, Maciel August P, Scortegagna Crestani M, Brum Saccomori A, Dal Magro BM, Moura Maurmann R, et al. Adaptive effects of gestational caloric restriction in the mitochondria of Wistar rats' brain: A DOHaD approach. Int J Dev Neurosci. 2019;79:1-10.
68. Morris TJ, Vickers M, Gluckman P, Gilmour S, Affara N. Transcriptional profiling of rats subjected to gestational undernourishment: implications for the developmental variations in metabolic traits. PLoS One. 2009;4(9):e7271.

69. Salmon AB, Dorigatti J, Huber HF, Li C, Nathanielsz PW. Maternal nutrient restriction in baboon programs later-life cellular growth and respiration of cultured skin fibroblasts: a potential model for the study of aging-programming interactions. Geroscience. 2018;40(3):269-78.
70. Thompson LP, Chen L, Polster BM, Pinkas G, Song H. Prenatal hypoxia impairs cardiac mitochondrial and ventricular function in guinea pig offspring in a sex-related manner. Am J Physiol Regul Integr Comp Physiol. 2018;315(6):R1232-R41.
71. Thompson LP, Song H, Polster BM. Fetal Programming and Sexual Dimorphism of Mitochondrial Protein Expression and Activity of Hearts of Prenatally Hypoxic Guinea Pig Offspring. Oxid Med Cell Longev. 2019;2019:7210249.
72. Al-Hasan YM, Pinkas GA, Thompson LP. Prenatal Hypoxia Reduces Mitochondrial Protein Levels and Cytochrome c Oxidase Activity in Offspring Guinea Pig Hearts. Reprod Sci. 2014;21(7):883-91.
73. Hellgren KT, Premanandhan H, Quinn CJ, Trafford AW, Galli GLJ. Sex-dependent effects of developmental hypoxia on cardiac mitochondria from adult murine offspring. Free Radic Biol Med. 2021;162:490-9.
74. Dunlop K, Sarr O, Stachura N, Zhao L, Nygard K, Thompson JA, et al. Differential and Synergistic Effects of Low Birth Weight and Western Diet on Skeletal Muscle Vasculature, Mitochondrial Lipid Metabolism and Insulin Signaling in Male Guinea Pigs. Nutrients. 2021;13(12).
75. Selak MA, Storey BT, Peterside I, Simmons RA. Impaired oxidative phosphorylation in skeletal muscle of intrauterine growth-retarded rats. Am J Physiol Endocrinol Metab. 2003;285(1):E130-7.
76. Peterside IE, Selak MA, Simmons RA. Impaired oxidative phosphorylation in hepatic mitochondria in growth-retarded rats. Am J Physiol Endocrinol Metab. 2003;285(6):E1258-66.
77. Gillberg L, Ronn T, Jorgensen SW, Perfilyev A, Hjort L, Nilsson E, et al. Fasting unmasks differential fat and muscle transcriptional regulation of metabolic gene sets in low versus normal birth weight men. EBioMedicine. 2019;47:341-51.
78. Hellgren LI, Jensen RI, Waterstradt MS, Quistorff B, Lauritzen L. Acute and perinatal programming effects of a fat-rich diet on rat muscle mitochondrial function and hepatic lipid accumulation. Acta Obstet Gynecol Scand. 2014;93(11):1170-80.
79. Pileggi CA, Hedges CP, Segovia SA, Markworth JF, Durainayagam BR, Gray C, et al. Maternal High Fat Diet Alters Skeletal Muscle Mitochondrial Catalytic Activity in Adult Male Rat Offspring. Front Physiol. 2016;7:546.
80. Jousse C, Muranishi Y, Parry L, Montaurier C, Even P, Launay JM, et al. Perinatal protein malnutrition affects mitochondrial function in adult and results in a resistance to high fat diet-induced obesity. PLoS One. 2014;9(8):e104896.
81. Park KS, Kim SK, Kim MS, Cho EY, Lee JH, Lee KU, et al. Fetal and early postnatal protein malnutrition cause long-term changes in rat liver and muscle mitochondria. J Nutr. 2003;133(10):3085-90.
82. Park HK, Jin CJ, Cho YM, Park DJ, Shin CS, Park KS, et al. Changes of mitochondrial DNA content in the male offspring of protein-malnourished rats. Ann N Y Acad Sci. 2004;1011:205-16.
83. Alba-Linares JJ, Perez RF, Tejedor JR, Bastante-Rodriguez D, Ponce F, Carbonell NG, et al. Maternal obesity and gestational diabetes reprogram the methylome of offspring beyond birth by inducing epigenetic signatures in metabolic and developmental pathways. Cardiovasc Diabetol. 2023;22(1):44.
84. Puttabyatappa M, Saadat N, Elangovan VR, Dou J, Bakulski K, Padmanabhan V. Developmental programming: Impact of prenatal bisphenol-A exposure on liver and muscle transcriptome of female sheep. Toxicol Appl Pharmacol. 2022;451:116161.
85. Saadat N, Puttabyatappa M, Elangovan VR, Dou J, Ciarelli JN, Thompson RC, et al. Developmental Programming: Prenatal Testosterone Excess on Liver and Muscle Coding and Noncoding RNA in Female Sheep. Endocrinology. 2022;163(1).

86. Cossin-Sevrin N, Hsu BY, Marciau C, Viblanc VA, Ruuskanen S, Stier A. Effect of prenatal glucocorticoids and thyroid hormones on developmental plasticity of mitochondrial aerobic metabolism, growth and survival: an experimental test in wild great tits. J Exp Biol. 2022;225(9).
87. Davies KL, Camm EJ, Smith DJ, Miles J, Forhead AJ, Murray AJ, et al. Developmental programming of mitochondrial substrate metabolism in skeletal muscle of adult sheep by cortisol exposure before birth. J Dev Orig Health Dis. 2023;14(1):77-87.
88. Gyllenhammer LE, Picard M, McGill MA, Boyle KE, Vawter MP, Rasmussen JM, et al. Prospective association between maternal allostatic load during pregnancy and child mitochondrial content and bioenergetic capacity. Psychoneuroendocrinology. 2022;144:105868.
89. Li N, Guenancia C, Rigal E, Hachet O, Chollet P, Desmoulins L, et al. Short-term moderate diet restriction in adulthood can reverse oxidative, cardiovascular and metabolic alterations induced by postnatal overfeeding in mice. Scientific reports. 2016;6:30817.
90. Neto JGO, Woyames J, Andrade CBV, de Almeida MM, Fassarella LB, Atella GC, et al. Effect of Gestational Fish Oil Supplementation on Liver Metabolism and Mitochondria of Male and Female Rat Offspring Programmed by Maternal High-Fat Diet. Molecular nutrition & food research. 2023;67(8):e2200479.
91. Puttabyatappa M, Ciarelli JN, Chatoff AG, Padmanabhan V. Developmental programming: Metabolic tissue-specific changes in endoplasmic reticulum stress, mitochondrial oxidative and telomere length status induced by prenatal testosterone excess in the female sheep. Mol Cell Endocrinol. 2021;526:111207.
92. Woodman AG, Mah R, Keddie D, Noble RMN, Panahi S, Gragasin FS, et al. Prenatal iron deficiency causes sex-dependent mitochondrial dysfunction and oxidative stress in fetal rat kidneys and liver. FASEB J. 2018;32(6):3254-63.
93. Gallier S, Vocking K, Post JA, Van De Heijning B, Acton D, Van Der Beek EM, et al. A novel infant milk formula concept: Mimicking the human milk fat globule structure. Colloids and surfaces B, Biointerfaces. 2015;136:329-39.
94. Michalski MC, Briard V, Michel F, Tasson F, Poulain P. Size distribution of fat globules in human colostrum, breast milk, and infant formula. J Dairy Sci. 2005;88(6):1927-40.
95. Hornell A, Lagstrom H, Lande B, Thorsdottir I. Breastfeeding, introduction of other foods and effects on health: a systematic literature review for the 5th Nordic Nutrition Recommendations. Food Nutr Res. 2013;57.
96. Kramer MS, Kakuma R. Optimal duration of exclusive breastfeeding. Cochrane Database Syst Rev. 2012;2012(8):CD003517.
97. Harder T, Bergmann R, Kallischnigg G, Plagemann A. Duration of breastfeeding and risk of overweight: a meta-analysis. Am J Epidemiol. 2005;162(5):397-403.
98. Bouwman LMS, Fernandez-Calleja JMS, van der Stelt I, Oosting A, Keijer J, van Schothorst EM. Replacing Part of Glucose with Galactose in the Postweaning Diet Protects Female But Not Male Mice from High-Fat Diet-Induced Adiposity in Later Life. J Nutr. 2019;149(7):1140-8.
99. Bouwman LMS, Swarts HJM, Fernandez-Calleja JMS, van der Stelt I, Schols H, Oosting A, et al. Partial replacement of glucose by galactose in the post-weaning diet improves parameters of hepatic health. The Journal of nutritional biochemistry. 2019;73:108223.
100. Ng M, Fleming T, Robinson M, Thomson B, Graetz N, Margono C, et al. Global, regional, and national prevalence of overweight and obesity in children and adults during 1980-2013: a systematic analysis for the Global Burden of Disease Study 2013. Lancet. 2014;384(9945):766-81.
101. Collaboration NCDRF. Worldwide trends in body-mass index, underweight, overweight, and obesity from 1975 to 2016: a pooled analysis of 2416 population-based measurement studies in 128.9 million children, adolescents, and adults. Lancet. 2017;390(10113):2627-42.

102. Teller IC, Hoyer-Kuhn H, Bronneke H, Nosthoff-Horstmann P, Oosting A, Lippach G, et al. Complex lipid globules in early-life nutrition improve long-term metabolic phenotype in intra-uterine growth-restricted rats. Br J Nutr. 2018;120(7):763-76.
103. Breij LM, Abrahamse-Berkeveld M, Vandenplas Y, Jespers SNJ, de Mol AC, Khoo PC, et al. An infant formula with large, milk phospholipid-coated lipid droplets containing a mixture of dairy and vegetable lipids supports adequate growth and is well tolerated in healthy, term infants. Am J Clin Nutr. 2019;109(3):586-96.
104. Teoh OH, Lin TP, Abrahamse-Berkeveld M, Winokan A, Chong YS, Yap F, et al. An Infant Formula with Large, Milk Phospholipid-Coated Lipid Droplets Supports Adequate Growth and Is Well-Tolerated in Healthy, Term Asian Infants: A Randomized, Controlled Double-Blind Clinical Trial. Nutrients. 2022;14(3).
105. van Beijsterveldt I, Myers PN, Snowden SG, Ong KK, Brix S, Hokken-Koelega ACS, et al. Distinct infant feeding type-specific plasma metabolites at age 3 months associate with body composition at 2 years. Clin Nutr. 2022;41(6):1290-6.
106. Sun Y, Rahbani JF, Jedrychowski MP, Riley CL, Vidoni S, Bogoslavski D, et al. Mitochondrial TNAP controls thermogenesis by hydrolysis of phosphocreatine. Nature. 2021;593(7860):580-5.
107. Friel JK, Martin SM, Langdon M, Herzberg GR, Buettner GR. Milk from mothers of both premature and full-term infants provides better antioxidant protection than does infant formula. Pediatr Res. 2002;51(5):612-8.
108. Turoli D, Testolin G, Zanini R, Bellu R. Determination of oxidative status in breast and formula milk. Acta Paediatr. 2004;93(12):1569-74.
109. Korchazhkina O, Jones E, Czauderna M, Spencer SA. Effects of exclusive formula or breast milk feeding on oxidative stress in healthy preterm infants. Arch Dis Child. 2006;91(4):327-9.
110. Malodobra-Mazur M, Cierzniak A, Myszczyszyn A, Kaliszewski K, Dobosz T. Histone modifications influence the insulin-signaling genes and are related to insulin resistance in human adipocytes. Int J Biochem Cell Biol. 2021;137:106031.
111. Castellano-Castillo D, Ramos-Molina B, Oliva-Olivera W, Ocana-Wilhelmi L, Queipo-Ortuno MI, Cardona F. Genome Profiling of H3k4me3 Histone Modification in Human Adipose Tissue during Obesity and Insulin Resistance. Biomedicines. 2021;9(10).
112. Matilainen O, Quiros PM, Auwerx J. Mitochondria and Epigenetics - Crosstalk in Homeostasis and Stress. Trends Cell Biol. 2017;27(6):453-63.
113. Giordano A, Cesari P, Capparuccia L, Castellucci M, Cinti S. Sema3A and neuropilin-1 expression and distribution in rat white adipose tissue. J Neurocytol. 2003;32(4):345-52.
114. Hung ND, Sok DE, Kim MR. Prevention of 1-palmitoyl lysophosphatidylcholine-induced inflammation by polyunsaturated acyl lysophosphatidylcholine. Inflamm Res. 2012;61(5):473-83.

Supplementary Material:

Table 1: Programming of mitochondrial function by perinatal events.

Timing	Factor	References
Prenatal		
Diet	High fat	(1-3)
	High salt	(4)
	Low protein	(5-9)
	Caloric restriction	(2, 10-13)
	Low iron	(14)
	Methyl deficient	(15)
	Fish oil	(16)
Maternal health	Obesity	(17)
	Diabetes	(18)
	Gestational diabetes	(17, 19)
	Stress	(20)
Hormones	Testosterone	(21, 22)
	Cortisol	(23)
	Glucocorticoids	(24)
Pollution	Bisphenol A	(25)
Other	Hypoxia	(26-29)
	High/low temperature	(30)
	IUGR/low birth weight	(31-35)
Perinatal		
Diet	High fat	(36, 37)
	Low protein	(38-40)
Pollution	Smoking	(41)
Postnatal		
Diet	Overnutrition by litter size reduction	(42)
	Low n6/n3	(43)
	Coenzyme Q	(44)
Other	High temperature	(45)

Selection of the publications: Pubmed search (date 05/23/23): ((mitochondria[Title/Abstract]) OR (mitochondrial[Title/Abstract]) OR (mtDNA[Title/Abstract]) OR (oxidative phosphorylation[Title / Abstract])) AND (programming[Title/Abstract]) AND ((perinatal[Title/Abstract]) OR (prenatal[Title/ Abstract]) OR (postnatal[Title/Abstract])), subsequently checked for appropriated readouts and timing. Studies with only direct effects (for example during fetal life) were excluded. Some extra studies were added based on own Endnote folder: (19, 32-35, 37, 39, 40).

References

1. Khamoui AV, Desai M, Ross MG, Rossiter HB. Sex-specific effects of maternal and postweaning high-fat diet on skeletal muscle mitochondrial respiration. J Dev Orig Health Dis. 2018;9(6):670-7.
2. Theys N, Ahn MT, Bouckenooghe T, Reusens B, Remacle C. Maternal malnutrition programs pancreatic islet mitochondrial dysfunction in the adult offspring. The Journal of nutritional biochemistry. 2011;22(10):985-94.
3. Borengasser SJ, Faske J, Kang P, Blackburn ML, Badger TM, Shankar K. In utero exposure to prepregnancy maternal obesity and postweaning high-fat diet impair regulators of mitochondrial dynamics in rat placenta and offspring. Physiol Genomics. 2014;46(23):841-50.
4. Stocher DP, Klein CP, Saccomori AB, August PM, Martins NC, Couto PRG, et al. Maternal high-salt diet alters redox state and mitochondrial function in newborn rat offspring's brain. Br J Nutr. 2018;119(9):1003-11.
5. Vidyadharan VA, Betancourt A, Smith C, Yallampalli C, Blesson CS. Prenatal Low-Protein Diet Affects Mitochondrial Structure and Function in the Skeletal Muscle of Adult Female Offspring. Nutrients. 2022;14(6).
6. Ferreira DJS, da Silva Pedroza AA, Braz GRF, da Silva-Filho RC, Lima TA, Fernandes MP, et al. Mitochondrial bioenergetics and oxidative status disruption in brainstem of weaned rats: Immediate response to maternal protein restriction. Brain Res. 2016;1642:553-61.
7. Tarry-Adkins JL, Fernandez-Twinn DS, Chen JH, Hargreaves IP, Neergheen V, Aiken CE, et al. Poor maternal nutrition and accelerated postnatal growth induces an accelerated aging phenotype and oxidative stress in skeletal muscle of male rats. Dis Model Mech. 2016;9(10):1221-9.
8. Aiken CE, Tarry-Adkins JL, Ozanne SE. Suboptimal nutrition in utero causes DNA damage and accelerated aging of the female reproductive tract. FASEB J. 2013;27(10):3959-65.
9. Oster M, Murani E, Metges CC, Ponsuksili S, Wimmers K. Transcriptional response of skeletal muscle to a low-protein gestation diet in porcine offspring accumulates in growth- and cell cycle-regulating pathways. Physiol Genomics. 2012;44(16):811-8.
10. Jorgensen W, Gam C, Andersen JL, Schjerling P, Scheibye-Knudsen M, Mortensen OH, et al. Changed mitochondrial function by pre- and/or postpartum diet alterations in sheep. Am J Physiol Endocrinol Metab. 2009;297(6):E1349-57.
11. Stone V, Maciel August P, Scortegagna Crestani M, Brum Saccomori A, Dal Magro BM, Moura Maurmann R, et al. Adaptive effects of gestational caloric restriction in the mitochondria of Wistar rats' brain: A DOHaD approach. Int J Dev Neurosci. 2019;79:1-10.
12. Morris TJ, Vickers M, Gluckman P, Gilmour S, Affara N. Transcriptional profiling of rats subjected to gestational undernourishment: implications for the developmental variations in metabolic traits. PLoS One. 2009;4(9):e7271.
13. Salmon AB, Dorigatti J, Huber HF, Li C, Nathanielsz PW. Maternal nutrient restriction in baboon programs later-life cellular growth and respiration of cultured skin fibroblasts: a potential model for the study of aging-programming interactions. Geroscience. 2018;40(3):269-78.
14. Woodman AG, Mah R, Keddie DL, Noble RMN, Holody CD, Panahi S, et al. Perinatal iron deficiency and a high salt diet cause long-term kidney mitochondrial dysfunction and oxidative stress. Cardiovasc Res. 2020;116(1):183-92.
15. Maloney CA, Hay SM, Reid MD, Duncan G, Nicol F, Sinclair KD, et al. A methyl-deficient diet fed to rats during the pre- and peri-conception periods of development modifies the hepatic proteome in the adult offspring. Genes Nutr. 2013;8(2):181-90.

16. Neto JGO, Woyames J, Andrade CBV, de Almeida MM, Fassarella LB, Atella GC, et al. Effect of Gestational Fish Oil Supplementation on Liver Metabolism and Mitochondria of Male and Female Rat Offspring Programmed by Maternal High-Fat Diet. Molecular nutrition & food research. 2023;67(8):e2200479.
17. Alba-Linares JJ, Perez RF, Tejedor JR, Bastante-Rodriguez D, Ponce F, Carbonell NG, et al. Maternal obesity and gestational diabetes reprogram the methylome of offspring beyond birth by inducing epigenetic signatures in metabolic and developmental pathways. Cardiovasc Diabetol. 2023;22(1):44.
18. Kamel MA, Helmy MH, Hanafi MY, Mahmoud SA, Abo Elfetooh H. Impaired peripheral glucose sensing in F1 offspring of diabetic pregnancy. J Physiol Biochem. 2014;70(3):685-99.
19. Kim J, Piao Y, Pak YK, Chung D, Han YM, Hong JS, et al. Umbilical cord mesenchymal stromal cells affected by gestational diabetes mellitus display premature aging and mitochondrial dysfunction. Stem Cells Dev. 2015;24(5):575-86.
20. Gyllenhammer LE, Picard M, McGill MA, Boyle KE, Vawter MP, Rasmussen JM, et al. Prospective association between maternal allostatic load during pregnancy and child mitochondrial content and bioenergetic capacity. Psychoneuroendocrinology. 2022;144:105868.
21. Saadat N, Puttabyatappa M, Elangovan VR, Dou J, Ciarelli JN, Thompson RC, et al. Developmental Programming: Prenatal Testosterone Excess on Liver and Muscle Coding and Noncoding RNA in Female Sheep. Endocrinology. 2022;163(1).
22. Puttabyatappa M, Ciarelli JN, Chatoff AG, Padmanabhan V. Developmental programming: Metabolic tissue-specific changes in endoplasmic reticulum stress, mitochondrial oxidative and telomere length status induced by prenatal testosterone excess in the female sheep. Mol Cell Endocrinol. 2021;526:111207.
23. Davies KL, Camm EJ, Smith DJ, Miles J, Forhead AJ, Murray AJ, et al. Developmental programming of mitochondrial substrate metabolism in skeletal muscle of adult sheep by cortisol exposure before birth. J Dev Orig Health Dis. 2023;14(1):77-87.
24. Cossin-Sevrin N, Hsu BY, Marciau C, Viblanc VA, Ruuskanen S, Stier A. Effect of prenatal glucocorticoids and thyroid hormones on developmental plasticity of mitochondrial aerobic metabolism, growth and survival: an experimental test in wild great tits. J Exp Biol. 2022;225(9).
25. Puttabyatappa M, Saadat N, Elangovan VR, Dou J, Bakulski K, Padmanabhan V. Developmental programming: Impact of prenatal bisphenol-A exposure on liver and muscle transcriptome of female sheep. Toxicol Appl Pharmacol. 2022;451:116161.
26. Thompson LP, Song H, Polster BM. Fetal Programming and Sexual Dimorphism of Mitochondrial Protein Expression and Activity of Hearts of Prenatally Hypoxic Guinea Pig Offspring. Oxid Med Cell Longev. 2019;2019:7210249.
27. Thompson LP, Chen L, Polster BM, Pinkas G, Song H. Prenatal hypoxia impairs cardiac mitochondrial and ventricular function in guinea pig offspring in a sex-related manner. Am J Physiol Regul Integr Comp Physiol. 2018;315(6):R1232-R41.
28. Al-Hasan YM, Pinkas GA, Thompson LP. Prenatal Hypoxia Reduces Mitochondrial Protein Levels and Cytochrome c Oxidase Activity in Offspring Guinea Pig Hearts. Reprod Sci. 2014;21(7):883-91.
29. Hellgren KT, Premanandhan H, Quinn CJ, Trafford AW, Galli GLJ. Sex-dependent effects of developmental hypoxia on cardiac mitochondria from adult murine offspring. Free Radic Biol Med. 2021;162:490-9.
30. Stier A, Monaghan P, Metcalfe NB. Experimental demonstration of prenatal programming of mitochondrial aerobic metabolism lasting until adulthood. Proc Biol Sci. 2022;289(1970):20212679.
31. Dunlop K, Sarr O, Stachura N, Zhao L, Nygard K, Thompson JA, et al. Differential and Synergistic Effects of Low Birth Weight and Western Diet on Skeletal Muscle Vasculature, Mitochondrial Lipid Metabolism and Insulin Signaling in Male Guinea Pigs. Nutrients. 2021;13(12).

32. Simmons RA, Suponitsky-Kroyter I, Selak MA. Progressive accumulation of mitochondrial DNA mutations and decline in mitochondrial function lead to beta-cell failure. J Biol Chem. 2005;280(31):28785-91.
33. Selak MA, Storey BT, Peterside I, Simmons RA. Impaired oxidative phosphorylation in skeletal muscle of intrauterine growth-retarded rats. Am J Physiol Endocrinol Metab. 2003;285(1):E130-7.
34. Peterside IE, Selak MA, Simmons RA. Impaired oxidative phosphorylation in hepatic mitochondria in growth-retarded rats. Am J Physiol Endocrinol Metab. 2003;285(6):E1258-66.
35. Gillberg L, Ronn T, Jorgensen SW, Perfilyev A, Hjort L, Nilsson E, et al. Fasting unmasks differential fat and muscle transcriptional regulation of metabolic gene sets in low versus normal birth weight men. EBioMedicine. 2019;47:341-51.
36. Hellgren LI, Jensen RI, Waterstradt MS, Quistorff B, Lauritzen L. Acute and perinatal programming effects of a fat-rich diet on rat muscle mitochondrial function and hepatic lipid accumulation. Acta Obstet Gynecol Scand. 2014;93(11):1170-80.
37. Pileggi CA, Hedges CP, Segovia SA, Markworth JF, Durainayagam BR, Gray C, et al. Maternal High Fat Diet Alters Skeletal Muscle Mitochondrial Catalytic Activity in Adult Male Rat Offspring. Front Physiol. 2016;7:546.
38. Jousse C, Muranishi Y, Parry L, Montaurier C, Even P, Launay JM, et al. Perinatal protein malnutrition affects mitochondrial function in adult and results in a resistance to high fat diet-induced obesity. PLoS One. 2014;9(8):e104896.
39. Park KS, Kim SK, Kim MS, Cho EY, Lee JH, Lee KU, et al. Fetal and early postnatal protein malnutrition cause long-term changes in rat liver and muscle mitochondria. J Nutr. 2003;133(10):3085-90.
40. Park HK, Jin CJ, Cho YM, Park DJ, Shin CS, Park KS, et al. Changes of mitochondrial DNA content in the male offspring of protein-malnourished rats. Ann N Y Acad Sci. 2004;1011:205-16.
41. Stangenberg S, Nguyen LT, Chen H, Al-Odat I, Killingsworth MC, Gosnell ME, et al. Oxidative stress, mitochondrial perturbations and fetal programming of renal disease induced by maternal smoking. Int J Biochem Cell Biol. 2015;64:81-90.
42. Li N, Guenancia C, Rigal E, Hachet O, Chollet P, Desmoulins L, et al. Short-term moderate diet restriction in adulthood can reverse oxidative, cardiovascular and metabolic alterations induced by postnatal overfeeding in mice. Scientific reports. 2016;6:30817.
43. Varshney R, Das S, Trahan GD, Farriester JW, Mullen GP, Kyere-Davies G, et al. Neonatal intake of Omega-3 fatty acids enhances lipid oxidation in adipocyte precursors. iScience. 2023;26(1):105750.
44. Tarry-Adkins JL, Fernandez-Twinn DS, Chen JH, Hargreaves IP, Martin-Gronert MS, McConnell JM, et al. Nutritional programming of coenzyme Q: potential for prevention and intervention? FASEB J. 2014;28(12):5398-405.
45. Ton R, Stier A, Cooper CE, Griffith SC. Effects of Heat Waves During Post-natal Development on Mitochondrial and Whole Body Physiology: An Experimental Study in Zebra Finches. Front Physiol. 2021;12:661670.

Summary and Samenvatting

Summary

The global prevalence of overweight and obesity has reached epidemic proportions and is considered a major public health threat. The causes of obesity are multifactorial and several contributing factors have been identified in early life, such as suboptimal fetal growth and maternal overnutrition during pregnancy. Nutrition in early life has been suggested to play an important role in setting the risk of metabolic health outcomes in later life, a concept called nutritional programming. Breastfeeding is associated with a differential growth and adiposity development and a protective effect on childhood overweight and adverse metabolic health outcomes. One contributing factor may be the distinctly different supramolecular structure of the human milk fat globule compared to lipid droplets in infant formula. Indeed, a postnatal diet with large, (milk)phospholipid coated lipid droplets i.e., mimicking some of the features of the human milk fat globule, previously showed to reduced adult adiposity in a mouse model for nutritional programming. Alterations in white adipose tissue (WAT) function and mitochondrial function were anticipated to contribute to these programming effects. Hence, in this thesis I investigated the effect of a postnatal diet containing large, (milk)phospholipid coated lipid droplets (Nuturis®, called Concept in this thesis) on WAT function and mitochondrial function, including the processes underlying and related alterations in the liver. **Chapter 1** provides a general introduction on early life programming of later life metabolic health with a particular focus on the role of WAT, mitochondrial function and liver development.

In **Chapter 2**, we examined the effect of early postnatal Concept feeding on markers of mitochondrial density and oxidative capacity in the visceral, retroperitoneal (RP) WAT of adult mice, with the aim to investigate potential programming effects of the Concept on WAT mitochondrial function. We showed that early postnatal Concept feeding increased levels of mitochondrial density markers i.e., citrate synthase (CS) and mitochondrial DNA (mtDNA), and protein expression of mitochondrial cytochrome c oxidase subunit I, a subunit of complex IV of the oxidative phosphorylation (OXPHOS) in RP WAT, following a western style diet (WSD) challenge in adulthood. Together, this may indicate an increased oxidative capacity in WAT of adult mice challenged with a WSD after being fed Concept in early postnatal life, potentially explaining the reduced adiposity observed in this and previous studies. However, in **Chapter 4**, we learned that mitochondrial density, measured as CS and mtDNA levels, was unaffected in epididymal (EPI), RP and inguinal (ING) WAT directly following the postnatal dietary intervention with the Concept. Interestingly, we did observe a reduced protein expression of OXPHOS subunits in the visceral (EPI and RP) WAT depots at that timepoint. Together, our results

indicated that the higher levels of mitochondrial density and oxidative markers in WAT of the mice fed Concept in early postnatal life followed by a WSD challenge in adulthood, were not the consequence of consistently increased levels of those markers from early life onwards, but rather a response to the WSD challenge in adulthood i.e., suggesting preserved mitochondrial flexibility. This increased mitochondrial flexibility may potentially explain the reduced WSD-induced adiposity observed in Concept fed mice.

In **Chapter 3**, the developmental trajectory of different WAT depots from weaning until young adulthood was investigated in a mouse model for nutritional programming. We showed that levels of markers for mitochondrial density i.e., CS activity and mtDNA, and OXPHOS subunits were higher in subcutaneous (ING) WAT compared to the tested visceral (EPI and RP) WAT depots and that mitochondrial density substantially declined from weaning until young adulthood. This decline in mitochondrial function markers was most pronounced in ING WAT, where it was paralleled by a decline in protein expression of OXPHOS subunits of complexes I, II and III and a reduction in brown adipocyte marker expression, indicating reduction of oxidative capacity and whitening of this WAT depot over time. Interestingly, in **Chapter 4** we observed that postnatal Concept feeding increased OXPHOS protein expression in ING WAT directly after the postnatal dietary intervention period, which may reflect a difference in thermogenic activity in ING WAT of Concept mice. Together, the substantial reduction in mitochondrial function and WAT browning markers over time suggests a window to program WAT function and browning in early postnatal life.

Mechanisms possibly explaining the Concept-associated differences in mitochondrial function markers include, next to the above-mentioned WAT browning, programming of adipocyte stem cells and epigenetic mechanisms i.e., mechanisms regulating gene expression via structural adaptations to chromosomal regions. In **Chapter 4**, we explored the possible involvement of DNA methylation, an example of an epigenetic mechanism, as underlying mechanism explaining the observed programming effects of the Concept. We showed that postnatal Concept feeding elevated total DNA methylation and increased methylation of pathways involved in growth and development of cells and tissues in EPI WAT. Despite the exploratory nature of these findings, this data suggests methylation might be one of the possible underlying processes for the observed long-term programming impact.

The improved mitochondrial oxidative capacity in WAT of the postnatal Concept fed mice may affect hepatic lipid and energy metabolisms, as impaired WAT health may lead to ectopic fat deposition in the liver, a step in the development of type 2 diabetes (T2D)

and non-alcoholic fatty liver disease (NAFLD). Hence, **Chapter 5** describes our research investigating the effect of postnatal Concept feeding on mitochondrial function in the liver in a mouse model for postnatal nutritional programming. Early postnatal Concept feeding increased maximum hepatic oxidative capacity linked to the TCA cycle direct after the postnatal diet intervention and the maximum hepatic oxidative capacity linked to β-oxidation following a WSD challenge in adulthood, together indicating programming of the maximum oxidative capacity in the liver in the Concept fed mice. We postulate that the improved oxidative capacity may have contributed to the reduced WSD-induced hyperinsulinemia and insulin resistance and cytosolic accumulation of 18:1 fatty acids containing diacylglycerols in the liver observed in Concept fed mice.

Phospholipid levels are disturbed in blood and liver with T2D and NAFLD and may indicate a disturbed phospholipid metabolism in the liver or skeletal muscle. In **Chapter 6**, we showed that levels of Lysophosphatidylcholine (LysoPC)18:2, a hydrolyzed phospholipid, were reduced in serum of young IUGR rat offspring, direct after the early postnatal dietary intervention period, and that those levels were restored by postnatal Concept compared to Control feeding. Furthermore, the LysoPC(18:2) levels in the young IUGR rat offspring correlated to fasted blood glucose levels later in life, indicating that LysoPC(18:2) levels may be a predictive biomarker for later life glucose levels. However, further research is needed to understand the link between this specific LysoPC and the glucose metabolism.

To conclude, in this thesis we found indications that exposure to a postnatal diet with large, (milk)phospholipid coated lipid droplets in early life has a lasting impact on mitochondrial oxidative capacity in later life. This improved mitochondrial oxidative capacity may (partly) explain previous described beneficial effects of postnatal Concept feeding on adult adiposity and metabolic health outcomes. Underlying processes and mechanisms involved in the programming effect of the Concept are to be elucidated but based on our initial explorations, these may include epigenetic mechanisms and changes to cell populations (WAT browning) and the hepatic (phospho)lipid metabolism.

Nederlandse samenvatting

De prevalentie van overgewicht en obesitas heeft wereldwijd epidemische proporties aangenomen en wordt beschouwd als een grote bedreiging voor de volksgezondheid. Er zijn meerdere oorzaken die bijdragen aan het ontstaan van obesitas, waaronder factoren in het vroege leven zoals overvoeding van de moeder tijdens de zwangerschap en suboptimale groei tijdens het prenatale en vroege postnatale leven. Voeding in het vroege leven kan het risico op metabole ziekten later in het leven beïnvloeden, een concept dat nutritionele programmering wordt genoemd. Borstvoeding wordt bijvoorbeeld geassocieerd met een andere groei en ontwikkeling van wit vetweefsel dan flesvoeding, en met een vermindering van het risico op overgewicht bij kinderen en andere nadelige metabole condities. Er is verondersteld dat de duidelijk andere supramoleculaire structuur van de vetdruppels in humane melk ten opzichte van de vetdruppels in standaard zuigelingenvoedingen mogelijk kan bijdragen aan deze beschermende effecten van borstvoeding. Inderdaad, in een muismodel voor nutritionele programmering is eerder aangetoond dat een postnataal dieet met grote, (melk)fosfolipide gecoate vetdruppels, waarmee een aantal eigenschappen van de vetdruppels in humane melk worden nagebootst, de vetstapeling in volwassenheid verminderde. Aangenomen werd dat veranderingen in de functie van wit vetweefsel en mitochondriën bijdragen aan deze programmeringseffecten. Daarom heb ik in dit proefschrift onderzocht wat het effect is van een postnataal dieet met grote vetdruppels omgeven door melk fosfolipiden (Nuturis®, in dit proefschrift Concept genoemd) op de functie van wit vetweefsel en mitochondriën, evenals de onderliggende processen en gerelateerde veranderingen in de lever. **Hoofdstuk 1** is een algemene inleiding over de programmering van de metabole gezondheid in het latere leven met als focus de rol van wit vetweefsel, mitochondriële functie en leverontwikkeling.

In **hoofdstuk 2** onderzochten we het effect van het Concept in het vroege postnatale dieet op markers van mitochondriële dichtheid en oxidatieve capaciteit in het retroperitoneale (RP), viscerale vetweefsel (buik vetweefsel) van volwassen muizen. Het doel van deze studie was om mogelijke programmeereffecten van het Concept op de mitochondriële functie van wit vetweefsel te onderzoeken. Daarom werd het effect van het Concept vergeleken met dat van een controle dieet met kleine vetdruppels, zonder fosfolipiden, zoals in standaard zuigelingenvoedingen. In deze studie toonden we aan dat het Concept in het vroege postnatale dieet in RP-vetweefsel een verhoging gaf van indicatoren voor mitochondriële dichtheid, zoals citraat synthase (CS) en mitochondrieel DNA (mtDNA), en een verhoging van eiwitexpressie van mitochondrieel cytochroom c-oxidase subunit I, een onderdeel van complex IV van de oxidatieve fosforylering

(OXPHOS), nadat de volwassen dieren enkele weken een westers dieet (WSD; hoog in vet) te eten kregen. Samen kunnen deze resultaten wijzen op een verhoogde oxidatieve capaciteit in vetweefsel van volwassen muizen die worden uitgedaagd met een WSD nadat ze in het vroege postnatale leven het Concept dieet hebben gekregen. Dit verklaart mogelijk de verminderde vetopslag van de Concept dieren zoals in deze en eerdere studies is gevonden. In **hoofdstuk 4** leerden we echter dat de mitochondriële dichtheid, gemeten als CS en mtDNA niveaus, direct na de postnatale voedingsinterventie met het Concept niet was veranderd in het epididymale (EPI), RP en inguinale (ING) vetweefsel. Interessant is dat we op datzelfde tijdstip, in het viscerale (EPI en RP) vetweefsel, een verminderde eiwitexpressie van sub-eenheden van OXPHOS hebben waargenomen. Deze resultaten kunnen er samen op wijzen dat de hogere hoeveelheden van de markers voor mitochondriële dichtheid en oxidatieve capaciteit in het vetweefsel van de volwassen muizen, die het Concept kregen in het vroege postnatale leven, niet het gevolg waren van consistent verhoogde hoeveelheden van de markers vanuit het vroege leven. Het ligt meer voor de hand dat dit een reactie was op het WSD in het volwassen leven en dit suggereert dat de mitochondriële flexibiliteit in de Concept dieren behouden is gebleven. Deze verhoogde mitochondriële flexibiliteit kan mogelijk de verminderde WSD-geïnduceerde vetstapeling verklaren die wordt waargenomen bij Concept gevoede muizen.

In **hoofdstuk 3** is het ontwikkelingstraject van verschillende vetdepots onderzocht, tijdens de leeftijd van spenen tot jongvolwassenheid, in een muismodel voor nutritionele programmering. We lieten in dit hoofdstuk zien dat niveaus van markers voor mitochondriële dichtheid, d.w.z. CS-activiteit en mtDNA, en OXPHOS-sub-eenheden hoger waren in subcutaan vetweefsel (onderhuids, ING-vetweefsel) in vergelijking met viscerale vetweefsel (EPI- en RP-vetdepots) en dat de mitochondriële dichtheid aanzienlijk daalde vanaf spenen naar jong volwassenheid. Deze afname van mitochondriële functiemarkers was het meest uitgesproken in ING-vetweefsel, waar het gepaard ging met een afname van de eiwitexpressie van OXPHOS-sub-eenheden van complexen I, II en III en een vermindering van de expressie van markers voor bruine vetcellen (die warmte kunnen produceren). Samen wijst dit op vermindering van de oxidatieve capaciteit en een overgang naar een witter fenotype van dit vetdepot vanaf spenen naar jonge volwassenheid. Interessant is dat we in **hoofdstuk 4** hebben gevonden dat het Concept in het postnatale dieet de OXPHOS-eiwitexpressie in ING-vetweefsel direct na de postnatale interventieperiode verhoogde, dit kan duiden op een verschil in thermogene activiteit in het ING-vetweefsel van de Concept muizen. De aanzienlijke verlaging van de markers voor mitochondriële functie en markers voor

de bruining van wit vetweefsel, over de tijd, suggereren samen dat er in het vroege postnatale leven een venster is om de functie van vetweefsel te programmeren.

Mechanismen die mogelijk de Concept-geassocieerde verschillen in mitochondriële functiemarkers verklaren, omvatten, naast het bovengenoemde bruinen van wit vetweefsel, programmering van stamcellen van het vetweefsel en epigenetische mechanismen, d.w.z. mechanismen die genexpressie reguleren via structurele aanpassingen aan chromosomale regio's. In **hoofdstuk 4** onderzochten we de mogelijke betrokkenheid van DNA-methylatie, een voorbeeld van een epigenetisch mechanisme, als onderliggend mechanisme dat de gevonden programmeereffecten van het Concept zou kunnen verklaren. We toonden aan dat het Concept in het postnatale dieet de totale DNA-methylatie in EPI-vetweefsel verhoogde en ook specifieke de methylatie van netwerken van genen die betrokken zijn bij groei en ontwikkeling van cellen en weefsels in het EPI vetweefsel. Ondanks dat de opzet van de studie harde conclusies niet toelaat, suggereren deze bevindingen wel dat methylatie een van de mogelijke onderliggende processen kan zijn voor de waargenomen programmeringseffecten van het Concept op de lange termijn.

De verbeterde mitochondriële oxidatieve capaciteit in wit vetweefsel van de muizen die het Concept kregen in postnatale dieet kan het lipide en energiemetabolisme in de lever beïnvloeden. Een verminderde gezondheid van het wit vetweefsel kan leiden tot vetafzetting in de lever, een stap in de ontwikkeling van type 2 diabetes (T2D; ouderdomssuikerziekte) en niet-alcoholische leververvetting (NAFLD). Daarom onderzochten we in **hoofdstuk 5**, in een muismodel voor postnatale nutritionele programmering, het effect van het Concept in het postnatale dieet op de mitochondriële functie in de lever.

Het Concept in het vroege postnatale dieet verhoogde, in de lever, de maximale oxidatieve capaciteit gekoppeld aan de citroenzuurcyclus direct na de postnatale dieetinterventie en de maximale oxidatieve capaciteit gekoppeld aan de vetzuur-oxidatie in de volwassen muizen die enkele weken uitgedaagd waren met een WSD. Deze resultaten wijzen samen op de programmering van de maximale oxidatieve capaciteit in de lever in de Concept gevoede muizen. We gaan ervan uit dat de verbeterde oxidatieve capaciteit kan hebben bijgedragen aan de eerder waargenomen verminderde WSD-geïnduceerde hyperinsulinemie en insuline resistentie, als ook de vermindering van de stapeling van diacylglycerolen die 18:1-vetzuren bevatten in het cytosol van levercellen, in de Concept gevoede muizen.

De hoeveelheid fosfolipiden in het bloed en de lever van mensen met T2D en NAFDL zijn verstoord, wat kan wijzen op een verstoord fosfolipidemetabolisme in de

lever of de skeletspieren. In **hoofdstuk 6** laten we zien dat de hoeveelheid van het gehydrolyseerd fosfolipide, Lysofosfatidylcholine (LysoPC) 18:2, direct na de postnatale voedingsinterventie verlaagd was in serum van jonge IUGR-ratten. We lieten ook zien dat de hoeveelheid LysoPC(18:2) in het serum werd hersteld door het Concept in het postnatale dieet. Bovendien correleerden de hoeveelheden LysoPC(18:2) in het serum van de jonge IUGR-ratten met de nuchtere bloedglucosespiegels later in het leven. Dit geeft aan dat de hoeveelheid LysoPC (18: 2) in het serum in het vroege leven de bloedglucosespiegels in het latere leven kan voorspellen, m.a.w. een biologische marker kan zijn voor glucosespiegels in het latere leven. Verder onderzoek is echter nodig om het verband tussen deze specifieke LysoPC en het glucosemetabolisme te begrijpen.
Concluderend, we vonden in dit proefschrift duidelijke aanwijzingen dat blootstelling aan een postnataal dieet met grote, vetdruppels omgeven door (melk)fosfolipiden in het vroege leven een blijvende invloed heeft op de mitochondriële oxidatieve capaciteit op latere leeftijd. Deze verbeterde mitochondriële oxidatieve capaciteit kan (gedeeltelijk) de eerder beschreven gunstige effecten van het Concept in het postnatale dieet op volwassen vetstapeling en metabole gezondheidsresultaten verklaren. Onderliggende processen en mechanismen die betrokken zijn bij het programmeringseffect van het Concept moeten verder worden onderzocht. Echter, de resultaten van onze eerste verkennende experimenten suggereren dat epigenetische mechanismen, veranderingen in celpopulaties (bruining van wit vetweefsel) en veranderingen van het (fosfo)lipiden metabolisme in de lever hieraan mogelijk bijdragen.

Appendices

Dankwoord

Na een lange periode van onderzoek, schrijven en herschrijven ben ik dan aan het laatste deel van mijn proefschrift aangekomen, het dankwoord. In ons team bij Danone hebben we lange tijd al onze nutritional programming studies een ruimte-naam gegeven. Om in dat thema te blijven, mijn promotietraject was een net als een ruimtereis een reis die ik niet alleen heb gemaakt. En ook de eindbestemming had soms wat weg van de maan, ver weg en bijna onbereikbaar. Maar het was ook een hele mooie reis die ik met veel plezier heb gemaakt en die een succes werd door de bijdrage, hulp, begeleiding en aanmoediging van een heleboel mensen die ik allemaal hartelijk wil bedanken.

Beste Jaap en Eline, hartelijk dank voor de kans die ik van jullie heb gekregen. Jullie waren fijne medereizigers! Jaap, al voordat mijn PhD officieel begon hadden wij regelmatig overleg over projecten. Je had snel door dat ik de ambitie had om een PhD te gaan doen en jouw support en inzet om dit mogelijk te maken zijn essentieel geweest. Onze meetings waren altijd erg inspirerend en je snelheid van reviewen ongeëvenaard, alhoewel ik soms wel eens hoopte dat het wat langer duurde voordat manuscripten weer op mijn bureau landden. Eline, ook al begon deze ruimtereis officieel pas eind 2019, al in 2010 begon mijn ruimtewandeling in jouw team. Wij wisten elkaar altijd te vinden op het onderzoek naar de ontwikkeling van wit vetweefsel en epigenetica en we hadden steeds grootse plannen. Alhoewel jij tijdens de reis een aantal keer bent uitgestapt bij verschillende ruimtestations ben ik heel blij dat wij deze reis samen hebben kunnen afronden! Ik heb van jullie beide veel geleerd over wetenschappelijk schrijven, het opstellen van goede onderzoeksvragen en creatief wetenschappelijk denken en heb jullie support zeker ook in de laatste paar jaar erg gewaardeerd.

Ik wil ook graag mijn andere medereizigers en onofficiële copromotors door de jaren heen, Annemarie, Bert en Marieke heel hartelijk bedanken de rol in mijn promotie traject. Annemarie, meer dan 12 jaar geleden bespraken we voor het eerst mijn ambitie voor een PhD traject. Het was niet altijd een makkelijk traject, ook niet voor jou als teamleider, maar ik waardeer erg dat je altijd de mogelijkheden hebt gecreëerd voor persoonlijke ontwikkeling en om aan projecten te werken die uiteindelijk in dit proefschrift terecht zijn gekomen. Bert, ook al wilde je richting je pensioen geen officiële rol meer als copromotor, ik heb je in de jaren dat ik in jouw team zat zeker zo gezien. Je hebt je hard gemaakt voor het officieel maken van mijn PhD traject (tijd voor boter bij de vis) en je inhoudelijke input voor de laatste projecten en tijdens het schrijven heb ik erg gewaardeerd! Marieke, de geitjes van mijn opa gaven ons contact altijd al iets extra's, maar het was echt heel fijn om na mijn ziekteverlof en na het vertrek van Bert en Eline bij Danone, samen met jou aan de afronding van dit proefschrift te werken. Je input

tijdens het schrijven was altijd grondig en hielp me altijd om mijn stukken verder aan te scherpen. Ik heb dat samen met je positieve insteek en humor erg gewaardeerd! Het lijkt er op dat het met deze PhD beter afloopt, dan met de geitjes en jullie appelboom!
I would also like to thank the assessment committee, Andries Kalsbeek, Marie-Caroline Michalski, Mariona Palou March en Renger Witkamp, for reviewing my thesis. I look forward meeting you at my PhD defense to discuss this thesis.
Lieve Laura en Saskia, wat superfijn dat jullie mijn paranimfen zijn! Laura, het was altijd al superfijn om jou als collega te hebben, maar tijdens de corona jaren waren onze digitale thee-momenten echt hoogtepunten! Je belangstelling en aandacht in de periode dat ik ziek was en de lastige weg terug was echt heel fijn en hielp om er doorheen te komen. Onze wandeling bij Austerlitz zal ik niet snel vergeten, we stonden echt veel te lang in de regen na te praten, maar het was echt top! Sas, wij zijn echt nooit uitgepraat en kunnen enorm veel lol hebben samen, maar ook goede gesprekken! Je digitale rondleiding door je nieuwe huis was blijkbaar niet echt onvergetelijk, maar toch fijn dat je de moeite nam. Je aanmoediging en adviezen voor mijn promotietraject waren echt heel fijn en onze dinertjes in Utrecht en de Escape rooms met de rest van de Escape enthousiastelingen onvergetelijk!
I would also like to thank all the coauthors for their contribution. A special thank you for Maryam Rakhshanderhoo and Dominik Pesta for finishing the submission and revision of Chapters 5 and 6 during my sick leave. I would also like to thank Eefje Engels and Tomas Jelenik for the nice collaboration for chapter 5, I wish you both all the best for the rest of your carriers! Also, a special thank you for Martijn Breeuwsma for your help with the analyses of the 3T3L1 experiments, I'm happy that part of your work is shared in the discussion of this thesis!
Laura Buelens, Nienke en Atanaska, bedankt voor jullie support, alle fijne gesprekken, lunchwandelingen, escape rooms en fietstochtjes. Ook jullie bezoek, berichtjes en telefoontjes tijdens mijn ziekteverlof heb ik erg gewaardeerd. Heel fijn dat jullie deze reis in de buurt waren en zo vaak een luisterend oor waren of gewoon tijd hadden voor gezelligheid!
Ook alle andere Danoners, oud-Danoners, team leden door de jaren heen en purple 4 collega's, heel erg bedankt voor jullie bijdrage. Speciale dank ook voor het lunch-team, het is altijd gezellig om bij jullie aan te schuiven!
Esther, ik wil ook jou bedanken voor je support en vriendschap. Met name op het begin van deze reis is jouw aanmoediging erg waardevol geweest! Het was heel leuk en leerzaam om het eerste hoofdstuk met jou hulp te schrijven en ook om samen Smart op te zetten. Het is altijd supergezellig om je weer te zien! En ik moet toegeven, je muziek is verrassend mooi. Je muzikale carrière wordt vast een succes!

Ook mijn andere Maastricht vrienden, Liesbeth, Karen en Ruth, heel erg bedankt voor alle fijne momenten de afgelopen jaren. We zien elkaar niet heel vaak, maar het is altijd erg gezellig om weer bij te praten!
Janneke, Femke en Machelina, heel erg bedankt voor jullie vriendschap en support de afgelopen jaren. Het is altijd fijn om met jullie af te spreken voor een etentje, wandeling, fietstocht of gewoon een kop thee. Laten we nog veel van zulke gezellige momenten plannen! (Oke, Janneke misschien geen rondjes Veerse meer bij 30 graden).
Lieve familie, papa, mama, Marieke, Ewout, Eelco, Celine, Marten en Hanneke, jullie aanmoedigingen, steun en humor is heel waardevol. Ik denk niet dat er een betere voorbereiding is voor een promotie traject dan de lange wandelingen en de fietsvakanties van vroeger, papa (zelfs die fietskar in het water, crisismanagement)! En mama, ik moet er vaak om lachen maar vind het ook leuk dat u trots op me bent! Ook alle tijd met jullie, Maud, Boaz, Floor, Jens, Tobias, Stef en Aron is altijd leuk en gezellig. Samen bakken, naar Sela, winkelen, spelletjes doen, of gewoon genieten van hoe blij jullie zijn met simpele dingen (zoals een vliegtuig dat ’s nachts van het plafond valt)! Het is fijn om naast mijn werk een sterk netwerk te hebben dat mij deze jaren gesteund heeft waardoor ik er ook vaak bij bepaald werd wat echt belangrijk is. Heel erg bedankt voor alles!

List of Publications

Full papers

Jelenik T., **Kodde A.,** Pesta D., Phielix E., Oosting A., Rohbeck E., Dewidar B., Mastrototaro L., Trenkamp S., Keijer J., Beek van der E.M., Roden M.; Dietary lipid droplet structure in postnatal life improves hepatic energy and lipid metabolism in a mouse model for postnatal programming, Pharmacol Res, 2022; 179:106193.

Kodde A., Mischke M., Rakhshandehroo M., Voggel J., Fink G., Nüsken E., Rauh M., Beek van der E.M., Dötsch J., Nüsken K.D.; The effect of dietary lipid quality in early life on serum LysoPC(18:2) levels and their association with adult blood glucose levels in intrauterine growth restricted rats, Nutr Metab (Lond), 2021; 18(1):101.

Kodde F.D., Rakhshandehroo M., Beek van der E.M., M.H. Oosterveer; Infant formula for reducing the risk of developing non-alcoholic fatty liver disease, 2021, WO2021099632, patent.

Kodde A., Engels E., Oosting A., Limpt van K., Beek van der E.M., Keijer J.; Maturation of white adipose tissue function in C57BL/6j mice from weaning to young adulthood, Front Physiol, 2019; 10:836.

Carlin G., Chaumontet C., Blachier F., Barbillon P., Darcel N., Delteil C., Beek van der E.M., **Kodde A.,** Heijning van de B., Tome D., Davila A.M.; Parinatal exposure of rats to a maternal diet with varying protein quantity and quality affects the risk of overweight in female adult offspring, J Nutr Biochem, 2020; 79:108333.

Carlin G., Chaumontet C., Blachier F., Barbillon P., Darcel N., Blais A., Delteil C., Guillin F.M., Blat S., Beek van der E.M., **Kodde A.,** Tome D., Davila A.M.; Maternal high-protein diet during pregnancy modifies rat offspring body weight and insulin signalling but not macronutrient preference in adulthood, Nutrients, 2019; 11(96).

Kodde A., Beek van der E.M., Phielix E., Engels E., Schipper L., Oosting A.; Supramolecular structure of dietary fats in early life modulates expression of markers for mitochondrial content and capacity in adipose tissue of adult mice, Nutr Metab (Lond), 2017; 14:37.

Baars A., Oosting A., Engels E., Kegler D., **Kodde A.**, Schipper L., Verkade H.J., Beek van der E.M.; Milk fat globule membrane coating of large lipid droplets in the diet of young mice prevents body fat accumulation in adulthood, Br J Nutr, 2016; 115(11):1930.

Oosting A., **Kodde F.D.**, Abrahamse-Berkeveld M., Beek van der E.M., Infant nutrition with lipid globules to increase energy expenditure and metabolic flexibility later in life, 2013, WO2014058318 A1, patent.

Maljaars P.W., Geraerdts M., Peters H., **Kodde A.**, Haddema E., Troost F., Masclee A., Lenght and site of small intestine exposed to fat influences hunger and food intake, Br J Nutr; 2011; 106(10):1609-15.

Hamer H., Jonkers D., Renes I.B., Vanhoutvin S.A., **Kodde A.**, Troost F.J., Venema K., Brummer R.J., Butyrate enamas do not affect human colonic MUC2 and TFF3 expression, Eur J Gastroenterol Hepatol, 2010; 22(9):1134-40.

Vanhoutvin S., Troost F.J., Lindsey P.J., Koek G.H., Jonkers D., **Kodde A.**, Venema K., Brummer R.J., Butyrate-induced transcriptional changes in human colonic mucosa, Plos ONE, 2009; 4(8):e6759.

Hamer H.M, Jonkers D.M.A.E., Loof A., Vanhoutvin S., Troost F.J., Venema K., **Kodde A.**, Koek G.H., Schipper R.G., Heerde van W.L., Brummer R.J., Analyses of human colonic mucus obtained by an *in vivo* sampling technique, Dig Liver Dis, 2009; 41(8):559-64.

Hamer H.M., Jonkers D.M.A.E., Bast A., Vanhoutvin S., Fischer M.A.J.G., **Kodde A.**, Troost F.J., Venema K., Brummer R.J., Butyrate modulates oxidative stress in the colonic mucosa of healthy humans, Clinical Nutrition, 2009; 28(1):88-93.

Troost F.J., Baarlen van P., Lindsey P., **Kodde A.**, Vos de W.M., Kleerebezem M., Brummer R.J., Identification of the transcriptional response of human intestinal mucosa to *Lactobacillus plantarum* WCFS1 *in vivo*, BMC Genomics, 2008; 9:374.

Renes J., Tilburg van J., Haaften van R., Bouwman F., **Kodde F.D.**, Evelo C., Noben J.P., Robben J., Mariman E., Thiazolidinediones regulate expression of proteins involved in triglyceride storage and fatty acid oxidation in 3T3-L1 preadipocytes, Adipocytes, 2006; 2(2):1-17.

Heuvelink A.E., Ahmed M., **Kodde F.D.**, Zwartkruis-Nahuis J.T.M., Boer de E., Enterobacter Sakazakii in melkpoeder, Ware(n) Chemicus, 2002; 32(1):17-30.

Abstracts:

Carlin G., Chaumontet C., Delteil C., **Kodde A.**, Heijning van de B., Beek van der E.M., Tome D., Davila A., Varying protein quantity and quality in the maternal diet during the perinatal period affects growth and adiposity risk in female adult offspring in rats, oral presentation, ASN, Baltimore, Maryland, USA, 2019.

Carlin G., Chaumontet C., Delteil C., **Kodde A.**, Heijning van de B., Tome D., Davila A., Perinatal exposure to a maternal diet varying in protein quantity and quality affects weight gain and adiposity of female adult offspring in rat, poster, SSIB, Utrecht, 2019.

Kodde A., Engels E., Oosting A., Limpt van K., Beek van der E.M., Keijer J., Remoddeling of mitochondria in white adipose depots in postweaning C57BL/6j mice, poster, Keystone symposium on Organ Crosstalk in Obesity and NAFLD, Keystone, Colorado, USA, 2018. (*poster*)

Carlin G., Chaumontet C., Delteil C., Darcel N., Heijning van de B., **Kodde A.**, Tome D., Davila A., Exposition périnatale à un régime de quantité et de qualité variables en protéines chez le rat-croissance, préférences alimentaires et risque de surpoids chez la descendance femelle adulte, poster, Journées Francophones de Nutrition, Nice, France, 2018.

Kodde A., Engels E., Oosting A., Limpt van K., Beek van der E.M., Keijer J., Differences in development of white adipose tissue depots in post-weaning C57BL/6j mice; poster presentation Dohad, Rotterdam, 2017. (*poster presentation*)

Carlin G., Chaumontet C., Darcel N., Blachier F., **Kodde A.**, Oosting A., Tome D., Davila A., High-protein exposure during gestation – Consequences on food preferences and health in adult rat offspring in self-selection models, oral presentation International congress of nutrition; Buenos Aires, Argentina, 2017.

Kodde A., Oosting A., Phielix E., Schipper L., Engels E., Beek van der E., Developmental programming of the mitochondrial function with dietary lipid structure may protect against obesity; poster presentation Keystone symposium on mitochondria, metabolism and heart failure; Santa Fe, US, January 2015. (*poster*)

Kodde A., Oosting A., Phielix., Schipper L., Engels., Beek van der E., Postnatal programming with dietary lipid structure may protect against obesity through enhanced mitochondrial function in the adipose tissue; poster of distinction Power of Programming conference; Munich, Germany, March 2014. (*poster presentation*)

Beek van der E., **Kodde A**., Engels E., Kegler D., Schipper L., Verkade H.J., Oosting A.; Physical properties of dietary lipid droplets in early life program adipose tissue development and gene expression in adult mice; poster presentation, world congress of pediatric gastroenterology hepatology and nutrition (WCPGHAN), Taipei, Taiwan, November 2012.

Kodde A., Oosting A., Schipper L., Engels E., Kegler D., Heijning van de B., Teller I., Beek van der E.; Physical porperties of lipid droplets in the early diet affect adipose tissue development in C57BL/6j mice; oral presentation, international society for fatty acids and lipids (ISSFAL), Vancouver, Canada, May 2012. (*presentation*)

Vanhoutvin S., Troost F., Hamer H., Jonkers D., **Kodde A.**, Venema K., Brummer R.J.; Butyrate modulates mucosal gene transcription in healthy subjects; poster presentation, digestive disease week (DDW), Chicago, VS, May 2009.

Vanhoutvin S., Troost F., Hamer H., Jonkers D., **Kodde A.**, Venema K., Brummer R.J.; Butyrate induces transcriptional changes in human colonic mucosa, poster presentation, NVGE Eindhoven, the Netherlands, March 2008

Hamer H., Jonkers D., Troost F., Vanhoutvin S., **Kodde A.**, Veneman K., Koek G., Brummer R.J.; Effects of butyrate on the colonic mucus layer in healthy humans *in vivo*, poster presentation, NVGE Eindhoven, March 2008

Vanhoutvin S., Troost F., Hamer H., Jonkers D., **Kodde A.**, Venema K., Brummer R.J.; Butyrate induces transcriptional changes in human colonic mucosa; poster presentation, darmendag, Utrecht, November 2007

Hamer H., Jonkers D., Schipper R., Loof A., Vanhoutvin S., Troost F.J., Koek G., **Kodde A.**, Venema K., Brummer R.J.; Novel technique for mucus sampling and proteomic analysis of human colonic mucus; poster presentation, digestive disease week (DDW) Washington DC, VS, May 2007, Gastroenterology, 2007; 132(4 Suppl 2): A208

Hamer H., Jonkers D., Schipper R., Groot de J., **Kodde A.**, Venema K., Vanhoutvin S., Troost F., Loof A., Brummer R.J.; *In vivo* sampling of mucus in the large intestine, oral presentation darmendag, Groningen, November 2006

About the Author

Francina Dorothea (Andrea) Kodde was born December 5th, 1978 in Goes, The Netherlands. In 1996 she received her HAVO diploma at the Greijdanus College in Zwolle and in 2001 her bachelor's degree in biomedical sciences at the Saxion Hogeschool Ijselland, Deventer. She subsequently worked for several years as research technician, first for the NVWA (Dutch food and consumer product safety authority) and subsequently for 7.5 years at Maastricht University. At Maastricht University she first worked at the department of Human Biology and subsequently at the department of Gastroenterology. During those years Andrea developed an interest in research on the interaction between nutrition and health. In 2010 she started as an assistant scientist, senior assistant from 2012 and scientist from 2019, at Danone Nutricia Research in the nutritional programming team. In this role she investigated the role of early life nutrition on the metabolism, specifically on white adipose tissue function. Next to the work described in the thesis, she was involved in several projects on the effect of early life nutrition (pre- or postnatal) on metabolic health.

The research described in this thesis was financial supported by Danone Nutricia Research.

Financial support from Danone Nutricia Research for printing and design of this thesis is gratefully acknowledged.

Cover design by David van Neerbos (davidvanneerbos.nl) and Barbara de Haas (fishwife design).

Illustrations lipid droplets on the cover adapted from Oosting A., Effect of dietary lipid structure in early postnatal life on mouse adipose tissue development and function in adulthood, Br J Nutr. 2014;111(2):215-26.

Figure 1,2 and 4 of the introduction and Figure 1 and 2 of the discussion by Barbara de Haan (fishwife design).

Printed by Ridderprint.